

# C–H and C–C Activation by Cobalt and Ruthenium Catalysis

**Dissertation**

for the award of the degree

“Doctor rerum naturalium”

of the Georg-August-University of Göttingen



within the doctoral program of chemistry

of the Georg-August-University School of Science (GAUSS)

submitted by

**Marc Philipp Moselage**

from Verl

Göttingen, 2017



**Thesis Committee**

Prof. Dr. Lutz Ackermann, Institute of Organic and Biomolecular Chemistry

Prof. Dr. Franc Meyer, Institute of Inorganic Chemistry

**Members of the Examination Board**

Reviewer: Prof. Dr. Lutz Ackermann, Institute of Organic and Biomolecular Chemistry

Second Reviewer: Prof. Dr. Franc Meyer, Institute of Inorganic Chemistry

**Further Members of the Examination Board**

Prof. Dr. Manuel Alcarazo, Institute of Organic and Biomolecular Chemistry

Prof. Dr. Dietmar Stalke, Institute of Inorganic Chemistry

Dr. Shoubhik Das, Institute of Organic and Biomolecular Chemistry

Dr. Franziska Thomas, Institute of Organic and Biomolecular Chemistry

**Date of the Oral Examination:** 15.11.2017





## Acknowledgment

Das Umfeld, die Unterstützung und die vielen Erlebnisse der letzten vier Jahre lassen sich wahrlich kaum in ein paar Zeilen zusammenfassen, dennoch verdienen einige Menschen eine besondere Anerkennung.

Zunächst gilt mein großer Dank meinen Mentor und Lehrer Prof Dr. Lutz Ackermann, mich in sein Team aufzunehmen und unter exzellenten Bedingungen zu forschen. Die Ausstattung, die internationale Besetzung, sowie der wissenschaftliche Output machen diesen Arbeitskreis sicherlich einzigartig. Ebenso bin ich sehr dankbar an hochrangigen internationalen Konferenzen teilgenommen haben zu dürfen.

Prof. Dr. Franc Meyer danke ich für die Übernahme des Zweitgutachtens. Ebenso vielen Dank den weiteren Mitgliedern der Prüfungskommission Prof. Dr. Manuel Alcarazo, Prof. Dr. Dietmar Stalke, Dr. Shoubhik Das und Dr. Franziska Thomas.

Ebenso möchte ich mich bei allen analytischen Abteilungen im Hause für das gewissenhafte und schnelle Messen jeglicher Arten von Substanzen herzlich bedanken. Im Besonderen gilt dies der NMR-Abteilung unter der Leitung von Dr. M. John für knapp 1500 NMR Spektren und der Massenspektrometrie unter der Leitung von Dr. H. Frauendorf für über 150 MS Spektren und den kompetenten Ratschlägen bei Problemen jeglicher Art.

Natürlich gebührt mein größter Dank auch den vielen Mitarbeitern und ehemaligen Mitarbeitern unseres Arbeitskreises. Vielen lieben Dank Svenja für schlichtweg alles, zunächst einmal, dass du es knapp drei Jahre mit mir in einem Labor ausgehalten hast, die vielen Gespräche über alles Mögliche und deine Unterstützung und Ratschlag auch bei nicht-chemischen Problemen. Vielen Dank auch an Nicolas, nicht nur für gemeinsame Projekte, sondern auch die große Schnittmenge an gemeinsamen Humor. Danke Karo, dass ich mich von Anfang an gleich willkommen fühlte, für deine stets gute Laune und positiven bis leicht verrückten Art.

Muito obrigado Elo for bringing sunshine into the lab for five wonderful months we could spend with you. Muchas Gracias Ana and Maria for sharing the (northern) Spanish way of life with us. Thanks also Alan for all and in particular, for watching football games. The times with you passed by too fast.

Besten Dank auch an Alex, Julian, Ralf, Torben und Thomas für diverse Unternehmungen in und um Göttingen und die vielen Erinnerungen. Danke an Gabi,

Karsten und Stefan dafür, dass Equipment, Geräte und Chemikalien stets einsatzbereit waren und alles Bürokratische zuverlässig bewältigt wurde.

Für das gewissenhafte Korrekturlesen des Folgenden bedanke ich mich sehr herzlich bei Dr. Svenja Warratz, Nicolas Sauermann und Torben Rogge.

Bedanken möchte ich mich auch bei allen Studenten, die ich im Rahmen eines Forschungspraktikums, der Bachelor- oder Masterarbeit oder im Rahmen des FoLL-Projekts begleiten durfte

Nicht unerwähnt bleiben soll auch Prof. Dr. Thorsten Glaser, bei denen ich nicht nur während der Masterarbeit, aber auch während des gesamten Studiums stets optimale Betreuung und Förderung erhielt.

Mein größter Dank jedoch gebührt meiner Familie, die mir mein Studium überhaupt erst ermöglicht hat und mich jederzeit und bei allen Entscheidungen bestmöglich unterstützt hat. Ohne euch wäre all dies nie möglich gewesen. Zum Schluss vielen Dank an meine liebe Julia, dass du mich gerade in den letzten Tagen der Promotion bestmöglich unterstützt hast.

Göttingen, Oktober 2017

Marc Moselage,





## Contents

<b>1</b>	<b>Introduction .....</b>	<b>1</b>
1.1	Transition Metal-Catalyzed C–H Functionalizations .....	1
1.2	Cobalt-Catalyzed C–H Activation .....	4
1.2.1	C–H Activation by low-valent Cobalt Catalysis .....	6
1.2.2	C–H Activation by Cp*Co(III) Catalysis.....	14
1.3	Transition Metal-Catalyzed C–C Functionalizations .....	23
1.3.1	Functionalization of Strained Substrates .....	25
1.3.2	Functionalization of Unstrained Substrates .....	28
<b>2</b>	<b>Objectives.....</b>	<b>33</b>
<b>3</b>	<b>Results and Discussion.....</b>	<b>36</b>
3.1	Cobalt-Catalyzed Alkenylation with Enol Derivatives.....	36
3.1.1	Optimization Studies .....	36
3.1.2	Scope of the Cobalt-Catalyzed C–H Alkenylation with Enolates.....	43
3.1.3	C–H Alkenylation with Alkenyl Phosphates, Carbamates and Carbonates .....	49
3.1.4	C–H Alkenylation of Ferrocenes.....	51
3.1.5	Mechanistic Studies .....	54
3.1.6	Cleavage of the Pyrimidyl Directing Group.....	65
3.2	Cobalt-Catalyzed C–H Allylation with Allyl Acetates .....	65
3.2.1	Optimization Studies .....	65
3.2.2	Scope of the Cobalt-Catalyzed C–H Allylation with Allyl Acetates .....	67
3.2.3	Mechanistic Studies .....	72
3.3	Cobalt-Catalyzed C–H/N–O Functionalization.....	74
3.3.1	Scope for the Cobalt-Catalyzed C–H/N–O Functionalization.....	75
3.3.2	Mechanistic Studies .....	78
3.4	Ruthenium(II)-Catalyzed Decarbamoylative and Decarboxylative C–C Arylations.....	80
3.4.1	Optimization Studies .....	81
3.4.2	Scope for the Ruthenium(II)-Catalyzed Decarbamoylative C–C Arylation	84
3.4.3	Decarboxylative and Dealkanolative C–C Arylation.....	91
3.4.4	Ruthenium(II)-Catalyzed Hydroarylation by C–C Bond Cleavage.....	94
3.4.5	Mechanistic Studies .....	95

3.4.6	Diversification of the Pyrazoles .....	98
3.5	Ruthenium(II)-Catalyzed Decarboxylative C–C Alkylation .....	100
3.5.1	Optimization Studies .....	100
3.5.2	Scope for the Decarboxylative Ruthenium(II)-Catalyzed C–C Alkylation with Alkyl Halides .....	104
3.5.3	Mechanistic Studies .....	109
3.5.4	Ozonolysis of the Pyrazole Directing Group .....	112
<b>4</b>	<b>Summary and Outlook.....</b>	<b>114</b>
<b>5</b>	<b>Experimental Part .....</b>	<b>119</b>
5.1	General Remarks.....	119
5.2	General Procedures .....	122
5.3	Cobalt-Catalyzed C–H Alkenylation with Enol Derivatives.....	124
5.3.1	Experimental Procedures and Analytical Data .....	124
5.3.2	Mechanistic Studies .....	140
5.4	Cobalt-Catalyzed Allylation with Allyl Acetates .....	147
5.4.1	Experimental Procedures and Analytical Data .....	147
5.4.2	Mechanistic Studies .....	153
5.5	Cobalt-Catalyzed C–H/N–O Functionalization.....	155
5.5.1	Experimental Procedures and Analytical Data .....	155
5.6	Ruthenium(II)-Catalyzed C–C Arylation of Amides and Acids .....	161
5.6.1	Experimental Procedures and Analytical Data .....	161
5.6.2	Mechanistic Studies .....	184
5.7	Ruthenium(II)-Catalyzed C–C Alkylation of Acids .....	186
5.7.1	Experimental Procedures and Analytical Data .....	186
5.7.2	Mechanistic Studies .....	199
5.7.3	Selected 2D-NMR Spectra.....	201
<b>6</b>	<b>References .....</b>	<b>210</b>

## List of Abbreviations

Ac	acetyl
acac	acetyl acetate
Ad	adamantyl
Alk	alkyl
Am	amyl
AMLA	ambiphilic metal ligand activation
Ar	aryl
atm	atmospheric pressure
ATR	attenuated total reflection
BDMAE	1,1'-oxybis( <i>N,N</i> -dimethylmethanamine)
BHT	2,6-di- <i>tert</i> -butyl-4-methylphenol
BIES	base-assisted internal electrophilic substitution
Bn	benzyl
Boc	<i>tert</i> -butoxycarbonyl
Bu	butyl
calc.	calculated
<i>cat.</i>	catalytic
CMD	concerted metalation deprotonation
cod	1,5-cyclooctadiene
Cp*	pentamethylcyclopentadienyl
Cy	cyclohexyl
$\delta$	chemical shift
d	doublet
DBU	1,8-diazabicyclo[5.4.0]undec-7-ene
DCE	1,2-dichloroethane
DMF	<i>N,N</i> -dimethylformamide
DMPU	1,3-dimethyl-3,4,5,6-tetrahydro-2(1 <i>H</i> )pyrimidinone
DMSO	dimethyl sulfoxide
dppb	1,3-bis(diphenylphosphino)butane
dppe	1,3-bis(diphenylphosphino)ethane
dppm	1,3-bis(diphenylphosphino)methane
dppp	1,3-bis(diphenylphosphino)propane
ee	enantiomeric excess
EI	electron ionization
equiv	equivalents

ESI	electrospray ionization
Et	ethyl
EWG	electron-withdrawing group
g	gram
GC	gas chromatography
GPC	gel permeation chromatography
GVL	$\gamma$ -valerolactone
h	hour or hextet
HASPO	heteroatomic secondary phosphine oxide
hept	heptet
Het	hetero(aryl)
HFIP	1,1,1,3,3,3-hexafluoro-2-propanol
HPLC	high performance liquid chromatography
HRMS	high resolution mass spectrometry
Hz	Hertz
<i>i</i>	iso
ICyHCl	1,3-dicyclohexyl-1 <i>H</i> -imidazol-3-ium chloride
IES	internal electrophilic substitution
IMesHCl	1,3-dimesityl-1 <i>H</i> -imidazol-3-ium chloride
Ind	indazolyl
IPrHCl	1,3-bis(2,6-diisopropylphenyl)-1 <i>H</i> -imidazol-3-ium chloride
IR	infrared
J	Joule
<i>J</i>	coupling constant
KIE	kinetic isotope effect
L	ligand or liter
Leu	leucine
LiHMDS	lithium bis(trimethylsilyl)amide
LLHT	ligand-to-ligand hydrogen transfer
M	metal
<i>m</i>	meta
m	multiplet
M.p.	melting point
<i>m/z</i>	mass-to-charge ratio
mA	milliampere
Me	methyl
Mes	mesityl



mg	milligram
MHz	megahertz
min	minutes
mmol	millimol
MS	mass spectrometry
MTBE	methyl- <i>tert</i> -butyl ether
μm	microgram
MW	microwave
Naph	naphthyl
nbd	2,5-norbanadiene
NBP	<i>N</i> -bromophthalimide
NBS	<i>N</i> -bromosuccinimide
NCTS	<i>N</i> -cyano- <i>N</i> -phenyl- <i>para</i> -toluenesulfonamide
NHC	N-heterocyclic carbene
NIS	<i>N</i> -iodosuccinimide
NMP	<i>N</i> -methylpyrrolidinone
NMR	nuclear magnetic resonance
<i>o</i>	<i>ortho</i>
<i>p</i>	<i>para</i>
Pent	pentyl
Ph	phenyl
Piv	pivaloyl
PMP	<i>para</i> -methoxyphenyl
ppm	parts per million
Pr	propyl
py	pyridyl
pym	pyrimidyl
pyphos	2-[2-(diphenylphosphaneyl)ethyl] pyridine
pyz	pyrazolyl
q	quartet
R	(organic) rest
( <i>r</i> )DG	(removable) directing group
s	singulet
sat.	saturated
SET	single electron transfer
S <sub>N</sub>	nucleophilic substitution
SPS	solvent purification system

<i>t</i>	<i>tert</i>
t	triplet or time
T	temperature
TEMPO	2,2,6,6-tetramethylpiperidine- <i>N</i> -oxide
Tf	trifluoromethanesulfonyl
TFA	trifluoroacetic acid
TFE	2,2,2-trifluoroethanol
THF	tetrahydrofuran
TLC	thin layer chromatography
TM	transition metal
TMS	trimethylsilyl
Tos	<i>para</i> -toluenesulfonyl
UV	ultraviolet
VE	valence electrons
WCA	weakly coordinating anion





## 1 Introduction

Within the last decades, an immense amount of compounds have been made for a plethora of applications in pharmaceutical and agrochemistry, polymer science and important other areas. While all these materials have doubtlessly improved the life quality of many people, their ecological footprint in terms of pollution and contamination of earth, water and air demands for more ecological synthesis. Therefore catalysis is an important technique for the present and even more so, for the future. Within their *12 Principles of Green Chemistry*, Warner and Anastas declared catalysis as one key principle.<sup>[1]</sup> Furthermore, the reduction of stoichiometric to catalytic amounts also inherently reduces the waste production, declared as the first principle.

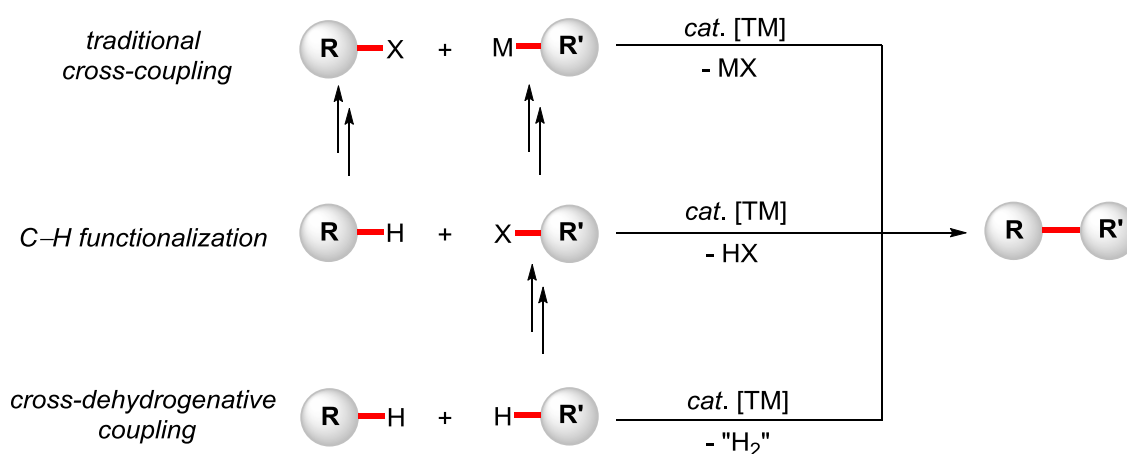
For the industrial manufacture, not just ecological, but also economical aspects influence the synthetical strategy. That includes easily available and cost-effective chemicals including catalysts, mild reaction conditions as well as robust and versatile reactions. This demand is further increased in times of generics and expiring patents.<sup>[2]</sup> Catalysis is one possible solution to fulfill these requirements, in particular, the activation and functionalization of the most abundant bonds in organic compounds, namely C–H and C–C bonds.

### 1.1 Transition Metal-Catalyzed C–H Functionalizations

The selective formation of C–C or C–Het bonds by catalytic methods is more important than the activation process and is of key importance for organic synthesis. In particular, the application towards the formation of biaryls is their biggest potential as the access to these omnipresent scaffolds is limited.<sup>[3]</sup>

Early works by Ullmann enabled the access to biaryls using stoichiometric or even catalytic amounts of copper.<sup>[4]</sup> With harsh reaction conditions, low selectivities and moderate yields, the application of this method continues to be limited. Almost 70 years later, a breakthrough in the field of selective C–C coupling was achieved with the development of palladium-catalyzed cross-coupling reactions. Namely, the Kumada-Corriu,<sup>[5]</sup> Negishi,<sup>[6]</sup> Magita-Kosogi-Stille,<sup>[7]</sup> Suzuki-Miyaura<sup>[8]</sup> and Hiyama<sup>[9]</sup> cross-coupling enabled the efficient and selective synthesis of biaryls, while the Mizoroki-Heck<sup>[10]</sup> reaction allowed for the selective alkenylation of aryl halides and the Sonogashira-Hagihara<sup>[11]</sup> reaction represents a powerful tool for alkynylation. These reactions became widely applicable tools for C–C coupling reactions with numerous applications, even in late stage-diversifications.<sup>[12]</sup> Therefore, this research was recognized with the Nobel Prize in 2010 to A. Suzuki, E.-i. Negishi and R. F. Heck.<sup>[13]</sup>

While these methods have clearly revolutionized organic syntheses, they still face significant problems. Thus, a pre-functionalization is necessary and not only for organic (pseudo)halides, but even more so for the employed organic nucleophiles, which usually require multiple synthetic steps. Moreover, these compounds can be difficult to handle and store, e.g.  $\text{RMgX}$ ,  $\text{R}_2\text{Zn}$ , and toxic, e.g.  $\text{R}'_3\text{RSn}$ . Therefore, the selective C–H functionalization<sup>[14]</sup> represents an elegant tool to circumvent these problems, combining the broad practicability of cross-couplings with the atom economical, environmentally-friendly and need nature of C–H activation (Figure 1.1). Furthermore, C–C bond formation can also occur by twofold C–H activation in a dehydrogenative fashion. These reactions usually require stoichiometric amounts of an oxidant.

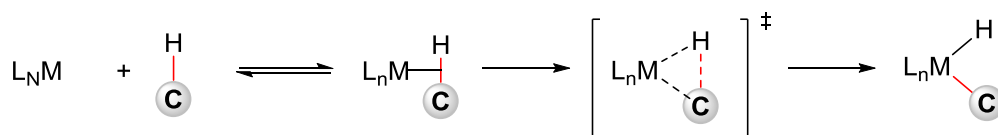


**Figure 1.1:** Comparison of traditional cross-coupling *versus* C–H activation.

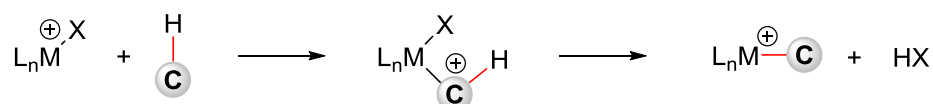
The field of C–H activation has attracted major attention and has become a widely investigated area of research. Its key-step, the cleavage of the C–H bond, has been extensively examined. Excluding radical-type outer-sphere mechanisms,<sup>[15]</sup> the bond dissociation proceeds *via* five different pathways, depending on the nature of the metal, its ligands and oxidation states (Figure 1.2).<sup>[14b, 14c]</sup> These methods comprise oxidative addition, electrophilic substitution,  $\sigma$ -bond metathesis, 1,2-addition and base-assisted metalation. The oxidative addition is a typical reaction pathway for late and electron-rich transition metals in low oxidation states, such as ruthenium(0), rhodium(I) and palladium(0). This mechanism is also postulated for low-valent cobalt-catalysis (*vide infra*). Most late transition metals in higher oxidation states tend to undergo C–H activation by an electrophilic substitution in which the metal acts as a Lewis acid. Early transition metals as well as lanthanides which cannot undergo oxidative addition can react *via*  $\sigma$ -bond metathesis. The 1,2-addition is observed for metals with an unsaturated  $\text{M}=\text{X}$  bond, mostly metal imido-complexes. This mode usually takes place for early transition metals. A more recently discovered mode for C–H cleavage is the base-mediated C–H

activation.<sup>[14b]</sup> Here the base facilitates the proton abstraction upon C–H activation with the transition metal.

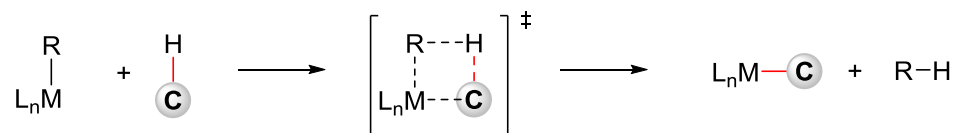
oxidative addition:



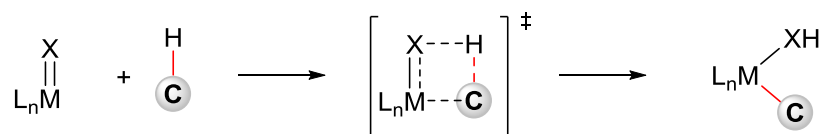
electrophilic substitution:



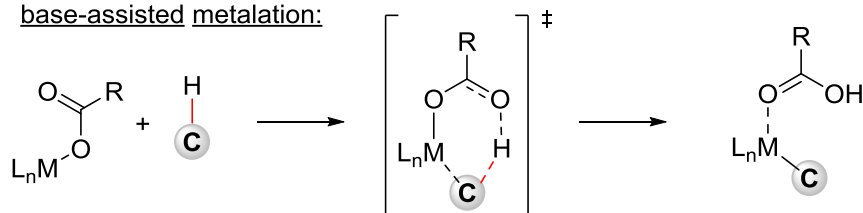
$\sigma$ -bond metathesis:



1,2-addition:



base-assisted metalation:



**Figure 1.2:** Different modes for organometallic C–H activation.

This base-assisted C–H cleavage underwent further investigation and three transition states were reported, demonstrating the cooperation of base and metal (Figure 1.3). The *concerted metalation deprotonation* (CMD)<sup>[16]</sup> and the *ambiphilic metal ligand activation* (AMLA),<sup>[17]</sup> where a six-membered transition state is proposed, were disclosed independently. In contrast, the *intermolecular electrophilic substitution* (IES)<sup>[18]</sup> proceeds via a more strained 4-membered transition state and is typical for alkoxide bases. The very recently presented *base-assisted intermolecular substitution* (BIES)<sup>[19]</sup> rationalizes the preferred reactivity of electron-rich arenes.

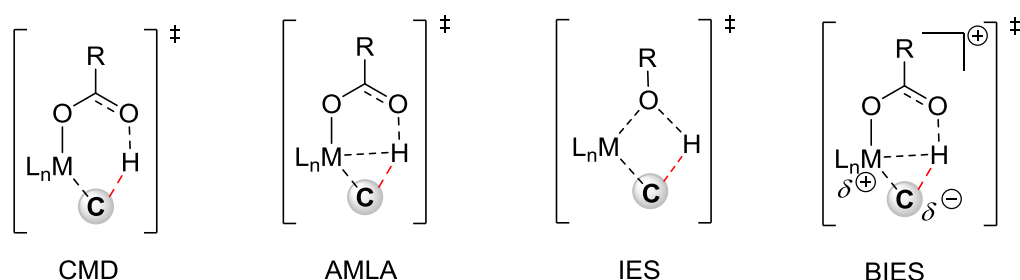


Figure 1.3: Base-assisted metalation.

C–H bonds are omnipresent in organic molecules with almost identical bond dissociations energies. En route for sustainable C–H functionalization, the control of selectivity is of major importance. This selectivity can be gained by electronic bias, steric control, or a directing group that coordinates to the transition metal in proximate position to a C–H bond (Figure 1.4).<sup>[20]</sup>

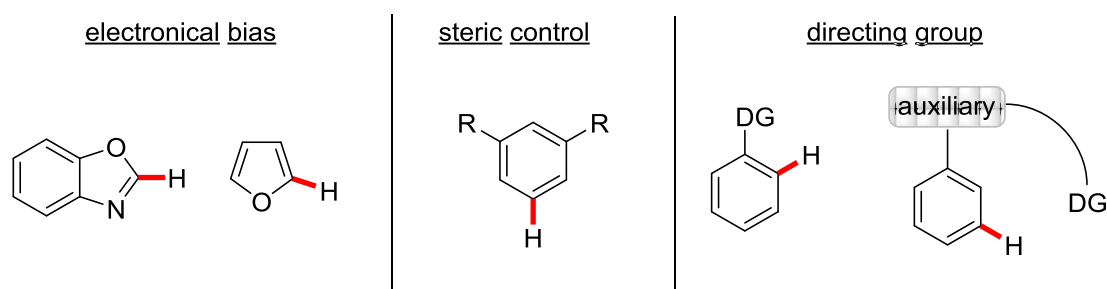


Figure 1.4: Selectivity in C–H activation.

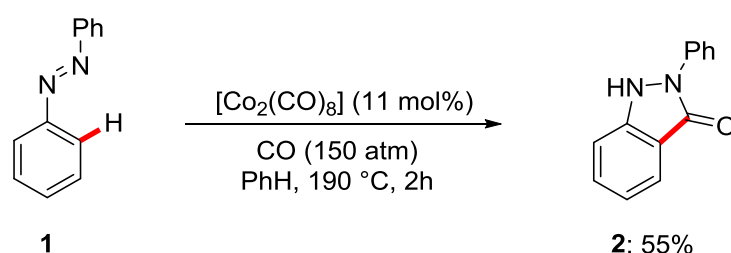
The control by electronic and steric properties usually relies on the substrate itself and therefore limits the number of useable compounds. In contrast, a directing group can be added to a huge variety of different substrates and in many cases also be removed after the transformation (removable directing group).<sup>[21]</sup> This removal does not necessarily require an additional cleavage step, but can proceed in the same reaction as the desired functionalization (traceless directing group). In the best case, addition of the directing group, C–H functionalization and cleavage take place in a single reaction (transient directing group).

## 1.2 Cobalt-Catalyzed C–H Activation

The last decade established the transition metal-catalyzed C–H activation as an increasingly viable and powerful tool for a very broad range of different transformations, a success that was mostly contributed to 4d and 5d transition metals.<sup>[14]</sup> Despite indisputable achievements, the relatively high costs<sup>[22]</sup> and low abundance demanded for the development of more economical and sustainable catalysts. Therefore, catalysts based on 3d metals attracted significant attention throughout the last years.<sup>[23]</sup> In

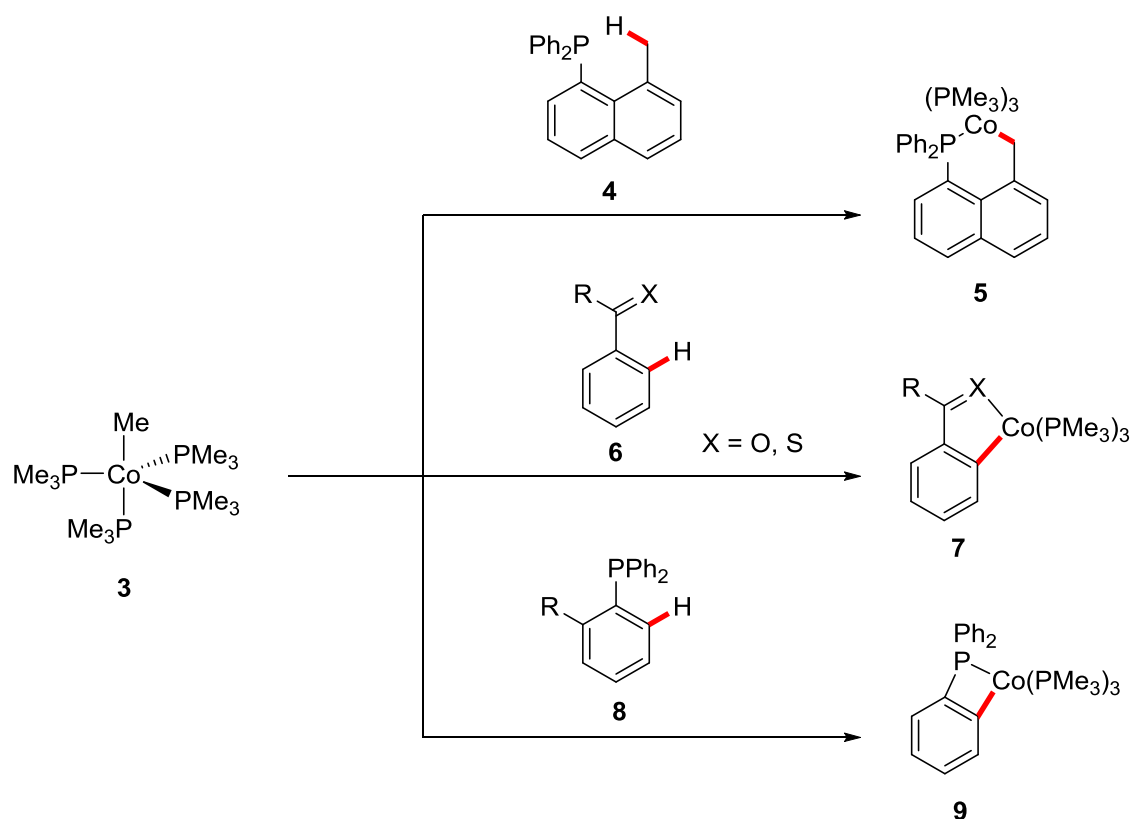


particular, cobalt became the metal of choice of many research groups.<sup>[23a, 24]</sup> Its catalytic coupling performance was discovered already in 1941 by Karash and Fields with the homocoupling of Grignard reagents<sup>[25]</sup> and was reflected in many important transformations, such as the Phausen-Khand<sup>[26]</sup> reaction, the Bönnemann pyridine synthesis<sup>[27]</sup> and also hydroformylation<sup>[28]</sup> reactions. The activity of cobalt complexes for C–H activation was discovered at an early stage, with a groundbreaking work of Murahashi and coworkers.<sup>[29]</sup> They succeeded in performing a cobalt-catalyzed carbonylative cyclization of azobenzene (**1**) and later on with imines (Scheme 1.1), a contribution that not only represents the first for cobalt catalysis, but also one of the first examples of chelation assisted C–H activation.



**Scheme 1.1:** Cobalt-catalyzed carbonylative cyclization.

Although this cobalt-catalyzed C–H activation suffered from very harsh reaction conditions and offered space for improvement, the development of more sustainable and powerful catalysts stagnated for almost 40 years. With the beginning of the 1990's, Klein succeeded in the synthesis of different cyclocobaltated complexes by stoichiometric C–H activation using  $[\text{Co}(\text{CH}_3)(\text{PMe}_3)_4]$  (**3**) as the precursor.<sup>[30]</sup> This complex was powerful enough to generate 5-,<sup>[30a-d, 30f]</sup> 6-,<sup>[30d]</sup> and even strained 4-membered<sup>[30e]</sup> cobaltacycles (Scheme 1.2).

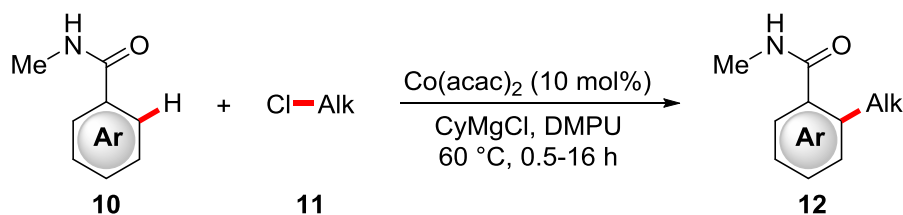


Scheme 1.2: Stoichiometric cyclocobaltation

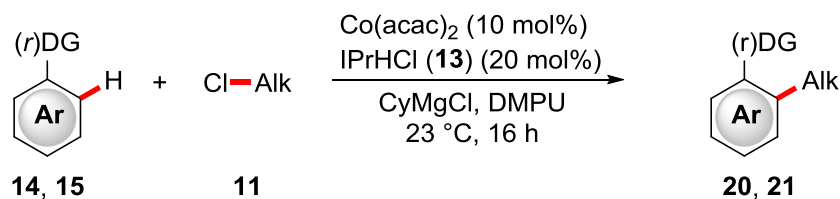
### 1.2.1 C–H Activation by low-valent Cobalt Catalysis

Despite these early achievements in catalysis and the understanding of cyclometalated species, the amount of contribution maintained manageable until Nakamura and coworkers reported a cobalt-catalyzed alkylation with alkyl halides (Scheme 1.3a).<sup>[31]</sup> The key factor was the *in situ* generation of the active catalyst by the use of inexpensive  $\text{Co}(\text{acac})_2$  and a Grignard reagent that allowed for the cobalt-catalyzed C–H activation with organic electrophiles. Limitations of the first system were the relatively small scope as well as the restriction to benzamides **10**. Significant improvements of this system were contributed by the groups of Ackermann<sup>[32]</sup> and Yoshikai.<sup>[33]</sup> In independent studies, both groups discovered the increase in performance with a N-heterocyclic carbene (NHC) as ligand that enabled the desired reaction at room temperature. Ackermann and coworkers established a system with  $\text{Co}(\text{acac})_2$  and  $\text{IPrHCl}$  (**13**) (Figure 1.5), which succeeded in the alkylation of aryl pyridines **14** and biologically important indoles **15** (Scheme 1.3b).<sup>[32]</sup> In contrast, Yoshikai's system utilizes  $\text{CoBr}_2$  and compounds **16** or **17** as carbene precursors (Scheme 1.3c).<sup>[33]</sup> It afforded the alkylation of ketimines **18** that, after subsequent hydrolysis, delivered the *ortho*-alkylated ketones **19**.

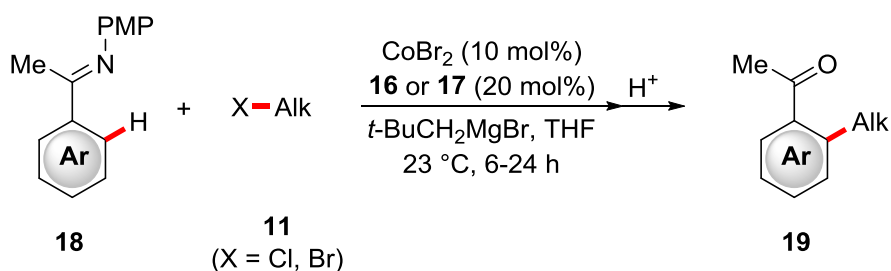
(a) Nakamura (2011)



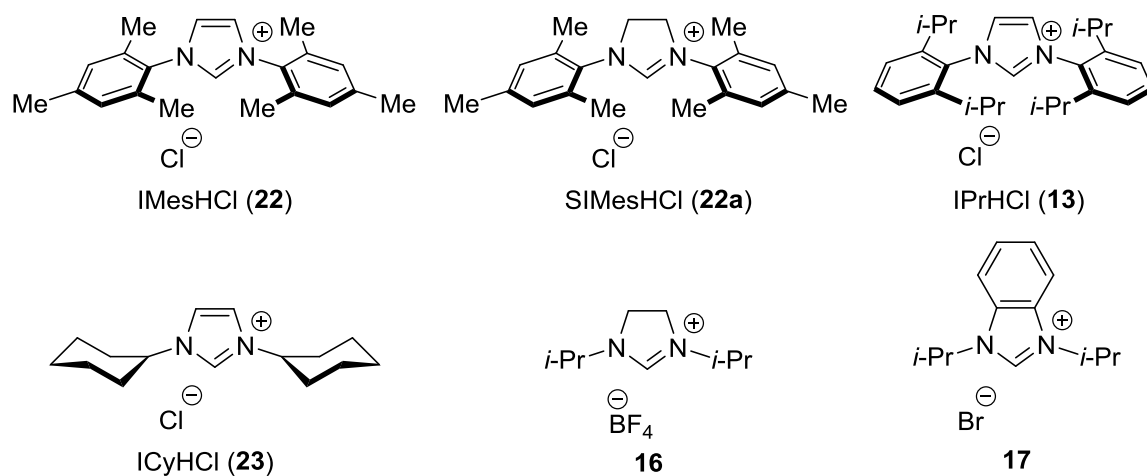
(b) Ackermann (2013)



(c) Yoshikai (2013, 2014)

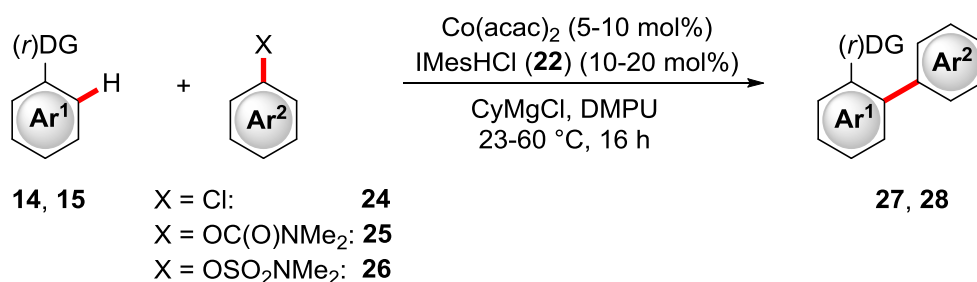
**Scheme 1.3:** Cobalt-catalyzed C–H alkylation with alkyl halides **11**.

The choice of appropriate ligands proved to be crucial for the success of the reactions. In particular, N-heterocyclic carbenes<sup>[34]</sup> found most application in these reactions. The most often utilized are listed below (Figure 1.5).

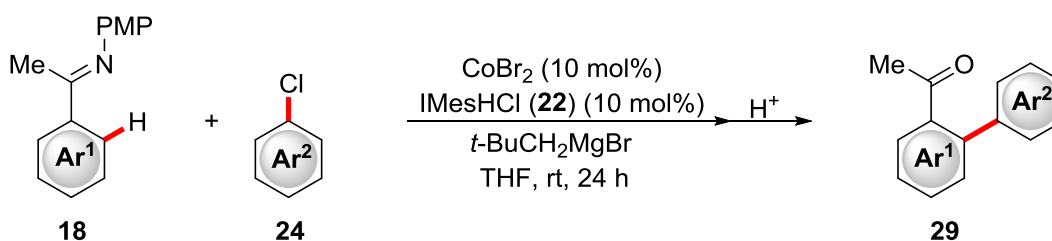
**Figure 1.5:** Common NHC preligands for the cobalt-catalyzed C–H functionalization.

Beside the C–H alkylation, methods for the selective C–H arylations are arguably even more important. The formed biaryl compounds play an important role in *inter alia* agrochemical and pharmaceutical chemistry and their syntheses usually require transition metal-catalyzed methods.<sup>[35]</sup> By replacing the IPrHCl (**13**) preligand with IMesHCl (**22**), Ackermann and coworkers presented the first cobalt-catalyzed C–H arylation (Scheme 1.4a).<sup>[32, 36]</sup> Again, the broad use of this low-valent cobalt chemistry could be underlined. The reaction allowed for the C–H arylation of aryl pyridines **14** as well as pyri(mi)dyl indoles **15** with aryl chlorides **24**, carbamates **25** and sulfamates **26** by C–Cl or C–O bond cleavage. In subsequent studies the group of Yoshikai presented a C–H arylation protocol that allowed for the conversion of ketimines **18** (Scheme 1.4b).<sup>[37]</sup> The catalytic system differs from the Ackermann system by using CoBr<sub>2</sub> instead of Co(acac)<sub>2</sub> and by employing the very expensive *neo*-pentyl Grignard.<sup>[38]</sup> An expansion of this C–H arylation system was reported by Ackermann and coworkers (Scheme 1.4c).<sup>[19d, 39]</sup> The improved system enabled the arylation of, among others, benzamides **10** and aryl tetrazoles. With these features the reaction gives access to angiotensin-II-receptor-blockers (ARBs) such as Losartan and Valsartan, which are blockbuster drugs for hypertension treatment.<sup>[35b]</sup>

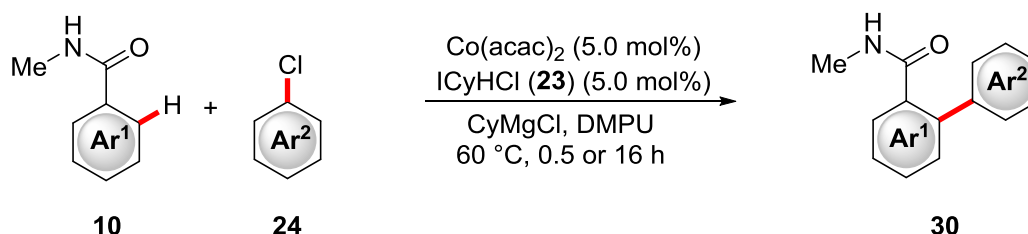
(a) Ackermann (2012, 2013)



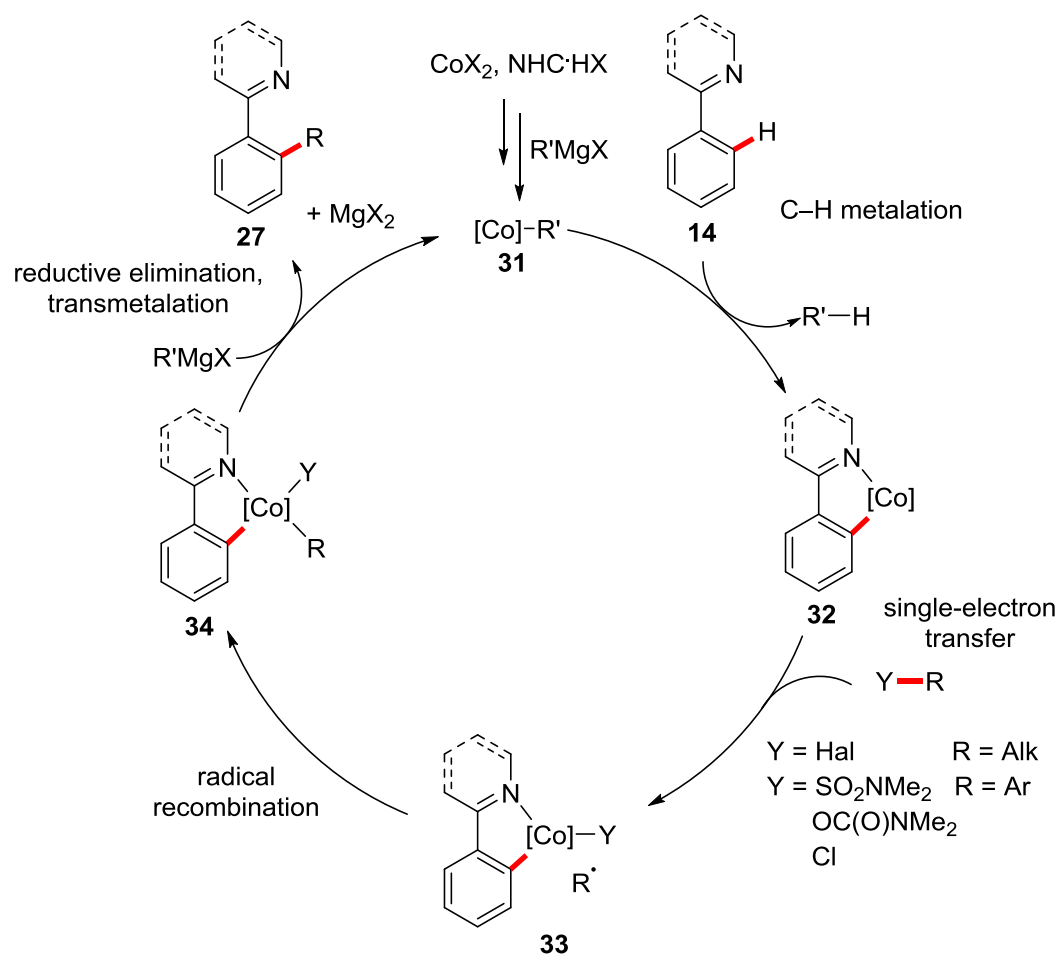
(b) Yoshikai (2012)



(c) Ackermann (2015)

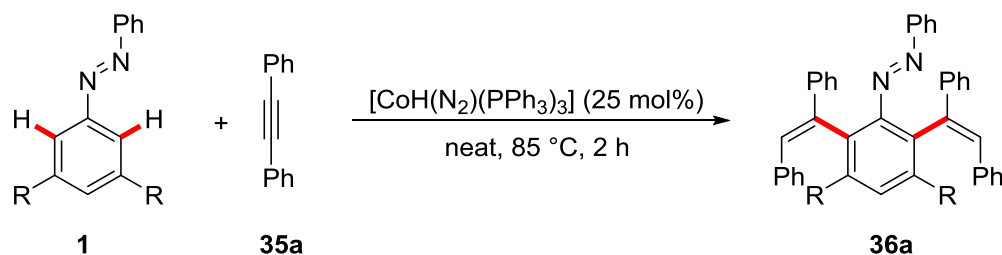
**Scheme 1.4:** Cobalt-catalyzed C–H arylation.

Despite the continuous progress in cobalt-catalyzed C–H alkylation and arylation, the mechanisms of these transformations remain widely undiscovered.<sup>[23a, 24c-f]</sup> It is proposed that it commences by an ill-defined low-valent organometallic cobalt species **31** that undergoes C–H metalation by an oxidative addition, reductive elimination cascade (Scheme 1.5). The following C–Hal or C–O bond cleavage is supposed to occur by a SET type process, which upon radical rebound results in complex **34**. Finally, reductive elimination delivers the alkylated or arylated arenes **27** and transmetalation with a Grignard molecule regenerates the active catalytic species.



**Scheme 1.5:** Proposed catalytic cycle for the cobalt-catalyzed C–H alkylation and arylation.

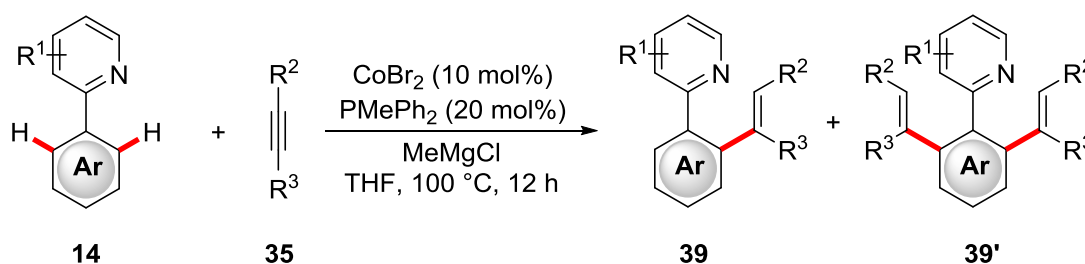
In contrast to the relatively limited examples of arylation and alkylation by low-valent cobalt catalysis, addition reactions of alkynes and alkenes are widely known for a series of different cobalt complexes and became benchmark reactions for novel catalysts.<sup>[23a, 24]</sup> The origin of these hydroarylation reactions can be dated back to Kisch's seminal work on the hydroarylation of tolane (**35a**) with azobenzenes **1** (Scheme 1.6).<sup>[40]</sup> Irrespective of its novelty, the “scope” of two examples and relatively uneconomical reaction conditions limited further applications.



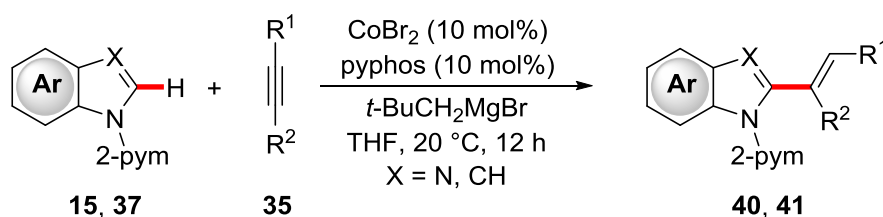
**Scheme 1.6:** First cobalt-catalyzed C–H hydroarylation.

A further achievement in cobalt-catalyzed alkyne hydroarylation was made by Yoshikai and coworkers using the previously described low-valent system based on  $\text{CoBr}_2$ , a phosphine ligand and Grignard reagent.<sup>[41]</sup> With this system, alkenylation of a broad range of arenes and heteroarenes could be made possible, namely aryl pyridines **14** (Scheme 1.7a)<sup>[41c]</sup>, pyri(mi)dyl indoles **15**, benzimidazoles **37** (Scheme 1.7b)<sup>[41a]</sup> and ketimines **18** (Scheme 1.7c),<sup>[41b]</sup> which, upon subsequent hydrolysis, delivered alkenylated ketones **38**.

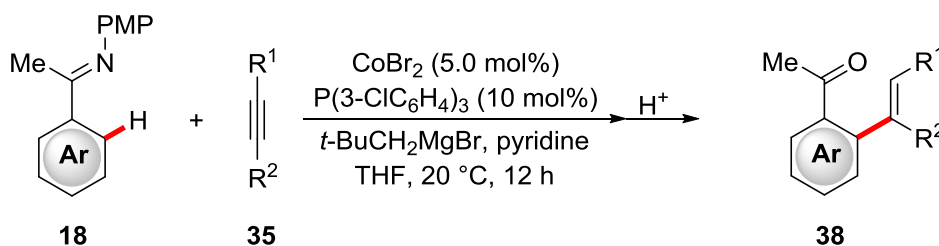
(a) hydroarylation with aryl pyridines **14**:



(b) hydroarylation with pyrimidyl indoles and benzimidazoles **15**, **37**:



(c) hydroarylation with imines **18**:

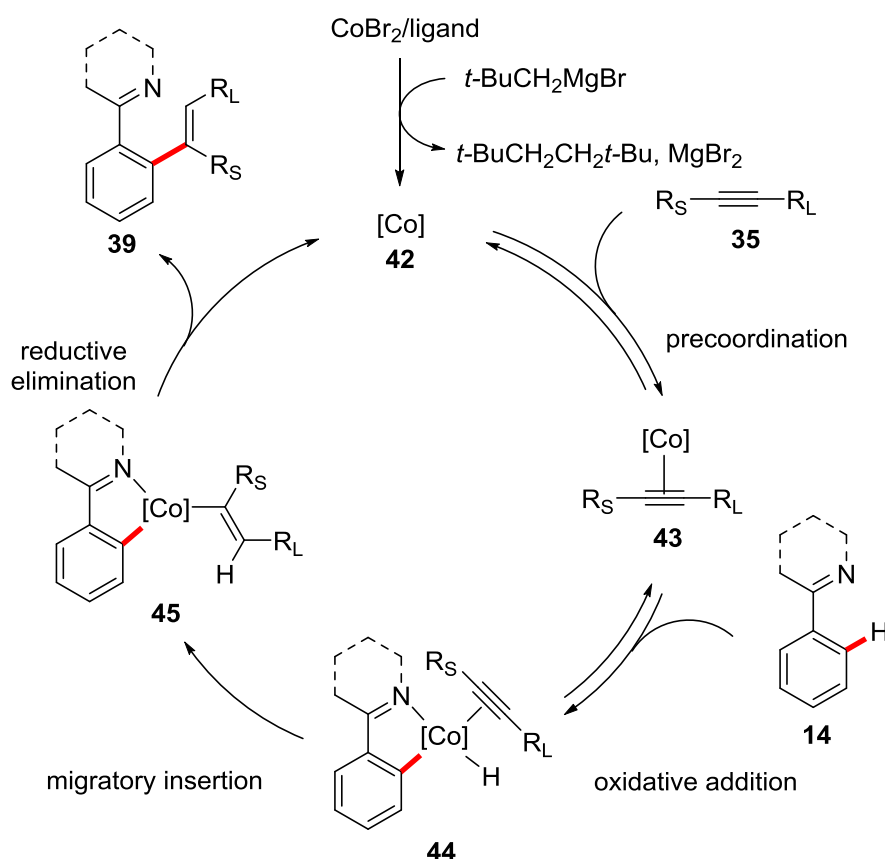


**Scheme 1.7:** Cobalt-catalyzed C–H alkenylation by alkyne hydroarylation.

Beside this *in situ* system with a Grignard reagent, Petit and coworkers succeeded in performing a hydroarylation reaction with a single-component catalyst.<sup>[42]</sup> They enabled the hydroarylation of alkynes **35** with ketimines **18** affording the alkenylated arenes with *Z* configuration.

The mechanism of the above mentioned examples commences in the same way as for the alkylation and arylation reaction, with an oxidative addition of the *in situ* generated

cobalt catalyst into the C–H bond forming complex **44** (Scheme 1.8).<sup>[41]</sup> For this reaction, alkyne coordination is assumed prior to the C–H activation step. Instead of reductive elimination, a 1,2-migratory insertion of the alkyne into the C–H bond is supposed to occur and finally reductive elimination from **45** delivers the reaction product and regenerates the active catalyst.



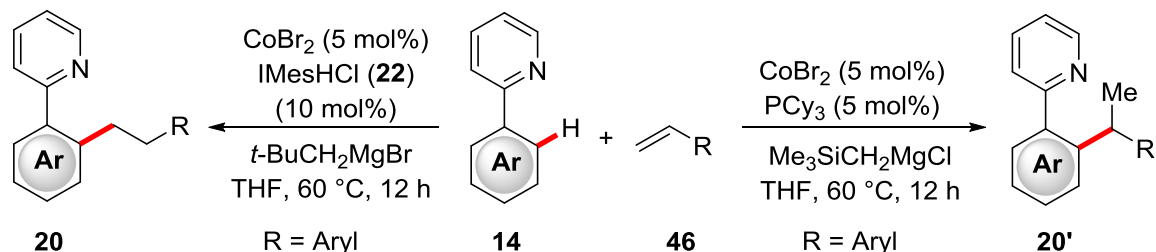
**Scheme 1.8:** Proposed catalytic cycle for the cobalt-catalyzed alkyne hydroarylation.

Limitations of these methods were found, when alkynes with similar  $\text{R}_\text{S}$  and  $\text{R}_\text{L}$  rests were employed, resulting in difficult to separate mixtures of regioisomers.

Apart from hydroarylation of alkynes, Nakamura<sup>[43]</sup> and Yoshikai<sup>[44]</sup> also enabled the successful addition of benzamides and amines to alkenes, giving access to alkylated arenes with solely *anti*-Markovnikov selectivity. The control of selectivity is arguably one of the greatest challenges in alkene addition reactions. An elegant solution for full control in selectivity was presented by Yoshikai and coworkers with two different catalytic systems allowing for the Markovnikov and *anti*-Markovnikov-selective alkene hydroarylation (Scheme 1.9).<sup>[45]</sup> With an oxidative addition/alkene insertion/reductive elimination manifold proposed, the authors assume the last step to be turnover-limiting as well regioselectivity-determining. The key to selectivity was the crucial choice of the NHC and phosphine ligand. While the bulky IMesHCl (**22**) favors the linear addition of



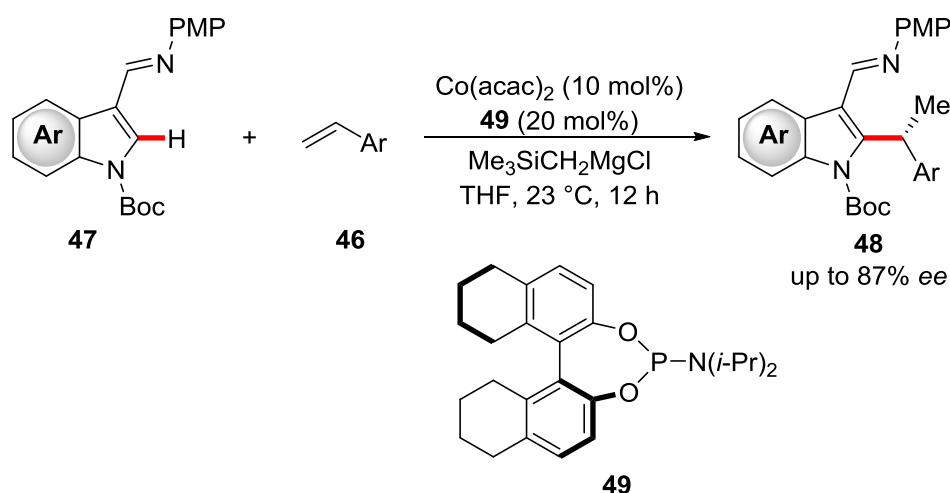
the alkene **46**, the phosphine ligand facilitates the branched insertion as a more stabilized benzylic cobalt species is formed.<sup>[46]</sup> Despite these highly selective catalytic systems, the employed alkenes are mostly restricted to styrenes and a substrate dependence on the selectivity must be conceded.<sup>[45]</sup>



**Scheme 1.9:** Linear- and branched-selective alkene hydroarylation by cobalt catalysis.

Recently, Ackermann and coworkers presented a cobalt(III)-catalyzed alkene hydroarylation that allowed for non-activated alkenes (*vide infra*).<sup>[47]</sup> In another update, the group of Yoshikai improved the Markovnikov-selective styrene hydroarylation by replacing the harsh Grignard reagent by magnesium turnings in sub-stoichiometric amounts of 50 mol%.<sup>[48]</sup> In light of this improvement, a significantly higher functional group tolerance was not reached.

Beside the control of Markovnikov-selective hydroarylations, an enantioselective approach to these chiral compounds represents an even greater challenge. Indeed, the Yoshikai group also established a highly side-selective and enantioselective alkene hydroarylation reaction using *N*-Boc-protected indoles **47** (Scheme 1.10), representing the first enantioselective cobalt-catalyzed C–H activation.<sup>[49]</sup> Among several tested chiral phosphines, phosphoramidate **49** was the best compromise between yield and enantioselectivity. In general, the reaction provides good stereoselectivities for a broad range of styrenes. It should be noted, that the Boc-protecting group remained crucial, as tosyl, benzyl, phenyl and carbamyl groups led to a significant drop in yield and enantioselectivity.

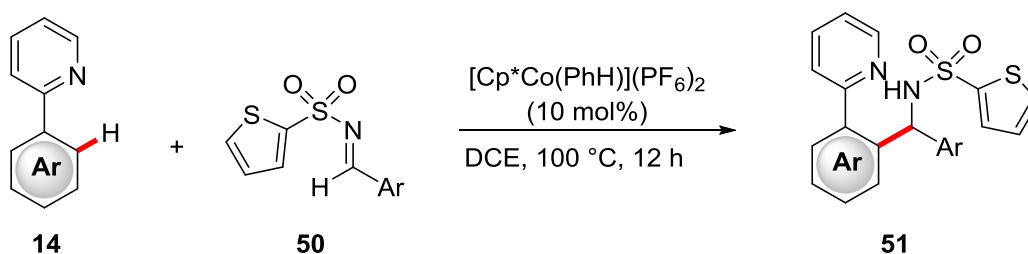


**Scheme 1.10:** Cobalt-catalyzed enantioselective alkene hydroarylation.

### 1.2.2 C–H Activation by $\text{Cp}^*\text{Co(III)}$ Catalysis

In view of the above described transformations, these low-valent cobalt catalysts are doubtlessly a milestone in cobalt-catalyzed C–H activation. The variety of reactions and the mostly mild reaction temperatures are beyond the scope for any other 3d transition metal. However, the omnipresent Grignard reagent limits its potential for future applications. And even the few reactions without Grignard reagent could not afford a higher functional group tolerance.

Therefore, a demand for robust and stable cobalt catalysts that allow for multiple transformations under mild reaction conditions was noted. A pathbreaking step towards this demand was achieved by Matsunaga/Kanai by establishing  $\text{Cp}^*\text{Co(III)}$ <sup>[50]</sup> complexes for cobalt-catalyzed C–H functionalizations. In their first findings, they disclosed the addition of imines **50** to aryl pyridines<sup>[51]</sup> **14** (Scheme 1.11) and with slight modifications also of pyrimidyl indoles<sup>[52]</sup> **15** and with enones.<sup>[51]</sup>

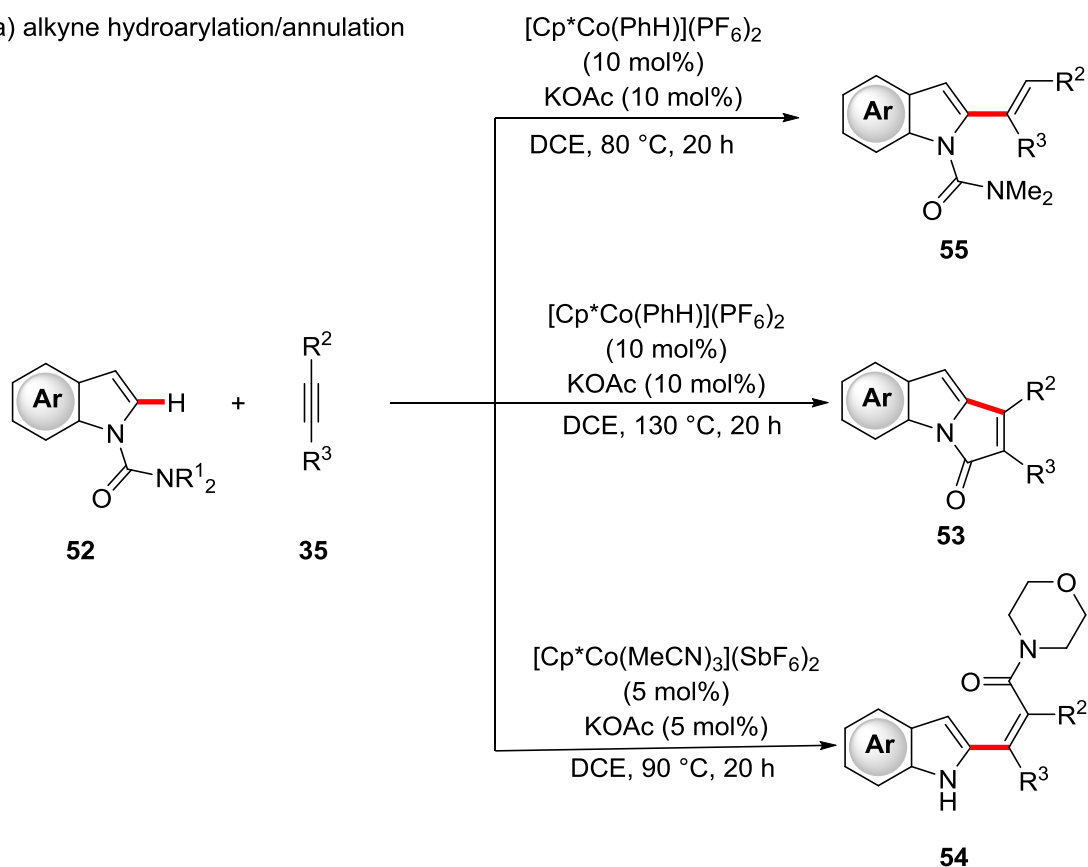


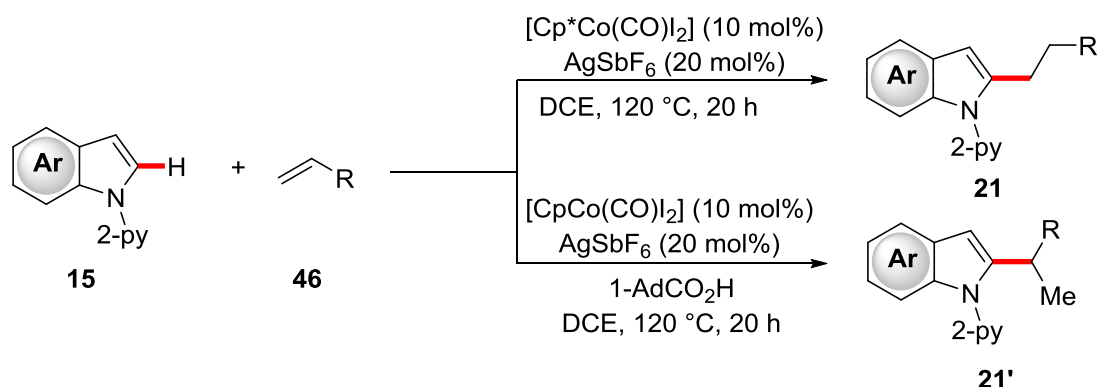
**Scheme 1.11:** Hydroarylation of imines by cobalt(III) catalysis.

These addition reactions were not limited to double bonds, but could also be realized with alkynes, as the benchmark reaction for novel cobalt catalysts. The cobalt sandwich complex  $[\text{Cp}^*\text{Co}(\text{PhH})](\text{PF}_6)_2$  proved to be active for the alkyne hydroarylation with 2-carbamoyl indoles **52** (Scheme 1.12a).<sup>[53]</sup> In fact, related reactions yielding alkenylated

indoles have been published before by rhodium(III) catalysis<sup>[54]</sup> and bear the same limitations, i.e. that the regioselectivity is determined by the steric properties of the alkyne, but the cobalt-catalyzed variant goes beyond alkenylation. After the C–H metalation and alkyne insertion, the formed cobalt–carbon bond is more polarized than the related rhodium–carbon bond, due to its lower electronegativity.<sup>[55]</sup> Dependent on the rest R on the carbamate, the more nucleophilic carbon-atom can perform a nucleophilic substitution and  $\beta$ -nitrogen elimination releases the annulated product **53**,<sup>[53]</sup> or the  $\alpha,\beta$ -unsaturated amide **54**, as recently reported.<sup>[56]</sup> This selectivity control is not just attributed to alkyne additions. In a recent report, Ackermann and coworkers demonstrated the selective and controllable Markovnikov/*anti*-Markovnikov Addition of alkenes **46** (Scheme 1.12b).<sup>[19a]</sup> The bulky carboxylic acid 1-AdCO<sub>2</sub>H was the crucial additive whose presence enabled the Markovnikov-selective hydroarylation while the linear product is obtained without. Detailed mechanistic studies provided evidence for a switch in the C–H activation mode. Thus, linear selectivity follow a ligand-to-ligand hydrogen transfer (LLHT)<sup>[57]</sup> while branched selectivity is the consequence of a base-assisted internal electrophilic substitution (BIES).<sup>[19]</sup>

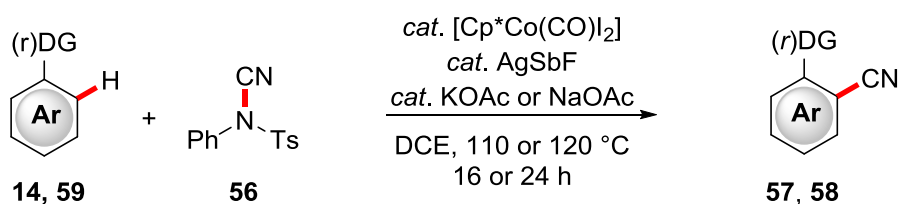
(a) alkyne hydroarylation/annulation



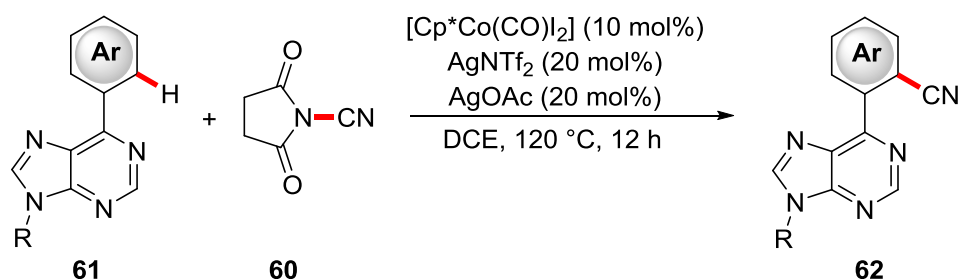
(b) Markovnikov/*anti*-Markovnikov alkene hydroarylation**Scheme 1.12:** Control of region-selectivity in cobalt(III)-catalyzed C–H functionalizations.

The continuous success of the Cp\*Co(III)-catalyzed C–H functionalizations goes beyond addition reactions. Beginning in 2014, substitution reactions with organic electrophiles were reported with the installation of valuable functional groups. In parallel works, the groups of Ackermann<sup>[58]</sup> and Glorius<sup>[59]</sup> independently developed a cobalt-catalyzed C–H cyanation with *N*-cyano-*N*-phenyl-*p*-toluenesulfonamide (NCTS, **56**) as cyanide source (Scheme 1.13a). The reaction delivers aryl nitriles **57**, **58** selectively for aryl pyri(mi)dines **14** and pyrazoles **59**. Both systems are comparable, with a catalyst loading of 10 mol% for the Glorius system,<sup>[59]</sup> compared to 2.5 mol% for the system of Ackermann.<sup>[58]</sup> In a follow-up work, Chang and coworkers made use of *N*-cyanosuccinimide (**60**) as an also easily preparable and storable cyanide source (Scheme 1.13b).<sup>[60]</sup> Beside the above mentioned arenes, they succeeded in the C–H cyanation of important 6-aryl purines **61** in good yields. However, this system required two costly silver salts as additives.

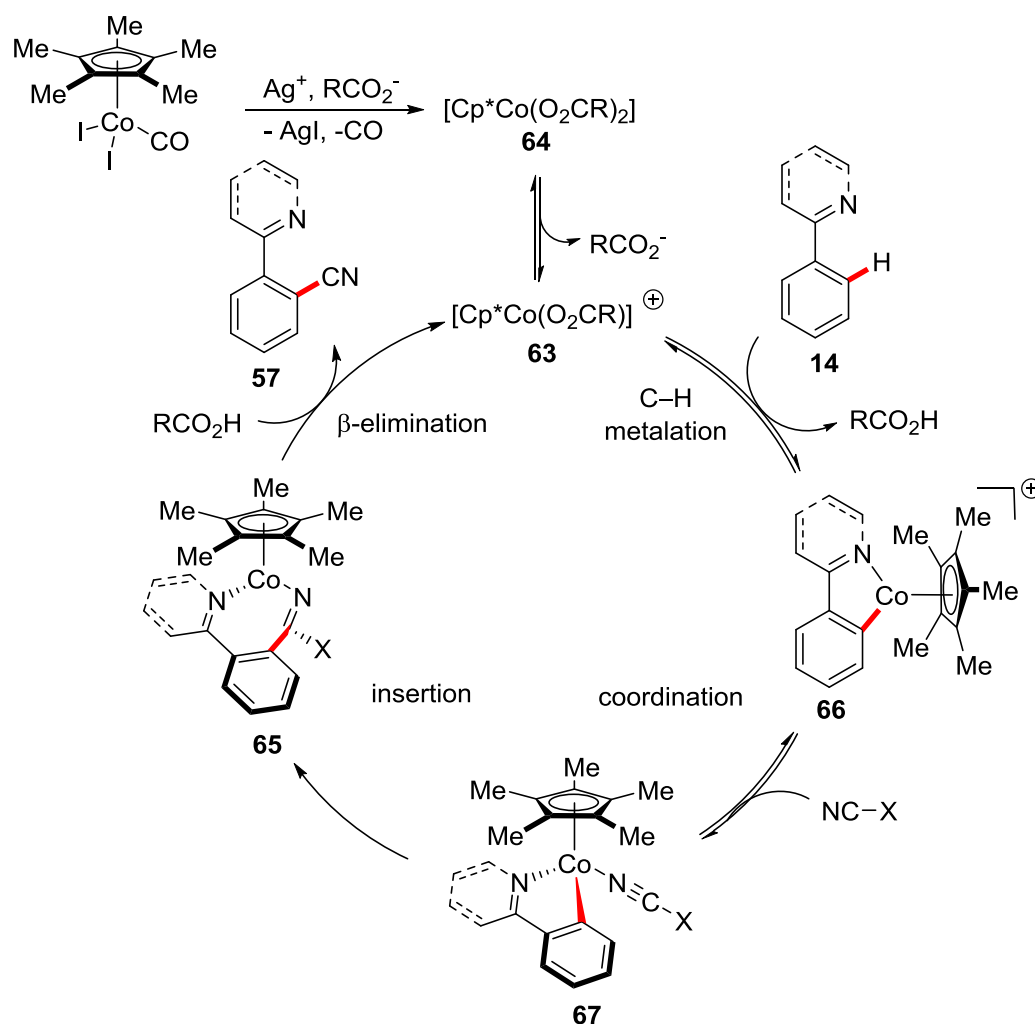
(a) Ackermann, Glorius (2014)



(b) Chang (2015)

**Scheme 1.13:** Cobalt(III)-catalyzed cyanation of (hetero)arenes.

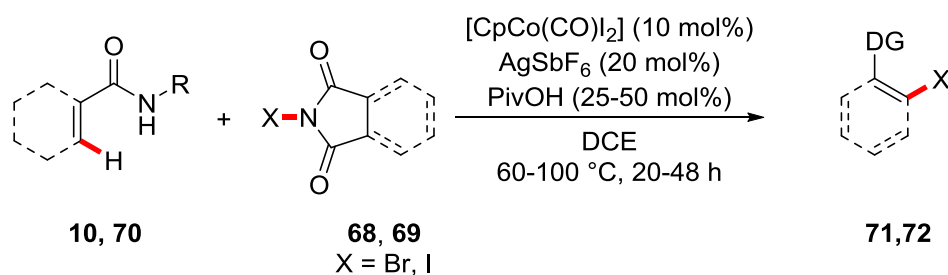
The catalytic cycle for the cobalt(III)-catalyzed cyanation<sup>[58-60]</sup> is exemplary for many cobalt(III)-catalyzed transformations (Scheme 1.14). It is initiated by the generation of a cationic 16 VE cobalt species **63**. If [Cp\*Co(CO)I<sub>2</sub>] is the precatalyst, the species is delivered through halide abstraction by a silver salt, CO dissociation and acetate coordination in an equilibrium with resting state **64**. This active catalyst **63** undergoes reversible C–H metalation which is supposed to proceed *via* a CMD/AMLA<sup>[17, 61]</sup> or BIES<sup>[19]</sup> type process. In the next step,<sup>[58-60]</sup> the electrophile coordinates to the cobalt, followed by a migratory insertion from the multiple bond into the Co–C bond. Then, the seven-membered cycle **65** is formed and β-elimination takes place which releases the product **57** and regenerates the catalyst **63**.



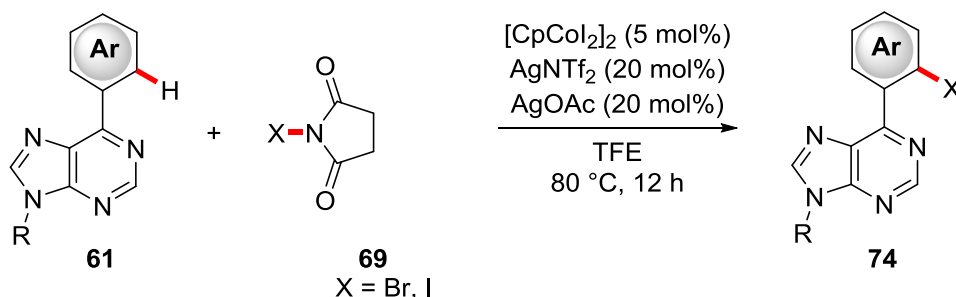
**Scheme 1.14:** Proposed catalytic cycle for the cobalt-catalyzed cyanation.

As the cyano group is a pseudo-halide, a related halogenation reaction went to the focus of many researchers. In 2014, the Glorius group thus reported about the cobalt(III)-catalyzed bromination and iodination with *N*-bromophthalamide (NBP, **68**) and *N*-iodosuccinimide (NIS, **69a**) as halogen sources (Scheme 1.15a).<sup>[59]</sup> The reaction conditions are comparable to the cyanation and the system turned out to be useful for aryl pyridines **14**, acrylamides **70**, as well as benzamides **10**, delivering their (*Z*)-3-halo acrylamides **71**, 2-halo benzamides **72** and ortho-halogenated aryl pyridines **73**. Recently, Pawar discovered a related cobalt-catalyzed halogenation of 6-aryl purines **61** with *N*-iodosuccinimide (NIS) or *N*-bromosuccinimide (NBS, **69b**) (Scheme 1.15b).<sup>[62]</sup> This system offers many similarities to the cyanation protocol of Chang,<sup>[60]</sup> along with the drawback to require two additional silver salts.

(a) Glorius (2014)



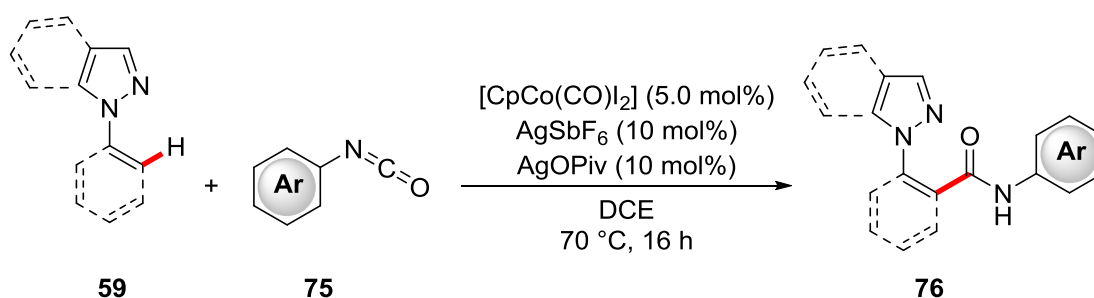
(b) Pawar (2016)

**Scheme 1.15:** Cobalt(III)-catalyzed halogenations.

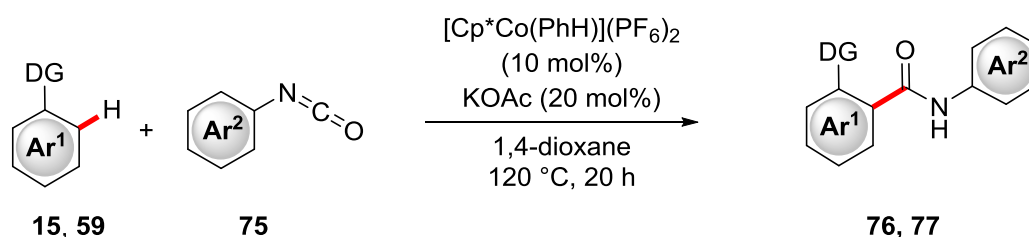
The mechanism for these halogenations<sup>[59, 62]</sup> proceeds in a similar way as for the C–H cyanation, except that a nucleophilic attack and ligand exchange takes place instead of an insertion/elimination manifold.

Besides (pseudo)halides, the versatile cobalt(III) catalysis could also be applied to the addition of isocyanate yielding aromatic amides. As these reactions were dominated by 4d and 5d transition metal catalysts,<sup>[63]</sup> Ackermann and coworkers presented the first cobalt-catalyzed reaction of this kind for the aminocarbonylation of aryl pyrazoles and indazoles **59** with isocyanates **75** as well as acyl azides (Scheme 1.16a).<sup>[64]</sup> In a subsequent work, Ellman and coworkers established a similar system by using the sandwich complex  $[\text{Cp}^*\text{Co}(\text{PhH})](\text{PF}_6)_2$  and KOAc as the additive.<sup>[65]</sup> In contrast to the system of Ackermann, this reaction does not require silver salts as additives, though the reactions are conducted at elevated temperature.

(a) Ackermann (2015)



(b) Ellman (2015)

**Scheme 1.16:** Cobalt(III)-catalyzed aminocarbonylation.

Competition experiments revealed electron-rich arenes and electron-deficient isocyanates to react fastest, rendering a migratory insertion to be rate-determining.<sup>[64]</sup>

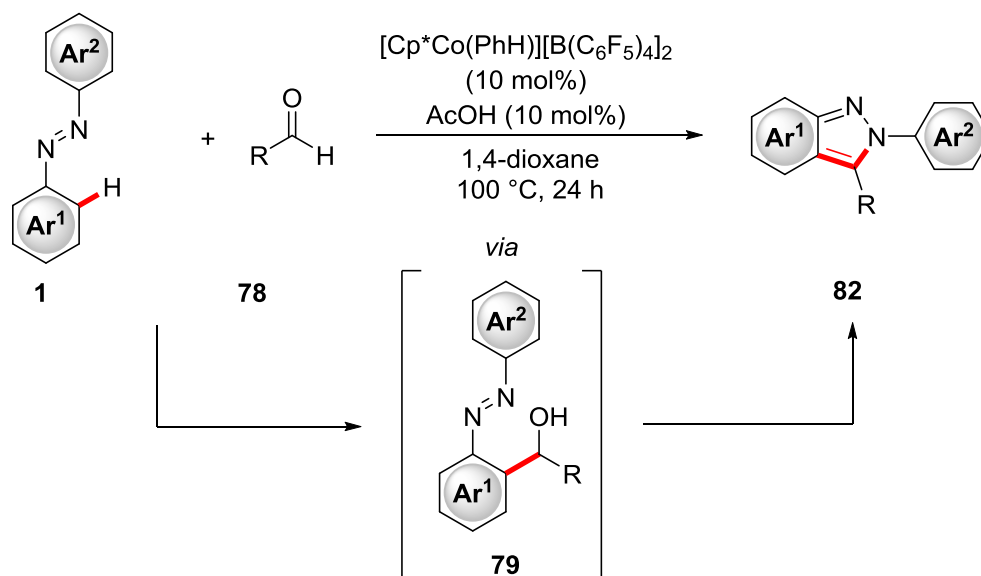
En route to sustainable synthesis, modern techniques should not only comprise the functionalization of (hetero)arenes, but also the *de-novo* synthesis of heterocycles, the role of which in pharmaceutical chemistry and material science is particularly high.<sup>[66]</sup> Within the various methods for the construction of heterocycles, C–H functionalizations became a promising alternative to traditional methods.<sup>[67]</sup> Many of these methods can be considered as domino reactions<sup>[68]</sup>, consisting of a C–H functionalization followed by cyclization.<sup>[67]</sup> Within this strategy, cobalt can play a key role. Its lower electronegativity compared to other group 9 elements<sup>[55]</sup> results in a more nucleophilic organometallic species which may undergo novel and unprecedented cyclizations. This concept was elegantly exploited by Ellman and coworkers within their indazole synthesis from azobenzenes **1** and aldehydes **78** (Scheme 1.17a).<sup>[69]</sup> This reactions proceeded *via* an addition reaction of aldehydes generating alcohol **79**. Under the present conditions, this alcohol undergoes an intramolecular substitution reaction in a dehydrative fashion what the authors described as cyclative capture. Mechanistic studies resulted in a reversible alcohol formation which is also an early example of a cobalt-catalyzed C–C functionalization.

In the same contribution, this method was also applied to the synthesis of furans from  $\alpha,\beta$ -unsaturated oximes **80** (Scheme 1.17b). Under the reaction conditions, the *in situ*

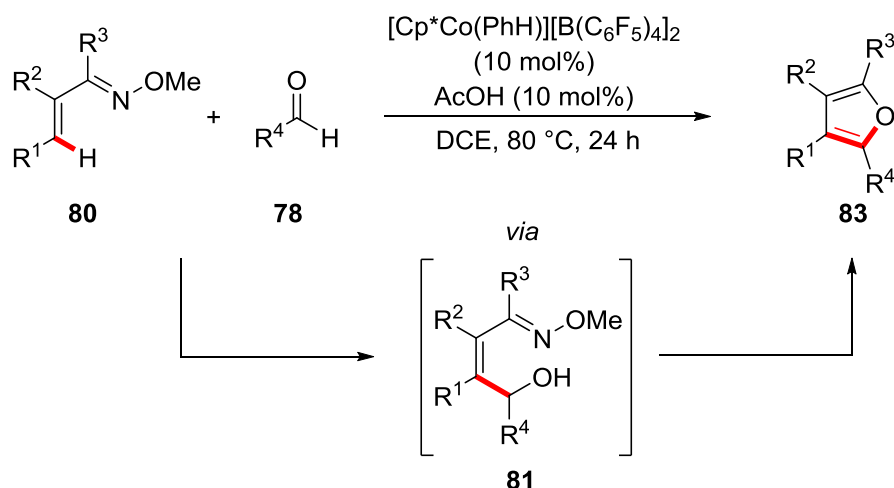


formed alcohol **81** attacks the carbon on the oxime which yields the furan by release of methoxyamine. Another highlight of the reaction is the single-component catalyst  $[\text{Cp}^*\text{Co}(\text{PhH})][\text{B}(\text{C}_6\text{F}_5)_4]_2$ . By the use of this sandwich complex, just 10 mol% of acetic acid as additive were required. Instead, when using the often employed complex  $[\text{Cp}^*\text{Co}(\text{CO})\text{I}_2]$ , two additional silver salts were necessary to obtain comparable results. It should be noted that cobalt-catalyzed reactions resulted in higher yields than a related reaction under rhodium(III) catalysis.<sup>[70]</sup>

(a) indazole synthesis



(b) furan synthesis

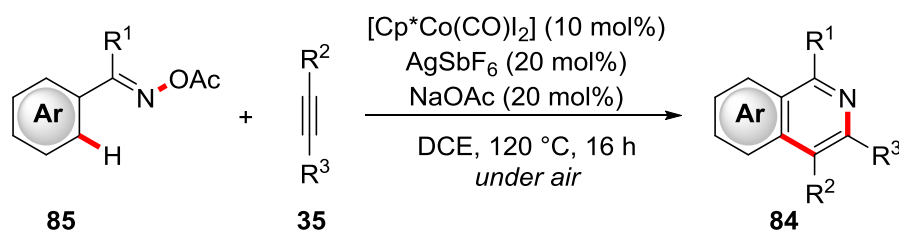


**Scheme 1.17:** Cobalt(III)-catalyzed indazole and furan synthesis by addition/annulation pathway.

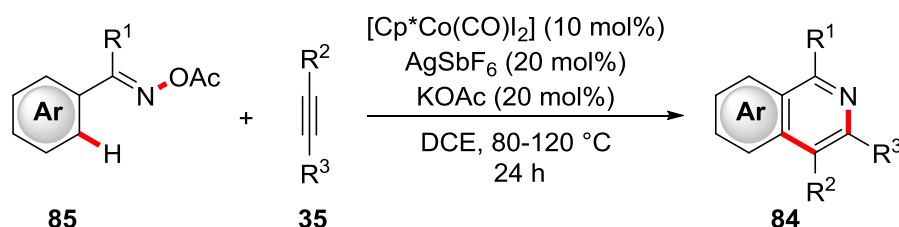
The reaction manifold of C–H/N–O functionalization could also be applied to the synthesis of isoquinolines **84** by cobalt catalysis that was independently disclosed by

Ackermann, Matsunaga/Kanai and Sundararaju (Scheme 1.18). In the Ackermann reaction,<sup>[71]</sup> a catalytic system with  $[\text{Cp}^*\text{Co}(\text{CO})\text{I}_2]$ ,  $\text{AgSbF}_6$  and  $\text{NaOAc}$  enabled the synthesis from *O*-acyl-oximes **85** and alkynes **35** even when performed under air (Scheme 1.18a), whereas Matsunaga/Kanai used an atmosphere of  $\text{N}_2$  (Scheme 1.18b).<sup>[72]</sup> In contrast, the system of Sundararaju offers certain differences (Scheme 1.18c).<sup>[73]</sup> The group employed unsubstituted oximes **86** instead of *O*-acyl ones and their reaction proceeded also in the absence of a silver salt. However, the costly TFE had to be employed as the solvent.<sup>[74]</sup> In these reactions, the unique role of cobalt becomes striking. Similar reaction have been reported by Chiba and Zhao/Jia/Li using rhodium(III) complexes, but their systems are limited to internal alkynes and face regioselectivity problems.<sup>[75]</sup>

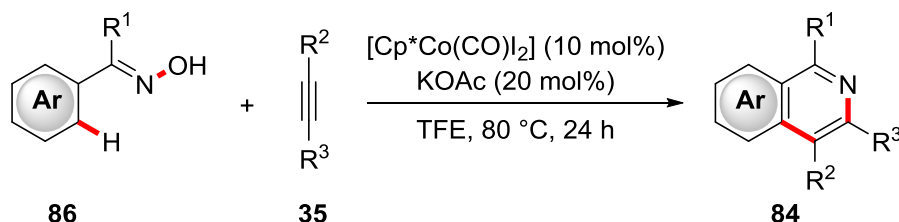
(a) Ackermann (2015)



(b) Matsunaga/Kanai (2015)



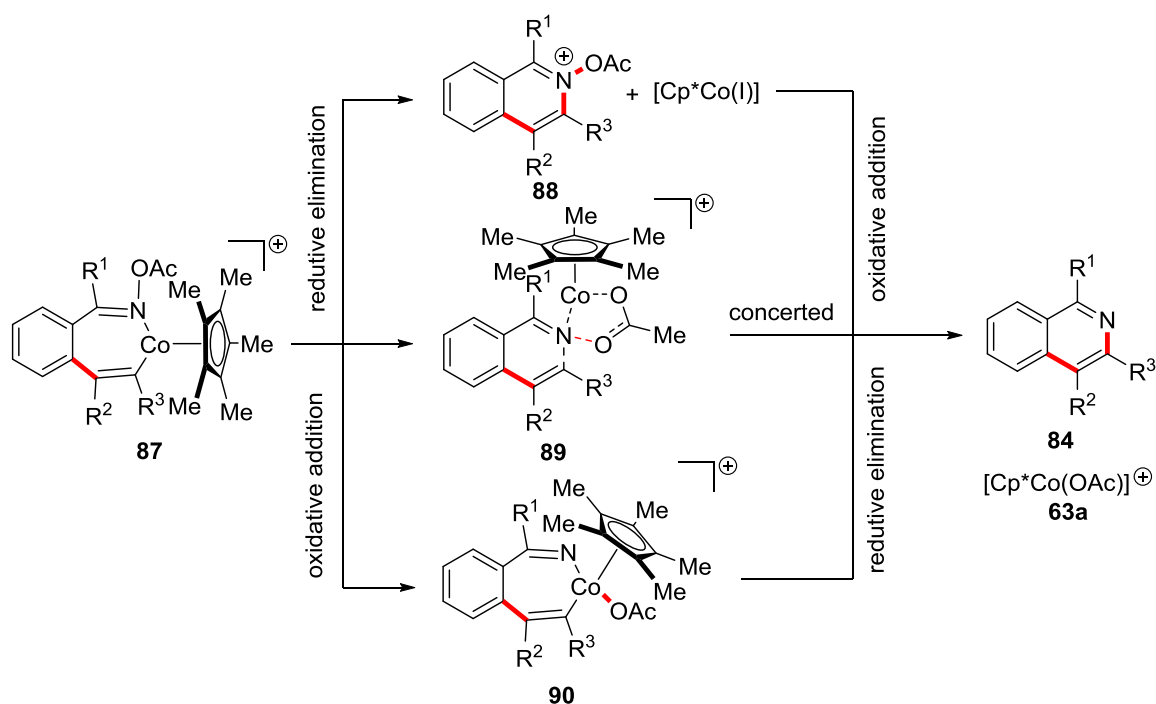
(c) Sundararaju (2015)



**Scheme 1.18:** Isoquinoline synthesis by cobalt(III)-catalyzed C–H/N–O activation.

The mechanism of this isoquinoline synthesis starts with a reversible C–H cobaltation, followed by alkyne insertion leading to intermediate **87** (Scheme 1.19).<sup>[71-73]</sup> The following N–O cleavage and C–N formation are not completely understood, but three general pathways are taken into consideration. These mechanisms are *i*) reductive elimination,

providing the isoquinolinium acetate **88** and a cobalt(I) species, followed by oxidative addition to yield the product and the cobalt(III) catalysts, *ii*) a concerted acetate transfer, presumably by keeping a cobalt(III) species and *iii*) *visé versa* to *i*), an oxidative addition from the cobalt centre into the N–O bond giving a high-valent cobalt(V) species which upon reductive elimination results in the product and the cobalt(III) catalyst. Matsunaga/Kanai proposed all three pathways as possible,<sup>[72]</sup> whereas Ackermann assumed a concerted acetate transfer.<sup>[71]</sup> In contrast, Sundararaju postulated a reductive elimination/oxidative addition pathway.<sup>[73]</sup>



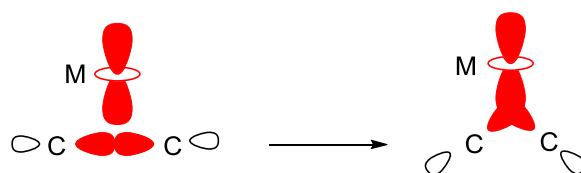
**Scheme 1.19:** Possible reaction pathways for C–N forming and N–O cleavage.

### 1.3 Transition Metal-Catalyzed C–C Functionalizations

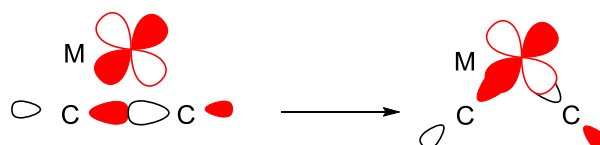
The last decades established the field of C–H activation as one of the most important and investigated research areas.<sup>[14]</sup> In contrast, the selective functionalization of omnipresent C–C bond remained limited.<sup>[76]</sup> This lack in scientific contributions mainly originates from the intrinsic difficulties in activating C–C bonds versus other  $\sigma$ -bonds in terms of thermodynamics and kinetics. Concerning thermodynamics, the relatively high bond dissociation energy of roughly 375 kJ/mol<sup>[77]</sup> renders this bond quite stable and even more, most C–C functionalizations end up with another C–C bond formation with almost identical energies of product and starting material. The biggest challenge, however, is to overcome the energetic barrier from the C–C to M–C bond upon activation. These M–C bond energies are in a range of 120–170 kJ/mol (for M = Pd)<sup>[77]</sup> offering a significant energy gap.

Moreover, also kinetical aspects render this reaction challenging. A simplified model of the metal-carbon interactions is depicted in Scheme 1.20 and involves overlaps of the  $d_z^2$  orbital of the metal with the bonding  $\sigma$ -C-C orbital (Scheme 1.20a), and of the  $d_{xz}$  or  $d_{yz}$  metal-orbital with the antibonding  $\sigma^*$ -C-C orbital (Scheme 1.20b).<sup>[76b]</sup> The constrained nature of the  $\sigma$ -orbitals along the bond axis hinders a broad overlap with the metal orbital and lowers the resonance integral. This effect is further amplified by the large energy difference between the  $\sigma$  and  $\sigma^*$  and the ones of the metal d-orbitals. Overcoming these effects by applying more forcing conditions may end up in side reaction due to orbital interactions with other functional groups.

(a) C-C bonding orbital with  $d_z^2$  metal orbital



(b) C-C anti-bonding orbital with  $d_{xz}$  or  $d_{yz}$  metal orbital



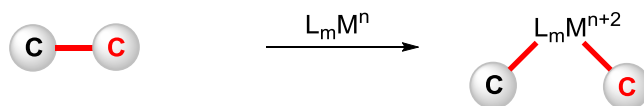
**Scheme 1.20:** Insertion scenarios of  $\sigma$ -C-C bonds with transition metals.

A last effect can also be contributed to steric reasons. In contrast to C-H or C-Hal bonds, carbons are usually not terminal atoms and the more shielded C-C bond affords more steric hindrance for the metal.

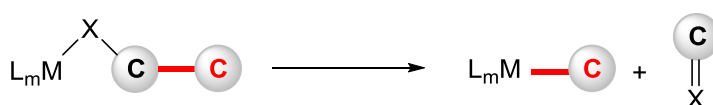
Despite all these intrinsic difficulties, the C-C functionalization did not rest as an unsolved challenge. Indeed, a manageable, but increasing amount of methodologies exists and further increases.<sup>[76a, 76b, 76d-k]</sup> The biggest challenge is arguably the activation step of the C-C bond. Today, this *modus operandi* is explained by three different pathways (Scheme 1.21), which are *i*) oxidative addition, *ii*)  $\beta$ -carbon elimination and *iii*) retro-allylation. Related to C-H activation and cross-coupling chemistry, the oxidative addition (Scheme 1.21a) requires an electron-rich transition metal in a low oxidation state, mostly rhodium(I), nickel(0) and palladium(0).<sup>[76a, 76b, 76d, 76f, 76g, 76i, 76k]</sup> This pathway is often observed for the opening of strained rings, but can also proceed in non-strained systems. The  $\beta$ -carbon elimination is analogous to the  $\beta$ -hydride elimination (Scheme 1.21b). After binding to the substrate, the carbon cleavage is facilitated through the

formation of a strong C=X bond.<sup>[76b, 76g, 76h, 76j]</sup> The third pathway, the retro-allylation, is much rarer reported than the two other methods (Scheme 1.21c). It takes place when the metal binds to a homoallylic compound and proceeds *via* a 6-membered transition state by also creating a C=X bond.<sup>[76g, 78]</sup>

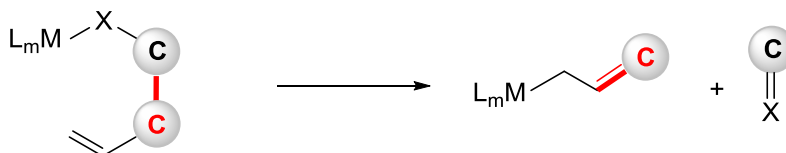
(a) oxidative addition



(b)  $\beta$ -carbon elimination



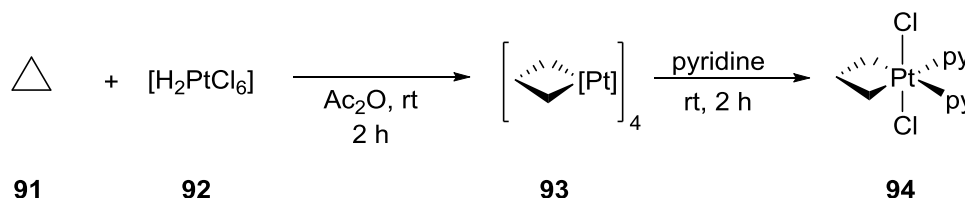
(c) retro-allylation



**Scheme 1.21:** Modes for transition metal-catalyzed C–C bond activation.

### 1.3.1 Functionalization of Strained Substrates

The beginning of C–C bond cleavage by metalation dates back to 1955 when Tipper reacted cyclopropane (**91**) with “PtCl<sub>2</sub>” and succeeded in a ring opening by an oxidative addition (Scheme 1.22).<sup>[79]</sup> Later, Chatt<sup>[80]</sup> and Bailey<sup>[81]</sup> corrected that not PtCl<sub>2</sub>, but [H<sub>2</sub>PtCl<sub>6</sub>] (**92**) is the active species performing an oxidative addition to a platinum(VI) compound.<sup>[82]</sup> This complex **93** was found to be a platinum-tetramer and a monomeric platinum(IV) complex **94** is yielded when treating with pyridine.



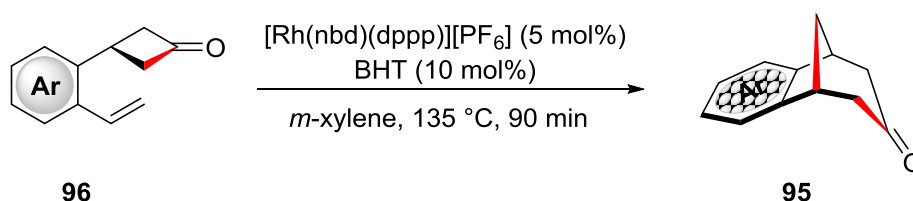
**Scheme 1.22:** Stoichiometric C–C cleavage by oxidative addition of Pt with cyclopropane (**91**).

The oxidative addition was enabled by the release of ring strain of the cyclopropane which is assigned as 121 kJ/mol.<sup>[83]</sup> Using the release of ring strain energy became a role model for a number of C–C functionalizations of strained molecules.<sup>[76a, 76d, 76g]</sup>

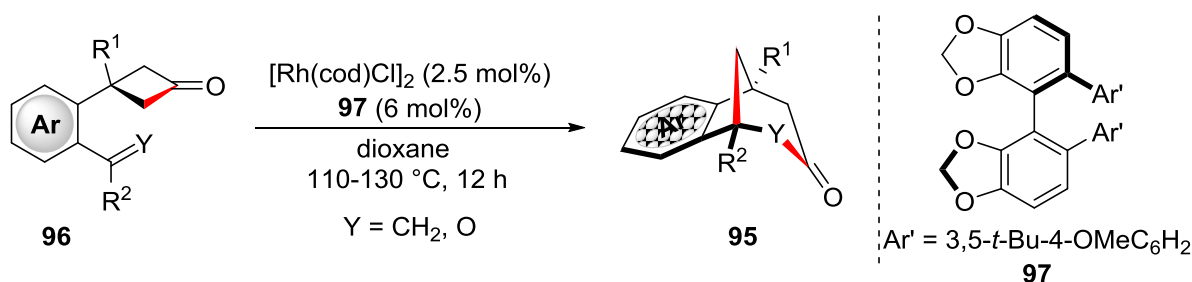
Beyond the simple cyclometalation, the bond cleavage was coupled with other metal-organic transformations, in many cases insertion reactions into the M–C bond.

In seminal studies, Murakami and coworkers demonstrated that rhodium(I) complexes can undergo oxidative addition into the C–C(O) bond of cyclobutanones.<sup>[84]</sup> With this knowledge they made use of the oxidative addition/insertion scaffold within the synthesis of benzobicyclo[3.2.1]octenone (**95**) from 3-(2-vinylphenyl)cyclobutanone (**96**) (Scheme 1.23a).<sup>[85]</sup> For this synthesis, the type of phosphorous ligand was of crucial importance. While dppp gave best results, dppb resulted in undesired decarbonylation. In contrast, a smaller cone angle in dppe afforded  $\beta$ -hydride elimination after oxidative addition (Scheme 1.24). Later on, the group of Cramer enabled an enantioselective version using a chiral ligand **97** (Scheme 1.23b).<sup>[86]</sup> In the same year, the group applied this reaction to a migration reaction of aldehydes, also in an enantioselective fashion.<sup>[87]</sup>

(a) Murakami (2002)



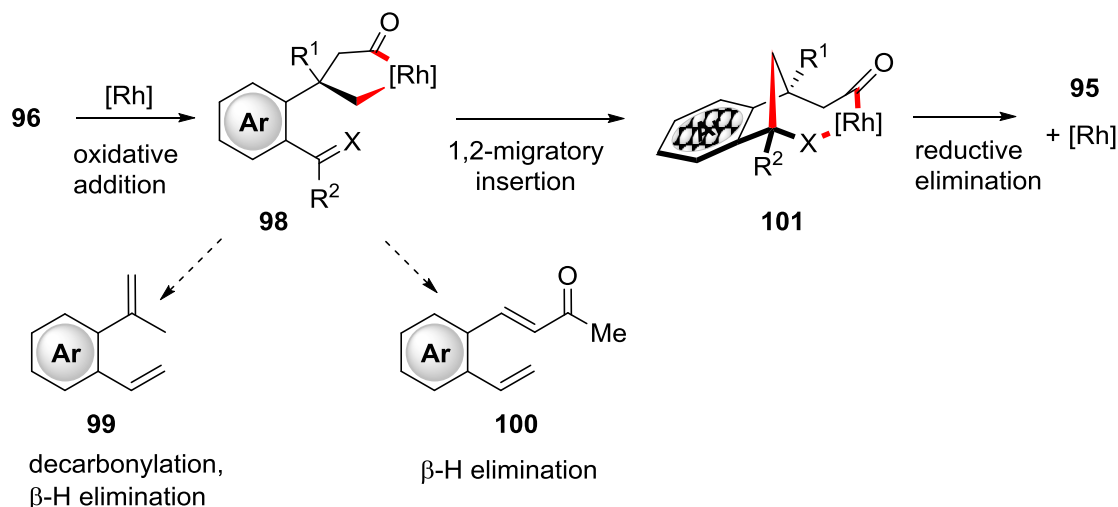
(b) Cramer (2014)



**Scheme 1.23:** Rhodium-catalyzed bicycle synthesis by C–C functionalizations of cyclobutanone.

The mechanisms of these reactions start with a C–C(O) bond activation by oxidative addition (Scheme 1.24). This is followed by a migratory insertion of the vinylic double bond or carbonyl function selectively into the Rh–C(sp<sup>3</sup>) bond and reductive elimination finally delivers the product. As mentioned above, the choice of ligand was of major importance.<sup>[85]</sup> Alternatively, decarbonylation from the rhodacycle **98** and  $\beta$ -hydride

elimination gave 1-(prop-1-en-2-yl)-2-vinylbenzene (**99**), whereas  $\beta$ -hydride elimination from **98** resulted in the ketone **100**.

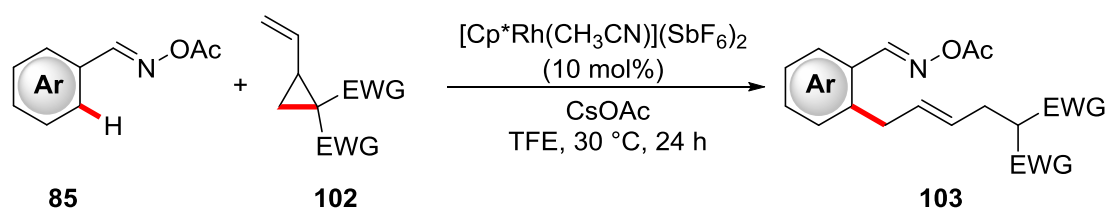


**Scheme 1.24:** Postulated mechanism for C–C functionalization of cyclobutanones.

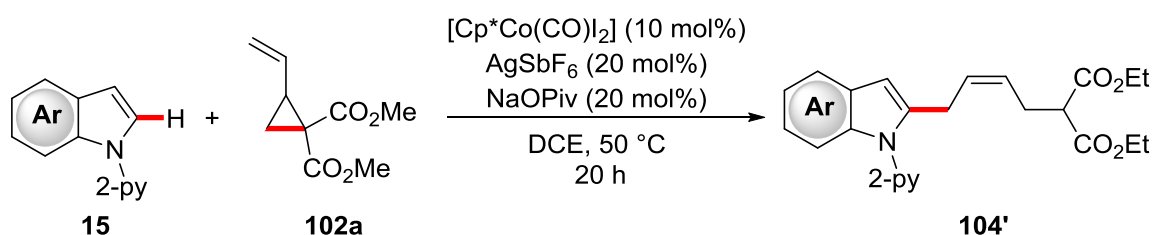
Another promising approach towards sustainable synthesis is to combine C–C with C–H activation as the most abundant bonds in organic molecules. Pioneering works of Fürstner and Aissa reported a C–H activation of aldehydes coupled with C–C ring opening of alkenylidene cyclopropanes,<sup>[88]</sup> which could also be performed in an enantioselective reaction.<sup>[89]</sup> Later, Huang/Li/Wang established a C–H/C–C cascade with vinyl cyclopropanes **102** (Scheme 1.25a).<sup>[90]</sup> Their method allowed for the preparation of allylated nitrones **103**, benzamides **104** and indoles **105**. However, this reaction as well as the pioneering works required precious rhodium catalysts.

That was changed by a work of Ackermann and coworkers in 2016.<sup>[91]</sup> The group successfully applied inexpensive cobalt(III) catalysis (Section 1.2.2) for the cyclopropane addition (Scheme 1.25b). The reaction coruscates with a broad functional group tolerance and gave access to allylated indoles **105'**, but also aryl pyridines **106'** and pyrazoles **107'**. Its highlight, however, is the formation of the thermodynamically less stable (*Z*)-isomer which is unknown for this type of reaction. This is explained by a shorter C–Co distance and a more compact organometallic species. In a recent work, the group presented a manganese-catalyzed variant of this reaction (Scheme 1.25c).<sup>[92]</sup> Though it required a higher reaction temperature, it offered a remarkable functional group tolerance that even allowed for the C–H allylation of tryptophanes. Here, the double bond configuration was found to be *E*, which was attributed to dispersion interactions.

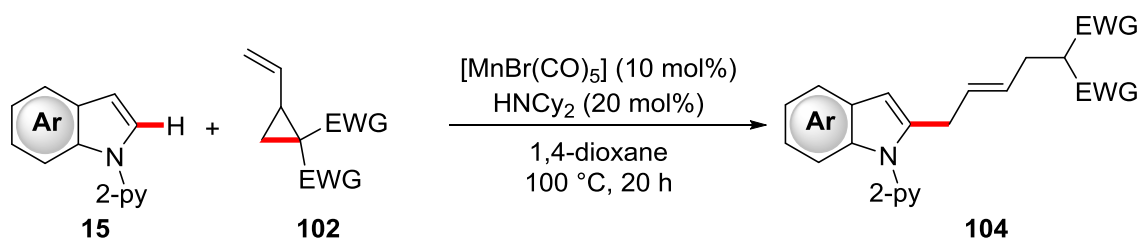
(a) Huang/Li/Wang (2015)



(b) Ackermann (2016)



(c) Ackermann (2017)

**Scheme 1.25:** Combined C-H/C-C functionalizations with vinyl cyclopropanes.

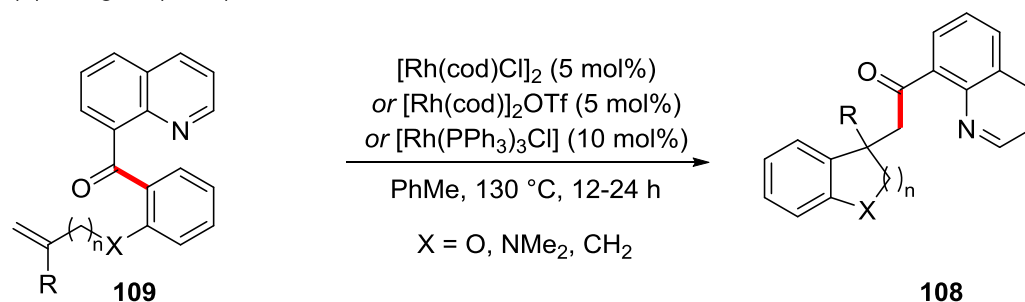
These reactions are supposed to commence by a reversible cyclometalation, followed by double bond insertion. Then, the C-C bond gets cleaved by  $\beta$ -carbon elimination.

### 1.3.2 Functionalization of Unstrained Substrates

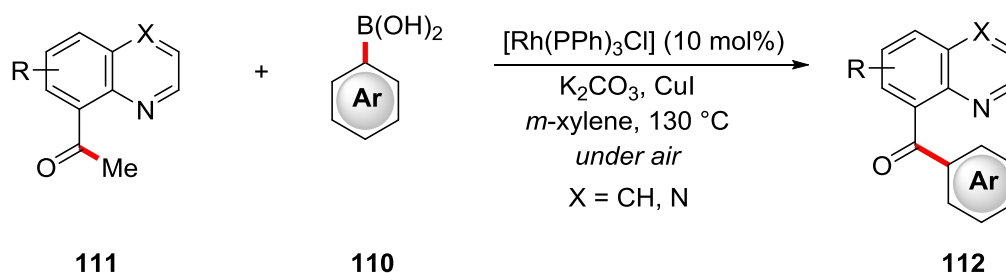
Methodologies for C-C activations are not limited to strained ring systems, such as cyclopropanes or cyclobutanones, but alternatives to the release of ring tension also exist. Related to C-H activation, C-C functionalizations can also occur *via* chelation assistance<sup>[14b]</sup> in which quinolines or quinoxalines turned out to be valuable directing groups.<sup>[76b, 76d, 76g]</sup> Using this principle, Douglas and coworkers presented indane, indoline and dihydrobenzofurane synthesis **108** by an intramolecular C-C activation/insertion reaction from 8-acylquinolines **109** (Scheme 1.26a).<sup>[93]</sup> An intermolecular substitution reaction with aryl boronic acids **110** was demonstrated by Wang and coworkers three years later (Scheme 1.26b).<sup>[94]</sup> Both reactions proceed by a chelation-assisted oxidative addition from the rhodium(I) species into the C(O)-C bond.



(a) Douglas (2009)



(b) Wang (2012)

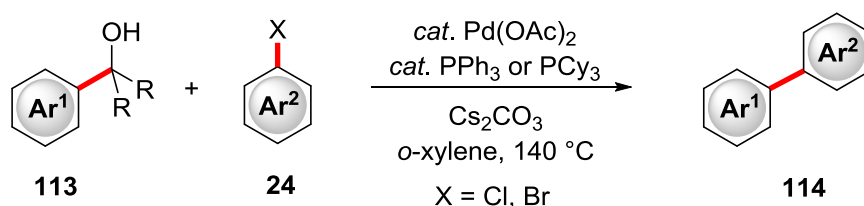
**Scheme 1.26:** C–C functionalization by chelation assistance.

Apart from oxidative additions, these functionalizations can be applied to more substances than strained ring systems or 8-acylquino(xa)lines. In the early 2000s, Miura and Nomura discovered that benzylic alcohols **113** can undergo C–C bond cleavage by palladium catalysis.<sup>[95]</sup> This method could be used for the C–C arylations with simple aryl halides **24** (Scheme 1.27a).<sup>[95–96]</sup> The activation process is supposed to occur *via*  $\beta$ -carbon elimination and the alcohol fragment of **113** results in the formation of a ketone or aldehyde.

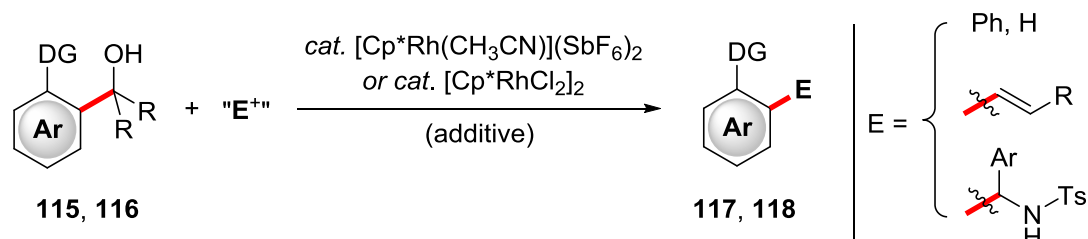
A widely applicable reaction manifold by this dealkanolative cleavage was reported by Shi about ten years later (Scheme 1.27b).<sup>[97]</sup> After  $\beta$ -carbon elimination, the rhodium-catalyzed reaction allowed for various modifications, including arylations,<sup>[98]</sup> oxidative alkenylations<sup>[99]</sup>, hydroarylations<sup>[100]</sup> or protonation.<sup>[94]</sup> In contrast to Miura's work<sup>[95–96]</sup>, the use of a pyridine or pyrazole directing group was mandatory.

Related to this chemistry, Morandi reported a cobalt-catalyzed dealkanolative reaction that allowed for further transformations complementary to rhodium (Scheme 1.27c).<sup>[101]</sup> It should be noted that C–H activation under the present conditions gave lower yields.

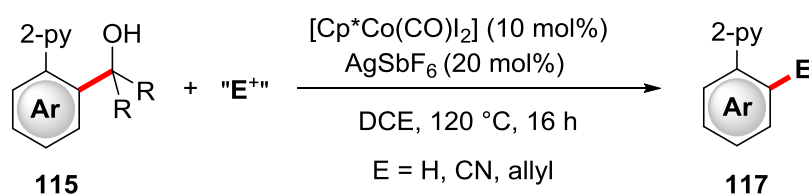
(a) Miura/Nomura (2001, 2003)



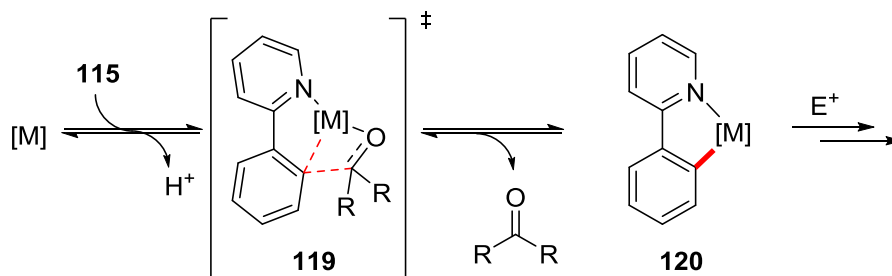
(b) Shi (2011, 2012)



(c) Morandi (2015)

**Scheme 1.27:** C–C functionalizations of alcohols by palladium, rhodium and cobalt catalysis.

In all cases, the former alcohol function resulted in the formation of a ketone or aldehyde as a hint for  $\beta$ -carbon elimination. For rhodium(III) and cobalt(III)-catalyzed reactions, the cleavage process is shown in Scheme 1.28. After pre-coordination to the directing group,  $\beta$ -carbon elimination occurs by the release of a carbonyl compound.<sup>[76g, 76h, 76j]</sup> The thus obtained cyclometalated species **120** undergoes further organometallic transformations.

**Scheme 1.28:** Chelation-assisted C–C bond cleavage by  $\beta$ -C-elimination.

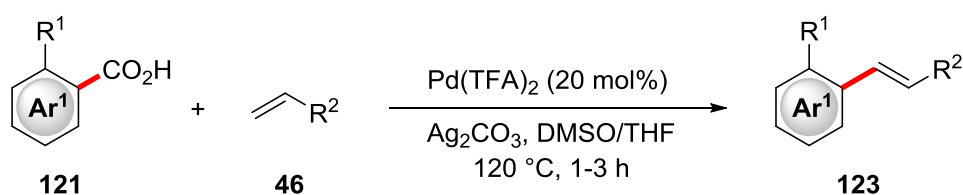
A different order is found for palladium-catalyzed reactions.<sup>[96, 102]</sup> The aryl halide adds to the *in situ* formed palladium(0) species the palladium(II)-aryl species coordinates to the

alcohol whereas  $\beta$ -C-elimination generates a  $\text{Ar-Pd(II)Ar'}$  species. Finally, reductive elimination delivers the biaryl species and the palladium(0) catalyst.

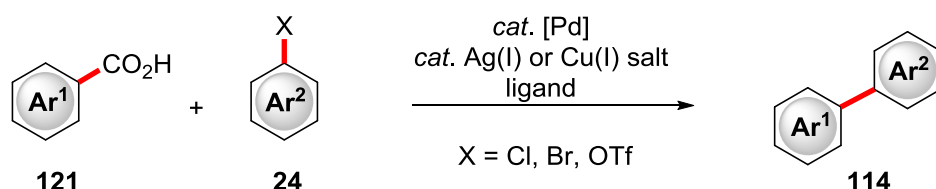
Besides the functionalization of benzylic alcohols, the catalytic functionalization of more abundant C–C bonds was continued to be in great demand. Essentially, the activation of benzoic acids in a decarboxylative fashion date back to 1966, when Nilsson discovered that benzoic acid underwent decarboxylation with stoichiometric amount of  $\text{Cu}_2\text{O}$ .<sup>[103]</sup> The first catalytic decarboxylation was presented by Myers showing a decarboxylative Heck reaction (Scheme 1.29a).<sup>[104]</sup> It proved viable for a wide range of terminal alkenes. Also substitution at the aryl moiety was tolerated. However, an *ortho*-substituent remained necessary for high yields as it facilitates the decarboxylation. Later, the C–C cleavage process could be elucidated to proceed via  $\beta$ -elimination though the authors did not name it by this.<sup>[105]</sup>

Besides alkenylation, Gooßen<sup>[106]</sup> and Forgione/Bilodeau<sup>[107]</sup> developed a decarboxylative arylation of benzoic acids **121** with aryl halides **24** (Scheme 1.29b and c). Similar to Myers' results,<sup>[104]</sup> first reports of Gooßen also required an *ortho*-substituent to facilitate the decarboxylation.<sup>[106b, 106d, 106e]</sup> This substrate dependence could be avoided when employing aryl triflates instead of aryl halides. The authors explained these findings with an *in situ* generated  $\text{Cu(OTf)}$  species that bears a higher reactivity in the decarboxylation process. Another resemblance to Myers' system is the necessity of a second metal, like copper(I) or silver(I) salts. This dependence was cancelled by Forgione/Bilodeau by establishing a palladium-only system for the decarboxylative arylation of heteroaromatic carboxylic acids **122**.<sup>[107]</sup> However, their system suffered from challenging C–H arylation on the heteroarenes and the selectivity was mostly controlled by the positional reactivity of the C–C or C–H bond. A similar work for the multiple arylation of thiophene-2-carboxylic acid was published in 2008 by Miura.<sup>[108]</sup> The proposed mechanism for these systems differs somewhat from the Myers system. Gooßen suggested a synergistic catalysis, with a copper-catalyzed decarboxylation pathway and a palladium-catalyzed “cross-coupling” cycle.<sup>[106c-e]</sup> Forgione/Bilodeau postulated a 1,2-Pd shift that cleaves the C–C bond.<sup>[107, 109]</sup> However, both mechanism are controversial and cannot rule out a  $\beta$ -elimination pathway.<sup>[76g]</sup>

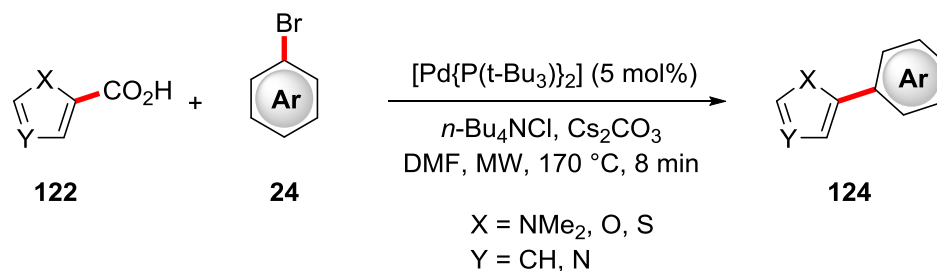
(a) Myers (2002)



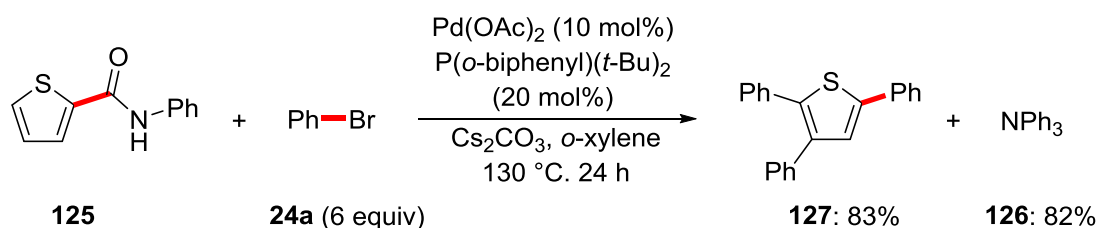
(b) Gooßen (2006)



(c) Forgione/Bilodeau (2006)

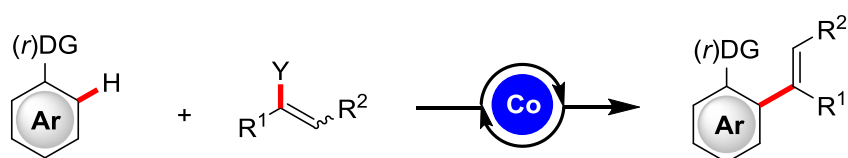
**Scheme 1.29:** Decarboxylative C–C arylations.

In contrast to the wide field of decarboxylative C–C functionalizations, examples with not less valuable amides in a decarbamoylative fashion are rare.<sup>[108, 110]</sup> Similar to the decarboxylative arylation, Miura succeeded in a decarbamoylative arylation of amide **125** with bromo benzene **24a** (Scheme 1.30).<sup>[108]</sup> However, the desired C–C arylation only took place with an excess of aryl bromide. Kinetic analysis revealed C–H arylations at the 3 and 2 positions to occur first, followed by a decarbamoylative C–C arylation. Surprisingly, the cleaved amide function was converted to triphenyl amine (**126**) that is unexpected for a  $\beta\text{-C}$  elimination pathway. Therefore, the origin of the C–C activation remains unclear here.

**Scheme 1.30:** Palladium-catalyzed decarbamoylative C–C arylation.

## 2 Objectives

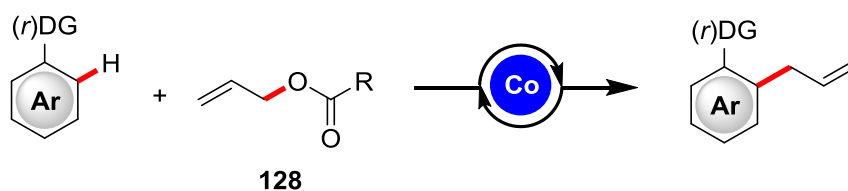
C–H activation has significantly improved the way organic synthesis is practiced. In particular, the last ten years have generated 3d metal catalysts<sup>[23a, 23b, 23d]</sup> as potent, but also earth-abundant and cost-effective alternatives to their precious 4d and 5d counterparts. Especially cobalt with its broad range of catalysts from low-valent systems<sup>[23a, 24c-f]</sup> up to high-valent Cp\*Co(III)<sup>[23a, 24a, 24b]</sup> complexes gained a key role for numerous transformations. The C–H alkenylation by alkyne hydroarylation became a model reaction for novel cobalt catalysts and was reported with low-valent systems by Kisch,<sup>[40]</sup> Yoshikai<sup>[41]</sup> and Petit<sup>[42]</sup> and also with high valent Cp\*Co(III) by Matsunaga/Kanai.<sup>[53, 56]</sup> However, all these reactions suffered from the same limitations i.e. restrictions to the synthesis of acyclic alkenes and a regioselectivity that is purely determined by the steric properties of the triple bond substituents. To address these restrictions, a cobalt-catalyzed C–H alkenylation with organic electrophiles, such as alkenyl esters, would overcome these limitations (Scheme 2.1).



**Scheme 2.1:** Cobalt-catalyzed C–H alkenylation with organic electrophiles.

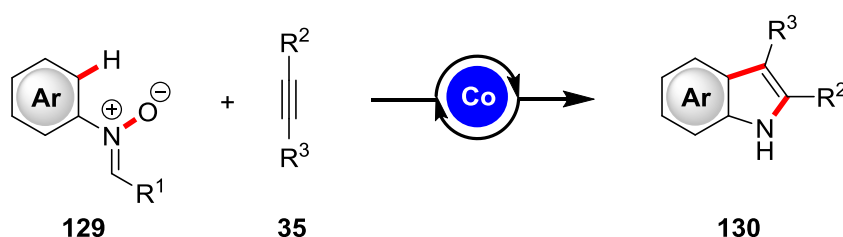
In the history of cobalt-catalyzed alkenylation, this approach has not been published and indeed this transformation bears several challenges. Cobalt-catalyzed cross-coupling reactions of alkenyl esters or halides with Grignard reagents are known<sup>[111]</sup> and a seriously taken side reaction. Therefore, the catalytic system does not only need to be optimal for the desired reactions, but also has to suppress this undesired side reaction. An even greater challenge is the control of the double bond configuration. As acyclic alkenyl esters offer a mixture of *E* and *Z* isomer, the impact of the catalytic system on this ratio would be of highest interest.

The unique performance of low-valent cobalt catalysis offered a broad range of new reactions.<sup>[23a, 24c-f]</sup> In spite of this versatility, the Grignard reagent limits its functional group tolerance and therefore its general applicability. With establishing Cp\*Co(III)-complexes, a new class of cobalt compounds enabled new and improved transformations under mild reaction conditions.<sup>[23a, 24a, 24b]</sup> These complexes should be applied for the allylation of (hetero)arenes with allyl esters **128** (Scheme 2.2). Beside the importance of a post-modifiable allyl group, the mechanism of this transformation is worth investigating.



**Scheme 2.2:** Cobalt(III)-catalyzed allylation with allyl esters.

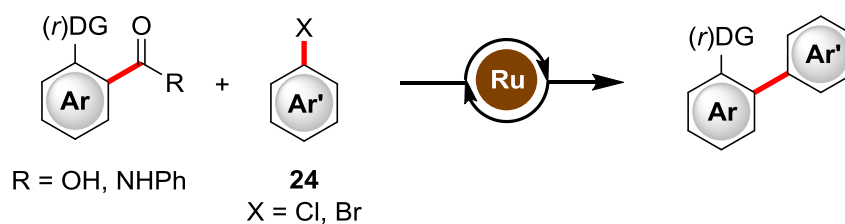
Heterocycles are particularly important in pharmaceutical chemistry and beyond.<sup>[66]</sup> In addition to the C–H functionalizations, the *de novo* synthesis of these compounds by catalytic reactions is an essential tool for a broad access to functionalized heteroarenes. In view of the increasing amount of methods by C–H activation in this field<sup>[67]</sup> and the importance of indoles **130**,<sup>[112]</sup> a *de novo* synthesis of this important heteroarene by cobalt(III) catalysis came to focus. This should be achieved by employing easily accessible nitrones **129** and alkynes **35** in a C–H alkenylation/cyclization cascade (Scheme 2.3).



**Scheme 2.3:** Cobalt(III)-catalyzed indole synthesis.

The difficulty in this reaction is the control of selectivity in the alkyne insertion step. The question arises which substituents  $R^2$  and  $R^3$  on the alkyne influence the selectivity in which way or even offer a different reactivity. Furthermore it need to be examined how the cobalt system differs from a related reaction under rhodium catalysis.<sup>[113]</sup>

The high and increasing amount of contributions on C–H activation<sup>[14a-d]</sup> is unreached for the not less important functionalization of C–C bonds. In spite of the above described difficulties with activation of C–C  $\sigma$ -bonds (*vide supra*), a ruthenium-catalyzed functionalization of aromatic amides and acids should be established, starting with a decarbamoylative and decarboxylative arylation with aryl halides (Scheme 2.4). Mechanistic studies should unravel the C–C bond cleavage process.



**Scheme 2.4:** Ruthenium(II)-catalyzed decarboxylative and decarbamoylative C–C arylation.

Beside the C–C arylation, the identified catalytic system should be applied to other transformation to enlarge the spectra of ruthenium-catalyzed C–C functionalizations. In particular, decarboxylative alkylations with electrophiles appear challenging as those reactions have not been reported with palladium or rhodium catalysis as of yet.



**Scheme 2.5:** Ruthenium(II)-catalyzed decarboxylative C–C alkylation.

The intrinsic problem for this alkylation reaction is certainly the esterification of benzoic acids with alkyl halides under basic conditions. In this way, the decarboxylative alkylation has to be faster than this undesired side reaction. Moreover, with the experiences on *meta*-selective C–H alkylation in mind,<sup>[114]</sup> the selectivity of this decarboxylative alkylation is an exciting research topic in terms of alkylation at the *ipso*-C position or by C–C/C–H functionalization.

### 3 Results and Discussion

#### 3.1 Cobalt-Catalyzed Alkenylation with Enol Derivatives

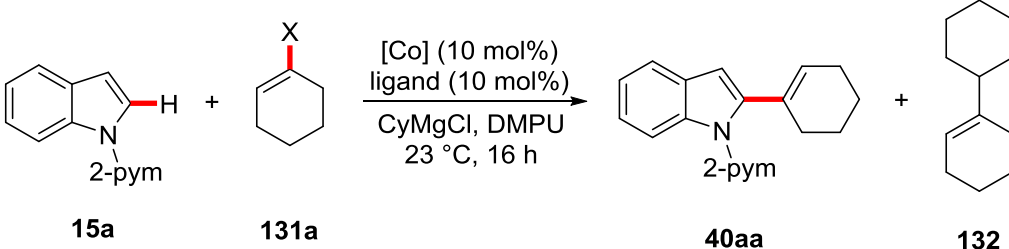
Methods for C–H activation by low-valent cobalt catalysis have emerged as a powerful technique for diverse C–C bond forming reaction with inactivated substrates.<sup>[23a, 24c-f]</sup> In particular, a plethora of methods for alkenylation reactions by addition of alkynes have been reported using a broad variety of cobalt catalysts (*vide supra*). In contrast to these achievements, a direct method for the alkenylation with organic electrophiles was thus far not established by cobalt catalysis and was just achieved by ruthenium catalysis under relatively harsh reaction conditions.<sup>[115]</sup> Therefore, a method for selective C–H alkenylation reactions with easily accessible organic electrophiles would be highly desirable.

##### 3.1.1 Optimization Studies

Given the broad applicability of aryl and alkyl halides for the cobalt-catalyzed arylation and alkylation, published by our group,<sup>[32, 39]</sup> Nakamura<sup>[31]</sup> and Yoshikai,<sup>[33b, 37, 116]</sup> we commenced our studies by probing various reaction conditions for the envisioned C–H alkenylation using cyclohexenyl chloride and bromide **131** with pyrimidyl indole (**15a**) under various reaction conditions (Table 3.1).

Unfortunately, a representative set of cobalt salts, NHC ligands and bases that proved suitable for the above mentioned reactions,<sup>[31-32, 33b, 37, 39, 116]</sup> did not deliver the desired product **40aa**. Instead, 1-cyclohexenyl cyclohexane (**132**) could be isolated in up to 29% (Entry 2).

**Table 3.1:** Initial experiments for the cobalt-catalyzed alkenylation with alkenyl halides **131a**.<sup>[a]</sup>

					
Entry	X	[Co]	Ligand	Yield of <b>40aa</b>	Yield of <b>132</b>
1	Cl	Co(acac) <sub>2</sub>	IMesHCl ( <b>22</b> )	---	20%
2	Br	Co(acac) <sub>2</sub>	IMesHCl ( <b>22</b> )	---	29%

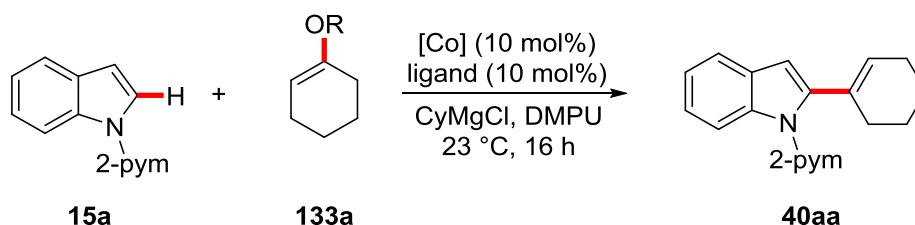


Entry	X	[Co]	Ligand	Yield of 40aa	Yield of 132
3	Cl	Co(acac) <sub>2</sub>	IPrHCl ( <b>13</b> )	---	10%
4	Cl	Co(acac) <sub>2</sub>	---	---	17%
5	Cl	CoCl <sub>2</sub>	IMesHCl ( <b>22</b> )	---	12%
6	Cl	Co(acac) <sub>2</sub>	ICyHCl ( <b>23</b> )	---	19%

<sup>[a]</sup> Reaction conditions: **15a** (0.50 mmol), **131a** (0.75 mmol), [Co] (10 mol%), ligand (10 mol%), CyMgCl (2.0 equiv), solvent (1.5 mL), 23 °C, 16 h.

These first results and especially the coupling of the alkenyl halide with the Grignard reagent which was reported before by Cahiez,<sup>[111]</sup> renders alkenyl halides as not suitable substrates for the desired transformation. To circumvent this problem, different enolates were tested in the desired C–H/C–O activation reaction (Table 3.2). The use of alkenyl acetates proved to be successful with 25% isolated yield in a non-optimized reaction (entry 1), whereas alkenyl tosylates and sulfamates did not show any conversion under otherwise identical reaction conditions.

**Table 3.2:** Different enolates **133a** for the cobalt-catalyzed C–H alkenylation.<sup>[a]</sup>



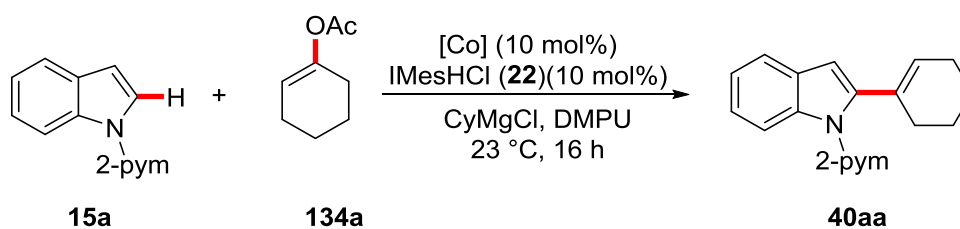
Entry	R	[Co]	Ligand	Yield / %
1	Ac	CoCl <sub>2</sub>	IMesHCl ( <b>22</b> )	25
2	Ac	Co(acac) <sub>2</sub>	IMesHCl ( <b>22</b> )	10
3	Ac	CoCl <sub>2</sub>	ICyHCl ( <b>23</b> )	8
4	Tos	CoCl <sub>2</sub>	IMesHCl ( <b>22</b> )	---
5	Tos	Co(acac) <sub>2</sub>	IMesHCl ( <b>22</b> )	---
6	Tos	CoCl <sub>2</sub>	ICyHCl ( <b>23</b> )	---
7	SO <sub>2</sub> NMe <sub>2</sub>	CoCl <sub>2</sub>	IMesHCl ( <b>22</b> )	---

Entry	R	[Co]	Ligand	Yield / %
8	SO <sub>2</sub> NMe <sub>2</sub>	Co(acac) <sub>2</sub>	IMesHCl ( <b>22</b> )	---
9	SO <sub>2</sub> NMe <sub>2</sub>	CoCl <sub>2</sub>	ICyHCl ( <b>23</b> )	---

<sup>[a]</sup> Reaction conditions: **15a** (0.50 mmol), **133a** (0.75 mmol), [Co] (10 mol%), ligand (10 mol%), CyMgCl (2.0 equiv), DMPU (1.5 mL), 23 °C, 16 h.

Besides these promising attempts, alkenyl acetates are stable, easy to handle and many derivatives can be easily prepared from the corresponding ketone.<sup>[117]</sup> To identify the best reaction conditions for the C–H/C–O alkenylation reaction, a variety of cobalt sources, (pre)ligands, bases and solvents were tested for the reaction of pyrimidyl-indole (**15a**) with cyclohexenyl acetate (**134a**). The optimization study began with probing different cobalt sources (Table 3.3). Among the tested cobalt halides, CoI<sub>2</sub> turned out to be optimal with 32% isolated yield (entry 3). Other cobalt salts, such as acetyl acetonate, nitrate and sulfate resulted in reduced yields (entries 4-7). In this aspect, the use of Co(acac)<sub>2</sub> and Co(acac)<sub>3</sub> gave comparable yields (entries 4 and 5), which indicates that the cobalt is probably reduced rapidly by the Grignard reagent and neither cobalt(II), nor cobalt (III) is the catalytical active species, which corresponds to previous findings by our group.<sup>[36]</sup> It is furthermore worth mentioning that no reaction takes place in the absence of a cobalt source.

**Table 3.3:** Cobalt sources for the cobalt-catalyzed alkenylation.<sup>[a]</sup>



Entry	[Co]	Yield / %
1	CoCl <sub>2</sub>	27
2	CoBr <sub>2</sub>	24
3	CoI <sub>2</sub>	32
4	Co(acac) <sub>2</sub>	20
5	Co(acac) <sub>3</sub>	19

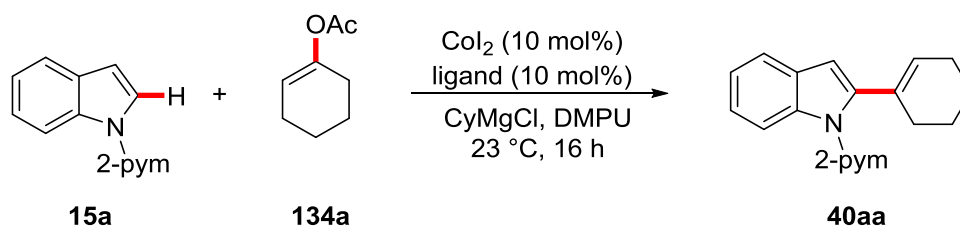
Entry	[Co]	Yield / %
6	Co(NO <sub>3</sub> ) <sub>2</sub>	9
7	CoSO <sub>4</sub>	11
8	Co <sub>2</sub> (CO) <sub>8</sub>	---
9	---	---

<sup>[a]</sup> Reaction conditions: **15a** (0.50 mmol), **134a** (0.75 mmol), [Co] (10 mol%), IMesHCl (**22**) (10 mol%), CyMgCl (2.0 equiv), DMPU (1.5 mL), 23 °C, 16 h.

With the best cobalt source being identified, the optimization continued with identifying the best ligands or ligand precursors (Table 3.4). No reaction took place in the absence of a ligand (entry 1). As N-heterocyclic carbenes are broadly implemented in low-valent cobalt catalysis,<sup>[23a, 24e]</sup> a variety of carbenes were screened. Among these, solely carbenes based on an imidazole core showed good conversion, whereas cyclic amino alkyl carbenes (CAAC)<sup>[118]</sup> **135** and cyclopropylidene-<sup>[119]</sup> based carbenes **136** were inactive (entries 6 and 7). Moreover, the substitution pattern on the imidazole core was highly crucial for the reaction progress. Best yields were obtained with the IPr carbene (**13**) (entry 3), whereas doubling of the amount of ligand led to a reduced yield, probably due to the formation of a less active cobalt complex (entry 4). Changing the substitution pattern on the arenes led a significant decrease in yield (entry 2) and replacing the arenes by alkyl groups led to a further decrease with both more or less bulky substituents **137-139** (entries 8-10). Furthermore, substitution on the 3 and 4 position of the imidazole was counterproductive, as ligand **138** gave low, but significant yield (entry 9), whereas **140a** und **140b** shut down the reaction completely (entries 11-12). In order to stabilize possible cyclocobalted complexes, a further donor atom was attached on one arene on the carbene. However, the ligand **141** did not afford any conversion (entry 13). In view of the high dependence on the steric properties on the carbene the question arose whether the sterics are rather necessary for the success of the reaction than the electronic character. To this extend the heteroaromatic secondary phosphine oxide<sup>[120]</sup> (HASPO) ligand **142** was submitted to the reaction mixture (entry 14), but no conversion could be observed. Cobalt-catalyzed C–H functionalization reactions using cobalt-phosphine complexes were successfully accomplished by Yoshikai and coworkers.<sup>[23a, 24e]</sup> To proof its activity a set of representative phosphines were tested (entries 17-20), but none of them showed activity. Finally, ligands with nitrogen donor atoms were submitted to the reaction (entries 21-22). Though these ligands showed considerable

success in nickel-catalyzed C–H activation reactions,<sup>[121]</sup> their *in situ* formed cobalt complexes were inactive. The structure of some ligand precursors are shown below (Figure 3.1).

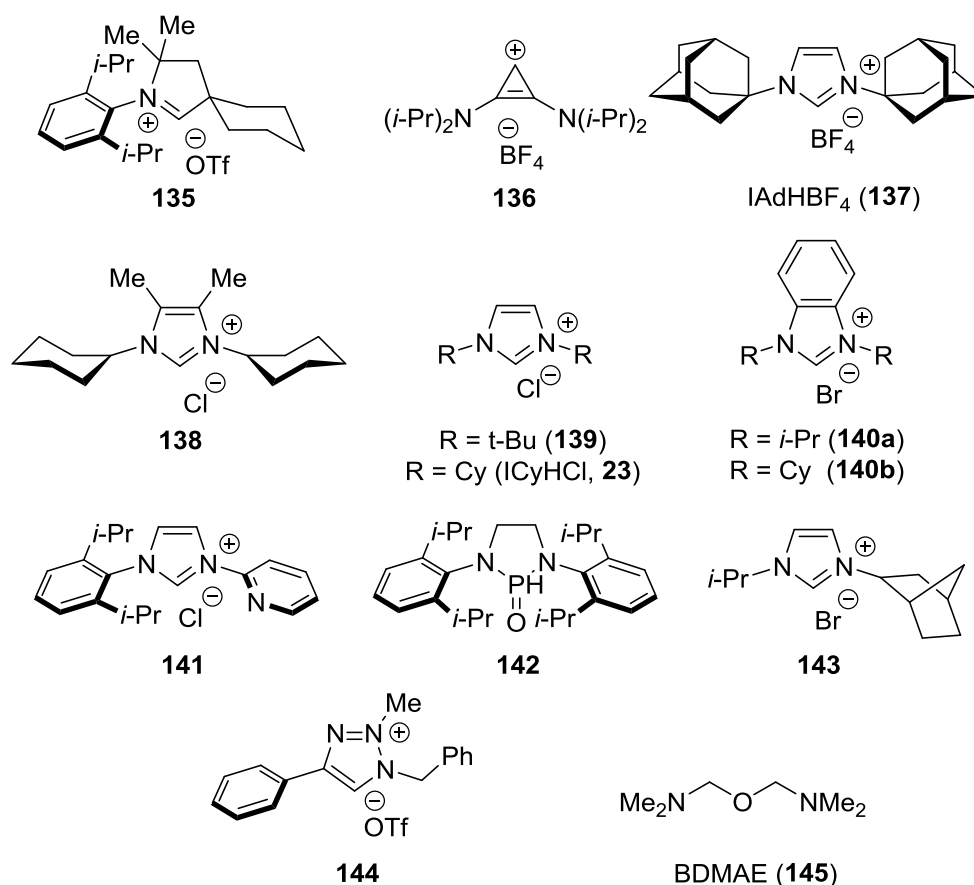
**Table 3.4:** Screening of different (pre)ligands for the cobalt-catalyzed alkenylation.<sup>[a]</sup>



Entry	(Pre-)Ligand	Yield / %
1	---	---
2	IMesHCl ( <b>22</b> )	32
3	IPrHCl ( <b>13</b> )	88
4	IPrHCl ( <b>13</b> )	79 <sup>[b]</sup>
5	ICyHCl ( <b>23</b> )	11
6	<b>135</b>	5
7	<b>136</b>	---
8	IAdHBF <sub>4</sub> ( <b>137</b> )	8 <sup>[c]</sup>
9	<b>138</b>	20
10	<b>139</b>	---
11	<b>140a</b>	10
12	<b>140b</b>	3 <sup>[c]</sup>
13	<b>141</b>	---
14	<b>142</b>	---
11	<b>143</b>	10
14	<b>144</b>	8 <sup>[c]</sup>

Entry	(Pre-)Ligand	Yield / %
17	PPh <sub>3</sub>	---
18	PCy <sub>3</sub>	---
19	dppe	---
20	pyphos	10
21	2,2-bipyridine	---
22	BDMAE ( <b>145</b> )	---

<sup>[a]</sup> Reaction conditions: **15a** (0.50 mmol), **134a** (0.75 mmol), CoI<sub>2</sub> (10 mol%), ligand (10 mol%), CyMgCl (2.0 equiv), DMPU (1.5 mL), 23 °C, 16 h. <sup>[b]</sup> IPrHCl (20 mol%). <sup>[c]</sup> GC-conversion using *n*-dodecane as internal standard.

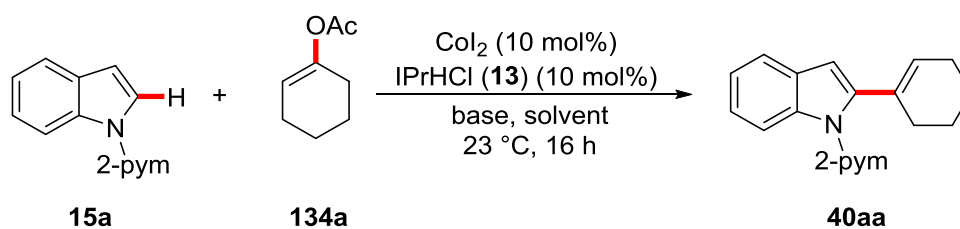


**Figure 3.1:** Structures of some applied ligand and ligand precursors.

Finally, the reaction was optimized regarding bases and solvents (Table 3.5). Among the tested Grignard reagents, cyclohexylmagnesium chloride and bromide gave best results (entries 1 and 2) without significant differences in the yields. The use of the very

expensive neopentyl magnesium chloride, which Yoshikai and coworkers employed in several transformations,<sup>[23a, 24e]</sup> resulted in a less efficient conversion (entry 5). In general, applying Grignard reagents remained necessary for the success of the reaction, as related strong bases, such as LiHMDS, KO $t$ -Bu or  $n$ -BuLi, failed to give any conversion (entries 7-9). That renders the organomagnesium compound to not only act as a base, but presumably also as a reducing agent to generate a catalytically active cobalt complex for this low-valent cobalt catalysis.<sup>[23a, 24e, 24f]</sup> A short solvent test did not afford a solvent preferable to DMPU. Employing THF resulted in a more complex reaction mixture where among other side products, 1-cyclohexyl cyclohexene (**132**) was found, and, therefore, the yield of the desired product decreased (entry 10). Using toluene just led to trace amounts of product **40aa** (entry 12), probably due to the low solubility of the Grignard species. Moreover, a slightly elevated reaction temperature of 60 °C did not result in improved yields (entry 13).

**Table 3.5:** Bases and solvents for the cobalt-catalyzed C–H/C–O alkenylation.



Entry	Base	Solvent	Yield / %
1	CyMgCl	DMPU	88
2	CyMgBr	DMPU	87
3	$i$ -PrMgCl	DMPU	62
4	$t$ -BuMgCl	DMPU	20
5	$t$ -BuCH <sub>2</sub> MgCl	DMPU	69
6	MeMgCl	DMPU	---
7	LiHMDS	DMPU	---
8	KO $t$ -Bu	DMPU	---
9	$n$ -BuLi	DMPU	---

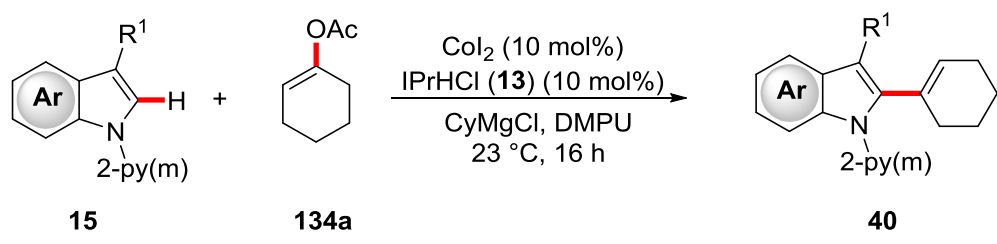
Entry	Base	Solvent	Yield / %
10	CyMgCl	THF	21
11	CyMgCl	NMP	11
12	CyMgCl	PhMe	traces
13	CyMgCl	DMPU	80 <sup>[b]</sup>

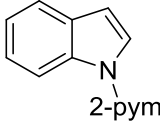
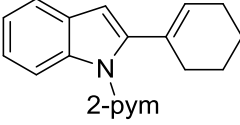
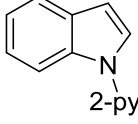
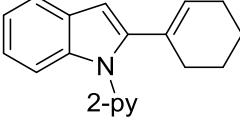
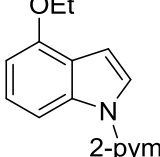
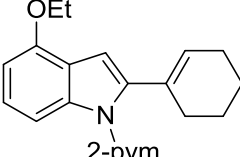
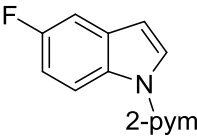
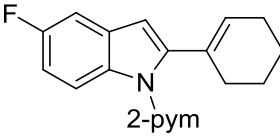
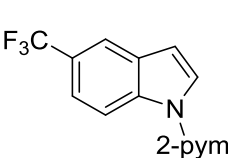
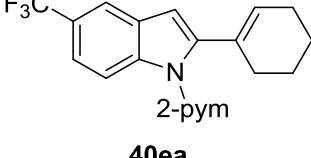
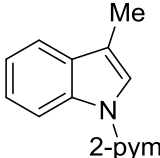
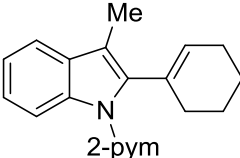
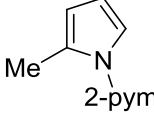
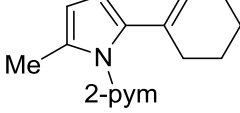
<sup>[a]</sup> Reaction conditions: **15a** (0.50 mmol), **134a** (0.75 mmol), CoI<sub>2</sub> (10 mol%), IPrHCl (**13**) (10 mol%), base (2.0 equiv), solvent (1.5 mL), 23 °C, 16 h. <sup>[b]</sup> Reaction performed at 60 °C.

### 3.1.2 Scope of the Cobalt-Catalyzed C–H Alkenylation with Enolates

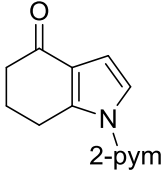
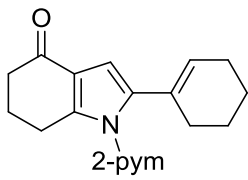
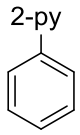
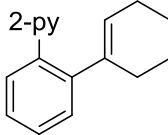
With the identified best catalytic system, we tested the versatility of the cobalt-catalyzed C–H/C–O alkenylation protocol for differently substituted indoles **15** as well as different vinyl acetates **134**. Probing various substitution patterns on the indole, we were delighted to observe that most of the substituents on different positions of the arenes were well tolerated (Table 3.6). Both, the pyrimidyl- as well as the pyridyl group served as valuable and cleavable directing groups (entries 1 and 2).<sup>[122]</sup> Furthermore, this method could be applied for the C–H alkenylation of electron-rich as well as electron-deficient indoles giving the desired products **40** in good yields (entries 3 and 5). Moreover, substitution pattern on several positions of the indole core, such as the 4, 5 and sterically more congested 3 position were not problematic (entries 3, 4 and 6). An extension of this method to other (hetero)arenes could also be successfully accomplished for the alkenylation of pyrroles **146** and 2-phenyl pyridines **14** (entries 7, 8 and 9). In the latter case, the C–H alkenylation proceeded with excellent levels of site-selectivity on the *ortho*-position of the arene with slight changes in the catalytic system.

**Table 3.6:** Scope of the cobalt-catalyzed C–H/C–O alkenylation.<sup>[a]</sup>

			
Entry	15	40	Yield / %

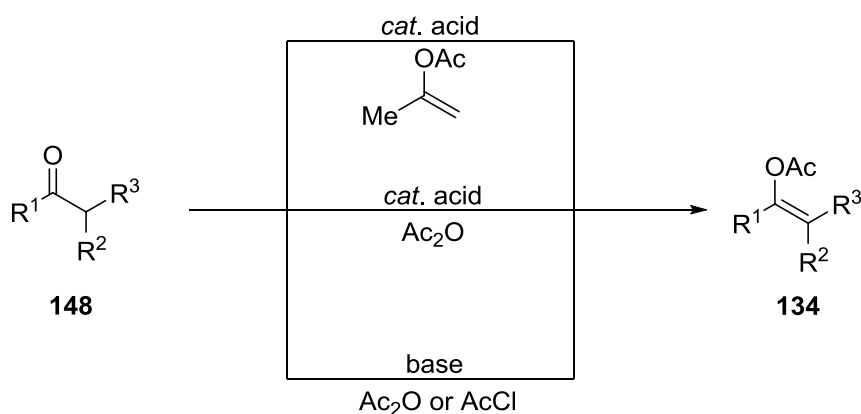
Entry	15	40	Yield / %
1	 <b>15a</b>	 <b>40aa</b>	88
2	 <b>15b</b>	 <b>40ba</b>	91
3	 <b>15c</b>	 <b>40ca</b>	60
4	 <b>15d</b>	 <b>40da</b>	75
5	 <b>15e</b>	 <b>40ea</b>	71
6	 <b>15f</b>	 <b>40fa</b>	93
7	 <b>146a</b>	 <b>147aa</b>	69



Entry	15	40	Yield / %
8	 <b>146b</b>	 <b>147ba</b>	54
9	 <b>14a</b>	 <b>39aa</b>	54 <sup>[b]</sup>

<sup>[a]</sup> Reaction conditions: **15** (0.50 mmol), **134a** (0.75 mmol),  $\text{CoI}_2$  (10 mol%),  $\text{IPrHCl}$  (**13**) (10 mol%),  $\text{CyMgCl}$  (2.0 equiv), DMPU (1.5 mL), 23 °C, 16 h. <sup>[b]</sup> Using  $\text{ICyHCl}$  (**23**) (10 mol %).

Motivated by the wide range of tolerated indoles and other heterocycles, the applicability was further investigated by testing different alkenyl acetates. In general, the use of vinyl acetates was of great benefit as a wide range of these compounds can be synthesized by three methods (Scheme 3.1). These pathways are *i*) treatment with isopropenyl acetate with catalytic amounts of acids,<sup>[117a, 117b]</sup> *ii*) reaction with acetic anhydride under acid catalysis,<sup>[117c]</sup> or *iii*) deprotonation and trapping of the enolate with acetic chloride or anhydride.



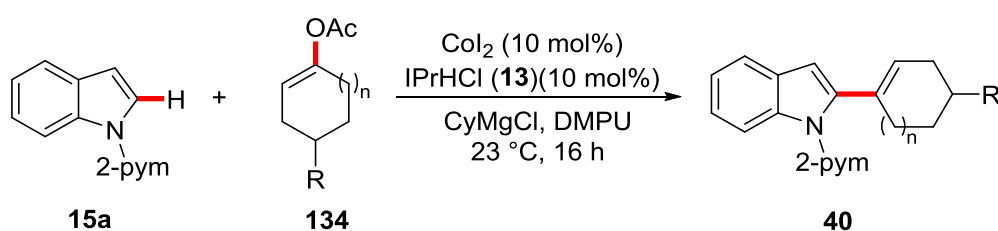
**Scheme 3.1:** General methods for the preparation of alkenyl acetates **134** from ketones **148**.

The first method provided very good yields for aliphatic ketones, especially cyclic ones. The second method improved the yields for some aliphatic vinyl acetates, whereas the third method was the one of choice for aryl ketones. Beside their broad accessibility, the

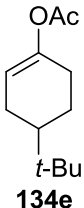
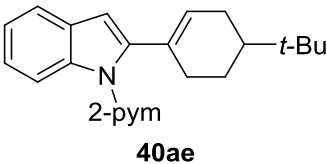
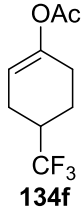
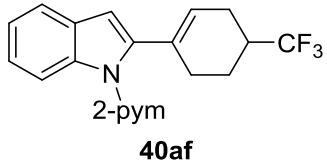
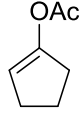
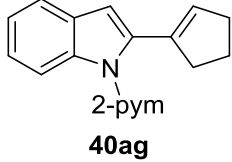
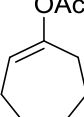
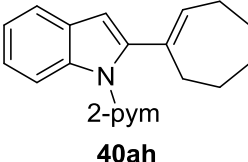
employed alkenyl acetates are bench-stable and can be stored for at least two years without detectable degradation.<sup>[123]</sup>

Beginning with cyclic alkenyl acetates, we were delighted to observe that a number of six-membered enolates were converted in very good yields (Table 3.7). In particular, enolates bearing electron-rich, as well as electron-withdrawing groups gave comparably good results (entries 3 and 5) and also a bulky *tert*-butyl group did not mismatch with the catalytic system (entry 4). However, the yields dropped significantly when employing enolates with other ring sizes. Poor yields were obtained with cyclopentenyl acetate (entry 6) and moderate yields with cycloheptenyl acetate (entry 7).

**Table 3.7:** Scope of cyclic alkenyl acetates **134** for the cobalt-catalyzed C–H alkenylation.<sup>[a]</sup>



Entry	Alkenyl Acetate	Product	Yield / %
1	<p><b>134b</b></p>	<p><b>40ab</b></p>	90
2	<p><b>134c</b></p>	<p><b>40ac</b></p>	89
3	<p><b>134d</b></p>	<p><b>40ad</b></p>	85

Entry	Alkenyl Acetate	Product	Yield / %
4	 <b>134e</b>	 <b>40ae</b>	84
5	 <b>134f</b>	 <b>40af</b>	86
6	 <b>134g</b>	 <b>40ag</b>	8
7	 <b>134h</b>	 <b>40ah</b>	35

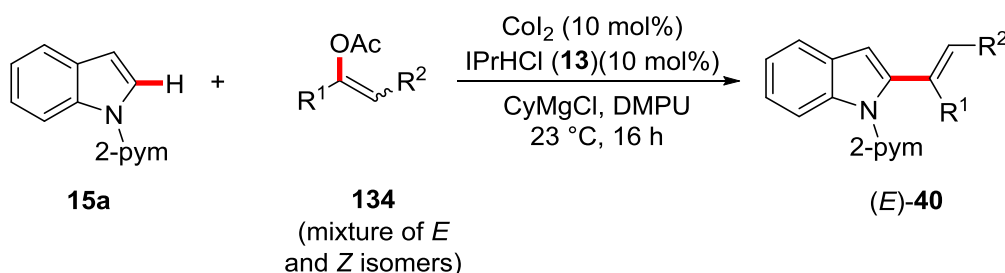
<sup>[a]</sup> Reaction conditions: **15a** (0.50 mmol), **134** (0.75 mmol),  $\text{CoI}_2$  (10 mol%),  $\text{IPrHCl}$  (**13**) (10 mol%),  $\text{CyMgCl}$  (2.0 equiv), DMPU (1.5 mL), 23 °C, 16 h.

It should be noted that all given examples in Table 3.7 cannot be prepared by hydroarylation reactions. As to the work of Kisch<sup>[40]</sup> and coworkers in 1994, this reaction provides an important expansion in the more than 20 year old history of cobalt-catalyzed C–H alkenylation chemistry.

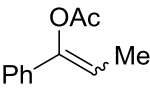
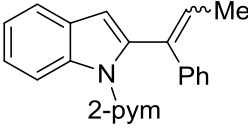
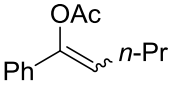
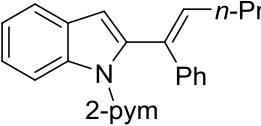
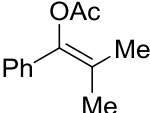
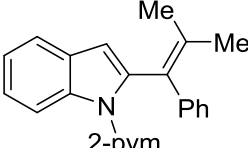
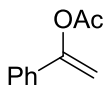
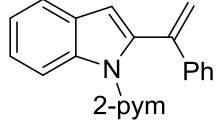
In contrast to cyclic vinyl acetates, the C–H/C–O alkenylation with acyclic enolates was not of less importance. As these enolates are usually obtained in a mixture of (*E*)- and (*Z*)- isomers with an excess of the (*Z*)- enolate depending on the method (*vide supra*), the question arose whether our catalytic system can affect this diastereomeric ratio and in which way. To shine light onto this question, the scope of acyclic alkenyl acetates **134** was performed with pyrimidyl indole (**15a**) (Table 3.8). To our great delight, all products in the scope afforded the double bond solely with (*E*)- configuration and in acceptable to good yields. This method also proved applicable to aliphatic enol acetates, as well as for

those bearing an aryl moiety (entries 3 and 5). In particular, the selectivity of this reaction with bis-alkyl enolates is another major advantage of this reaction towards other methods (entry 1 and 2). Also here, neither the (*Z*)-isomer, nor a regioisomer could be detected. In contrast, attempts to obtain these products by hydroarylation reactions of alkynes would lead to a mixture of regioisomers with hardly any level of selectivity, as shown by Yoshikai.<sup>[41a]</sup> The selectivity of those reactions is mostly controlled by steric interactions, rendering again the potential of these direct alkenylation by C–H/C–O bond cleavage. Minimum amounts of the (*Z*)-configured product could be observed when the reaction temperature is increased to 60 °C (entry 4). As also the yield dropped at this temperature, there is no good reason to perform this reaction at higher reaction temperatures. Limitations of the reaction appear when using fully substituted enol acetates (entry 6) as well as for those bearing a terminal double bond (entry 7).

**Table 3.8:** Scope for acyclic enol acetates **134** for the cobalt-catalyzed C–H alkenylation.<sup>[a]</sup>



Entry	Alkenyl Acetate	<i>E/Z</i> Ratio	Product	Yield / %
1	 <b>134i</b>	34/66	 <b>(E)-40ai</b>	50
2	 <b>134j</b>	37/63	 <b>(E)-40aj</b>	56
3	 <b>134k</b>	27/73	 <b>(E)-40ak</b>	80

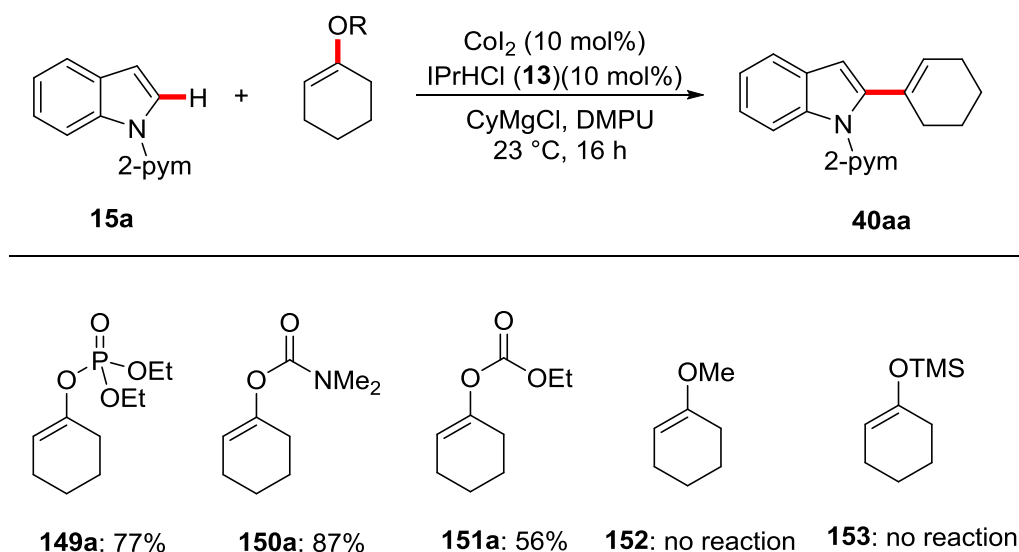
Entry	Alkenyl Acetate	E/Z Ratio	Product	Yield / %
4	 <b>134k</b>	27/73	 <b>40ak</b> (E/Z: 19/1)	67 <sup>[b]</sup>
5	 <b>134l</b>	29/71	 <b>(E)-40al</b>	54
6	 <b>134m</b>	---	 <b>40am</b>	10
7	 <b>134n</b>	---	 <b>40an</b>	Traces

<sup>[a]</sup> Reaction conditions: **15a** (0.50 mmol), **134** (0.75 mmol),  $\text{CoI}_2$  (10 mol%),  $\text{IPrHCl}$  (**13**) (10 mol%),  $\text{CyMgCl}$  (2.0 equiv), DMPU (1.5 mL), 23 °C, 16 h. <sup>[b]</sup> Reaction performed at 60 °C.

### 3.1.3 C–H Alkenylation with Alkenyl Phosphates, Carbamates and Carbonates

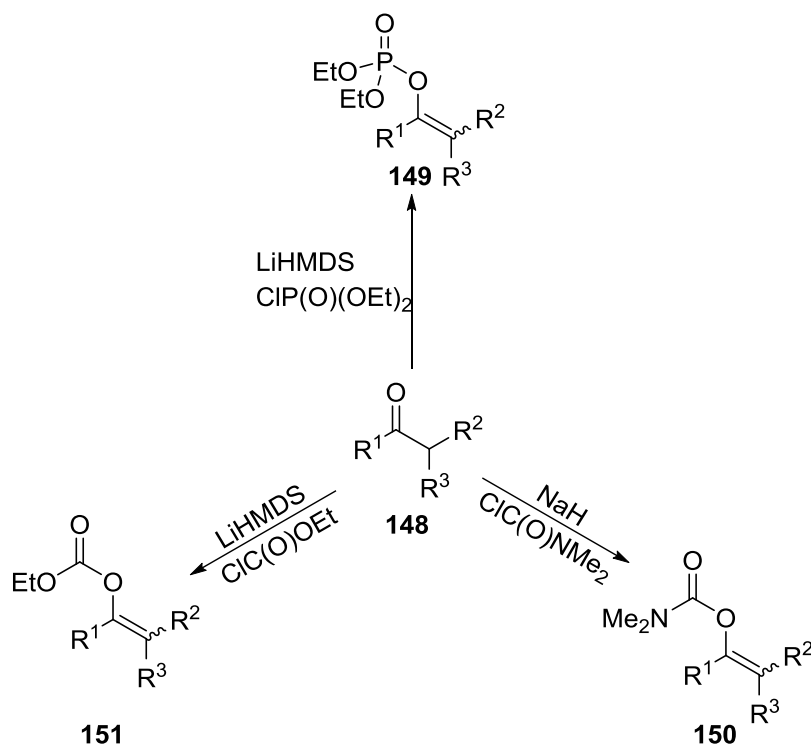
Inspired by the success of the C–H alkenylation with vinyl acetates **134** by C–O bond cleavage, a further study on other vinyl esters for the envisioned alkenylation reaction appeared meaningful. As tosylates and sulfamates were unsuccessful (*vide supra*), attention was centered on other vinyl esters, such as phosphates **149**, carbamates **150** and carbonates **151** without changes in the catalytic system. We investigated their performance using the established catalytic system, pyrimidyl indole (**15a**) and the cyclohexenyl ester of the tested enolate as these esters previously showed best results (Scheme 3.2). Indeed, a number of organic electrophiles proceeded well in this reaction. The carbamate **150a** gave comparable very good yields as the acetate and also the alkenyl phosphate **149a** was satisfactory. Alkenyl carbonate **151a** also provided the desired product, albeit with somewhat less efficiency. Unfortunately, no reaction was

observed when using vinyl ethers, such as cyclohexenyl methyl ether (**152**) or cyclohexenyl trimethylsilyl ether (**153**).



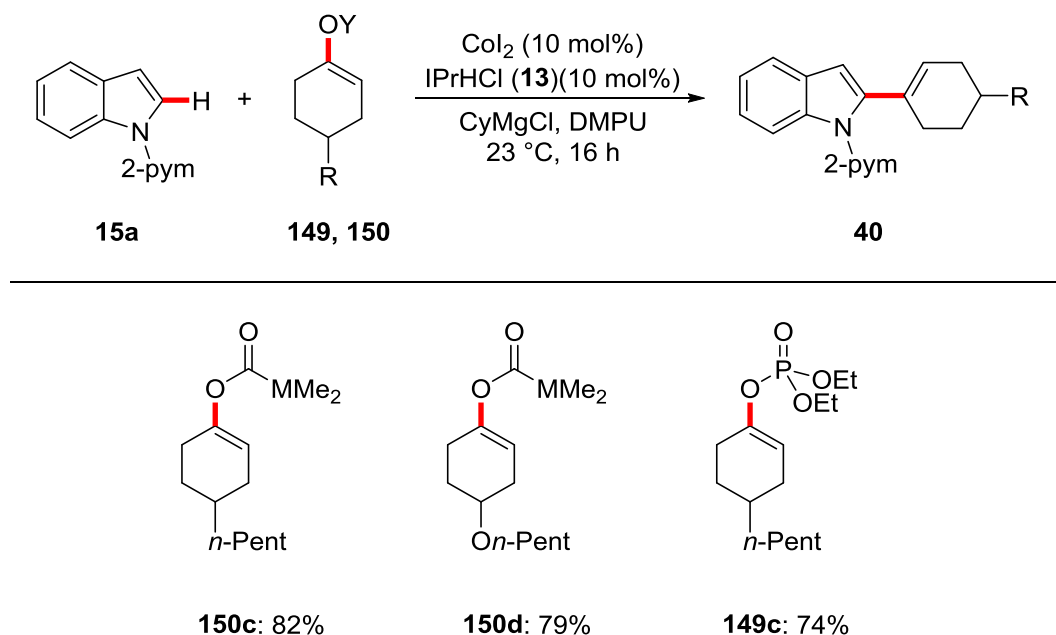
**Scheme 3.2:** Cobalt-catalyzed C-H alkenylation with organic electrophiles by C–O bond cleavage.

Also these esters are stable and can be stored for long time. Similar to alkenyl acetates, they can be prepared from the corresponding ketones by deprotonation with a strong base and trapping the enolate with an electrophile (Scheme 3.3).<sup>[124]</sup>



**Scheme 3.3:** Typical methods for the preparation of alkenyl phosphates **149**, carbamates **150** and carbonates **151**.

With good results being achieved with alkenyl phosphate **149a** and carbamate **150a**, a substrate scope of representative enolates was performed to probe again the versatility of this reaction (Scheme 3.4). The two alkenyl carbamates **150** proceeded well with good yields (entries 1 and 2). Also vinyl phosphates **149** proceeded well, with somewhat reduced efficiency. A representative scope with alkenyl phosphate was performed by N. Sauermann.<sup>[125]</sup> It revealed cyclic and acyclic phosphates **150** to be active substrates and in the latter case the desired indole **40** were obtained solely on (*E*)-configuration.



**Scheme 3.4:** Cobalt-catalyzed alkenylation with alkenyl phosphates **149** and carbamates **150**.

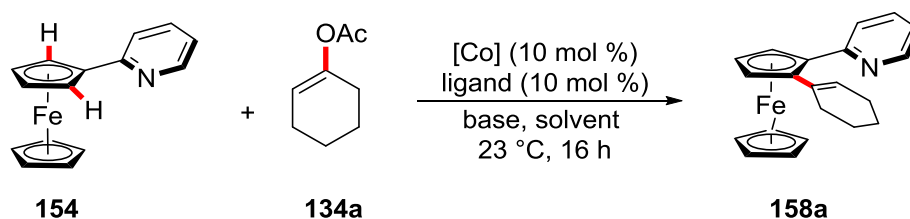
### 3.1.4 C–H Alkenylation of Ferrocenes

In order to expand the range of arenes, the alkenylation of much more challenging ferrocenes by the established catalytic system appeared promising towards their potential for asymmetric catalysis and ligand design.<sup>[126]</sup> With the success of the pyridyl directing group, we probed several reaction conditions using pyridyl ferrocene (**154**) as model substrate.<sup>[127]</sup> With careful tuning of some reaction parameters, the alkenylation of ferrocenes could be accomplished in acceptable yields. (Table 3.9). The optimized reaction conditions for the C–H alkenylation of indoles did not show any conversion (entry 1), which was not of great surprise, considering the different sterical and electronical properties of ferrocenes and indoles. As the ligand is of highest importance for many low-valent cobalt-catalyzed C–H functionalizations,<sup>[23a, 24e]</sup> a series of carbene type ligands have been chosen. Best yields were obtained with ICyHCl (**23**) as the preligand (entry 2). Surprisingly, also the ring size of the cycloalkyl group was of crucial importance so that imidazole based NHCs with a cyclopentyl for **155** as well as a

cycloheptyl group for **156** (Figure 3.2) provided less good yields (entries 9 and 10) and also a ligand with the more bulky adamantyl group **137** failed to give isolable conversion (entry 3). All other employed ligands did not lead to improved yields. However, the efficiency of the reaction could be improved by the use of  $\text{Co}(\text{acac})_2$  instead of  $\text{CoI}_2$  (entry 14). Changes in base and solvent were not successful (entries 17-21) as well as an elevated temperature of 60 °C (entry 22).

As the planar chirality of the ferrocene is its basis for asymmetric synthesis, an enantioselective alkenylation reaction would be of high demand. To this end inducing chirality by chiral groups on the ligand may lead to an enantioselective reaction. However, replacing the cyclohexyl group by a chiral bornyl group in IBornHCl (**157**) did not just dropped the yield to 15% (entry 11), but also provided a racemic mixture.

**Table 3.9:** Cobalt-catalyzed C–H alkenylation of ferrocene **154**.<sup>[a]</sup>

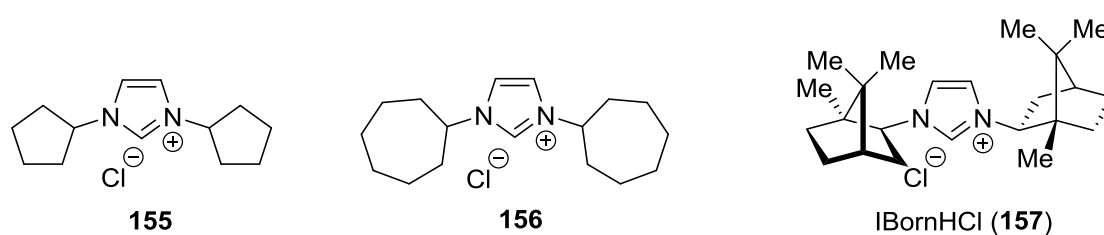


Entry	[Co]	Base	Ligand	Solvent	Yield / %
1	$\text{CoI}_2$	$\text{CyMgCl}$	IPrHCl ( <b>13</b> )	DMPU	---
2	$\text{CoI}_2$	$\text{CyMgCl}$	ICyHCl ( <b>23</b> )	DMPU	21
3	$\text{CoI}_2$	$\text{CyMgCl}$	IAdHBF <sub>4</sub> ( <b>137</b> )	DMPU	traces
4	$\text{CoI}_2$	$\text{CyMgCl}$	<b>135</b>	DMPU	traces
5	$\text{CoI}_2$	$\text{CyMgCl}$	<b>138</b>	DMPU	10
6	$\text{CoI}_2$	$\text{CyMgCl}$	<b>140a</b>	DMPU	6
7	$\text{CoI}_2$	$\text{CyMgCl}$	<b>140b</b>	DMPU	---
8	$\text{CoI}_2$	$\text{CyMgCl}$	<b>144</b>	DMPU	traces
9	$\text{CoI}_2$	$\text{CyMgCl}$	<b>155</b>	DMPU	19
10	$\text{CoI}_2$	$\text{CyMgCl}$	<b>156</b>	DMPU	8



Entry	[Co]	Base	Ligand	Solvent	Yield / %
11	CoI <sub>2</sub>	CyMgCl	IBornHCl ( <b>157</b> )	DMPU	15
12	CoCl <sub>2</sub>	CyMgCl	ICyHCl ( <b>23</b> )	DMPU	15
13	CoBr <sub>2</sub>	CyMgCl	ICyHCl ( <b>23</b> )	DMPU	traces
14	Co(acac) <sub>2</sub>	CyMgCl	ICyHCl ( <b>23</b> )	DMPU	48
15	Co(acac) <sub>3</sub>	CyMgCl	ICyHCl ( <b>23</b> )	DMPU	28
16	Co(OAc) <sub>2</sub>	CyMgCl	ICyHCl ( <b>23</b> )	DMPU	traces
17	Co(acac) <sub>2</sub>	MeMgCl	ICyHCl ( <b>23</b> )	DMPU	traces
18	Co(acac) <sub>2</sub>	<i>t</i> -BuMgCl	ICyHCl ( <b>23</b> )	DMPU	Traces
19	Co(acac) <sub>3</sub>	<i>t</i> -BuCH <sub>2</sub> MgCl	ICyHCl ( <b>23</b> )	DMPU	35
20	Co(acac) <sub>2</sub>	CyMgCl	ICyHCl ( <b>23</b> )	THF	traces
21	Co(acac) <sub>2</sub>	CyMgCl	ICyHCl ( <b>23</b> )	NMP	30
22	Co(acac) <sub>2</sub>	CyMgCl	ICyHCl ( <b>23</b> )	DMPU	40 <sup>[b]</sup>

<sup>[a]</sup> Reaction conditions: **154** (0.50 mmol), **134a** (0.75 mmol), [Co] (10 mol%), ligand (10 mol%), base (2.0 equiv), solvent (1.5 mL), 23 °C, 16 h. <sup>[b]</sup> Reaction performed at 60 °C.



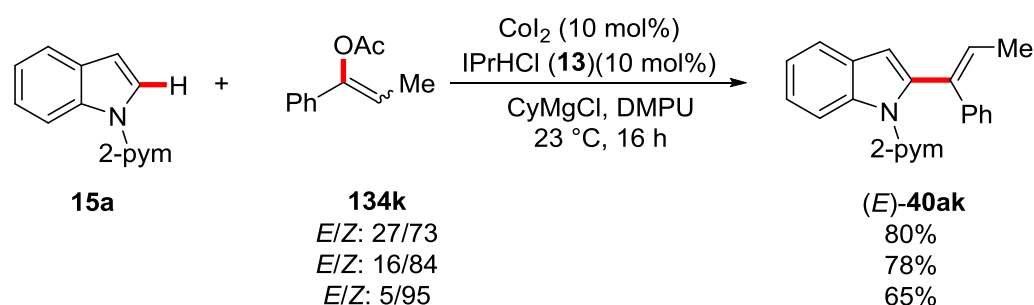
**Figure 3.2:** Additional (Pre)ligands for the Cobalt-Catalyzed alkenylation of ferrocenes.

Though the optimization studies just reached moderate yields, it represents the first example of cobalt-catalyzed C–H functionalization of ferrocenes. It should be noted that catalytic methods for alkenylation reactions on ferrocenes are rare<sup>[128]</sup> and most are accomplished by cost-intensive iridium<sup>[129]</sup> or palladium catalysts.<sup>[126b, 130]</sup> The only example based on ruthenium catalysis gave low yields.<sup>[131]</sup> Moreover, the above described methods require predominantly higher temperatures. On the route to

enantioselective C–H functionalizations on ferrocenes, our established system constitutes a promising basis.

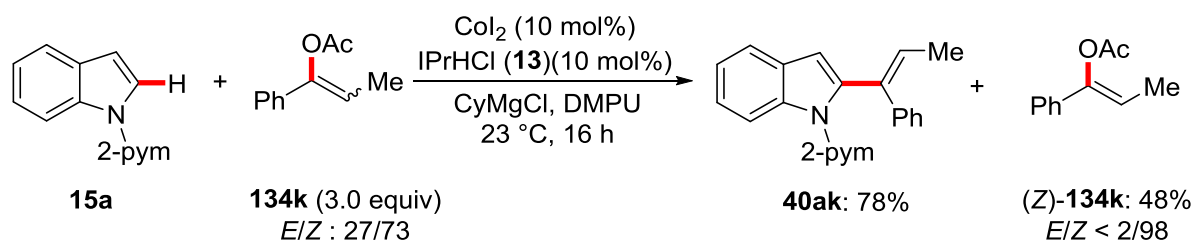
### 3.1.5 Mechanistic Studies

In order to get a deeper insight into the mechanism of this transformation, a series of experiments were performed to elucidate its mode of action. At first, the isomerization process of the enolate drew our attention. We wanted to know how the *E/Z* ratios of the acyclic enolates affect the reaction outcome. To answer this question, we repeated the reaction of pyrimidyl-indole (**15a**) and acetate **134k** (Table 3.8, entry 3) several times with different *E/Z* ratios of the alkenyl acetate (Scheme 3.5). Changing the ratio from *E/Z* 27/73 to 16/84 did not affect the yield significantly. Just when almost exclusively the *Z*-enolate was present with a ratio of 5/95, a small decrease in yield was the consequence. Again, in all three examples, the product **40ak** was isolated solely with (*E*)-configured double bond, where a complete isomerization from almost only (*Z*) to strictly (*E*) took place. Though this goes in hand with a slightly reduced yield, the affect of the ratio of isomers has just a minor effect on the reaction progress.



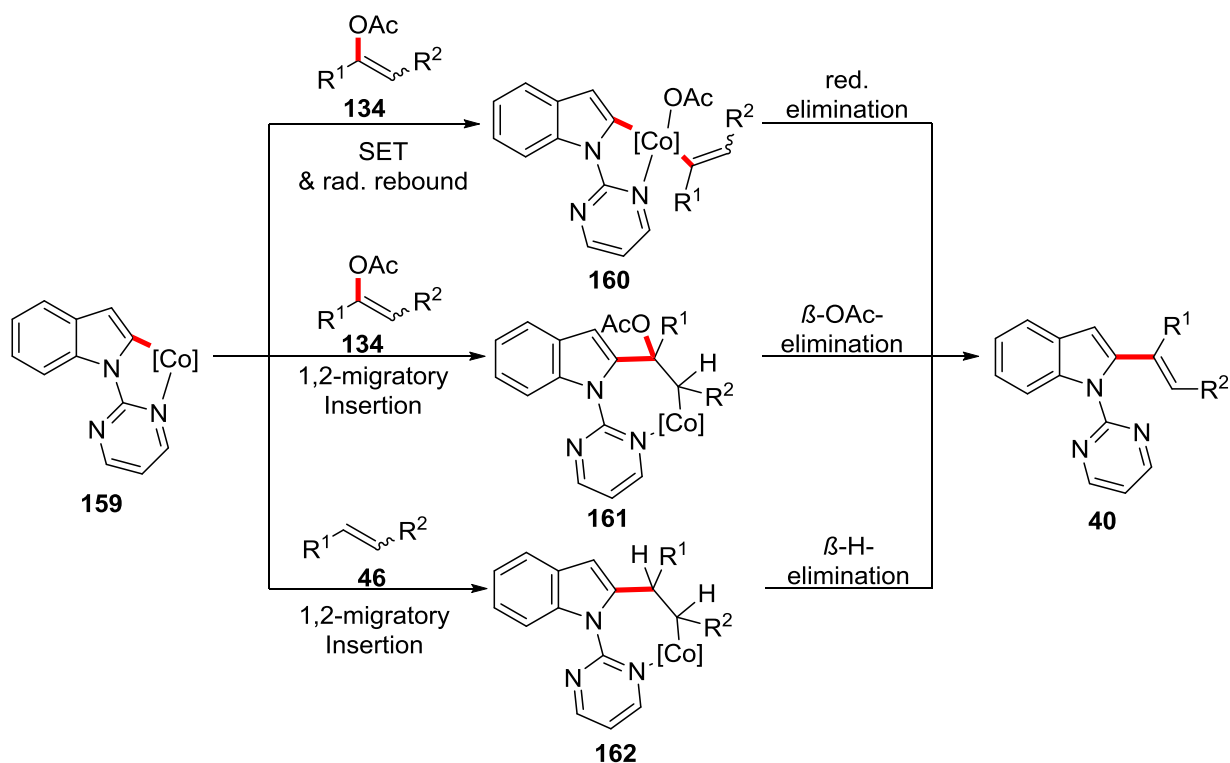
**Scheme 3.5:** Varying the isomeric ratio of the alkenyl acetate **134k**.

To further confirm the alkene isomerization process an excess of the enolate **134k** (3.0 equiv) was submitted to the reaction with the aim to explore the double bond configuration of the reisolated enolate (Scheme 3.6). As the yield and selectivity of the alkenylated product **40ak** stayed unaffected, the reisolated vinyl acetate **134k** was isolated in its pure isomer *Z*-isomer.



**Scheme 3.6:** Isomerization of the alkenyl acetate (**134k**).

With this isomerization process being identified, the focus was set to explore its origin, which is directly associated with the C–O activation and C–C bond forming processes. Starting from a cyclometalated cobalt complex **159**, three general pathways appear plausible for the activation of the alkenyl ester (Scheme 3.7). With respect to C–H alkylation and arylation reactions by low-valent cobalt catalysts (*vide supra*), a single electron transfer (SET) process was taken into consideration. Homolytical C–O bond cleavage would generate a cobalt acetate complex that, after subsequent radical recombination with the resulting alkenyl radical, would generate the oxidized complex **160**. Reductive elimination then delivers the product. Another possible pathway may commence with a 1,2-migratory insertion of the alkenyl acetate into the C–Co bond, generating a seven-membered cobaltacycle **161**.  $\beta$ -acetoxy elimination delivers the product and a cobalt-acetate species that, upon treatment with the Grignard reagent gives the active cobalt species. If we consider an insertion and  $\beta$ -elimination to be operative, not just the alkenyl acetate, but a possible *in situ* generated alkene **46** may also undergo insertion and  $\beta$ -H elimination delivers the product.

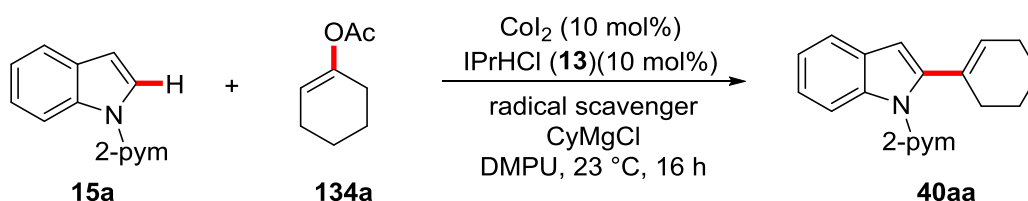


**Scheme 3.7:** Possible pathways for the C–O cleavage and C–C formation steps.

To check whether a radical mechanism is at work, radical scavengers, such as TEMPO or styrene were submitted to the reaction mixture (Table 3.10). The use of catalytic amounts of TEMPO did not affect the reaction outcome (entry 2), whereas one

equivalent lead to a significant drop in yield to 24% (entry 3). Also stoichiometric amounts of styrene decreased the yield (entry 4) with no detectable hydroarylation products.

**Table 3.10:** Influence of radical scavengers in the cobalt-catalyzed alkenylation.



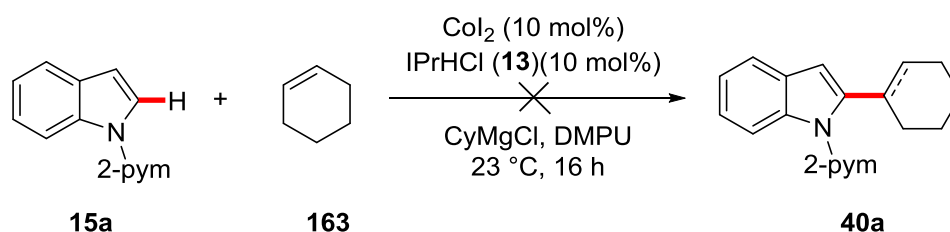
Entry	Radical Scavenger	Equiv	Yield / %
1	---		88
2	TEMPO	0.1	86
3	TEMPO	1.0	24
4	Styrene	1.0	42

<sup>[a]</sup> Reaction conditions: **15a** (0.50 mmol), **134a** (0.75 mmol), [Co] (10 mol%), ligand (10 mol%), base (2.0 equiv), solvent (1.5 mL), 23 °C, 16 h. <sup>[b]</sup> Reaction performed at 60 °C.

Judging from these results a complete rationalization whether a radical mechanism is operative cannot be made. Since TEMPO is a reactive compound, other inhibition reactions of TEMPO with the catalyst are possible. These include oxidation or coordination that will both inactivate the catalyst for the desired transformation. Also the loss of catalytic performance when styrene (1.0 equiv) is present can be contributed to other inhibition reactions. And even if a radical mechanism is assumed it cannot explain the remarkable stereoconvergent character of this reaction. Since the (*E*)- and (*Z*)-alkenyl radicals are both highly reactive species it is not reasonable why the (*Z*)-radical selectively rebounds to the cobalt. Moreover, since the formation of these radicals is related to the bond dissociation energy of the C–O bond, alkenyl halides with a weaker C–X bond are supposed to be more active. However, as shown above, cyclohexenyl bromide as well as cyclohexenyl chloride do not work at all (Table 3.1).

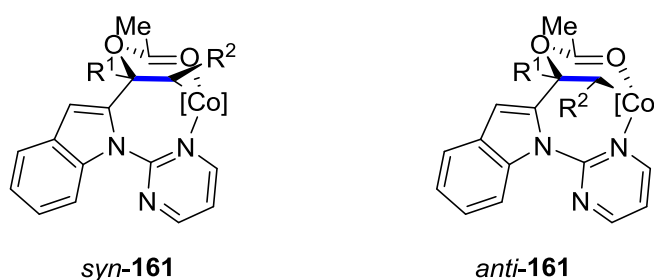
Thus, C–C bond formation by an insertion/elimination pathway seems plausible. The question is if it is the enolate that inserts into the C–Co bond or another, *in situ* formed species, e.g. the corresponding alkene which Kakiuchi and coworkers proposed for a

ruthenium-catalyzed alkenylation.<sup>[115a]</sup> To exclude this pathway, the cyclohexenyl acetate **134** was replaced by cyclohexene (**163**) with the result that no reaction, neither alkenylation, nor hydroarylation, took place (Scheme 3.8). Moreover, the insertion of an alkene would also lead to regioisomeric mixtures which were never observed for any compound.



**Scheme 3.8:** Attempted alkenylation or hydroarylation with cyclohexene (**163**).

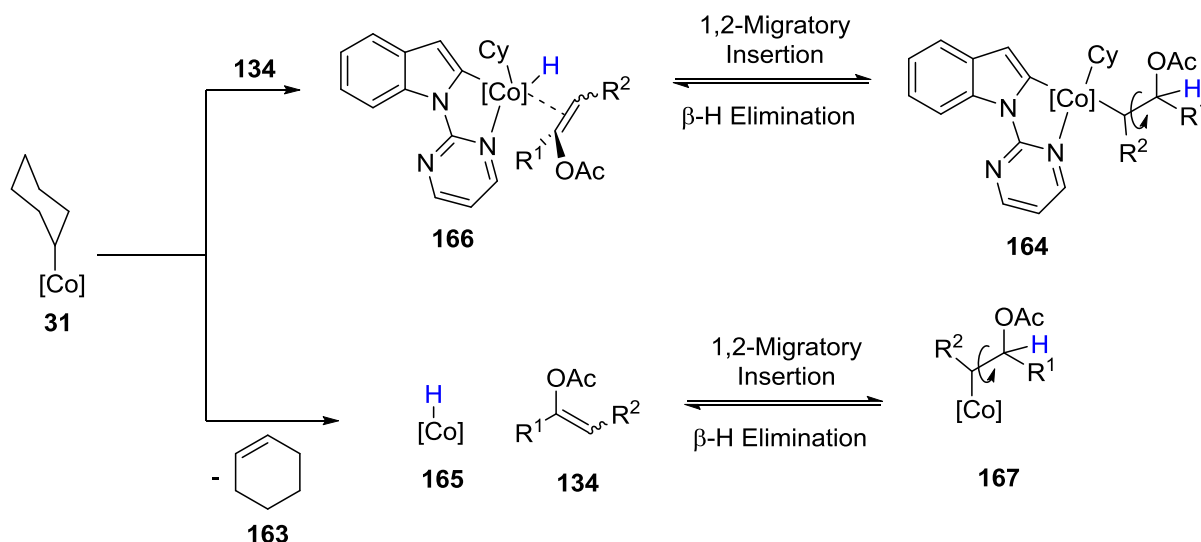
Though insertion of an enolate followed by  $\beta$ -O-elimination seems to be plausible, the origin of the stereoconvergent character is not completely understood which is also attributed to the fact that the exact coordination sphere on the cobalt is not clear. Furthermore, assumptions can be made regarding a possible scenario for the divergent reaction manifold. The 1,2-migratory insertion will proceed in a *syn* fashion and is most likely an irreversible step. To the thus formed 7-membered cobaltacycle a secondary interaction of the acetate to the cobalt may take place that will form a cobalta bicyclo[4.3.1] species giving either *syn*-**161** after insertion of the *E*-enolate or hypothetically *anti*-**161** for the *Z*-enolate, respectively (Figure 3.3). As rotation about the C–C bond (marked in blue) is not possible, the insertion step is also selectivity-determining and a conversion from *syn*-**161** to *anti*-**161** can be omitted. The reason why the proposed *syn*-intermediate is formed solely can be explained by either the higher reactivity of the *E*-enolate and/or a preferred geometry of the intermediate.



**Figure 3.3:** Insertion of alkenyl acetate **134** with *syn*- and *anti*- configured intermediates.

This however, also means that the alkenyl ester isomerization takes place prior to the irreversible insertion step.

Therefore, another insertion reaction with a free rotation among the carbon-carbon bond appears plausible. In particular, the insertion reaction of a double bond in cobalt-hydrogen bond is well known for C–H activation (*vide supra*), but also hydroformylations.<sup>[28]</sup> In this reaction, the formation of two cobalt-hydride complexes is possible (Scheme 3.9). The most feasible results from the C–H activation step by an oxidative addition, as this C–H activation step is postulated for the most low-valent cobalt reactions. Usually, reductive elimination of an alkane (the alkyl rest results from the Grignard) generates the active species. However, it is also possible that the double bond inserts in the Co–H bond (upper path). As rotation among the C–C bond is possible in complex **164**, both isomers can be found after subsequent  $\beta$ -hydride elimination. Alternatively, after transmetalation with the Grignard reagent, the cobalt alkyl species **31** may undergo  $\beta$ -hydride elimination resulting in a cobalt hydride species **165** which can also perform this isomerization (lower path).

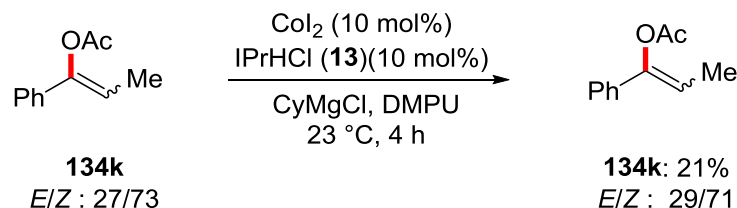


**Scheme 3.9:** Possible pathways for the isomerization of alkenyl esters.

The 1,2-migratory insertion of a double bond into a metal–hydride bond as well as the reverse  $\beta$ -hydride elimination are usually much faster for many transition metals than the insertion into a M–C bond, followed by  $\beta$ -O elimination.<sup>[132]</sup> For this, the upper path appears possible, as a fast process prior to reductive elimination of cyclohexane from **166** which then enables the C–C bond formation.

To exclude the lower pathway, the isomerization reaction (Scheme 3.6) was performed in absence of the pyrimidyl indole (**15a**) for alkenyl acetate **134k** (Scheme 3.10). Surprisingly, the alkenyl esters suffers from a rapid degradation that just 21% can be

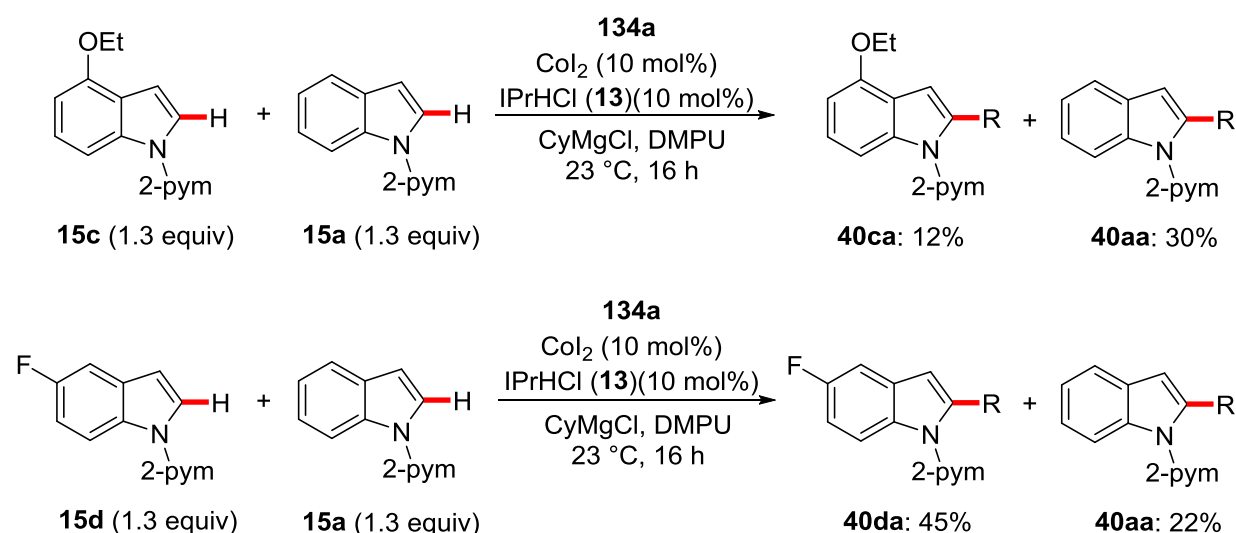
isolated after 4 h reaction time. However, its *E/Z* ratio stays unchanged within the margin of accuracy. Among others, coupling with the Grignard reagent occurred (Table 3.1).



**Scheme 3.10:** Attempted isomerization of alkenyl acetate **134k** in absence of pyrimidyl indole.

In view of the low mass balance and, the assumption can at least be made that an isomerization process may not occur in the absence of the pyrimidyl indole **15**.

Given this remarkable stereoconvergent character of the C–H alkenylation reaction, further mechanistic experiments were performed to unravel its mode of action. To explore electronic effects on the indole, competition experiments between electron-rich **15c** and electron-deficient arenes **15d** were performed (Scheme 3.11). In particular, two competition experiments between both the electronically modified arene and the neutral pyrimidyl indole (**15a**) were conducted. With this setup, we could *i*) exclude a positional dependence of the functional group, *ii*) omit any sort of interaction between the arenes and *iii*) get a hint whether any other effects of the functional group have a further effect. The first experiment between the electron rich arene **15c** and the standard pyrimidyl indole (**15a**) clearly renders the one bearing an ethoxy group as less reactive. In contrast, when employing an electron-deficient fluoroindole **15d**, it turned out to be more reactive than the neutral indole **15a**. From these two experiments, the conclusion can be made that electron-deficient arenes show higher reactivity than electron neutral arenes, which are still more active than electron rich arenes. These experiments are in good agreement with those conducted for cobalt-catalyzed alkylation and arylations.<sup>[32, 36, 39]</sup>



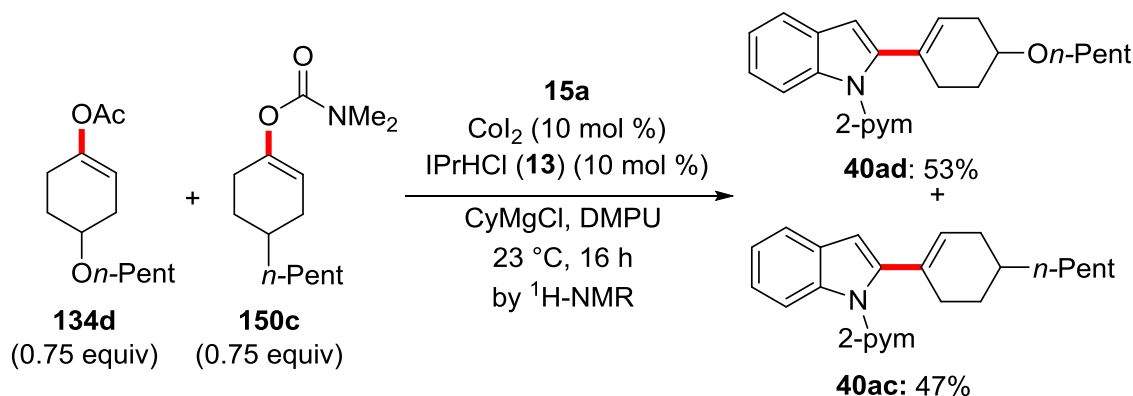
**Scheme 3.11:** Intermolecular competition experiment between different indoles. R = 1-Cyclohexenyl.

Moreover, two findings are notable. First, the experiment with the electron-rich arene **15c** gave a less overall yield as the one with the electron-deficient one (42% versus 67% combined yield). Second, though indole **15d** reacted preferentially, its yield in the single experiment is lower than the one with pyrimidyl indole (**15a**) (75% versus 88% isolated yield, Table 3.6). The lower overall yield can be rationalized in terms of a minor reactivity of the 4-ethoxy indole **15c** compared to the 5-fluoro derivative **15d**. It can be explained by a faster oxidative addition step of the fluoro arene **15d** which is supposed to be irreversible (*vide infra*). Hence, the fluoroarene binds most of the active cobalt species irreversibly and less is left for the other arene. The following steps (elimination, insertion of the enolate etc) are apparently slower for the electron-deficient arene as for electron-neutral one.

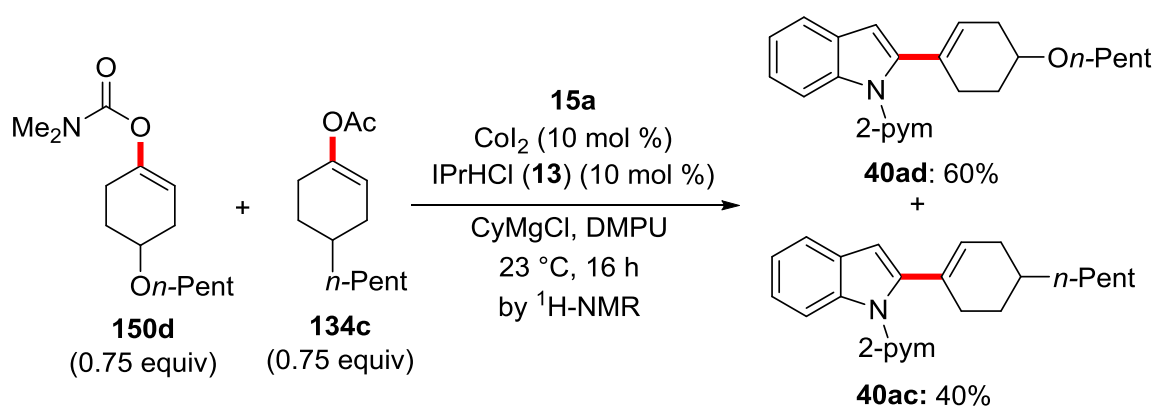
With the behavior of indoles in hand, we now tested the impact of the alkenyl esters on the reaction progress. Since alkenyl acetates, carbamates and phosphates, provided very good yields, competition experiments were of certain interest to identify the most reactive ester. Thus, intermolecular competition experiments between different enolates were performed. To distinguish both alkenyl esters those with a pentyl and pentoxy group at the 4-position of the cyclohexenyl moiety were tested as we first assumed that these alkenyl rests show similar reactivity. We first compared alkenyl acetates **134** and carbamates **150** (Scheme 3.12). To check whether the pentyl or pentoxy groups make a difference in the reaction, both esters with both groups were tested. Indeed, we observed that the 4-pentoxycyclohexenyl ester reacted preferentially in both cases. Judging from the conversion that was determined by <sup>1</sup>H-NMR spectroscopy, no significant difference between alkenyl acetates and carbamates could be measured.



(a) competition experiment between enol acetate **134d** and carbamate **150c**

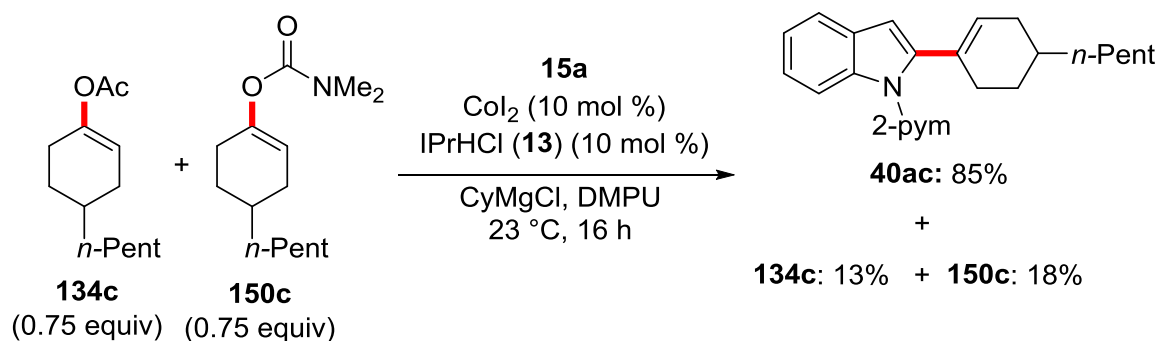


(b) competition experiment between enol acetate **134c** and carbamate **150d**



**Scheme 3.12:** Intermolecular competition experiments I between enol acetates **134** and carbamates **150**.

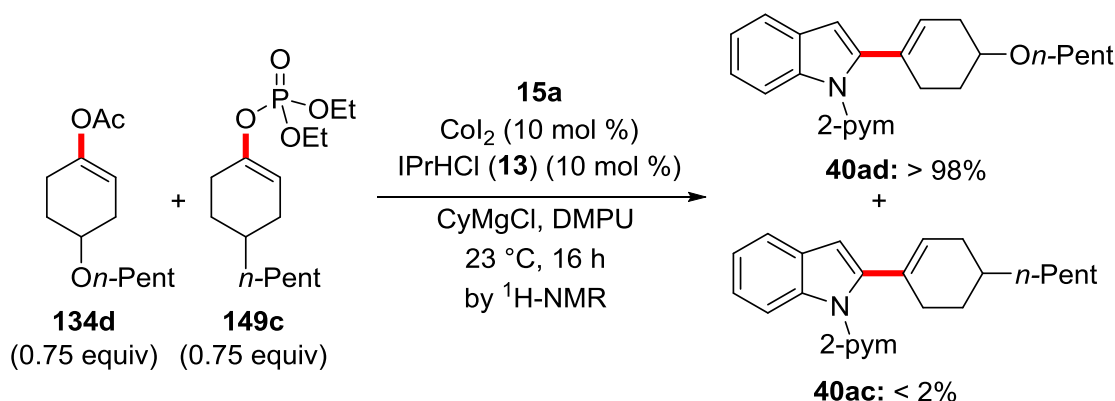
However, the significant dependence of the rest on the cyclohexenyl group demanded another kind of experiment. To exclude any effects on the substitution pattern, a competition experiment between vinyl acetate **134c** and carbamate **150c** with the same ester rest was conducted. As both enolates delivered the same product the preference in reactivity was determined by the reisolated alkenyl esters (Scheme 3.13). In terms of reproducibility, with 13% reisolated vinyl acetate **134c** and 18% reisolated vinyl carbamate **150c**, the amount of converted enolates is almost identical. As a consequence, we assume that vinyl acetates showed similar reactivity as carbamates, presupposed that the alkenyl acetate **134c** and carbamate **150c** have similar stability under the present reaction conditions.



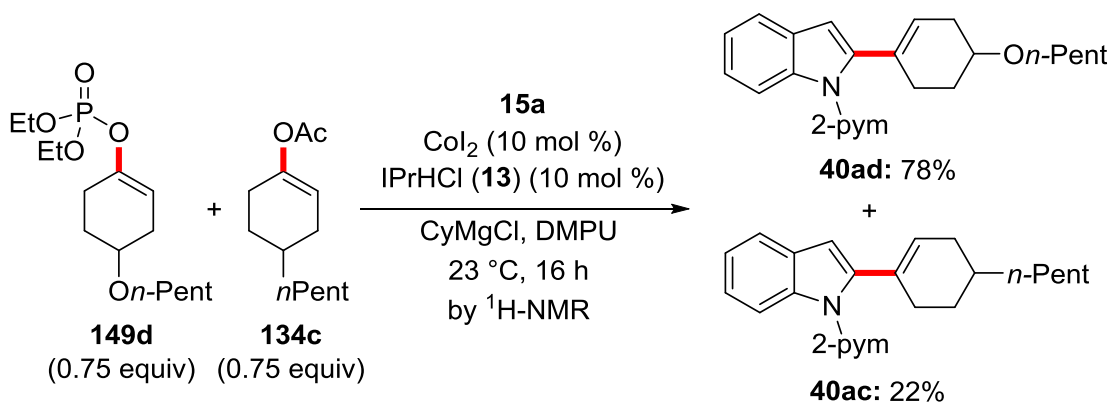
**Scheme 3.13:** Intermolecular competition experiments II between alkenyl acetates **134** and carbamates **150**.

The same types of experiments were conducted again to compare the reactivity between vinyl acetates **134** and phosphates **149**. Again at first, intermolecular competition experiments between alkenyl acetates and phosphates bearing a 4-pentylcyclohexenyl or 4-pentoxycyclohexenyl were performed (Scheme 3.14). The increased reactivity of the pentoxy *versus* the pentyl group was observed for both enolates. However, a significant difference in reactivity between acetates and phosphates was observed as well. With the vinyl acetate **134d** against the vinyl phosphate **149c**, only the acetate converted to the product, as far as determinable by  $^1\text{H-NMR}$  spectroscopy (Scheme 3.14a). In the cross experiment with the vinyl acetate **134c** and phosphate **149d**, the alkenyl phosphate showed higher conversion, but with significant conversion of the alkenyl acetate with a ratio of 78% to 22% (Scheme 3.14b).

(a) competition experiment between enol acetate **134d** and phosphate **149c**

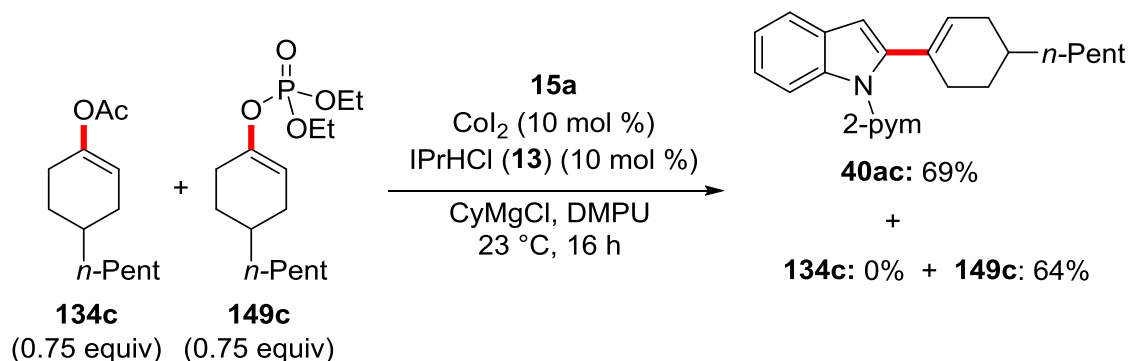


(b) competition experiment between enol acetate **134c** and phosphate **149d**



**Scheme 3.14:** Intermolecular competition experiments between alkenyl acetates **134** and phosphates **149**.

When using the same rests for the alkenyl acetate and phosphate, no alkenyl acetate **134c** could be reisolated whereas 64% of the alkenyl phosphate **149c** were recollected (Scheme 3.15). Again, it is assumed that both alkenyl acetate **134c** and phosphate **149c** afford the same stability under the present reaction conditions.



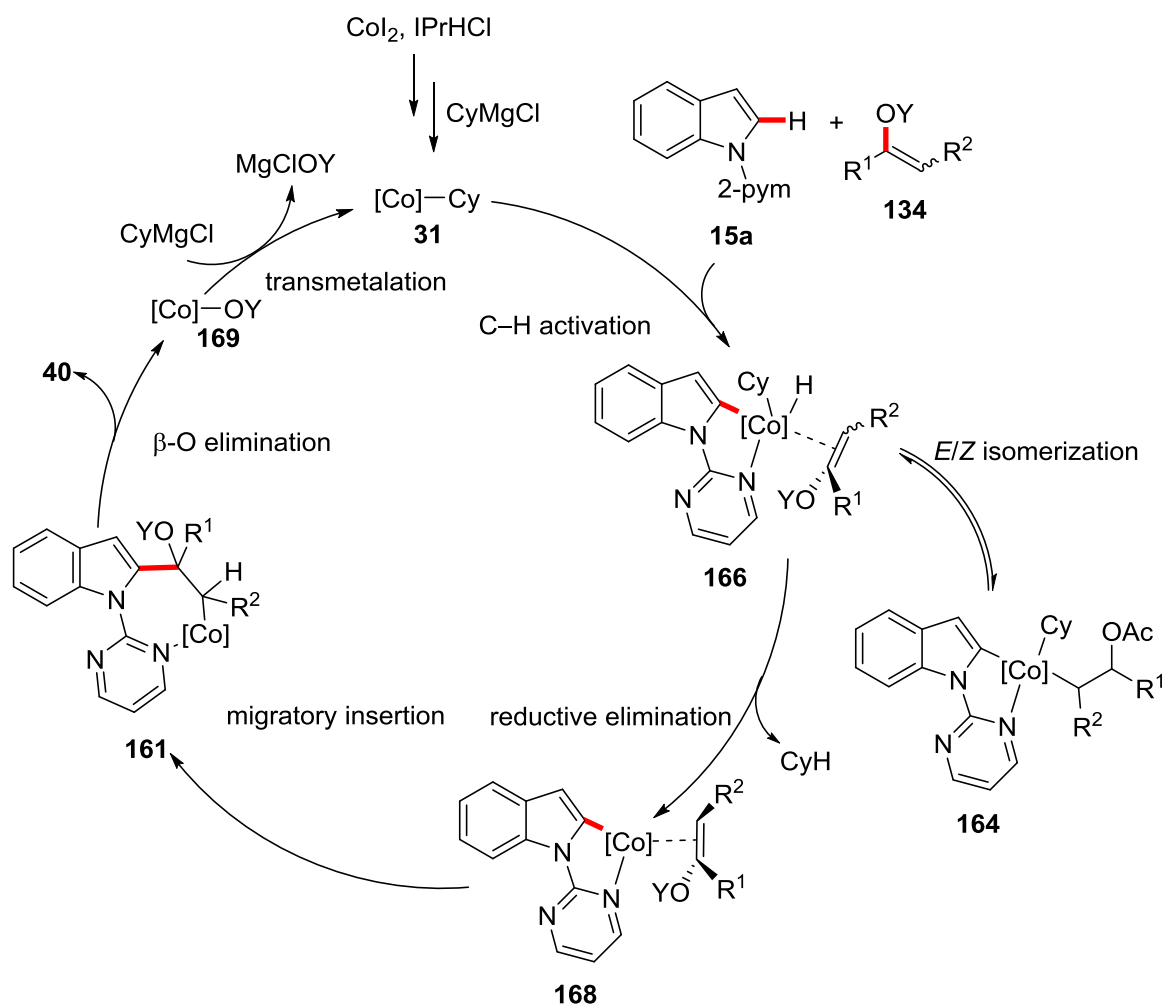
**Scheme 3.15:** Intermolecular competition experiment II between alkenyl acetates **134** and phosphates **149**.

These findings render alkenyl phosphates less reactive than acetates. Therefore, the following order of reactivity could be established for alkenyl electrophiles:



These findings appear surprising as they are not in order with the C–O dissociation energies.

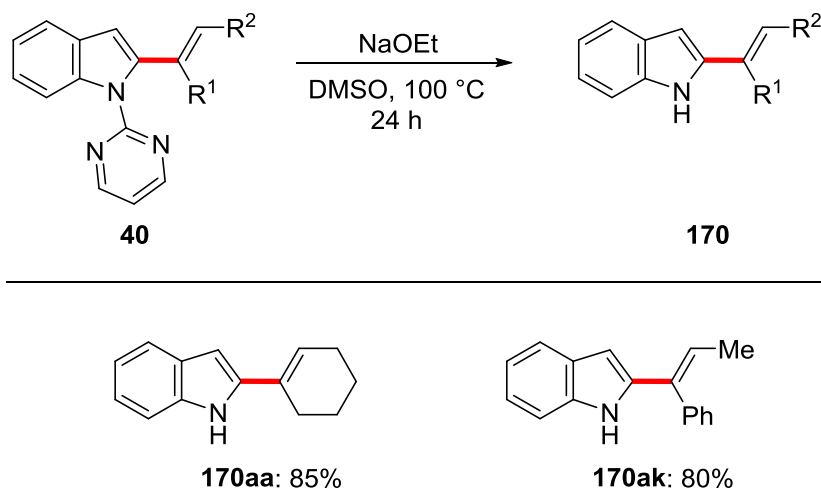
Based on our mechanistic findings, the cycle for the cobalt-catalyzed alkenylation commences with the generation of a low-valent organocobalt species **31** (Scheme 3.16). C–H activation by oxidative addition follows to give a cobalt-hydride species **166**. This complex can further react in two ways, (i) reversible migratory insertion of the alkenyl ester into the Co–H bond leads to isomerization of the double and (ii) irreversible reductive elimination delivers the complex **168** by the loss of cyclohexane. This allows for 1,2-migratory insertion into the Co–C bond yielding the 7-membered cobaltacycle **161**. Finally,  $\beta$ -O elimination yields the product **40** and transmetalation of the cobalt-acetate **169** complex with the Grignard reagent regenerates the active catalyst **31**.



**Scheme 3.16:** Postulated catalytic cycle for the cobalt-catalyzed alkenylation with alkenyl esters.

### 3.1.6 Cleavage of the Pyrimidyl Directing Group

Finally the removal of the pyrimidyl directing group provided access to 2-alkenylated *NH*-free indoles **170** which amplifies the applicability of this novel transformation. A general method to cleave to pyrimidyl rest by treatment with sodium ethanolate was established by our group.<sup>[122]</sup> To our delight, this procedure could be applied to 2-alkenylated pyrimidyl indoles, which is shown for a cyclic as well as a non-cyclic alkenyl group (Scheme 3.17). The cleavage led to very good yields without double bond isomerization



**Scheme 3.17:** Cleavage of the pyrimidyl directing group.

## 3.2 Cobalt-Catalyzed C–H Alkylation with Allyl Acetates

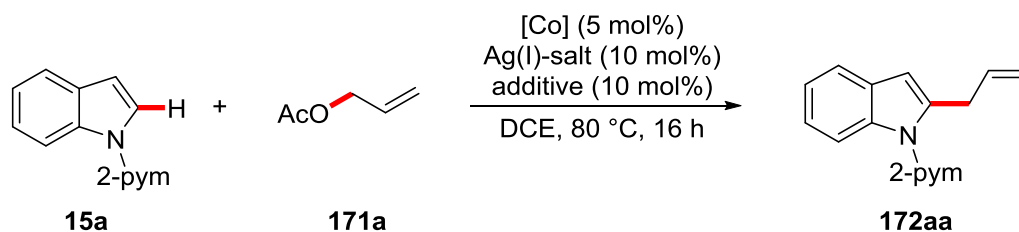
Though a broad range of important transformations could be achieved by low-valent cobalt catalysis, the use of a Grignard reagent somehow limits the functional group tolerance and demanded for milder reaction conditions for cobalt catalysis. With the successful application of Cp\*Co(III) catalysis in C–H activation in 2013,<sup>[51]</sup> Matsunaga/Kanai made major advances this aim. With the idea of installing a modifiable allyl group on a molecule, a C–H alkylation reaction by mild and robust Cp\*Co(III) catalysis gained our interest.

### 3.2.1 Optimization Studies

For establishing a C–H alkylation strategy, optimization reactions should unravel the best catalytic system in terms of mild and robust with a stable and easy accessible allyl source. With the success we have made with C–C forming reactions by C–H/C–O activation and in particular the cleavage of C–OAc bonds, we chose allyl acetate **171a** as inexpensive, stable and, for allyl compounds, relatively harmless compound.<sup>[133]</sup> We also selected indole as model heteroarene due to its key importance<sup>[112, 134]</sup> and because of the easy attachment and removal of the pyrimidyl or pyridyl directing groups.<sup>[122]</sup>

We initiated our studies by taking the cobalt complex  $[\text{Cp}^*\text{Co}(\text{CO})\text{I}_2]$ ,<sup>[135]</sup> a silver(I) salt to remove the iodide from the complex and catalytic amounts of a carboxylate to generate the active catalytic species (Table 3.11). Among screening these two additives,  $\text{AgSbF}_6$  and KOAc provided almost quantitative conversion with 96% yield (entry 2). Similar results were obtained when using pivalic acid instead of KOAc (entry 4). In contrast, attempts to replace the costly silver salt by the cationic cobalt complex  $[\text{Cp}^*\text{Co}(\text{PhH})](\text{PF}_6)_2$  (entries 6-7) or the dimer  $[\text{Cp}^*\text{CoCl}_2]_2$  (entry 8) were unsuccessful. To check whether an organometallic cobalt complex is necessary, simple cobalt salts, such as  $\text{Co}(\text{OAc})_2$  and  $\text{CoCl}_2$ , were tested, but without any success (entries 9 and 10). The choice of the silver counteranion was equally crucial. Replacing the hexafluoroantimonate anion by an also weakly-coordinating hexafluorophosphate anion led to a decreased yield of 18% (entry 12). It could be questioned whether catalytic amounts of potassium acetates were necessary, since stoichiometric amounts of acetate are generated during the reaction. Indeed, omitting this additive just gave minor yields of 29% (entry 5). Most likely, catalytic amounts of KOAc are needed to generate the active cobalt complex (*vide infra*). Moreover, the reaction did not take place in the absence of a cobalt or a silver source (entries 13 and 14).

**Table 3.11:** Optimization studies for the cobalt-catalyzed allylation with allyl acetates.<sup>[a]</sup>



Entry	[Co]	Ag(I)-salt	Additive	Yield / %
1	$[\text{Cp}^*\text{Co}(\text{CO})\text{I}_2]$	$\text{AgSbF}_6$	$\text{K}_2\text{CO}_3$	14
2	$[\text{Cp}^*\text{Co}(\text{CO})\text{I}_2]$	$\text{AgSbF}_6$	KOAc	96
3	$[\text{Cp}^*\text{Co}(\text{CO})\text{I}_2]$	$\text{AgSbF}_6$	NaOAc	75
4	$[\text{Cp}^*\text{Co}(\text{CO})\text{I}_2]$	$\text{AgSbF}_6$	PivOH	94
5	$[\text{Cp}^*\text{Co}(\text{CO})\text{I}_2]$	$\text{AgSbF}_6$	---	29
6	$[\text{Cp}^*\text{Co}(\text{PhH})](\text{PF}_6)_2$	$\text{AgSbF}_6$	KOAc	traces
7	$[\text{Cp}^*\text{Co}(\text{PhH})](\text{PF}_6)_2$	---	KOAc	traces

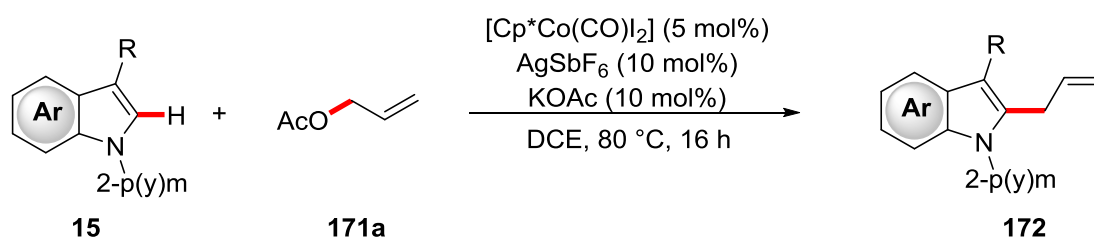
Entry	[Co]	Ag(I)-salt	Additive	Yield / %
8	[Cp*CoCl <sub>2</sub> ] <sub>2</sub>	---	KOAc	---
9	Co(OAc) <sub>2</sub>	AgSbF <sub>6</sub>	KOAc	---
10	CoCl <sub>2</sub>	AgSbF <sub>6</sub>	KOAc	---
11	[Cp*Co(CO)I <sub>2</sub> ]	AgCO <sub>3</sub>	KOAc	5 <sup>[b]</sup>
12	[Cp*Co(CO)I <sub>2</sub> ]	AgPF <sub>5</sub>	KOAc	18
13	---	AgSbF <sub>6</sub>	KOAc	---
14	[Cp*Co(CO)I <sub>2</sub> ]	---	KOAc	---

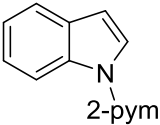
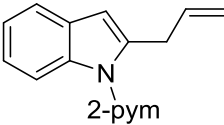
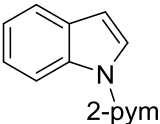
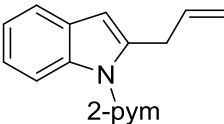
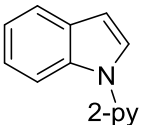
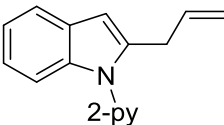
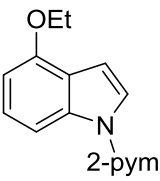
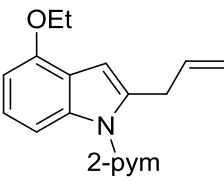
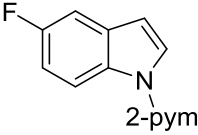
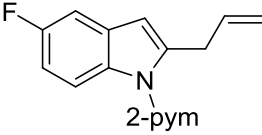
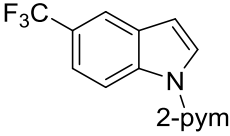
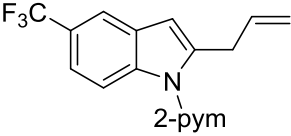
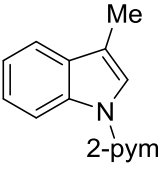
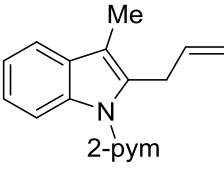
<sup>[a]</sup> Reaction conditions: **15a** (0.50 mmol), **171a** (1.00 mmol), [Co] (5 mol%), additive (10 mol%), DCE (1.5 mL), 80 °C, 16 h. <sup>[b]</sup> GC-conversion using *n*-dodecane as internal standard.

### 3.2.2 Scope of the Cobalt-Catalyzed C–H Allylation with Allyl Acetates

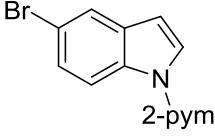
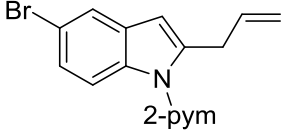
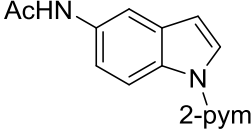
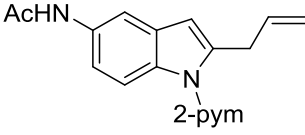
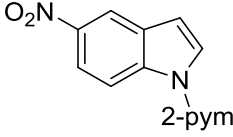
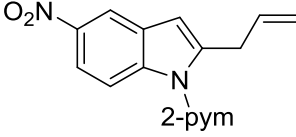
With the optimized reaction conditions in hand, the range of application was examined, beginning with the substitution pattern on the indole (Table 3.12). As for the directing group, both the pyrimidyl (entry 1) and pyridyl (entry 3) group succeeded in the reaction, with somewhat better results for the pyrimidyl group. A reaction on a 2 mmol scale worked as well with comparable yield (entry 2). Substitution on the indole was successfully tested on the 4,5 and the sterically more challenging 3 position with very good yields (entries 4-7). More importantly, the labile aryl bromide bond was unproblematic (entry 8), as well as the basic amide group (9) and even a nitro group furnished the desired product in very good yield (entry 10). That could not be taken for granted, as nitro groups caused problems in ruthenium-catalyzed reactions (*vide infra*) and the starting material **15i** as well as the allylated product **172ia** have very poor solubility in DCE and related solvents. Moreover, also electron-rich, and electron-deficient arenes were tolerated well (entries 4 and 5,6).

**Table 3.12:** Scope of indoles **15** in the cobalt-catalyzed C–H allylation.<sup>[a]</sup>



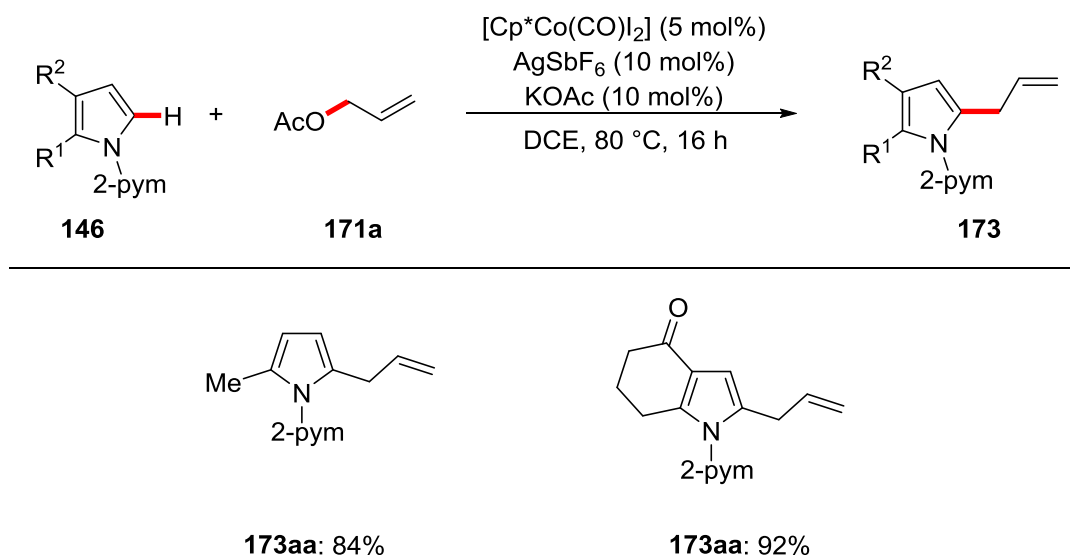
Entry	Indole	Product	Yield / %
1	 <b>15a</b>	 <b>172aa</b>	96
2	 <b>15a</b>	 <b>172aa</b>	92 <sup>[b]</sup>
3	 <b>15b</b>	 <b>172ba</b>	76
4	 <b>15c</b>	 <b>172ca</b>	89 <sup>[c]</sup>
5	 <b>15d</b>	 <b>172da</b>	94
6	 <b>15e</b>	 <b>172ea</b>	84 <sup>[c]</sup>
7	 <b>15f</b>	 <b>172fa</b>	93 <sup>[c]</sup>



Entry	Indole	Product	Yield / %
8	 <b>15g</b>	 <b>172ga</b>	95
9	 <b>15h</b>	 <b>172ha</b>	78 <sup>[c]</sup>
10	 <b>15i</b>	 <b>172ia</b>	91 <sup>[c]</sup>

<sup>[a]</sup> Reaction conditions: **15** (0.50 mmol), **171a** (1.00 mmol), [Cp\*Co(CO)I<sub>2</sub>] (5 mol%), KOAc (10 mol%), DCE (1.5 mL), 80 °C, 16 h. <sup>[b]</sup> 2 mmol scale, <sup>[c]</sup> Performed by N. Sauermann.

The reaction was not limited to indoles **15**, but proved also applicable to pyrroles **146** (Scheme 3.18), shown for two representative examples.

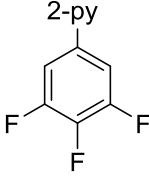
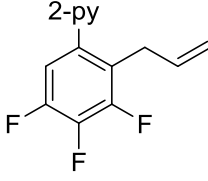


**Scheme 3.18:** Cobalt-catalyzed allylation of pyrroles **146**.

The scope of this reaction was not restricted to heteroarenes, but also arenes bearing a pyridyl or pyrimidyl directing group could be C–H allylated well (Table 3.13). Representative examples of aryl pyri(mi)dines **14** were allylated highly regioselectively at the *ortho*-position to the directing group with moderate to good yields. As the applicability of these compounds was limited, especially due to the lack of the directing group removal, the scope was not further extended. However, in contrast to indoles (Table 3.12), electronic properties had a significant impact on the reaction outcome in the way that electron-deficient arenes (entries 1,3,4) showed somewhat better yields than electron-neutral or rich arenes (entry 2). Though the difference is not very high, it is all in all a remarkable finding, because related C–H allylation reactions with rhodium<sup>[136]</sup> and parallel and follow-up efforts with cobalt<sup>[59, 137]</sup> delivered higher yields for electron-rich arenes.

**Table 3.13:** Cobalt-catalyzed allylation of phenyl pyri(mi)dines.<sup>[a]</sup>

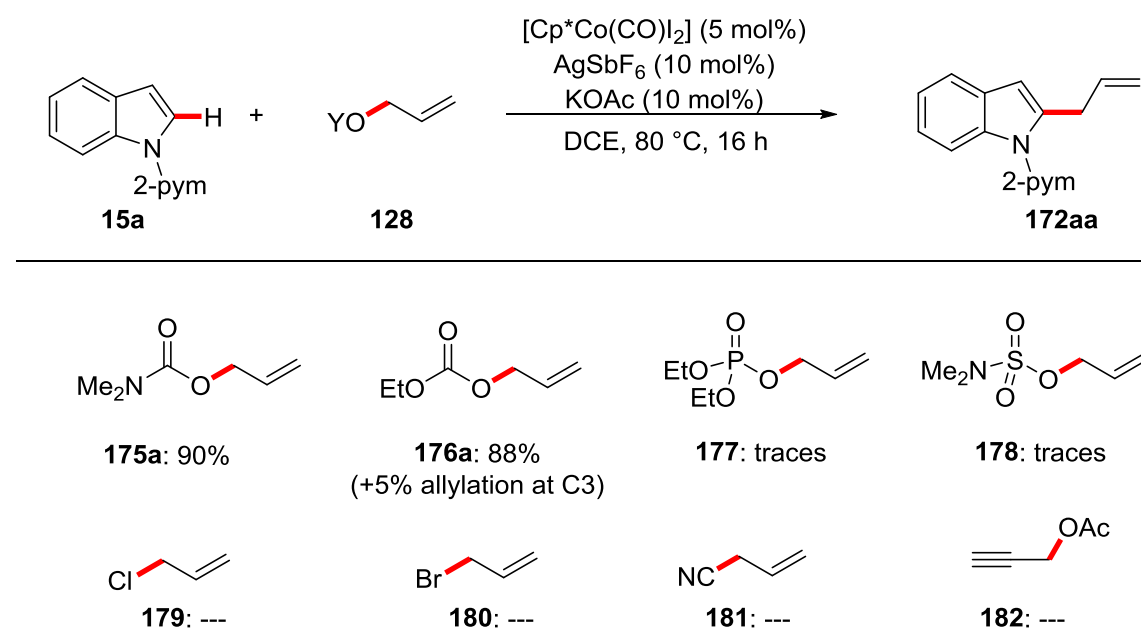
Entry	<b>14</b>	<b>174</b>	Yield / %
1	 <b>14b</b>	 <b>174ba</b>	57
2	 <b>14c</b>	 <b>174ca</b>	35
3	 <b>14e</b>	 <b>174ea</b>	61

Entry	14	174	Yield / %
4	 <p><b>14f</b></p>	 <p><b>174fa</b></p>	62

<sup>[a]</sup> Reaction conditions: **14** (0.50 mmol), **171a** (1.00 mmol), [Cp\*Co(CO)I<sub>2</sub>] (5 mol%), KOAc (10 mol%), DCE (1.5 mL), 80 °C, 16 h.

With the outstanding versatility towards different arenes and the great functional group tolerance in hand, we next tested differently substituted allyl acetates **171**. Unfortunately, the catalytic system turned out to be highly sensitive towards any substitution on the allyl moiety with the consequence of poor conversion and low selectivity under the optimized reaction conditions. Within a careful optimization for substituted allyl acetates J. Koeller discovered that the use of the bulky 1-AdCO<sub>2</sub>H instead of KOAc enabled the reaction with crotyl acetate to give a mixture of isomers in 63% overall yield.<sup>[138]</sup> The connectivity of the product mixture resembles to a S<sub>N</sub>/S<sub>N</sub>' ratio of 1.8.

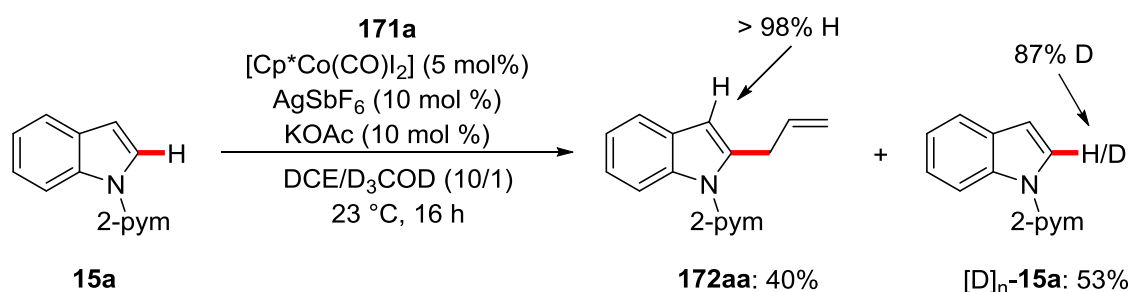
Then, different leaving groups on the allylic position have been tested (Scheme 3.19). We were pleased to observe that the C–H/C–O activation strategy can be extended to the use of allyl carbamates **175** and carbonates **176**, which also gave minor amounts of the C3-allylated product. In the latter case, Glorius and coworkers reported the cobalt-catalyzed allylation with allyl carbonates in a concurrent contribution.<sup>[59, 137a]</sup> In contrast, phosphates **177** and sulfamates **178** just led to minimal conversion and allyl halides **179** and **180** as well as cyanides **181** failed completely.



**Scheme 3.19:** Cobalt-catalyzed allylation with different electrophiles.

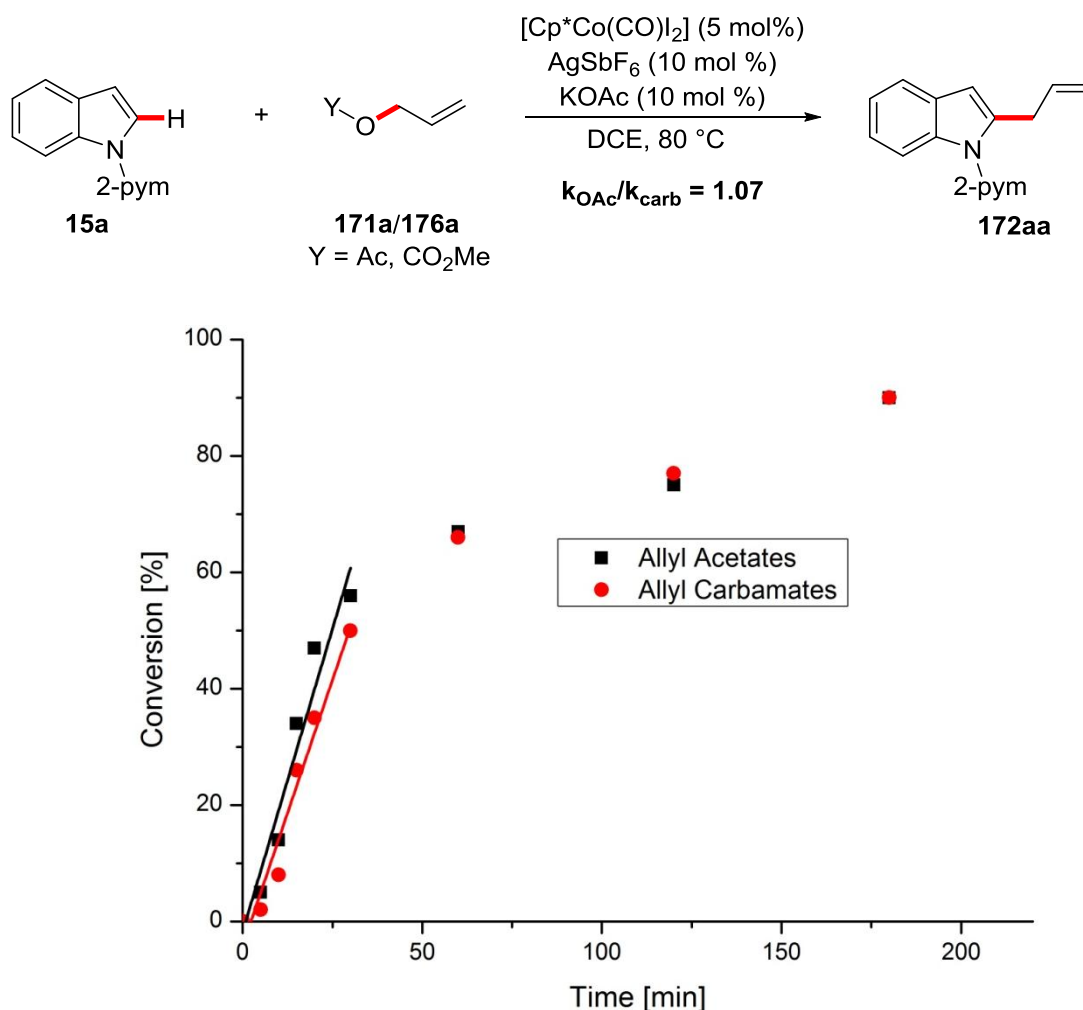
### 3.2.3 Mechanistic Studies

To get a better understanding of the reaction mechanism, experiments should shine light into its pathway. First, the reaction was performed in the presence of the deuterated co-solvent  $CD_3OD$  (Scheme 3.20) to examine the process of the C–H activation. No deuteration could be detected in the product **172aa**, whereas almost complete deuteration was observed at the C-2 position of the reisolated starting material  $[D]_n$ -**15a**. This result gave strong support for a reversible C–H metalation step. The fact that no deuterium was incorporated in the product molecule obviates a simple electrophilic type C–H activation which would result in deuteration at the C-3 position and also demonstrates the selective functionalization in the C-2 position *versus* an also possible C–H activation at the C-7 position which was observed in a related ruthenium-catalyzed C–H allylation.<sup>[139]</sup>



**Scheme 3.20:** H/D exchange with  $D_2O$  as the co-solvent.

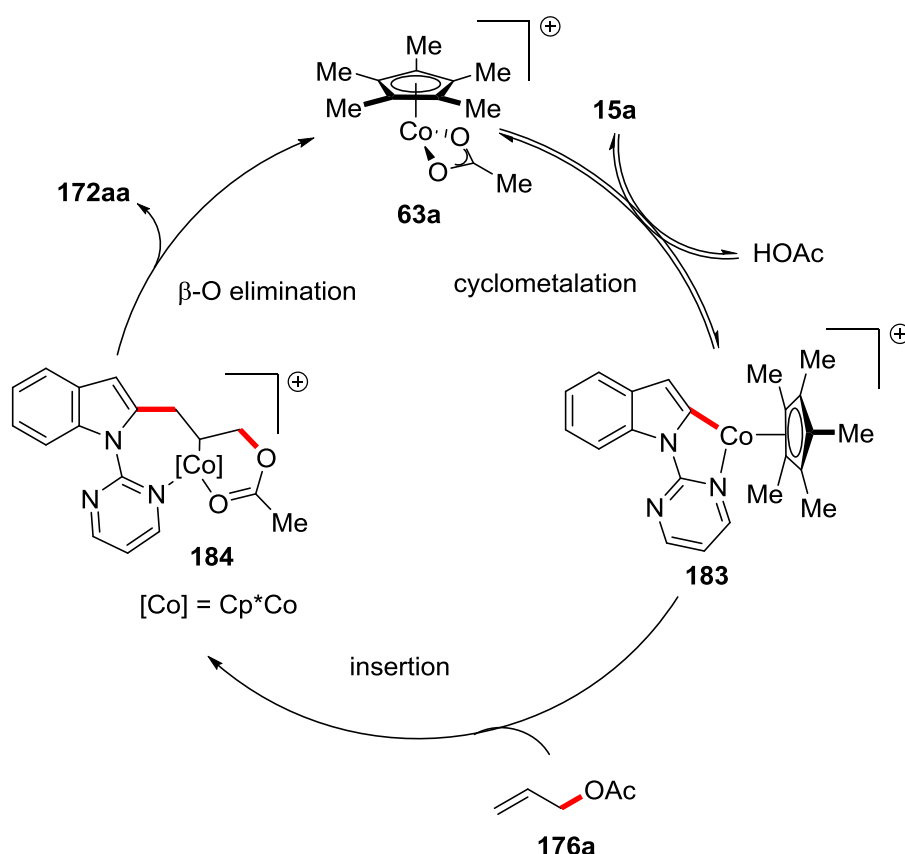
With the success of allyl acetates, carbamates and carbonates in the present reaction, we wanted to know, if the C–O cleavage has an effect on the initial rates for this reaction. To answer this question, the initial rates of the allylation reaction with allyl acetate (**171a**) and of the reaction with allyl carbonate **176a** were determined (Scheme 3.21). We chose these two substrates, because it is possible that these reactions proceed by different pathways. However, within the margin of error, no significant difference could be observed. Therefore it can be postulated that the reactivity of allyl acetate (**171a**) and allyl carbonate **176a** is identical.



**Scheme 3.21:** Intermolecular competition experiment between allyl acetate (**171a**) and carbamate **176a**. Conversion determined by GC using *n*-dodecane as internal standard.

Based on our mechanistic findings for this transformation, as well as on the findings for related reactions by other groups,<sup>[59, 137]</sup> we postulate the following catalytic cycle in which the active cobalt species is generated from the precatalyst  $[\text{Cp}^*\text{Co}(\text{CO})\text{I}_2]$  to result in a cationic  $[\text{Cp}^*\text{Co}(\text{OAc})]^+$  species **63a** (Scheme 3.22). This complex coordinates to the directing group and performs a reversible C–H activation presumably by a CMD/AMLA

type mechanism.<sup>[14b, 61]</sup> That can form a resting state (not shown) by coordination of an acetate anion to form a stable 18 VE complex. A related complex with phenyl pyridine was isolated and characterized.<sup>[53]</sup> Next, the allyl double bond performs a migratory insertion into the C–Co bond from complex **183**, generating a seven-membered cobaltacycle **184** with the leaving group weakly coordinating to the cobalt. The product is released by a  $\beta$ -O elimination process. This mechanism is also proposed for related rhodium(III) and ruthenium(II) reactions<sup>[136b, 136d, 136e, 139]</sup> and for related allylation with allyl carbamates and alcohols.

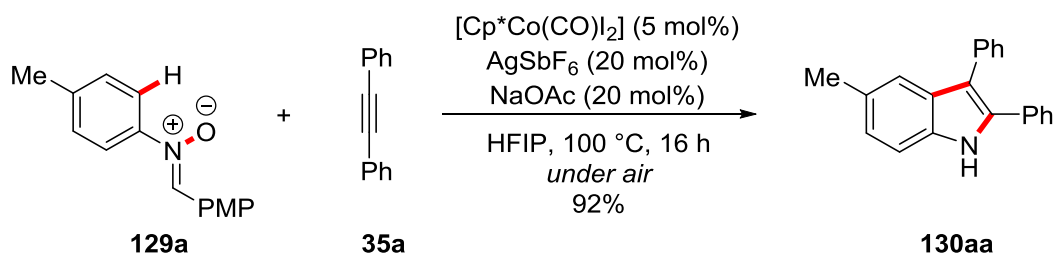


**Scheme 3.22:** Proposed catalytic cycles for the cobalt-catalyzed allylation.

### 3.3 Cobalt-Catalyzed C–H/N–O Functionalization

As mentioned before, the indole core plays a central role in medicinal and biomolecular chemistry<sup>[112, 134]</sup> and therefore methods to prepare or functionalize indoles are of great importance. As the above described methods allow the efficient allylation and alkenylation at the C-2 position of this heterocycle, a general method for a *de novo* synthesis of functionalized indoles would be desirable. To achieve this goal, H. Wang established a protocol that converts easily accessible nitrones **129** and alkynes **35** in a highly selective fashion to substituted indoles by mild cobalt(III) catalysis.<sup>[19b]</sup> The optimal catalytic system consisted of the versatile  $[\text{Cp}^*\text{Co}(\text{CO})\text{I}_2]$  precatalalyst,  $\text{AgSbF}_6$  and

NaOAc as additives in HFIP at 100 °C (Scheme 3.23). Since the importance of mono-protected amino acids in transition metal-catalyzed reactions gained more and more interest,<sup>[114b, 140]</sup> a careful screening revealed Piv-Leu-OH to give comparable good results (88%) as obtained with NaOAc. Replacing the PMP rest by a phenyl or mesityl rest which was optimal for a related rhodium(III)-catalyzed reaction,<sup>[113]</sup> gave worse results.

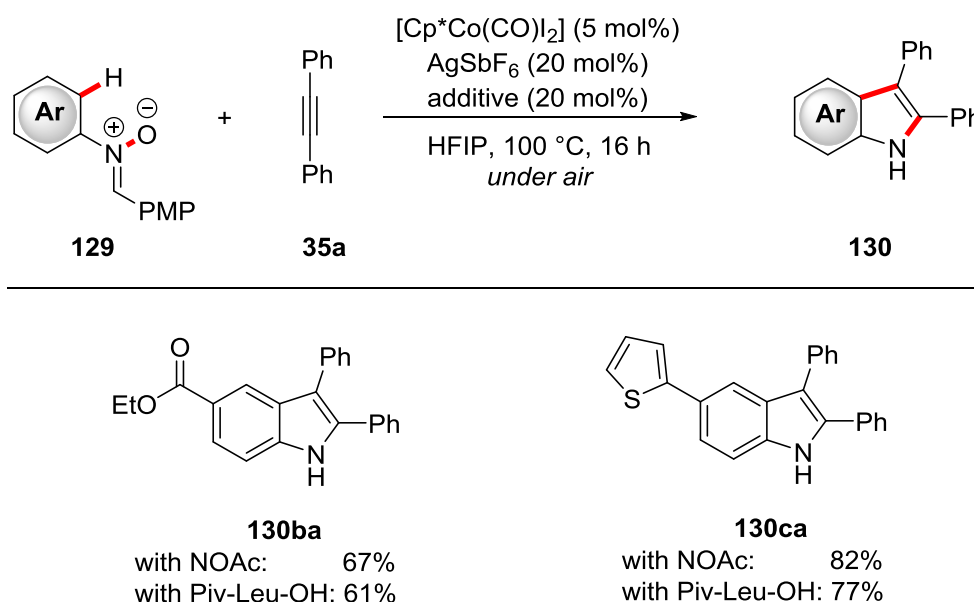


**Scheme 3.23:** Optimized reaction conditions for the C–H/N–O functionalization of nitron **129a** with alkyne **35a** (optimization performed by H. Wang).

### 3.3.1 Scope for the Cobalt-Catalyzed C–H/N–O Functionalization

With the best reaction conditions in hand, we next explored the applicability towards differently substituted nitrones **129** and alkynes **35**.

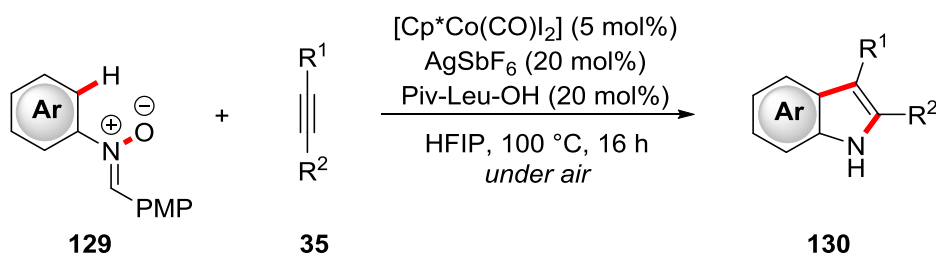
A representative scope with nitrones was performed by H. Wang.<sup>[19b]</sup> The amount of suitable nitrones for the envisioned indole synthesis could be extended by those bearing an ester moiety **129b** and a thiophenes heterocycle **129c** (Scheme 3.24).



**Scheme 3.24:** Scope for the cobalt-catalyzed C–H/N–O functionalization with nitrones **129**.

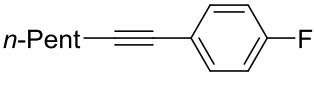
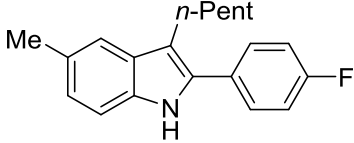
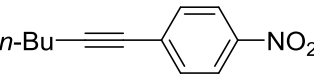
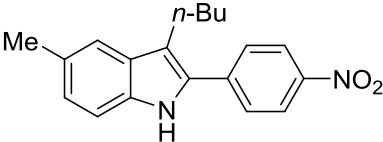
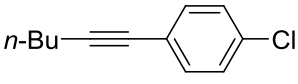
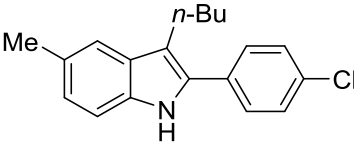
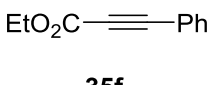
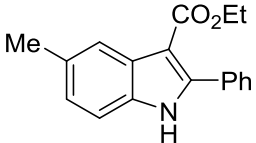
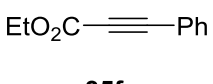
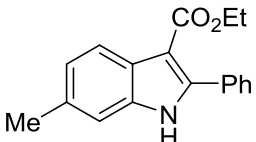
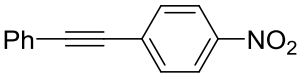
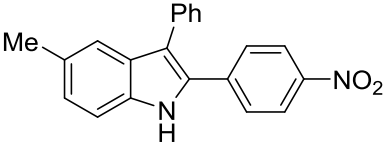
As a next step, the indole synthesis was conducted with different alkynes **35** to prepare 2- and 3-substituted indoles (Table 3.14). Whereas symmetrical bisaryl alkynes like **35b** proceeded well, the scope with unsymmetrical alkynes **35** was of considerable higher interest. Here, the selectivity of this transformation for alkyl aryl alkynes as well as for the much more challenging bisaryl alkynes could be estimated. Furthermore, indoles **130** with different substitution at the 2 and 3 positions have a significant broader applicability. In the reaction scope, all tested unsymmetrical alkynes gave the 2,3-functionalized indoles with perfect levels of regioselectivities in moderate to good yields. Using alkyl aryl alkynes, the aryl rest is located on the C-2 position of the indole and the alkyl moiety on the C-3 (entries 2-4). Moreover, the substitution pattern on the nitron does not have an impact on the regioselectivity (entries 5 and 6). These examples also show again the functional group tolerance with a propiolate being converted in sufficient yield. The highlight, however, of this scope is shown in entry 7, when even unsymmetrical bis aryl alkyne **35g** bearing a phenyl and 4-nitrophenyl group gave the desired product with perfect regioselectivity with the electron-withdrawing nitroarene at the C-2 position of the indole. It is indeed remarkable that only a nitro-group at the distal 4-position of the arene is sufficient for perfect selectivity. Along this line, if this reaction with **35g** is conducted under rhodium-catalysis the resulting indole is isolated as mixture of isomers with no level of selectivity.<sup>[113]</sup>

**Table 3.14:** Scope of alkynes **35** for the cobalt-catalyzed C–H/N–O functionalization.<sup>[a]</sup>



Entry	Alkyne	Product	Yield / %
1	<p style="text-align: center;"><b>35b</b></p>	<p style="text-align: center;"><b>130ab</b></p>	<p style="text-align: center;">78</p> <p style="text-align: center;">82<sup>[b]</sup></p>

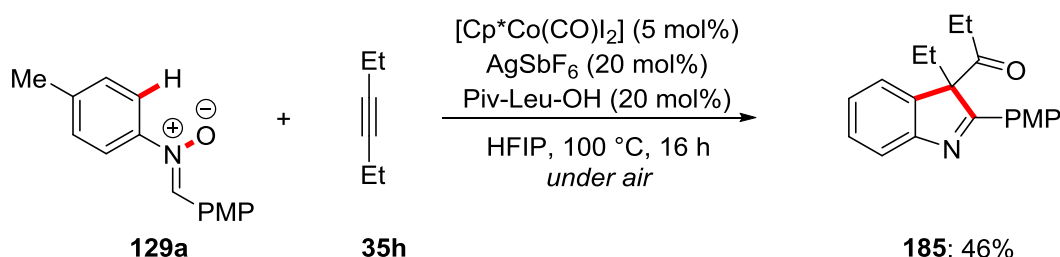


Entry	Alkyne	Product	Yield / %
2	 <b>35c</b>	 <b>130ac</b>	77
3	 <b>35d</b>	 <b>130ad</b>	54
4	 <b>35e</b>	 <b>130ae</b>	68
5	 <b>35f</b>	 <b>130af</b>	63
6	 <b>35f</b>	 <b>130df</b>	68
7	 <b>35g</b>	 <b>130ag</b>	64

<sup>[a]</sup> Reaction conditions: **129** (0.50 mmol), **35** (0.75 mmol), [Cp\*Co(CO)I<sub>2</sub>] (5 mol%), AgSbF<sub>6</sub> (20 mol%), Piv-Leu-OH (20 mol %), HFIP (2.0 mL), 100 °C, 16 h. <sup>[b]</sup> NaOAc (20 mol%) instead of Piv-Leu-OH.

As bisaryl as well as aryl alkyl alkynes were converted successfully in this reaction, the performance of bisalkyl alkynes was also examined. However, a rather messy reaction with undefined byproducts was observed. An exception from these findings was the

reaction with 3-hexyne (**35h**) (Scheme 3.25). Though with just moderate yield, this reaction delivered the unexpected 3*H*-indole **185** as the main product. This product with a keto and the PMP group attached to the molecule was never observed for any other tested examples and may indicate that for bisalkyl alkynes another mechanism is operative.



**Scheme 3.25:** Formation of 3*H*-indole **185** in the reaction of nitrone **129a** with 3-hexyne (**53h**).

### 3.3.2 Mechanistic Studies

Mechanistic experiments to get a better understanding of the reaction were performed by H. Wang.<sup>[19b]</sup> Among these were *i*) intermolecular competition experiments between electron-rich and electron-deficient nitrones and alkynes, *ii*) H/D exchange experiment with CD<sub>3</sub>OD as the co-solvent and *iii*) the determination of a kinetic isotope effect (KIE) by independent reactions. These experiments showed that

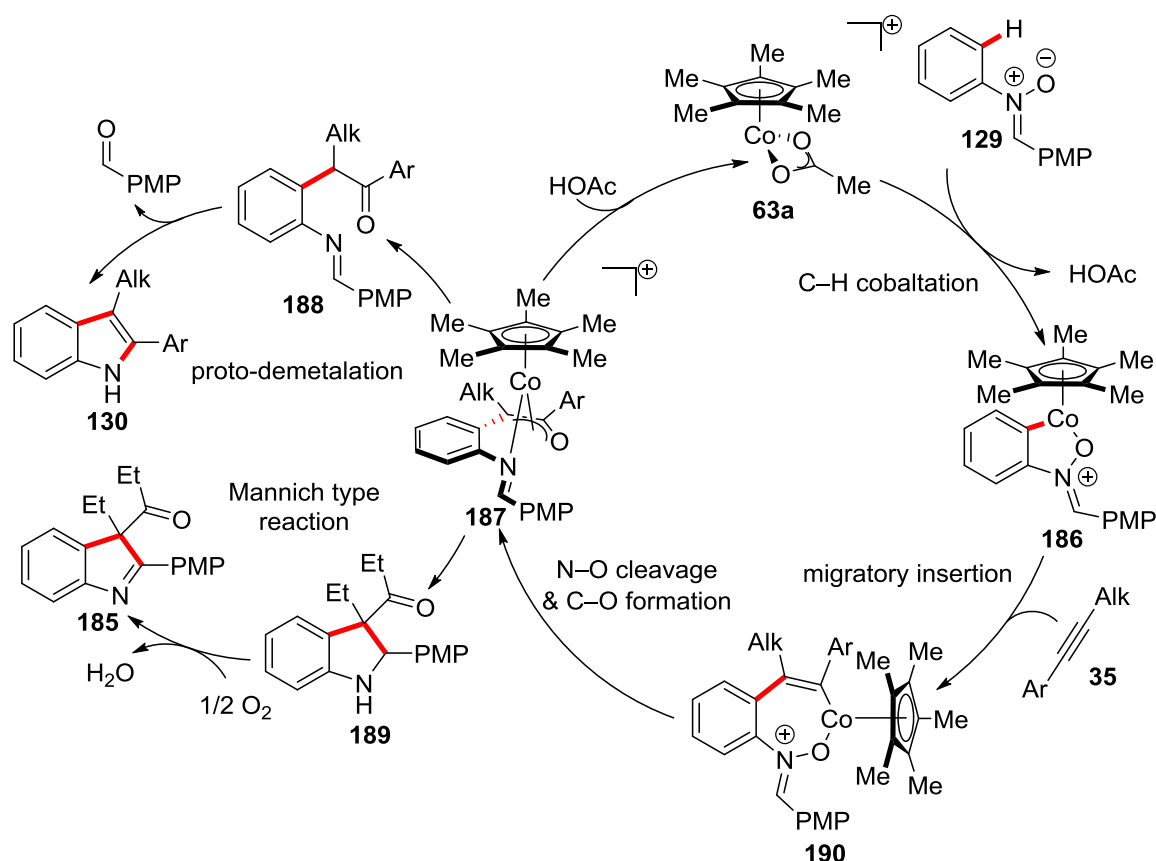
- Electron-rich nitrones as well as electron-rich alkynes react preferentially compared to electron deficient ones
- no deuterium incorporation was determined neither in the product nor in the reisolated starting material, when CD<sub>3</sub>OD was used as co-solvent and
- a KIE of 2.7 was determined by independent reactions.

The preferred reactivity of electron-rich nitrones can be rationalized by a base-assisted intramolecular electrophilic substitution type (BIES) mechanism<sup>[19e]</sup> and a kinetically relevant alkyne coordination may explain the preferred conversion of electron-rich alkynes. The fact that no deuterium incorporation was determined is rare for Cp\*Co(III)-catalyzed reactions and is also not observed for a related reaction with rhodium catalysts.<sup>[113]</sup> In consequence this reaction undergoes an irreversible C–H metalation step and combined with the estimated KIE of 2.7 a kinetically relevant, maybe rate-determining C–H activation step can be assumed.

With the regioselective nature of this reaction and the mechanistic studies in hand, we suggest the following catalytic cycle (Scheme 3.26). The catalytically active [Cp\*Co(OAc)]<sup>+</sup> species undergoes irreversible C–H metalation by a BIES<sup>[19e]</sup> type

mechanism to deliver the 5-membered cobaltacycle **186**. This is followed by coordination of the alkyne and subsequent migratory insertion into the Co–C bond. This step is also the regioselectivity-determining one in which the aryl group is placed in  $\alpha$ -position to the cobalt. In case for unsymmetrical biaryl alkynes the electron-deficient arene is placed proximal to the cobalt. An explanation for this could be that due to the high polarization of the C–Co bond and therefore the partially negative charge on the carbon atom, the neighboring arene delocalizes the charge over the ring and the stabilization is even higher with an electron deficient one. In contrast, an alkyl group on the  $\alpha$ -position with a +I-effect would further destabilize this intermediate. Next, the N–O bond is cleaved and the C–O bond is formed. The exact pathway for this transformation is not completely understood. Based on the efforts that have been made with rhodium(III) catalysis,<sup>[113, 141]</sup> two pathways appear plausible. That is *i*) an oxidative insertion of the cobalt into the N–O bond generating a cobalt(V)-oxo species and subsequent reductive elimination to form the C–O bond, or *ii*) reductive elimination provides the C–O bond and a cobalt(I) species and followed oxidative addition cleaves the N–O bond to generate **187**. In a subsequent report, Glorius and coworkers presented a cobalt-catalyzed indole synthesis from hydrazines.<sup>[142]</sup> Also here, the C–N formation and N–N cleavage was supposed to occur *via* a reductive elimination/ oxidative addition cascade. Depending on the alkyne, the key intermediate **187** can go along two reaction pathways. In most cases, proto-demetalation takes place and yields the imine **188**. Under the present condition this is hydrolyzed to the amine which immediately undergoes an intramolecular condensation reaction with the carbonyl group which yields the 1*H*-indole **130**.

Another pathway is followed when 3-hexyne (**35h**) is employed as the alkyne. We suppose that due to both alkyl groups and the missing charge delocalization a very nucleophilic enolate species is generated and in this particular case, an intramolecular Mannich reaction with the imine is faster than proto-demetalation. The *in situ* formed indoline **189** is not stable under the reaction condition and gets oxidized to the 3*H*-indole **185**.



**Scheme 3.26:** Proposed catalytic cycle for the cobalt(III)-catalyzed C-H/N-O functionalization.

### 3.4 Ruthenium(II)-Catalyzed Decarbamoylative and Decarboxylative C-C Arylations

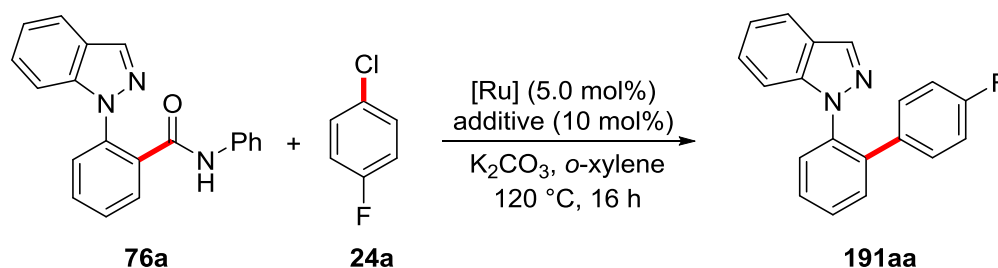
Catalytic C-H activation reactions have become an enormous and still increasing research area with a plethora of methods and reactions.<sup>[14e, 143]</sup> In contrast, examples for the selective activation of also omnipresent C-C bonds still continue to be rare.<sup>[76a-i, 76k]</sup> Though this area is mostly controlled by palladium and rhodium catalysis,<sup>[76a, 76b, 76d, 76f, 76g, 76i, 76j]</sup> significant progress has been made by the use of more cost-effective ruthenium catalysis.<sup>[144]</sup> However, substitution could only be achieved at the *ortho* position of a carboxylic acid by C-H functionalization, followed by decarboxylation. Therefore, the demand for a robust and direct C-C functionalization on the *ipso* position is highly desirable and hitherto, unreached for ruthenium catalysis.

Initial results for this goal by ruthenium catalysis were achieved in our group by J. Li.<sup>[145]</sup> Treating a benzamide with a pyrazole group at the *ortho* position with excess of an aryl chloride under ruthenium catalysis resulted in a double arylation at the *ortho* positions to the pyrazole directing group. As C-H arylation was expected, the C-C bond activation was completely unknown under these reactions conditions and shifted the focus to optimize a selective ruthenium-catalyzed C-C arylation.

### 3.4.1 Optimization Studies

With these promising initial results in hands, optimization studies have been performed to identify the best catalytic system for this novel transformation. The indazole moiety was chosen as directing group. This heterocycle, in particular 1-phenyl-1*H*-indazole represents an important scaffold in anti-inflammatory, antimicrobial and anticancer drugs<sup>[146]</sup> whereas their use as directing groups is relatively rare as compared to other *N*-containing heterocycles.<sup>[147]</sup> To establish the best catalytic conditions for this reaction, ruthenium sources, additives, bases, solvents and further reaction parameters were screened, beginning with the optimization for the ruthenium catalyst and additives (Table 3.15). Regarding the potential of ruthenium-cymene complexes in C–H activation, we tested a variety of different *in situ* and well-defined complexes with this structural motif. In absence of an additive, product formation was observed, albeit in very low yields (entry 1). Addition of carboxylic acids as additives, however, amplified the performance dramatically, with best results using 2,4,6-trimethyl benzoic acid (MesCO<sub>2</sub>H) (entry 4). The catalytically active ruthenium carboxylate complex is generated *in situ* under these reaction conditions, the well-defined [Ru(O<sub>2</sub>CMes)<sub>2</sub>(*p*-cymene)] gave comparable results in the present reaction (entry 5).<sup>[14b, 148]</sup> Switching from carboxylic acid to phosphine ligands shut down the reaction completely (entries 7-9). It should be noted that no reaction took place in the absence of ruthenium (entry 12) and moreover, other ruthenium sources, like [Ru<sub>3</sub>(CO)<sub>12</sub>] or the simple RuCl<sub>3</sub>·(H<sub>2</sub>O)<sub>*n*</sub>, were not successful either.

**Table 3.15:** Catalyst and additives for the ruthenium(II)-catalyzed decarbamoylative C–C arylation.<sup>[a]</sup>



Entry	[Ru]	Additive	Yield / %
1	[RuCl <sub>2</sub> ( <i>p</i> -cymene)] <sub>2</sub>	---	11
2	[RuCl <sub>2</sub> ( <i>p</i> -cymene)] <sub>2</sub>	1-AdCO <sub>2</sub> H	64
3	[RuCl <sub>2</sub> ( <i>p</i> -cymene)] <sub>2</sub>	PhCO <sub>2</sub> H	51
4	[RuCl <sub>2</sub> ( <i>p</i> -cymene)] <sub>2</sub>	MesCO <sub>2</sub> H	78

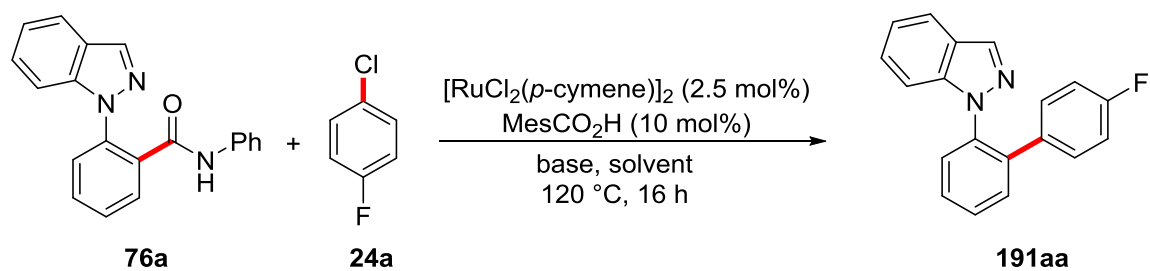
Entry	[Ru]	Additive	Yield / %
5	[Ru(O <sub>2</sub> CMe) <sub>2</sub> ( <i>p</i> -cymene)]	---	71
6	[RuCl <sub>2</sub> ( <i>p</i> -cymene)] <sub>2</sub>	AcOH	5
7	[RuCl <sub>2</sub> ( <i>p</i> -cymene)] <sub>2</sub>	PPh <sub>3</sub>	---
8	[RuCl <sub>2</sub> ( <i>p</i> -cymene)] <sub>2</sub>	PCy <sub>3</sub>	---
9	[RuCl <sub>2</sub> ( <i>p</i> -cymene)] <sub>2</sub>	dppm	---
10	[Ru <sub>3</sub> (CO) <sub>12</sub> ]	---	---
11	RuCl <sub>3</sub> ·(H <sub>2</sub> O) <sub><i>n</i></sub>	MesCO <sub>2</sub> H	---
12	---	MesCO <sub>2</sub> H	---

<sup>[a]</sup> Reaction conditions: **76a** (0.20 mmol), **24a** (0.40 mmol), [Ru] (5.0 mol%), additive (10 mol%), K<sub>2</sub>CO<sub>3</sub> (2.0 equiv), *o*-xylene (0.5 mL), 120 °C, 16 h.

Next, the screening of bases and solvents and further reaction parameters was performed (Table 3.16). First, the use of a base was necessary (entry 1) and its choice crucial. Hence, carbonates were the bases of choice (entries 2 and 3) and K<sub>2</sub>CO<sub>3</sub> gave best results. Also reducing the amounts to 1 equivalent led to a decrease in yield (entry 6). Other bases hardly gave any conversion, as KOAc failed (entry 4) and also a stronger base, such as DBU, were not successful (entry 5). The reaction can in principle be carried out in different solvents. Highest yields were achieved with *ortho*- or *meta*-xylene (entry 8), but performing the reaction in 1,4-dioxane or *t*-AmOH gave still acceptable results (entries 9 and 10). Taking the green solvent  $\gamma$ -valerolactone<sup>[149]</sup> resulted in a relatively low yield of 22% (entry 13). The reaction temperature of 120 °C turned out to be necessary, so that even a slight decrease in temperature to 100 °C reduced the yield severely (entry 16) and also a lower concentration of 0.2 M resulted in a slightly reduced efficiency (entry 17). To reduce the reaction time from 16 h to 30 minutes, the transformation could be performed under microwave irradiation at 200 W with an identical reaction outcome (entry 15).

### 3.4 Ruthenium(II)-Catalyzed Decarbamoylative and Decarboxylative C–C Arylations

**Table 3.16:** Optimization of ruthenium(II)-catalyzed decarbamoylative C–C functionalization.<sup>[a]</sup>



Entry	Base	Solvent	Yield / %
1	---	<i>o</i> -xylene	---
2	$\text{Na}_2\text{CO}_3$	<i>o</i> -xylene	38
3	$\text{Cs}_2\text{CO}_3$	<i>o</i> -xylene	66
4	KOAc	<i>o</i> -xylene	5
5	DBU	<i>o</i> -xylene	4
6	$\text{K}_2\text{CO}_3$	<i>o</i> -xylene	62 <sup>[b]</sup>
7	$\text{K}_2\text{CO}_3$	PhMe	45
8	$\text{K}_2\text{CO}_3$	<i>m</i> -xylene	76
9	$\text{K}_2\text{CO}_3$	1,4-dioxane	51
10	$\text{K}_2\text{CO}_3$	<i>t</i> -AmOH	41
11	$\text{K}_2\text{CO}_3$	DCE	---
12	$\text{K}_2\text{CO}_3$	<i>n</i> -Bu <sub>2</sub> O	---
13	$\text{K}_2\text{CO}_3$	GVL	22
14	$\text{K}_2\text{CO}_3$	MeOH	12
15	$\text{K}_2\text{CO}_3$	<i>o</i> -xylene	75 <sup>[c]</sup>
16	$\text{K}_2\text{CO}_3$	<i>o</i> -xylene	12 <sup>[d]</sup>
17	$\text{K}_2\text{CO}_3$	<i>o</i> -xylene	63 <sup>[e]</sup>

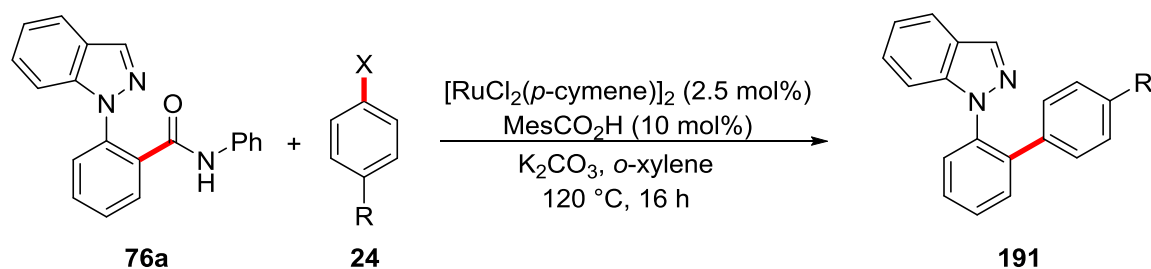
<sup>[a]</sup> Reaction conditions: **76a** (0.20 mmol), **24a** (0.40 mmol),  $[\text{RuCl}_2(p\text{-cymene})]_2$  (2.5 mol%),  $\text{MesCO}_2\text{H}$  (10 mol%), base (2.0 equiv), solvent (0.5 mL), 120 °C, 16 h. <sup>[b]</sup>

K<sub>2</sub>CO<sub>3</sub> (1.0 equiv). <sup>[c]</sup> Under microwave irradiation (200 W) for 30 min. <sup>[d]</sup> At 100 °C. <sup>[e]</sup> *o*-xylene (1.0 mL).

### 3.4.2 Scope for the Ruthenium(II)-Catalyzed Decarbamoylative C–C Arylation

At the end of these optimization studies, the best catalyst, additive, base and solvent were identified. This allowed for testing its performance towards different amides **76** and aryl halides **24**. To evaluate the influence of functional groups and electronic effects on the reaction, we initiated our studies with a plethora of 4-substituted aryl halides (Table 3.17). In general, our method was broadly applicable and compatible with aryl chlorides and bromides **24**. Electron-rich as well as electron-poor aryls were both converted in very good yields (entries 4 and 5). One remarkable feature of this transformation is the tolerance of functional groups. Indeed, nitriles, basic tertiary amines, ester and ketones delivered the desired product in good to very good yields. When using 1-bromo-4-chlorobenzene (**24k**) as the arylating reagent, the arylation occurred chemoselectively to yield the 4-chlorophenyl product, demonstrating the selective C–Br *versus* C–Cl cleavage (entry 11).

**Table 3.17:** Scope aryl halides **24** for the ruthenium(II)-catalyzed decarbamoylative C–C arylation.<sup>[a]</sup>



Entry	R	X	Yield / %
1	H	Br	81
2	Me	Br	83 <sup>[b]</sup>
3	OMe	Cl	79
4	OMe	Br	85
5	CF <sub>3</sub>	Br	88
6	CN	Br	63 <sup>[c]</sup>
7	NMe <sub>2</sub>	Br	59



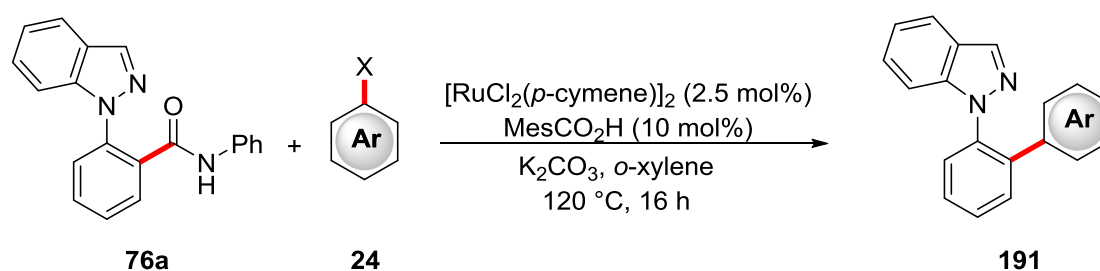
### 3.4 Ruthenium(II)-Catalyzed Decarbamoylative and Decarboxylative C–C Arylations

8	CO <sub>2</sub> Et	Cl	81
9	C(O)Ph	Br	79
10	C(O)Et	Br	72 <sup>[b]</sup>
11	Cl	Br	63 <sup>[b]</sup>

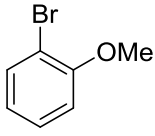
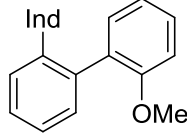
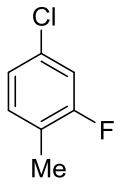
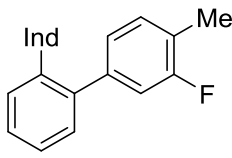
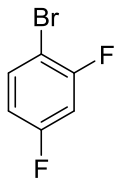
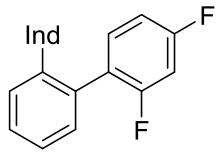
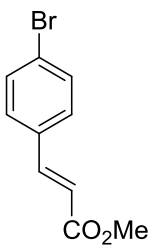
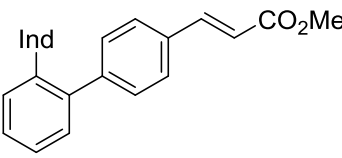
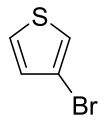
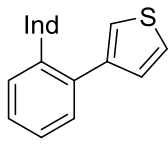
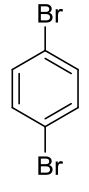
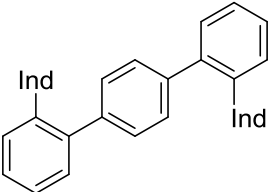
<sup>[a]</sup> Reaction conditions: **76a** (0.20 mmol), **24** (0.40 mmol), [RuCl<sub>2</sub>(*p*-cymene)]<sub>2</sub> (2.5 mol%), MesCO<sub>2</sub>H (10 mol%), K<sub>2</sub>CO<sub>3</sub> (2.0 equiv), *o*-xylene (0.5 mL), 120 °C, 16 h. <sup>[b]</sup> Performed by F. Kramm. <sup>[c]</sup> [RuCl<sub>2</sub>(*p*-cymene)]<sub>2</sub> (5.0 mol%).

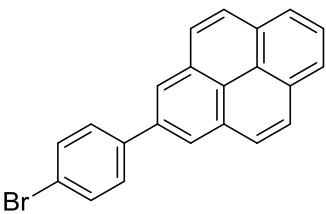
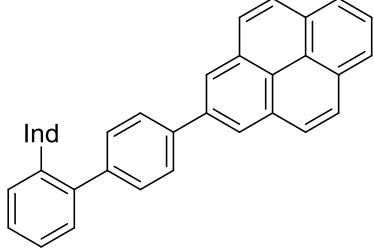
The studies on the reaction scope were continued with other substitution patterns on the aryl halide **24** (Table 3.18). Substituents at the 3 and the sterically more congested 2 position of the arene were well tolerated (entries 1 and 2) and even disubstituted arenes, like on 3,5-, or 2,4-position, did not mismatch with the catalytic system (entries 3 and 4). The scope was not restricted to phenyl-derived aryl halides, but also allowed the conversion of heteroarenes, such as a thiophene, in acceptable yield (entry 6). When 1,4-dibromobenzene (**24r**) was employed, a double C–C/C–Br activation was observed giving the triphenyl species **191ar** in remarkable good yield. Furthermore, this method can be applied for the installation of polycyclic aromatic hydrocarbons (PAH) like pyrenes (entry 8) for a possible utilization as fluorescent dye.

**Table 3.18:** Scope for further aryl halides **24** for the ruthenium(II)-catalyzed decarbamoylative C–C arylation.<sup>[a]</sup>



Entry	Aryl Halide	Product	Yield / %
1			69

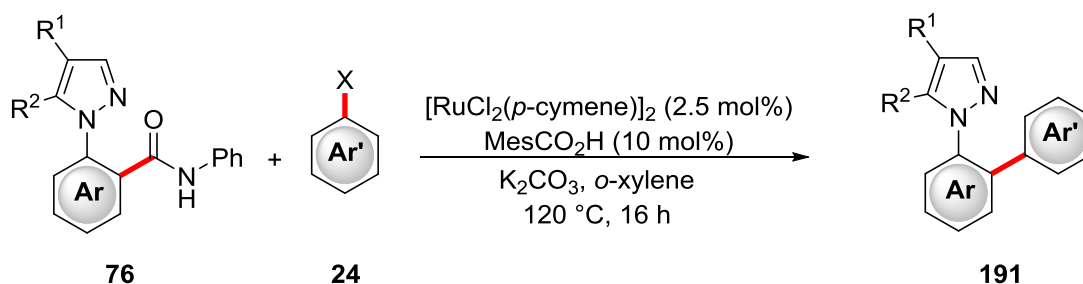
Entry	Aryl Halide	Product	Yield / %
2	 <b>24m</b>	 <b>191am</b>	75
3	 <b>24n</b>	 <b>191an</b>	73 <sup>[b]</sup>
4	 <b>24o</b>	 <b>191ao</b>	73 <sup>[b]</sup>
5	 <b>24p</b>	 <b>191ap</b>	70
6	 <b>24q</b>	 <b>191aq</b>	61
7	 <b>24r</b>	 <b>191ar</b>	80 <sup>[c]</sup>

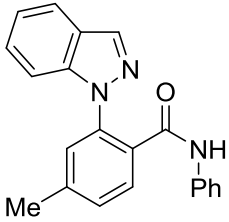
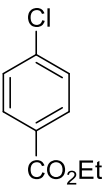
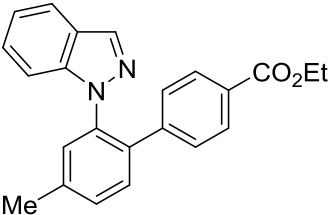
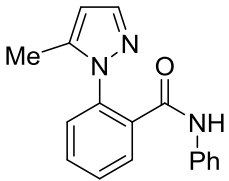
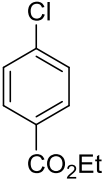
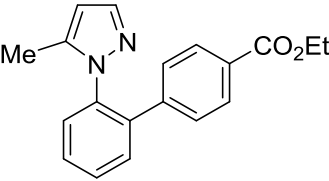
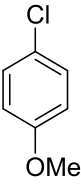
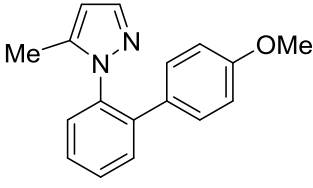
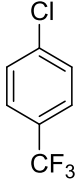
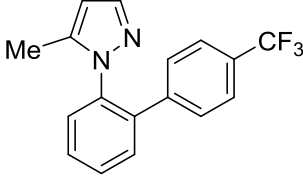
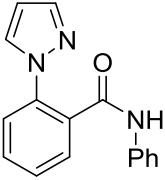
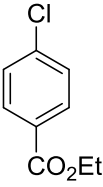
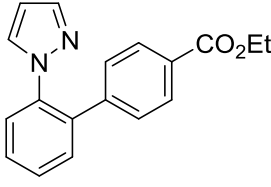
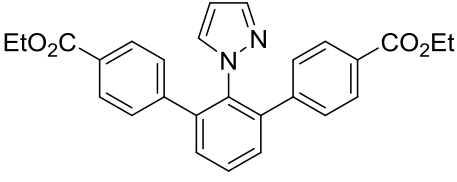
Entry	Aryl Halide	Product	Yield / %
8			70
	<b>24s</b>	<b>191as</b>	

<sup>[a]</sup> Reaction conditions: **76a** (0.20 mmol), **24** (0.40 mmol), [RuCl<sub>2</sub>(*p*-cymene)]<sub>2</sub> (2.5 mol%), MesCO<sub>2</sub>H (10 mol%), K<sub>2</sub>CO<sub>3</sub> (2.0 equiv), *o*-xylene (0.5 mL), 120 °C, 16 h. <sup>[b]</sup> Performed by F. Kramm. <sup>[c]</sup> **24r** (0.10 mmol).

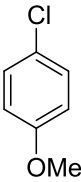
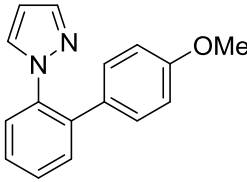
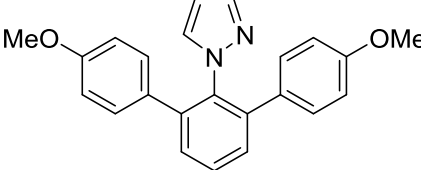
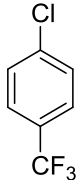
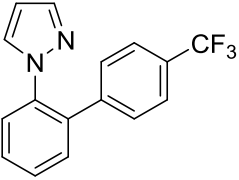
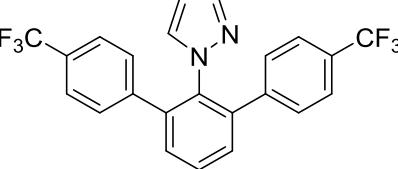
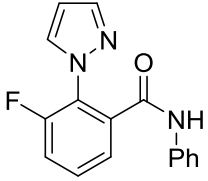
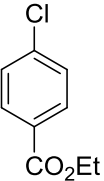
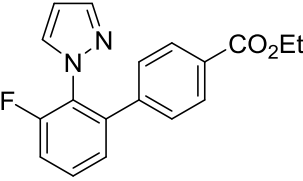
Motivated by the wide scope for different aryl halides **24**, the focus was shifted to substituted amides **76** as well as modifications of the directing group (Table 3.19) and indeed, related pyrazoles proved suitable. In particular, the 5-methyl pyrazole gained our interest. The desired arylation could be realized in good to very good yields (entries 2-4), and additionally the system allows for post modification opening a route acetanilides (*vide infra*). When the simple pyrazole group was employed, selective C–C arylation was accomplished in moderate to good yields in case of 1.1 equivalents of the aryl halide was used. However, its tendency for double arylation was reflected when an excess of aryl halide **24** was submitted (entries 5-10). It is noteworthy that the C–C cleavage occurred first, followed by a C–H arylation of the monoarylated arene. In all reactions, a mono C–H arylation of the amide could not be observed. *Ortho*- and *meta*-substitution at the amide was also tolerated by the catalytic system (entries 1, 11 and 12) and with *meta*-substitution, no second arylation took place. Again, the high functional group tolerance stood out. It did not only allow the successful transformation of a sulfamate **24t** (entry 13) in very good yield, but the mild reaction conditions enabled the transformation of the free NH<sub>2</sub> aniline **24u** (entry 14).

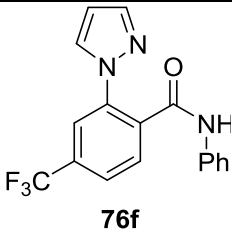

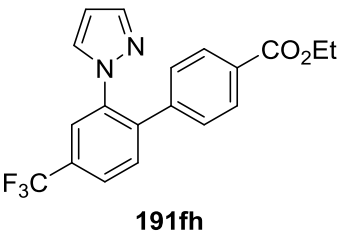
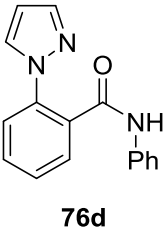
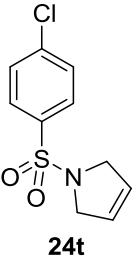
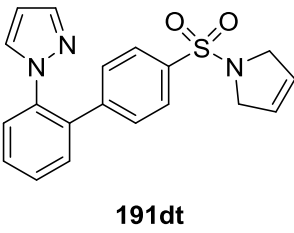
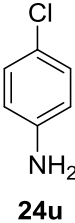
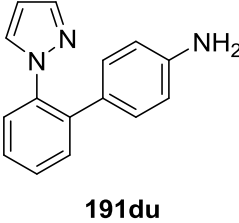
**Table 3.19:** Ruthenium(II)-catalyzed decarbamoylative C–C arylation of amides **76**.<sup>[a]</sup>



Entry	Amide	ArCl	Product	Yield / %
1	 <b>76b</b>	 <b>24h</b>	 <b>191bh</b>	72 <sup>[b]</sup>
2	 <b>76c</b>	 <b>24h</b>	 <b>191ch</b>	72 <sup>[b]</sup>
3	<b>76c</b>	 <b>24d</b>	 <b>191cd</b>	80
4	<b>76c</b>	 <b>24e</b>	 <b>191ce</b>	72
5	 <b>76d</b>	 <b>24h</b>	 <b>191dh</b>	66
6	<b>76d</b>	<b>24h</b>	 <b>191dh'</b>	60 <sup>[b]</sup>

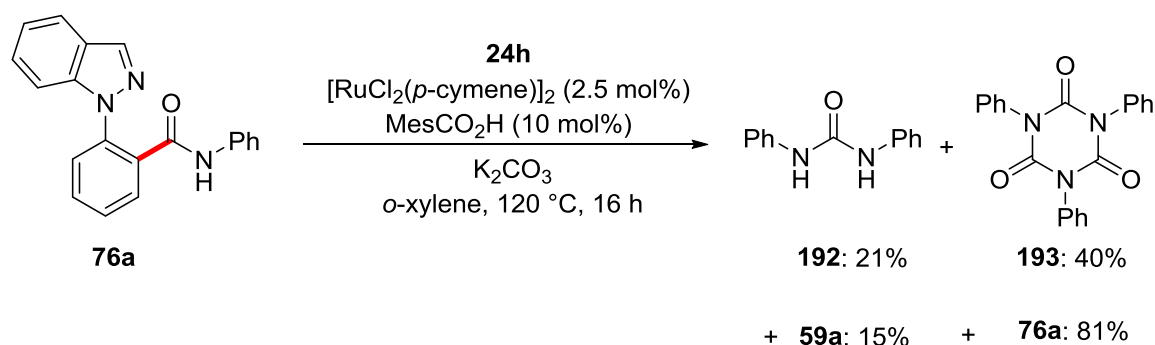
### 3.4 Ruthenium(II)-Catalyzed Decarbamoylative and Decarboxylative C–C Arylations

Entry	Amide	ArCl	Product	Yield / %
7	<b>76d</b>	 <b>24d</b>	 <b>191dd</b>	56
8	<b>76d</b>	<b>24d</b>	 <b>191dd'</b>	69 <sup>[b]</sup>
9	<b>76d</b>	 <b>24e</b>	 <b>191de</b>	71
10	<b>76d</b>	<b>24e</b>	 <b>191de'</b>	71 <sup>[b]</sup>
11	 <b>76e</b>	 <b>24h</b>	 <b>191eh</b>	83 <sup>[c]</sup>

Entry	Amide	ArCl	Product	Yield / %
12	 <b>76f</b>	<b>24h</b> 	 <b>191fh</b>	85 <sup>[c]</sup>
13	 <b>76d</b>	 <b>24t</b>	 <b>191dt</b>	84
14	<b>76d</b>	 <b>24u</b>	 <b>191du</b>	76

<sup>[a]</sup> Reaction conditions: **76** (0.20 mmol), **24** (0.22 mmol), [RuCl<sub>2</sub>(*p*-cymene)]<sub>2</sub> (2.5 mol%), MesCO<sub>2</sub>H (10 mol%), K<sub>2</sub>CO<sub>3</sub> (2.0 equiv), *o*-xylene (0.5 mL), 120 °C, 16 h.<sup>[b]</sup> **24** (0.40 mmol). <sup>[c]</sup> **24** (0.50 mmol), PhMe (1.0 mL), 120 °C, 18 h, Performed by J. Li.

In order to understand the C–C cleavage mechanism, the isolation of the carbamoyl leaving group or its reaction products were investigated. Among a careful analysis of all isolated compounds, *N,N*-diphenyl urea (**192**) as well as triphenylisocyanurates (**193**) were isolated (Scheme 3.27). These findings are a strong hint for the *in situ* formation of isocyanates that, under the reaction conditions, react to these compounds.

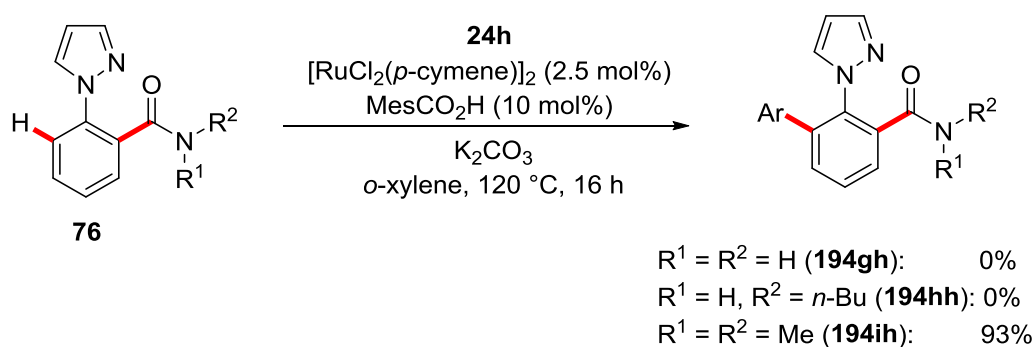


**Scheme 3.27:** Isocyanate adducts in the ruthenium(II)-catalyzed decarbamoylative C–C arylation.

This adduct formation of isocyanates is well known for various catalysts.<sup>[150]</sup> Surprisingly, a similar reaction has not been published yet by ruthenium catalysis.

With the identification of these reaction byproducts, it is even more remarkable that the C–C arylation proceeded with high conversions as the coordination of **192** and **193** with their donor atoms to the ruthenium can influence the catalytic activity.

In addition, the *N*-substitution pattern on the amide was tested (Scheme 3.28). The primary amide **76g** did not give any conversion and the same result was obtained with an aliphatic rest in substrate **76h**. In contrast, the tertiary amide **79i** enabled the C–H arylation at the other *ortho*-position in almost quantitative yields. These results demonstrate the importance of a deprotonable N–H bond which seems to be crucial for the C–C activation step.

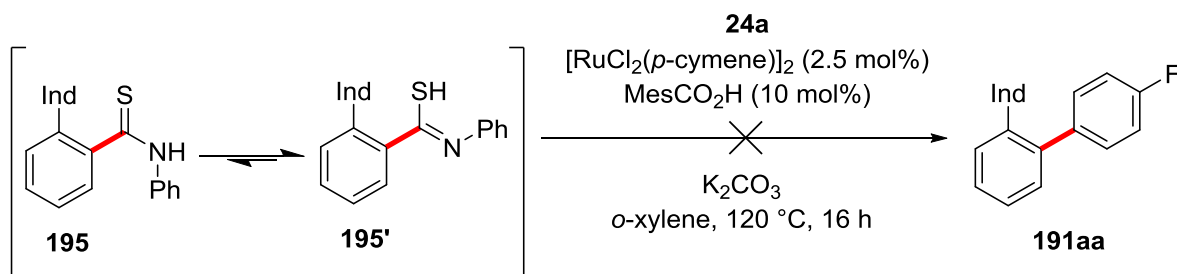


**Scheme 3.28:** Different amides for the ruthenium(II)-catalyzed C–C arylation.

### 3.4.3 Decarboxylative and Dealkanoylative C–C Arylation

With the release of isocyanate, the behavior of thioamides was of interest which were supposed to release isothiocyanates, an important class of compounds for among others flavoring substances.<sup>[151]</sup> The thioamide **195** is easily accessible from **76a** by treatment with the Lawesson's reagent. Unfortunately, it did not show any conversion in the C–C arylation reaction (Scheme 3.29) with almost quantitative reisolation of the starting

material. The reason can be found in the tautomerism of the amide.  $^1\text{H}$  and  $^{13}\text{C}$ -NMR suggested that not the expected thioamide **195** is present, but the tautomeric thioenamide **195'**.<sup>[152]</sup> Its thiol-like character can easily coordinate to the ruthenium and shut down its activity.



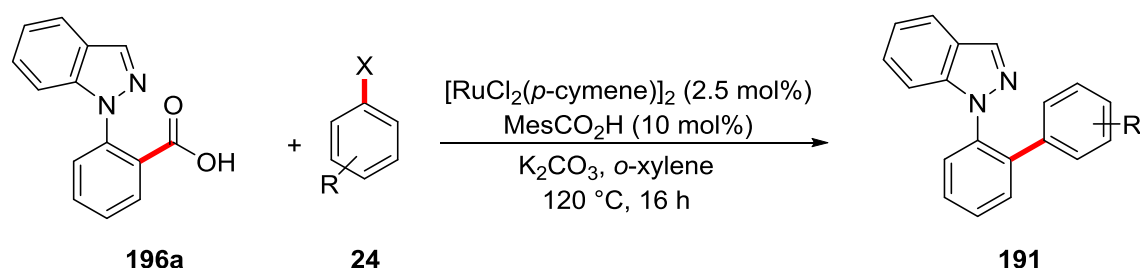
**Scheme 3.29:** Attempted C–C arylation with thioamides **195**.



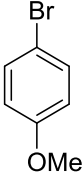
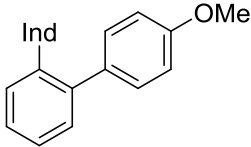
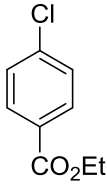
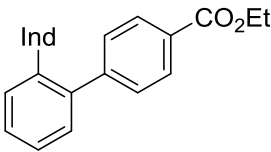
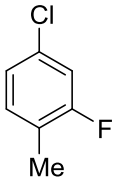
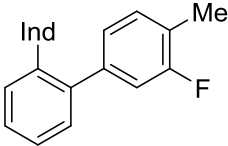
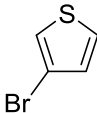
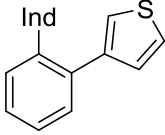
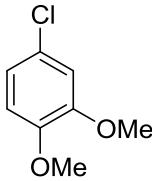
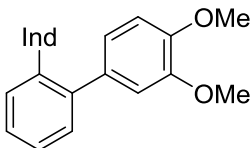
Beside (thio)amides we checked other leaving groups in this C–C functionalization reaction. Inspired by recent works on ruthenium-catalyzed C–H functionalization, followed by subsequent decarboxylation of benzoic acids,<sup>[153]</sup> we tested carboxylic acids **196** (

Table 3.20). Indeed, this decarboxylative arylation proceeded in very good yields, comparable with those obtained for amides and the same holds true for functional group tolerance, such as esters and heterocycles (entries 3 and 5). Also multiple substitution patterns with electron-donating and withdrawing groups were not problematic (entries 4 and 6). Furthermore, this decarboxylative C–C arylation bears two new innovations. First, in contrast to the aforementioned decarboxylative C–H functionalizations with ruthenium,<sup>[144]</sup> this reaction enabled the functionalization at the *ipso*-position to the acid. The second improvement is that this reaction does not require copper(II) or precious silver(I) salts as additives, which is the case for related palladium- or rhodium-catalyzed transformations.<sup>[154]</sup>

**Table 3.20:** Ruthenium(II)-catalyzed decarboxylative C–H arylation with acids **196**.<sup>[a]</sup>



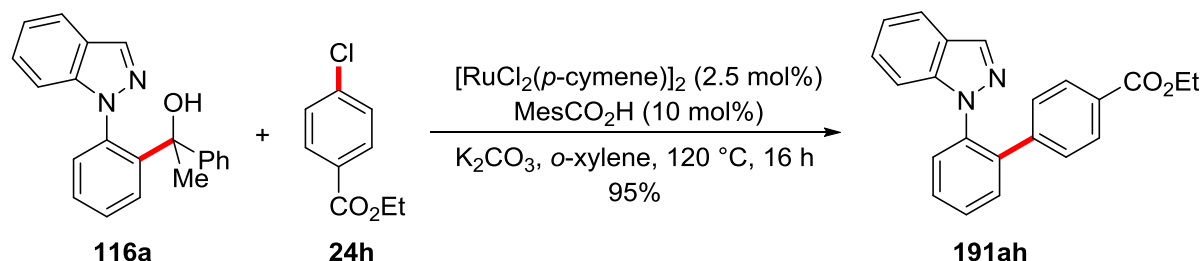
Entry	Aryl Halide	Product	Yield / %
1	<p style="text-align: center;"><b>24a</b></p>	<p style="text-align: center;"><b>191aa</b></p>	77

Entry	Aryl Halide	Product	Yield / %
2	 <b>24d</b>	 <b>191ad</b>	89
3	 <b>24h</b>	 <b>191ah</b>	79
4	 <b>24n</b>	 <b>191an</b>	71
5	 <b>24q</b>	 <b>191aq</b>	68
6	 <b>24v</b>	 <b>191av</b>	56

<sup>[a]</sup> Reaction conditions: **196a** (0.20 mmol), **24** (0.40 mmol), [RuCl<sub>2</sub>(*p*-cymene)]<sub>2</sub> (2.5 mol%), MesCO<sub>2</sub>H (10 mol%), K<sub>2</sub>CO<sub>3</sub> (2.0 equiv), *o*-xylene (0.5 mL), 120 °C, 16 h.

In order to expand the range of the C–C activation, other leaving groups were tested next. Moving away from carbonyl-containing groups to sp<sup>3</sup>-hybridized atoms, alcohols **116** attracted out attention. The oxygen atom can coordinate to the ruthenium and β-carbon elimination delivers the ketone or aldehyde. The arylation by C(sp<sup>2</sup>)–C(sp<sup>3</sup>) cleavage proceeded almost quantitatively with 95% yield, showing the first ruthenium-catalyzed dealkanolative C–C functionalization (Scheme 3.30). The expected

acetophenone was isolated in 85% yield. This again shows the versatile character of the C–C functionalization process by  $\beta$ -carbon elimination. C–C functionalization reactions of these benzyl alcohols were demonstrated with rhodium catalysts by Shi and coworkers<sup>[97-100]</sup> and also with cobalt catalysis by Morandi and coworkers.<sup>[101]</sup>

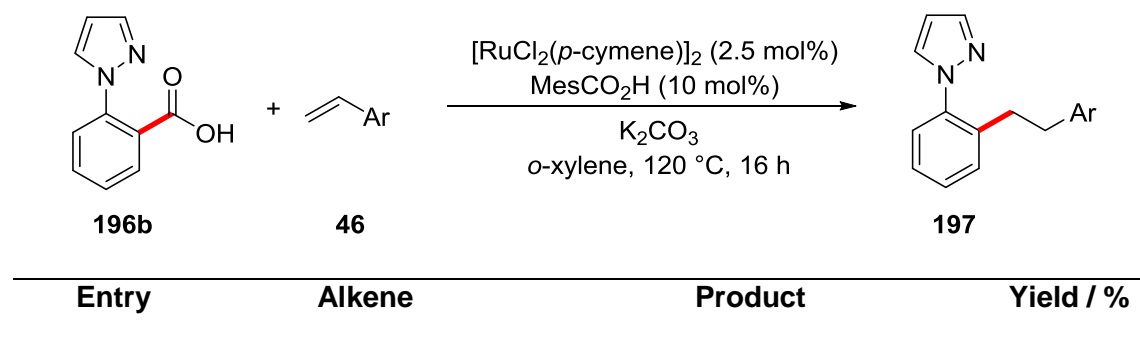


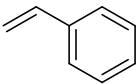
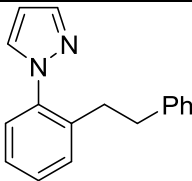
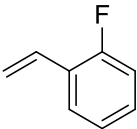
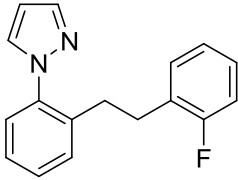
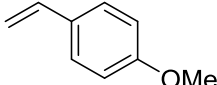
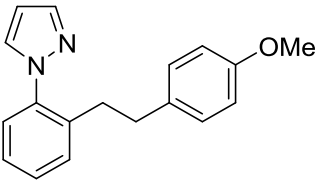
**Scheme 3.30:** Ruthenium(II)-catalyzed dealkanolative C–C arylation.

#### 3.4.4 Ruthenium(II)-Catalyzed Hydroarylation by C–C Bond Cleavage

Bearing a large scope including a high functional group tolerance and a variety of leaving groups highlight the applicability of this novel ruthenium-catalyzed transformation, it seems unlikely that this universal C–C functionalization reaction is limited to arylation reactions. Given the activation process to proceed by a  $\beta$ -elimination pathway renders a cycloruthenated species to be a probable reaction intermediate (*vide infra*) and therefore further transformations with this organoruthenium species should be possible. Beside the studied arylations by C–X bond cleavage, addition reactions to double bonds which are well known for related C–H activation<sup>[155]</sup> reactions were also investigated. Without changes in the catalytic system, a hydroarylation reaction of styrenes **46** by C–C bond cleavage could be achieved (Table 3.21). As a proof of principle, these three examples confirm the principle for multiple functionalizations by C–C bond cleavage.

**Table 3.21:** Ruthenium(II)-catalyzed hydroarylation of styrenes by C–C bond cleavage.<sup>[a]</sup>

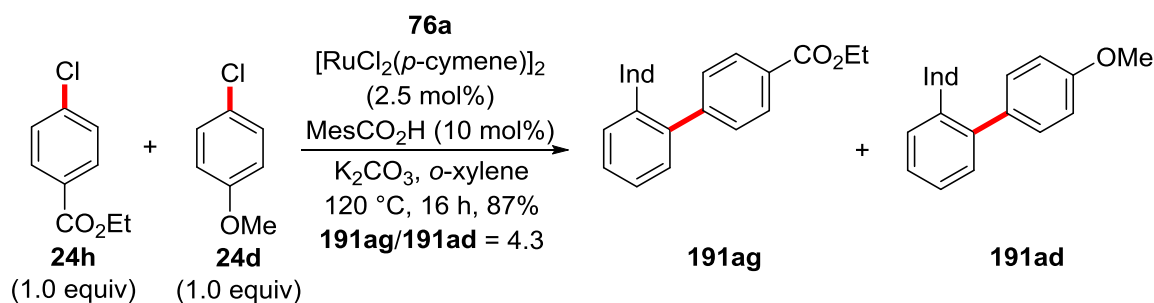


Entry	Alkene	Product	Yield / %
1	 46a	 197ba	74
2	 46b	 197bb	85
3	 46c	 197bc	56

<sup>[a]</sup> Reaction conditions: **196b** (0.20 mmol), **46** (0.40 mmol),  $[\text{RuCl}_2(p\text{-cymene})]_2$  (2.5 mol%), MesCO<sub>2</sub>H (10 mol%), K<sub>2</sub>CO<sub>3</sub> (2.0 equiv), *o*-xylene (0.5 mL), 120 °C, 16 h.

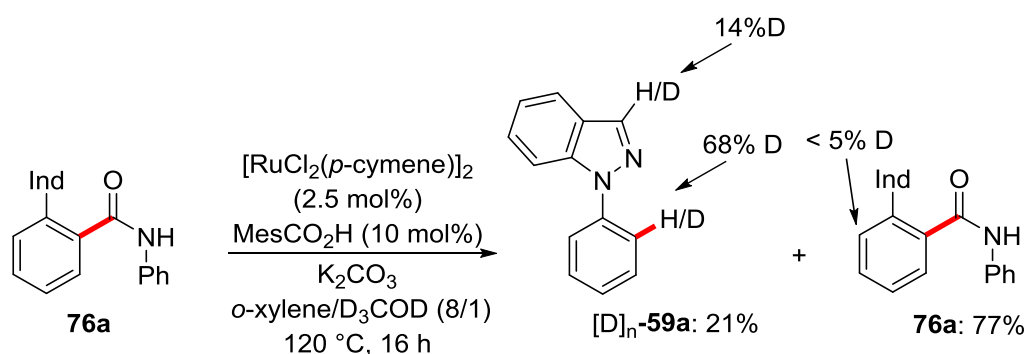
### 3.4.5 Mechanistic Studies

To gain insight into this new and versatile reaction manifold, mechanistic studies should unravel its mode of action. We initiated these studies by comparing electron-deficient and electron-rich aryl halides **24h** and **24d** in an intermolecular competition experiment (Scheme 3.31). In this experiment, a clear preference for the electron-deficient arene was detected.



**Scheme 3.31:** Intermolecular competition experiment between aryl halides **24**.

Next, a C–C cleavage reaction was performed in the absence of an aryl halide, but in the presence of  $D_3COD$  as the co-solvent (Scheme 3.32). The reaction yielded the decarbamoylated phenyl indazole **59a** in 21% and the starting material **76a** was isolated in 77%. Whereas no deuterium incorporation was determined in the starting material, the phenyl indazole showed a significant incorporation in the *ortho* position with 68% as well as in the 3-position of the indazole with 14%. The deuterium incorporation on the phenyl ring explicitly indicates the organometallic character of the C–C functionalization that includes a cycloruthenated species. The H/D exchange in the 3-position of the indazole may result from an electrophilic type C–H activation. It is noteworthy that no deuterium was detected in the reisolated starting material, in particular in the *ortho*-position. This clearly demonstrates that solely the C–C functionalization takes place and that a possible C–H activation of substrate **76a** can be ruled out.



**Scheme 3.32:** C–C Activation in the presence of deuterated co-solvent  $D_3COD$ .

To check whether this transformation involves any radical species, reactions were conducted in the presence of radical scavengers (Table 3.22). BHT and TEMPO as typical radical scavengers had a significant impact on the reaction outcome. Stoichiometric amounts of BHT reduced the efficiency to 53% (entry 3). The inhibition of TEMPO was even higher, as catalytic amounts decreased the yield already to 36% (entry 4) and one equivalent stopped the reaction completely (entry 5). However, it should be taken into consideration that TEMPO can interact in many ways with the catalytic system, e.g. through coordination, oxidation and other reactions. Yet, its impact is eminently higher as for the cobalt-catalyzed alkenylation (Table 3.10). Therefore, a clear statement cannot be made, but the assumption that this transformation involves a radical pathway seems reasonable.

**Table 3.22:** Influence of radical scavengers on the ruthenium(II)-catalyzed C–C arylation.<sup>[a]</sup>

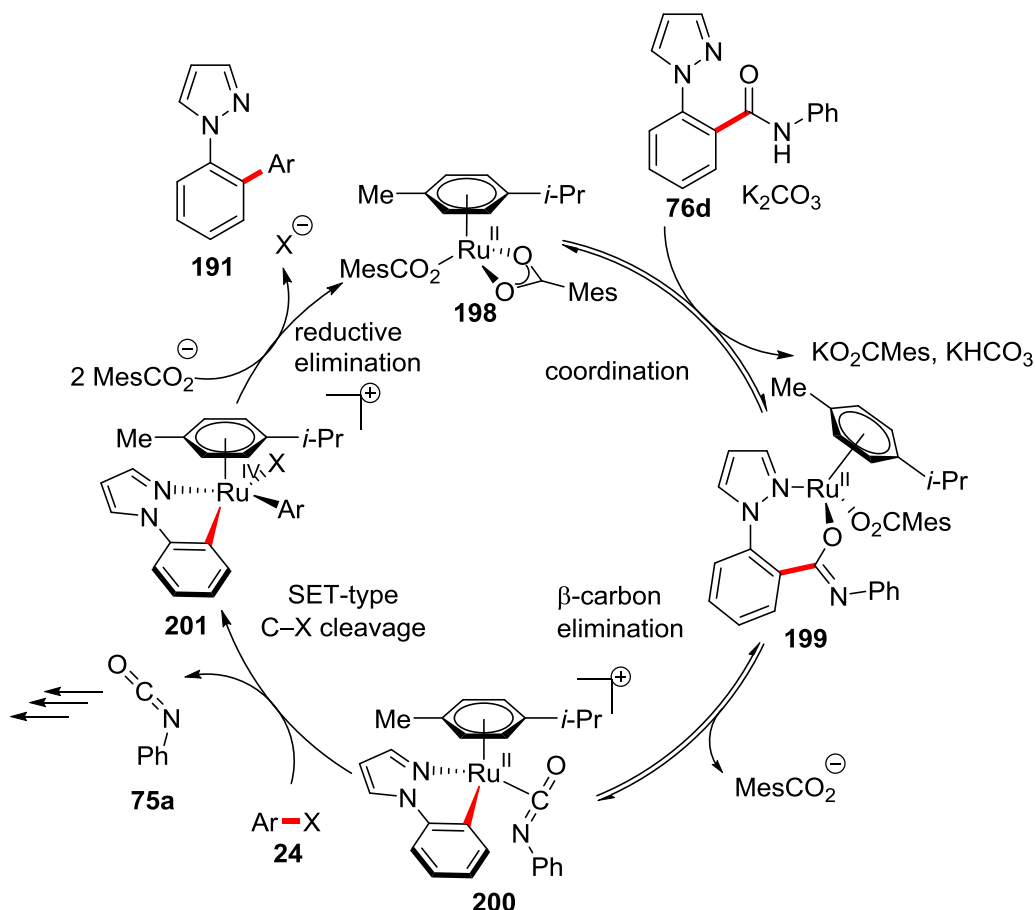
Entry	Radical Scavenger	Equiv	Yield / %
1	---	---	81
2	BHT	0.1	79
3	BHT	1.0	53
4	TEMPO	0.1	36
5	TEMPO	1.0	---

<sup>[a]</sup> Reaction conditions: **76a** (0.20 mmol), **24h** (0.40 mmol),  $[\text{RuCl}_2(p\text{-cymene})]_2$  (2.5 mol%), MesCO<sub>2</sub>H (10 mol%), K<sub>2</sub>CO<sub>3</sub> (2.0 equiv), radical scavenger, *o*-xylene (0.5 mL), 120 °C, 16 h.

To check whether the  $\beta$ -carbon elimination process is reversible, the reaction was performed with another isocyanate instead of aryl halide.<sup>[156]</sup> Indeed, another amide, derived from the submitted isocyanate, was isolated, demonstrating a reversible C–C cleavage.

Finally, after exploring the performance of this novel and versatile C–C activation reaction and based on our mechanistic studies, the following catalytic cycle was proposed (Scheme 3.33). The reaction is shown for the decarbamoylative C–C arylation of amides **76**, but the activation of acids **196** and alcohols **116** is suggested to work analogously. It starts with the  $[\text{Ru}(\text{O}_2\text{CMes})_2(p\text{-cymene})]$  (**198**) complex that can be submitted to the reaction directly or is generated *in situ*. Upon releasing MesCO<sub>2</sub><sup>−</sup> the cationic reactive complex coordinates to the amide and leads to deprotonation, generating the intermediate **199**. A similar coordination pattern can also be formulated for the acid and alcohol. In the next step, the C–C bond formation takes place *via* a  $\beta$ -C elimination that delivers the cycloruthenated species **200** and phenyl isocyanate (**75a**) that undergoes further reactions. In case of a decarboxylative or dealkanolative reaction CO<sub>2</sub> or a ketone are formed, respectively. This is followed by the C–X bond cleavage of

the aryl halide. Based on our mechanistic studies, it is plausible that this step proceeds *via* a single-electron-transfer (SET) from the ruthenium to the aryl halide followed by a subsequent radical recombination that forms a ruthenium(IV) complex **201**. However, other pathways, e.g. an oxidative addition into the C–X bond cannot be excluded. The thus formed high valent ruthenium(IV) species subsequently undergoes reductive elimination, generating the arylated arene **191** and coordination with carboxylic acid regenerates the active catalyst.



**Scheme 3.33:** Proposed catalytic cycle for ruthenium(II)-catalyzed decarbamoylative C–C arylation.

### 3.4.6 Diversification of the Pyrazoles

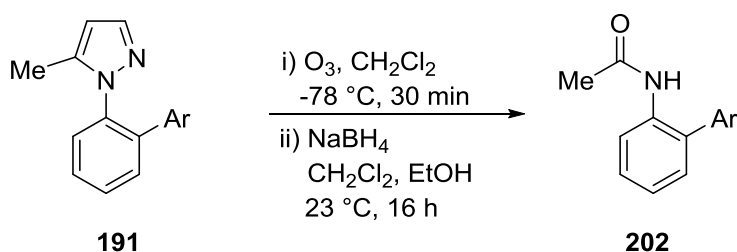
Though the pyrazole as well as the indazole moiety are important motifs in medicinal chemistry, further derivatizations will increase the applicability and therefore the impact of this reaction.

Promising diversification is represented the oxidation of the pyrazole core by ozonolysis.<sup>[157]</sup> In particular, the ozonolysis of 5-methyl pyrazoles yielding acetanilides are interesting. Because these oxidations are not reported with 5-methyl-1-aryl-1*H*-pyrazoles we first tested the reaction on 5-methyl-1-phenyl-1*H*-pyrazole (**191**) to find the

best reaction parameters and to prevent *inter alia* overoxidation. A preliminary optimization resulted in an initial current of 250 mA, an O<sub>3</sub>/O<sub>2</sub> flow of 50 L/h and a reaction time of 30 minutes at -78 °C to be the best parameters. After treatment with ozone, a reductive follow-up reaction delivered the desired acetanilides **202**.

With the optimal parameters identified, we applied the ozonolysis reaction to the C–C arylation products bearing a 5-methyl group (Table 3.23). We were delighted to obtain the biaryl anilides **202** for a representative set of substances. It should be noted that the isolated yields appeared moderate, but they are in line with related ozonolysis reactions.<sup>[158]</sup>

**Table 3.23:** Preparation of acetanilides **202** by ozonolysis.<sup>[a]</sup>



Entry	Pyrazole	Acetanilide	Yield / %
1	<p style="text-align: center;"><b>191ch</b></p>	<p style="text-align: center;"><b>202ch</b></p>	57
2	<p style="text-align: center;"><b>191cd</b></p>	<p style="text-align: center;"><b>202cd</b></p>	62
3	<p style="text-align: center;"><b>191ce</b></p>	<p style="text-align: center;"><b>202ce</b></p>	38



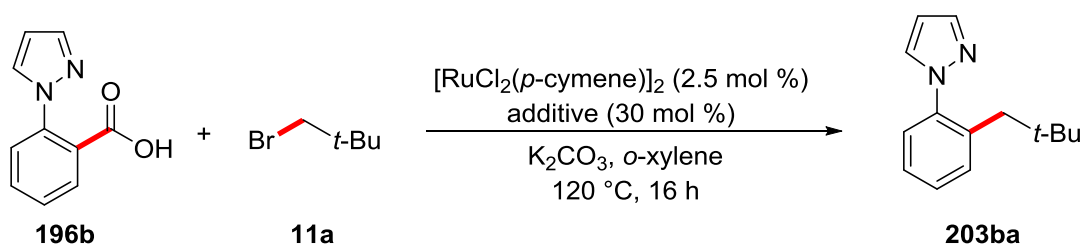
<sup>[a]</sup> Reaction conditions: **191** (0.20 mmol), O<sub>3</sub>/O<sub>2</sub> stream (Initial Current: 250 mA, Rate: 50 L/h), CH<sub>2</sub>Cl<sub>2</sub> (20 mL), –78 °C, 30 min, then NaBH<sub>4</sub> (4.0 equiv), CH<sub>2</sub>Cl<sub>2</sub>/MeOH, 23 °C, 16 h.

### 3.5 Ruthenium(II)-Catalyzed Decarboxylative C–C Alkylation

The above mentioned examples highlight the versatility of this novel ruthenium(II)-catalyzed C–C functionalization for arylation and hydroarylation reactions. In this aspect, a high interest was raised whether this protocol could be applied to important alkylation reactions with organic electrophiles. In addition, exploring the selectivity of this alkylation would be of equal importance with the experience in *meta*-selective C–H alkylations.<sup>[114, 159]</sup> However, performing a decarboxylative alkylation under basic conditions bears the intrinsic problem of esterification. Therefore, the C–C alkylation has to be optimized to be faster than the undesired esterification.

#### 3.5.1 Optimization Studies

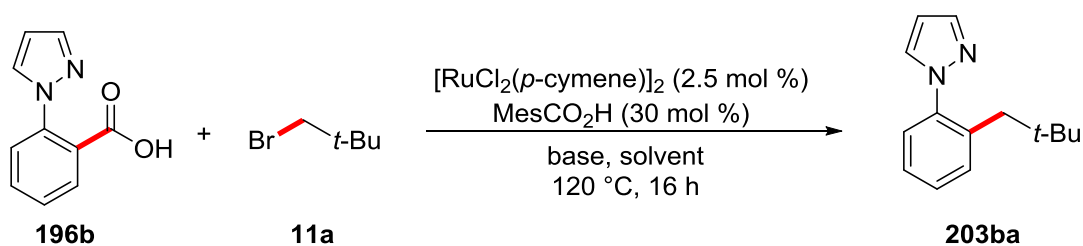
We commenced our studies by using 2-pyrazolyl benzoic acid (**196b**) and neopentyl bromide (**11a**) (Table 3.24). The neopentyl group was chosen for the optimization, since a certain bulk at the  $\beta$ -position on the alkane would hinder the non-desired esterification. We began this optimization with probing of different additives. With the key role of carboxylic acids for the related C–C arylation (Table 3.15), these additives might be the one of choice for the present reaction, too. However, the starting material itself is a carboxylic acid and may also serve as an additive. Indeed, in absence of an external carboxylic acid, the desired alkylation does proceed in acceptable yields (entry 1). Using the same catalytic system as for the arylation reaction with 10 mol% of MesCO<sub>2</sub>H, a significant improvement resulted (entry 2), showing that the starting material can act as an additive, but not as the best one. Yet, every carboxylic acid as additive would compete with the starting material for coordination to the ruthenium giving a mixture of carboxylate complexes and therefore a reduced activity. To circumvent this problem, the amount of acid was increased to get a higher amount of the more active complex. Fortunately, the use of 30 mol % of MesCO<sub>2</sub>H resulted in an almost quantitative yield of 95% (entry 3). The use of other carboxylic acids had just a minor effect on the yield (entries 4-6), and only acetic acid led to a significant decrease in conversion (entry 7). Identical to the C–C arylation, phosphorous based ligands, such PPh<sub>3</sub>, and PCy<sub>3</sub> shut down the reaction.

**Table 3.24:** Additives for the ruthenium(II)-catalyzed decarboxylative C–C alkylation.<sup>[a]</sup>

Entry	Additive	Yield / %
1	---	60
2	MesCO <sub>2</sub> H	75 <sup>[b]</sup>
3	MesCO <sub>2</sub> H	95
4	1-AdCO <sub>2</sub> H	81
5	PhCO <sub>2</sub> H	80
6	1-NaphCO <sub>2</sub> H	74
7	AcOH	59
8	PPh <sub>3</sub>	---
9	PCy <sub>3</sub>	---

<sup>[a]</sup> Reaction conditions: **196b** (0.50 mmol), **11a** (1.50 mmol), [RuCl<sub>2</sub>(*p*-cymene)]<sub>2</sub> (2.5 mol%), additive (30 mol%), K<sub>2</sub>CO<sub>3</sub> (2.0 equiv), *o*-xylene (1.0 mL), 120 °C, 16 h.<sup>[b]</sup> MesCO<sub>2</sub>H (10 mol%).

The optimization was continued with the testing of different bases and solvents (Table 3.25). Also for this reaction, the base proved necessary (entry 1), suggesting the deprotonation of the carboxylic acid as the initial step. In fact, this can be followed visually during the reaction. Beginning with a red/brown suspension, the formation of a yellow solid occurs after some minutes, indicating the formation of the less soluble carboxylate. After stirring for additional 1 hour, decarboxylation takes place and the reaction turns dark brown. Among the tested bases, just carbonates resulted in satisfactory yields without severe differences between Na<sub>2</sub>CO<sub>3</sub> and Cs<sub>2</sub>CO<sub>3</sub> (entries 5 and 6). The tolerance of different solvents was somewhat larger. Toluene, *m*-xylene and *t*-butyl benzene served as well (entries 8-10) and also 1,4-dioxane gave acceptable results (entry 11).

**Table 3.25:** Bases and solvents for the ruthenium(II)-catalyzed C–C alkylation.<sup>[a]</sup>

Entry	Base	Solvent	Yield / %
1	---	<i>o</i> -xylene	---
2	KOAc	<i>o</i> -xylene	10
3	K <sub>3</sub> PO <sub>4</sub>	<i>o</i> -xylene	---
4	NaOH	<i>o</i> -xylene	---
5	Na <sub>2</sub> CO <sub>3</sub>	<i>o</i> -xylene	89
6	Cs <sub>2</sub> CO <sub>3</sub>	<i>o</i> -xylene	91
7	DBU	<i>o</i> -xylene	---
8	K <sub>2</sub> CO <sub>3</sub>	PhMe	87
9	K <sub>2</sub> CO <sub>3</sub>	<i>m</i> -xylene	90
10	K <sub>2</sub> CO <sub>3</sub>	<i>t</i> -BuPh	85
11	K <sub>2</sub> CO <sub>3</sub>	1,4-dioxane	60
10	K <sub>2</sub> CO <sub>3</sub>	<i>t</i> -AmOH	38
11	K <sub>2</sub> CO <sub>3</sub>	GVL	10
10	K <sub>2</sub> CO <sub>3</sub>	H <sub>2</sub> O	---

<sup>[a]</sup> Reaction conditions: **196b** (0.50 mmol), **11a** (1.50 mmol), [RuCl<sub>2</sub>(*p*-cymene)]<sub>2</sub> (2.5 mol%), MesCO<sub>2</sub>H (30 mol%), base (2.0 equiv), solvent (1.0 mL), 120 °C, 16 h.

Subsequently, we also had a closer look on different ruthenium sources (Table 3.26). The well defined complex [Ru(O<sub>2</sub>CMes)<sub>2</sub>(*p*-cymene)] gave comparably high yield (entry 1) as compared to the system generated *in situ* from [RuCl<sub>2</sub>(*p*-cymene)]<sub>2</sub>. Simple ruthenium salts, like RuCl<sub>3</sub>·(H<sub>2</sub>O)<sub>n</sub>, and a ruthenium(0) complex, like [Ru<sub>3</sub>(CO)<sub>12</sub>], failed to

give any conversion (entries 2 and 3). To our delight, ruthenium nitrile complexes  $[\text{Ru}(t\text{-BuCN})_6][\text{BF}_4]_2$  and  $[\text{Ru}(\text{MeCN})_6][\text{BF}_4]_2$  turned out to be active catalysts for the desired reaction, though with a slight decrease in activity than the established ruthenium-cymene system (entries 4 and 5). The use of these cymene-free complexes gave already promising results in related C–H functionalization reactions.<sup>[160]</sup> It is also possible to substitute the tetrafluoroborate anion by a weakly coordinating anion (entry 6). Though the use of such complexes is not as synthetical useful, it represents the first application of WCAs in ruthenium-catalyzed C–H alkylation. Lastly, no reaction takes place in the absence of ruthenium compounds (entry 7).

**Table 3.26:** Ruthenium-sources for C–C alkylation.<sup>[a]</sup>

$\text{196b} + \text{11a} \xrightarrow[\text{K}_2\text{CO}_3, \text{ } o\text{-xylene}, 120^\circ\text{C}, 16\text{ h}]{[\text{Ru}] (5.0 \text{ mol } \%), \text{ additive } (30 \text{ mol } \%)}$ 
 $\text{203ba}$

Entry	[Ru]	Additive	Yield / %
1	$[\text{Ru}(\text{O}_2\text{CMes})_2(p\text{-cymene})]$	---	85
2	$[\text{Ru}_3(\text{CO})_{12}]$	---	---
3	$\text{RuCl}_3 \cdot (\text{H}_2\text{O})_n$	$\text{MesCO}_2\text{H}$	---
4	$[\text{Ru}(t\text{-BuCN})_6][\text{BF}_4]_2$	$\text{MesCO}_2\text{H}$	79
5	$[\text{Ru}(\text{MeCN})_6][\text{BF}_4]_2$	$\text{MesCO}_2\text{H}$	60
6	$[\text{Ru}(t\text{-BuCN})_6][\text{Al}(\text{hfp})_4]$	$\text{MesCO}_2\text{H}$	61 <sup>[b]</sup>
7	---	$\text{MesCO}_2\text{H}$	---

<sup>[a]</sup> Reaction conditions: **196b** (0.50 mmol), **11a** (1.50 mmol), [Ru] (5.0 mol%), additive (30 mol%),  $\text{K}_2\text{CO}_3$  (2.0 equiv), *o*-xylene (1.0 mL), 120 °C, 16 h. <sup>[b]</sup> Performed by K. Korvorapun.

### 3.5.2 Scope for the Decarboxylative Ruthenium(II)-Catalyzed C–C Alkyltion with Alkyl Halides

With the identified optimized reaction conditions, we tested its applicability in terms of different acids **196** and alkyl bromides **11**. Beginning with the latter, we probed a representative set of primary alkyl bromides **11** (Table 3.27). Though the scope is

somewhat limited, all reactions resulted in good to very good yields with perfect selectivity on the *ipso*-position of the acid. Moreover, undesired esterification could not be observed. However, primary alkyl halides **11** required a substituent at the  $\beta$ -position to the halide as esterification does occur in case of linear alkyl bromides.

**Table 3.27:** Scope for primary alkyl halides for ruthenium(II)-catalyzed decarboxylative alkylation.<sup>[a]</sup>

Entry	Alkyl Bromide	Product	Yield / %
1	 <b>11a</b>	 <b>203ba</b>	95
2	 <b>11b</b>	 <b>203bb</b>	80
3	 <b>11c</b>	 <b>203bc</b>	81

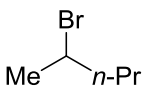
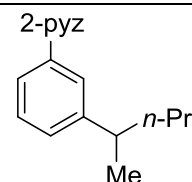
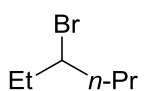
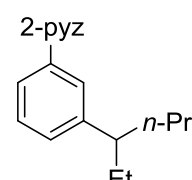
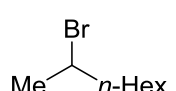
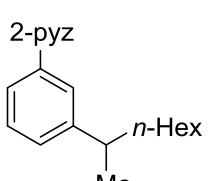

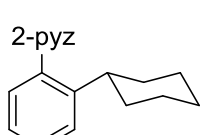
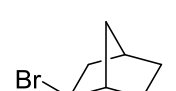
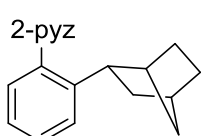
<sup>[a]</sup> Reaction conditions: **196b** (0.50 mmol), **11** (1.50 mmol),  $[\text{RuCl}_2(p\text{-cymene})]_2$  (2.5 mol%),  $\text{MesCO}_2\text{H}$  (30 mol%),  $\text{K}_2\text{CO}_3$  (2.0 equiv),  $\sigma$ -xylene (1.0 mL), 120 °C, 16 h.

Next, we studied secondary alkyl bromides (Table 3.28). Their alkylations are of high interest due to the *meta*-selective behavior of the related C–H alkylation.<sup>[114, 159]</sup> Indeed, the alkylation with secondary alkyl bromides proceeds *meta* to the directing group *via* a C–C/C–H activation pathway. The yields were good to moderate and this protocol is applicable to cyclic alkyl bromides with 5-, 7-, and 8-membered rings (entries 1-3) as well

as acyclic alkyl bromides (entries 4-7). All the alkylation proceeded with perfect regioselectivity and also esterification could not be observed in any example. The reactivity of cyclohexyl as well as norbornyl bromide (**11k** and **11l**) was striking. These six-membered cycloalkyl bromides gave the alkylated arene with *ortho*-substitution to the pyrazole directing group and also in perfect selectivity (entries 8 and 9).

**Table 3.28:** Scope for secondary alkyl halides for the ruthenium(II)-catalyzed decarboxylative alkylation.<sup>[a]</sup>

Entry	Alkyl Bromide	Product	Yield / %
1	 11d	 209bd	50
2	 11e	 209be	73
3	 11f	 209bf	55 <sup>[b]</sup>
4	 11g	 209bg	50

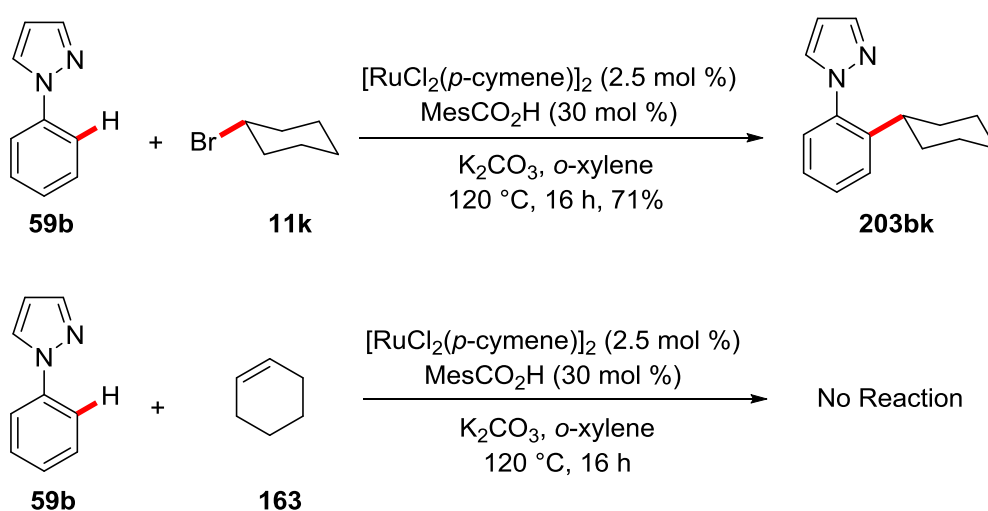
Entry	Alkyl Bromide	Product	Yield / %
5	 <b>11h</b>	 <b>209bh</b>	60
6	 <b>11i</b>	 <b>209bi</b>	59
7	 <b>11j</b>	 <b>209bj</b>	71
8	 <b>11k</b>	 <b>209bk</b>	75
9	 <b>11l</b>	 <b>209bl</b>	66

<sup>[a]</sup> Reaction conditions: **196b** (0.50 mmol), **11** (1.50 mmol), [RuCl<sub>2</sub>(*p*-cymene)]<sub>2</sub> (2.5 mol%), MesCO<sub>2</sub>H (30 mol%), K<sub>2</sub>CO<sub>3</sub> (2.0 equiv), *o*-xylene (1.0 mL), 120 °C, 16 h.

<sup>[b]</sup> [RuCl<sub>2</sub>(*p*-cymene)]<sub>2</sub> (5.0 mol%).

Especially the last two examples are the most astonishing ones in this scope and the question arose whether this effect originates from the C–C bond cleavage or rather from the electronic and steric effects of the directing group. To this end, we used the same catalytic system for the C–H alkylation of phenyl pyrazole (**59b**) with cyclohexyl bromide (**11k**) (Scheme 3.34). Again, the reaction product featured the cyclohexyl moiety in *ortho* position to the directing group. In contrast, a C–H alkylation of phenyl pyridine with

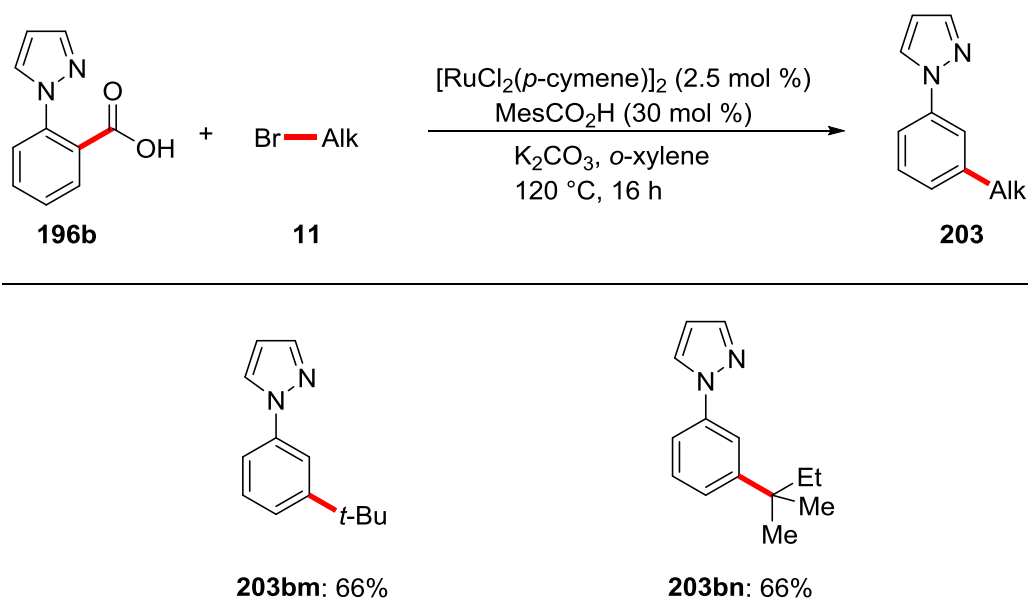
cyclohexyl bromide resulted in *meta*-substitution.<sup>[114c]</sup> Another possible explanation might be that the cyclohexyl bromide eliminates HBr and the *in situ* formed cyclohexene (**163**) undergoes migratory insertion. To test this hypothesis, the reaction was performed with cyclohexene (**163**), but no conversion was observed (Scheme 3.34). From these experiments the unexpected *ortho* alkylation with cyclohexyl bromide (**11k**) and norbornyl bromide (**11l**) originates from the pyrazole directing group. With the identified effect, it is not completely understood why cyclohexyl-containing rings afford this selectivity. Assuming a cycloruthenated species as reaction intermediate (*vide infra*), the addition of the cyclohexyl and norbornyl moiety to the ruthenium is apparently favored towards the addition to the arene.



**Scheme 3.34:** C–H Alkylation with cyclohexyl bromide (**11k**) and attempted hydroarylation.

Finally, the same catalytic system proved viable for the C–C alkylation with tertiary alkyl bromides **11** (Scheme 3.35). Though these two examples show moderate yields, it underlines the broad applicability for primary, secondary and tertiary alkyl bromides **11**.



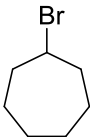
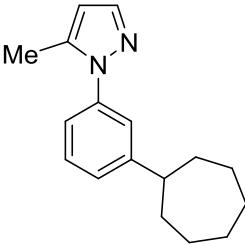
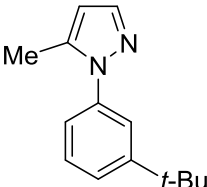
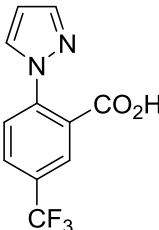
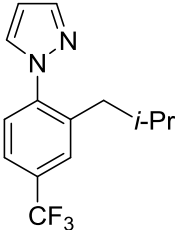
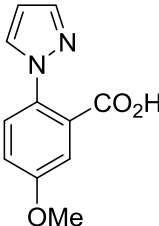
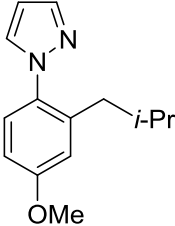


**Scheme 3.35:** Tertiary alkyl bromides for the ruthenium(II)-catalyzed decarboxylative alkylation.

Motivated by the large variety of alkyl bromides **11**, the substitution pattern on the arene and directing group was examined next (Table 3.29). In view of further derivatizations, the 5-methyl pyrazole was tested for primary, secondary and tertiary alkylation. To our delight, comparable yields were obtained as with the unsubstituted pyrazole (entries 1–3). As was observed for the C–C arylation, the 5-methyl pyrazole group gave access to acetanilides by ozonolysis (*vide infra*).<sup>[157]</sup> Furthermore, electron-withdrawing as well as donating groups on the arene were well tolerated (entries 4 and 5).

**Table 3.29:** Scope of the ruthenium(II)-catalyzed decarboxylative C–C alkylation with arenes **196**.<sup>[a]</sup>

Entry	Acid	Alkyl Bromide	Product	Yield / %
1	<p><b>196c</b></p>	<p><b>11b</b></p>	<p><b>203cb</b></p>	82

Entry	Acid	Alkyl Bromide	Product	Yield / %
2	<b>196c</b>	 <b>11e</b>	 <b>203ce</b>	77
3	<b>196c</b>	Br- <i>t</i> -Bu <b>11m</b>	 <b>203cm</b>	61
4	 <b>196d</b>	<b>11b</b>	 <b>203db</b>	88
5	 <b>196e</b>	<b>11b</b>	 <b>203eb</b>	90

<sup>[a]</sup> Reaction conditions: **196** (0.50 mmol), **11** (1.50 mmol), [RuCl<sub>2</sub>(*p*-cymene)]<sub>2</sub> (2.5 mol%), MesCO<sub>2</sub>H (30 mol%), K<sub>2</sub>CO<sub>3</sub> (2.0 equiv), *o*-xylene (1.0 mL), 120 °C, 16 h.

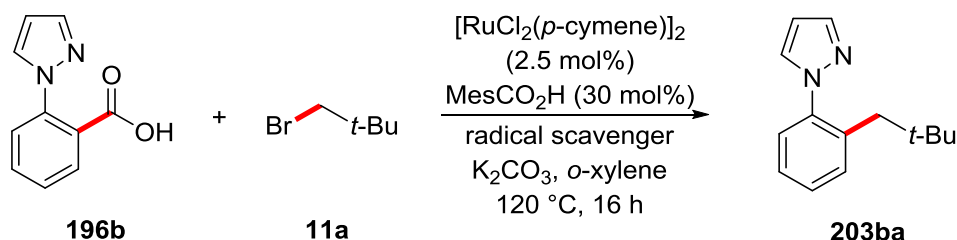
### 3.5.3 Mechanistic Studies

Given the broad applicability of this novel C–C alkylation reaction with primary, secondary and tertiary alkyl bromides, we became interested in understanding the mechanism of this transformation.

Related to the C–C arylation, a radical pathway could also be involved in this reaction. To this end, typical radical scavengers were employed in the primary and secondary alkylation. For the primary alkylation, stoichiometric amounts of BHT were necessary to

significantly decrease the yield (Table 3.30). In contrast, just 10 mol % of TEMPO lowered the yield to 22% and stoichiometric amounts stopped the reaction completely. Furthermore, no reaction takes place when the reaction was performed under air. These results are quite similar to the ones obtained for the C–C arylation (Table 3.22).

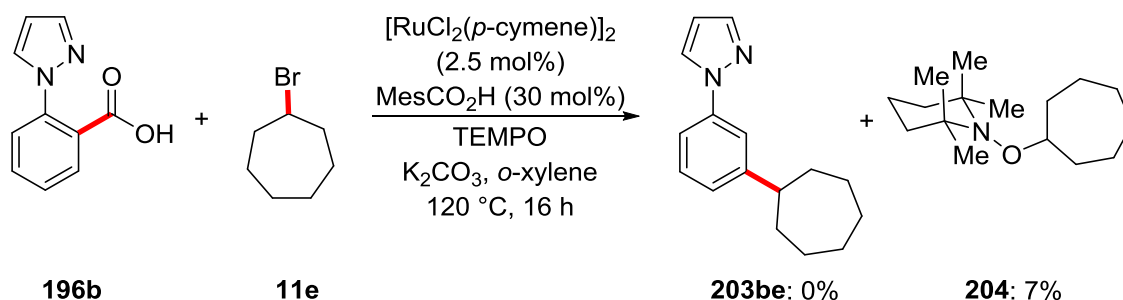
**Table 3.30:** Influence of radical scavengers for the ruthenium(II)-catalyzed decarboxylative C–C alkylation.



Entry	Radical Scavenger	Equiv	Yield / %
1	---	---	95
2	BHT	0.1	90
3	BHT	1.0	61
4	TEMPO	0.1	22
5	TEMPO	1.0	---
6	Air	---	---

<sup>[a]</sup> Reaction conditions: **196b** (0.50 mmol), **11a** (1.50 mmol),  $[\text{RuCl}_2(p\text{-cymene})]_2$  (2.5 mol%),  $\text{MesCO}_2\text{H}$  (30 mol%),  $\text{K}_2\text{CO}_3$  (2.0 equiv), radical scavenger, *o*-xylene (1.0 mL), 120 °C, 16 h.

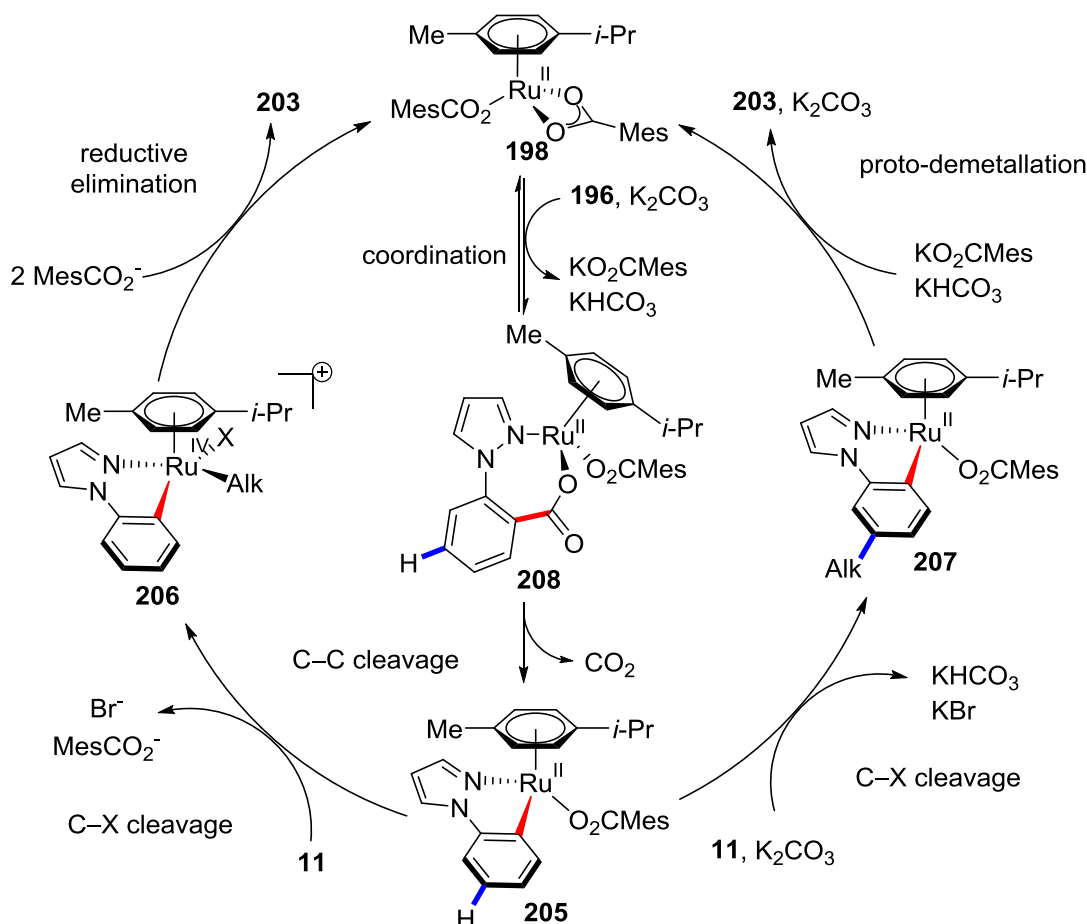
Though the inhibition with TEMPO is obvious, an alkyl adduct could neither be isolated nor detected. It is possible that the primary alkyl radical is too reactive and undergoes further reactions than addition to TEMPO. The picture is somewhat clearer in case of secondary alkyl bromides (Scheme 3.36). Also here, an equivalent of TEMPO shuts down the reaction completely but the cycloheptyl adduct could be detected by gas chromatography and even be isolated, albeit with just 7% yield.<sup>[161]</sup>



**Scheme 3.36:** Ruthenium(II)-catalyzed secondary alkylation in the presence of TEMPO. Reaction performed by K. Korvorapun.

These findings are comparable with those obtained for related C–H alkylation with secondary alkyl bromides where a radical SET-type C–X cleavage is supposed to be the *modus operandi*.<sup>[114b, 114c, 159]</sup> For the alkylation with primary halides the picture is somewhat more complicated and is still a subject of current research. Though a TEMPO-alkyl adduct could not be detected, we cannot completely exclude a radical pathway.

With the gained knowledge about the C–C alkylation reactions, the following catalytic cycle was proposed (Scheme 3.37). The reaction is commenced by the coordination of **200** to the ruthenium center. The C–C cleavage is achieved by  $\beta$ -elimination, generating the five-membered ruthenacycle **211** and CO<sub>2</sub>. The complex **211** can undergo two pathways, depending on the alkyl halide. In case of primary alkyl halides, the alkyl moiety adds to the ruthenium centre, presumably by a SET type process that generates the ruthenium(IV) species **212**. Subsequent reductive elimination is followed and results in the formation of the *ortho*-alkylated product **209** and regeneration of the active catalyst **202**. For most of the secondary and tertiary alkyl bromides, the alkyl radical adds to the arene in *para* position to the ruthenium that delivers the intermediate **213**. The product is released by proto-demetalation, which also regenerates the catalyst.

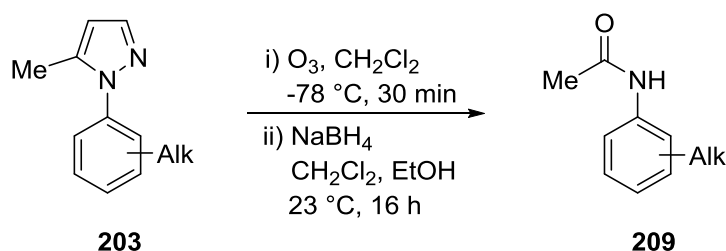


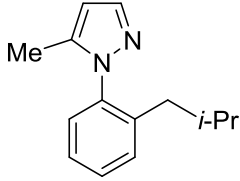
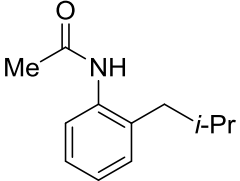
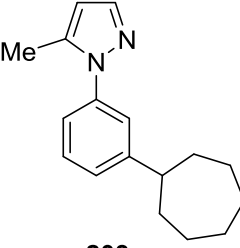
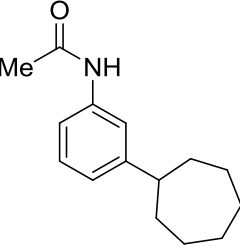
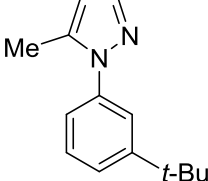
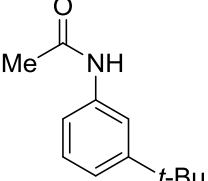
**Scheme 3.37:** Proposed catalytic cycles for the ruthenium(II)-catalyzed C–C alkylations.

### 3.5.4 Ozonolysis of the Pyrazole Directing Group

Considering the successful diversification of the C–C arylation products bearing a 5-methyl pyrazole directing group, we also tested this method for the C–C alkylation products. This diversification could be successfully applied to primary, secondary and tertiary alkylated compounds (Table 3.31). The yields with up to 71% are remarkably high as compared to related ozonolysis reactions.<sup>[157a, 158]</sup> Overall, this diversification rounds up the versatile character of the presented C–C alkylation, giving access to differently substituted acetanilides **209**.

**Table 3.31:** Ozonolysis of alkylated phenyl pyrazoles **203**.<sup>[a]</sup>



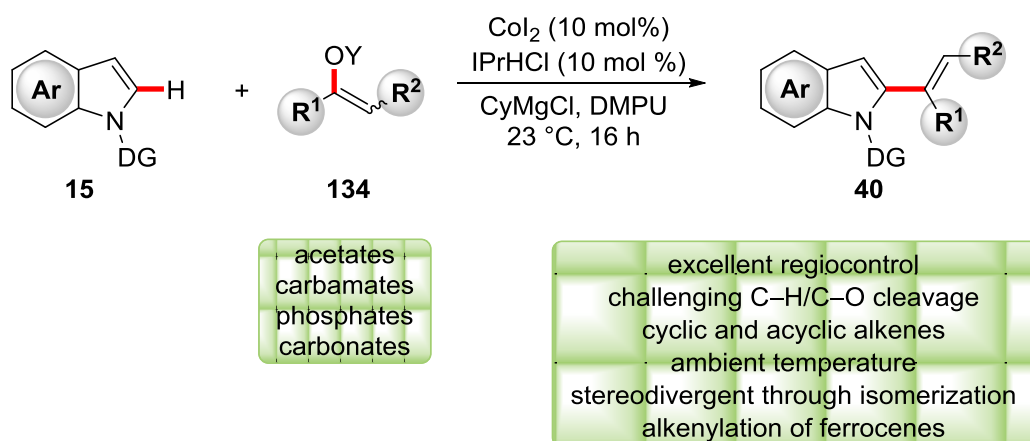
Entry	Pyrazole	Acetanilide	Yield / %
1	 <b>203cb</b>	 <b>209cb</b>	71
2	 <b>203ce</b>	 <b>209ce</b>	65
3	 <b>203cm</b>	 <b>209cm</b>	61

<sup>[a]</sup> Reaction conditions: **203** (0.20 mmol), O<sub>3</sub>/O<sub>2</sub> stream (Initial Current: 250 mA, Rate: 50 L/h), CH<sub>2</sub>Cl<sub>2</sub> (20 mL), -78 °C, 30 min, then NaBH<sub>4</sub> (4.0 equiv), CH<sub>2</sub>Cl<sub>2</sub>/MeOH, 23 °C, 16 h.

## 4 Summary and Outlook

C–H and C–C bonds belong to the most abundant motifs in organic molecules. Therefore, their selective functionalizations in an economical and ecological fashion are of greatest interest with an impact that outreaches academia and also increases the toolbox for many industrial applications.

In the first project, the cobalt-catalyzed C–H alkenylation with alkenyl esters was examined (Scheme 4.1).<sup>[125a]</sup> Thus far, the synthesis of alkenylated arenes by cobalt catalysis was restricted to hydroarylation reactions with alkynes. Despite the variety of methods, all these protocols just provided acyclic alkenes and furthermore, the regioselectivity of the alkyne insertion is mostly governed by sterics. Here, we managed to establish the first cobalt-catalyzed C–H alkenylation with organic electrophiles using cost-effective cobalt iodide and an easily accessible NHC precursor. This method allowed for the synthesis of cyclic as well as acyclic alkenes with perfect levels of regioselectivities. The highlight of this reaction is its stereoconvergent character that transforms alkenyl esters with a mixture of *E* and *Z* isomers highly selective to the *E* alkene. Mechanistic studies demonstrated that the catalytic system is able to isomerizes the enolate and an order in reactivity of the alkenyl esters could be estimated that is:  $\text{OAc} \approx \text{OC(O)NMe}_2 < \text{OP(O)(OEt)}_2$ . The choice of arenes was not restricted to heterocycles, such as indoles and pyrroles, but could also be extended to simple arenes and even more, this method can be applied to the C–H alkenylation of challenging ferrocenes. Though the yield of 48% percent is just moderate, it represents the first example of cobalt-catalyzed C–H activation on ferrocenes.

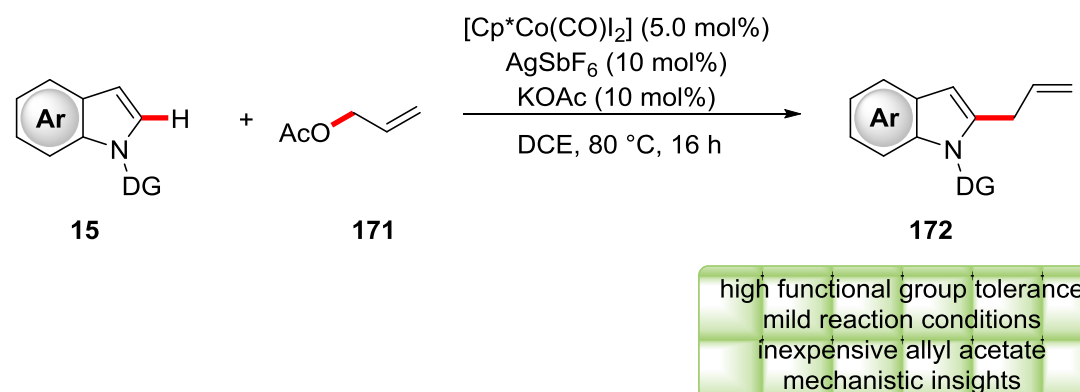


**Scheme 4.1:** Cobalt-catalyzed C–H alkenylation with alkenyl esters.

Though a series of mechanistic experiments were performed, the exact origin of the stereoconvergent character is not completely understood. Therefore, more effort could be spent for a better understand of this transformation. The aforementioned alkenylation

of ferrocenes set a promising base for enantioselective alkenylations by cobalt catalysis and the development of suitable chiral ligands may fulfill this goal. Related to this work, efforts have been made to extend this system. In a recent publication our group showed that not just imidazole derived NHCs, but also triazole-based ones could perform this reaction.<sup>[162]</sup> And also quite recently, Butenschön and coworkers developed a cobalt-catalyzed methylation of ferrocenes<sup>[163]</sup> based on our system.

In the second project, we moved from C–H alkenylation to C–H allylation and replaced the low-valent cobalt catalyst by a high valent Cp\*Co(III) complex. An active catalytic system could be established by using [Cp\*Co(CO)I<sub>2</sub>] as the precatalyst, catalytic amounts of AgSbF<sub>6</sub> and KOAc in DCE at 80 °C (Scheme 4.2).<sup>[138a]</sup> This allowed for the effective C–H allylation of phenyl rings, pyrroles and indoles with easily accessible allyl acetate by C–H/C–O activation. This reaction features a very high functional group tolerance that tolerates *inter alia* amides, halides and nitro groups. A surprising result was found when allyl acetate was replaced by crotyl acetate. As related reactions by rhodium, ruthenium, cobalt and manganese afforded the S<sub>N</sub>' (i.e. the branched product),<sup>[59, 136d, 136e, 137, 139, 164]</sup> our reaction delivered both the S<sub>N</sub>' and the S<sub>N</sub> (i.e. the linear)

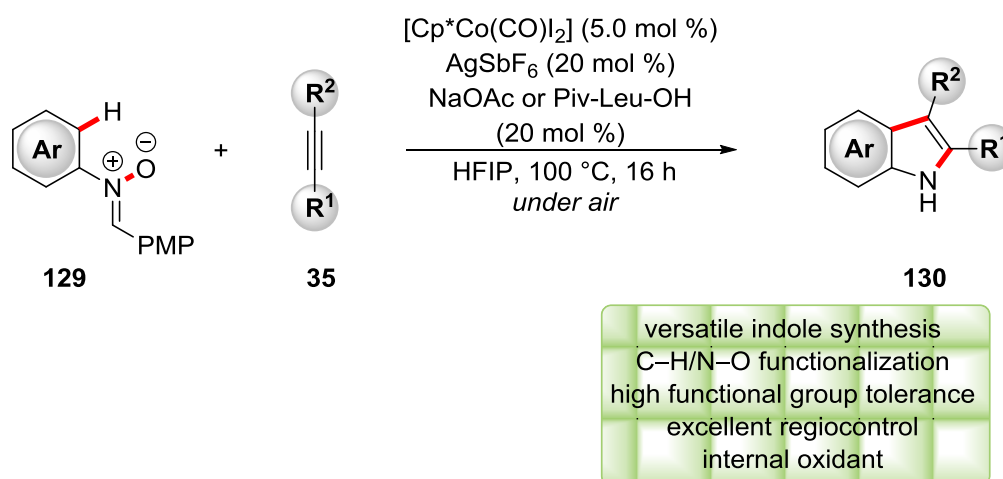


**Scheme 4.2:** Cobalt-catalyzed C–H allylation with allyl acetate (**171**).

The cobalt-catalyzed allylation gained great interest. In parallel and subsequent works, Glorius<sup>[59, 137a]</sup> and Matsunaga/Kanai<sup>[137b]</sup> published similar findings with allyl carbamates and allyl alcohols. A recent allylation reaction by ruthenium catalysis was published by Kapur and coworkers.<sup>[139]</sup> Very recently, Anbarasan reported on a cobalt-catalyzed allylation with allyl carbonates where also the S<sub>N</sub> product could be isolated, albeit in moderate yield.<sup>[165]</sup> The optimization of this reaction yielding the linear allylic compound would be worth optimizing, so that a change in the catalytic system would switch the selectivity.



The last project on cobalt-catalyzed C–H activation addressed the indole synthesis from nitrones by C–H/C–O bond activation. This heterocycle plays an important role in medicinal chemistry and the above described examples show the successful derivatization at the C-2 position by a cyclometalated reaction intermediate. For this reason, a cobalt-catalyzed *de novo* synthesis of substituted indoles would be useful. After careful screening of cobalt (pre-)catalysts, additives and solvents, H. Wang identified an active catalytic system for the selective indole synthesis from easily accessible nitrones and alkynes under cobalt(III) catalysis (Scheme 4.3).<sup>[19b]</sup> The scope of this reaction could be extended to more substitution patterns on the arene and unsymmetrical alkynes. Those with an alkyl aryl rest reacted with perfect levels of regioselectivities with the aryl group on C2-position of the indole, or in other words, proximal to the cobalt centre in the insertion step. The most surprising result was, however, the reaction with unsymmetrical bis aryl alkynes. Whereas these compounds showed no level of selectivity in related rhodium-catalyzed reactions,<sup>[113]</sup> the tested example showed excellent selectivity in our established system. A different reactivity was observed when 3-hexyne was submitted to the reaction. Here, the 3*H*-indole was formed, albeit in just moderate yield. This reactivity can be explained with a higher nucleophilic character after the alkyne insertion step with a consequent that a Manich type reaction takes place instead of the expected proto-demetalation.



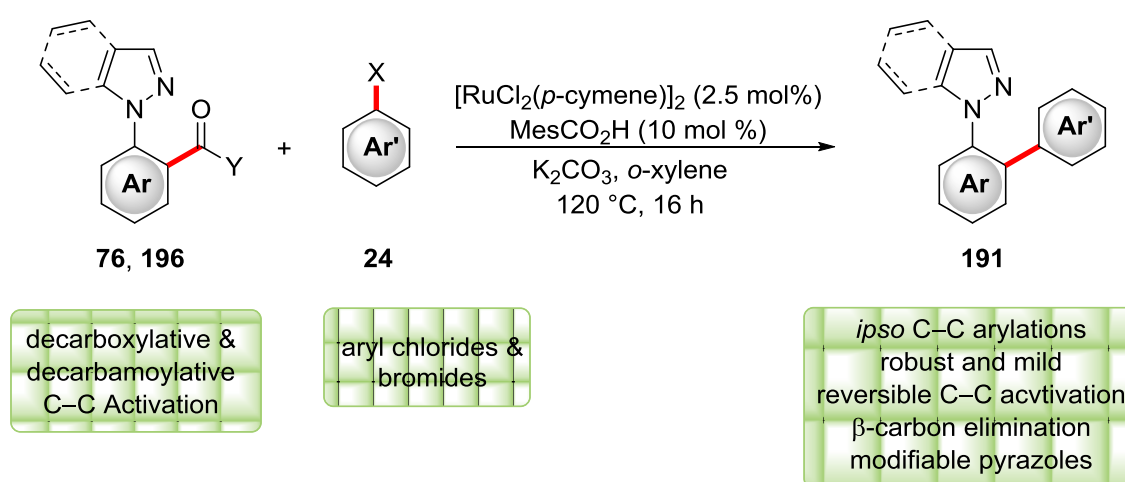
**Scheme 4.3:** Cobalt-Catalyzed Indole Synthesis by C–H/N–O Functionalization.

Overall, this method represents a useful method for the preparation of *NH*-free indoles with multiple substituents without an additional removal of a directing group at the 1-position. However, the atom-economy is nevertheless not high, because of the generation of 4-methoxybenzaldehyde as the side product. Furthermore, only 2- and 3-substituted indoles can be made possible, as the reaction does not proceed with terminal

alkynes. Then, the reaction can still be optimized to proceed with terminal alkynes and with smaller leaving groups on the nitron.

Also the cobalt-catalyzed indole synthesis arose interest in other research groups. In a subsequent work, Glorius reported on the cobalt-catalyzed indole synthesis from acetyl hydrazides and alkynes by N–N bond cleavage<sup>[142]</sup> and from acetanilides and alkynes in a dehydrogenative reaction.<sup>[166]</sup>

The next two projects examined the less explored C–C functionalization and in particular, the functionalization at the *ipso*-position by ruthenium(II) catalysis. It was possible to establish a highly versatile catalytic system that allowed for the decarboxylative, dealkanolative as well as decarbamoylative C–C arylation with aryl halides (Scheme 4.4).<sup>[156a]</sup> Notable features of this reaction were *inter alia* the very high functional group tolerance. Thus, halides, heterocycles and even NH<sub>2</sub>-free anilines were converted smoothly with exclusive C<sub>ipso</sub>-selectivity. The C–C transformation could be achieved with a pyrazole or indazole directing group. To our delight the C–C functionalization was not restricted to arylations, but migratory insertion could also be performed after the C–C bond cleavage. With this, C–C hydroarylations of styrenes could be made possible. Extensive mechanistic studies on this novel reaction type revealed an organometallic activation mode. Moreover, submitting an isocyanate to the reaction lead to the formation of another amide, thus demonstrating the reversible nature of the decarbamoylative C–C activation step. Furthermore, this method also allowed for optional post-functional diversification. Ozonolysis of the pyrazole directing group gave access to arylated acetanilides.



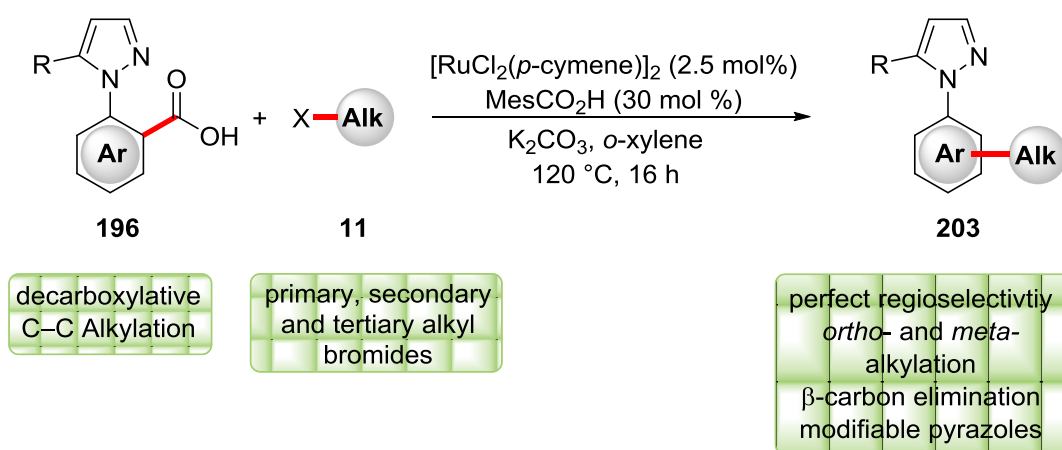
**Scheme 4.4:** Ruthenium(II)-Catalyzed Decarboxylative and Decarbamoylative C–C Arylations.

Though ongoing process is made for ruthenium(II)-catalyzed decarboxylative reactions,<sup>[153]</sup> up to now, no method exist for the *ipso* substitution. Those reactions can

be performed by palladium catalysis, but they suffer from problems with selectivity and require copper or silver additives.<sup>[144a]</sup> Therefore, this reaction is a breakthrough for achieving C–C arylations.

However, the relatively low atom-economy is a significant limitation of this reaction, since CO<sub>2</sub>, ketones and isocyanate adducts are formed as byproducts. Therefore, the development of a synthetically useful leaving group that could for example remain at the molecule at a remote position would be highly desirable. It would allow for new retrosynthetic analysis and increase the toolbox for synthetic chemistry.

Within the last project, we used the C–C activation protocol for alkylations with organic electrophiles. It was possible to establish a decarboxylative alkylation with a variety of alkyl bromides with perfect levels of regioselectivity (Scheme 4.5).<sup>[161]</sup> Reactions with primary alkyl halides led to *ortho*-selective C–C alkylation. The selectivity changed when moving to secondary and tertiary alkyl halides which mostly added to the *meta* position of the directing group. A notable exception from this rule was observed when secondary alkyl halides with a cyclohexyl moiety were submitted to the reaction. These compounds resulted in an *ortho*-selective C–C alkylation. Based on mechanistic investigations of this reaction an organometallic  $\beta$ -C elimination activation pathway was supposed. In contrast, the C–Br cleavage of the alkyl halide proceeded arguably by a radical SET-type process. Finally, diversification of the thus-obtained arylated products **203** could be demonstrated by ozonolysis, yielding the corresponding alkylated acetanilides.



**Scheme 4.5:** Ruthenium(II)-Catalyzed Decarboxylative C–C Alkylation.

Here, we have developed the first C–C alkylation reaction by C–C bond cleavage with organic electrophiles, a reaction manifold that was never described before. It demonstrates again the high versatility of the ruthenium catalyst for C–C activation. As predicted for the arylation, an improvement towards better atom-economy would make

this reaction a more broadly applicable method. Furthermore, the exact origin for *meta* and *ortho* substitution could be further investigated. In particular, the substrate dependence for the secondary alkylation is of key importance.

## 5 Experimental Part

### 5.1 General Remarks

All reactions involving moisture- or air-sensitive reagents or products were performed under an atmosphere of nitrogen using pre-dried glassware and standard Schlenk techniques. If not otherwise noted yields refer to isolated compounds, estimated to be >95% pure as determined by  $^1\text{H}$  NMR and GC analysis.

#### Vacuum

The following average pressure was measured on the used rotary vane pump RZ6 from Vacuubrand®:  $0.8 \cdot 10^{-1}$  mbar (uncorrected value)

#### Melting Points

Melting points were measured on a Stuart® Melting Point Apparatus SMP3 from Barloworld Scientific. Values are uncorrected.

#### Chromatography

Analytical thin layer chromatography (TLC) was performed on silica gel 60 F<sub>254</sub> aluminium sheets from Merck. Plates were either visualized under irradiation at 254 nm or 365 nm or developed by treatment with a potassium permanganate solution followed by careful warming. Chromatographic purification was accomplished by flash column chromatography on Merck Geduran® silica gel, grade 60 (40–63  $\mu\text{m}$ , 70–230 mesh ASTM).

#### Gas Chromatography

Monitoring of reaction process *via* gas chromatography or coupled gas chromatography-mass spectrometry was performed using a 7890 GC-system with/without mass detector 5975C (Triple-Axis-Detector) or a 7890B GC-system coupled with a 5977A mass detector, both from Agilent Technologies®.

#### Recycling Preparative HPLC

Recycling preparative HPLC (GPC) was performed on a system from JAI® (LC-92XX II Series, injection- and control-valve, UV and RI detector) connected to JAIGEL HH series columns. Chloroform of HPLC grade was employed.

### Infrared Spectroscopy

Infrared (IR) spectra were recorded using a Bruker® Alpha-P ATR spectrometer. Liquid samples were measured as film and solid samples neat. Spectra were recorded in the range from 4000 to 400  $\text{cm}^{-1}$ . Analysis of the spectral data were carried out using Opus 6. Absorption is given in wave numbers ( $\text{cm}^{-1}$ ).

### Nuclear Magnetic Resonance Spectroscopy

Nuclear magnetic resonance (NMR) spectra were recorded on Mercury Plus 300, VNMRS 300, Inova 500 and 600 from Varian®, or Avance 300, Avance III 300 and 400, Avance III HD 400 and 500 from Bruker®. Chemical shifts are reported in  $\delta$ -values in ppm relative to the residual proton peak or carbon peak of the deuterated solvent.

	$^1\text{H}$ NMR	$^{13}\text{C}$ NMR
$\text{CDCl}_3$	7.26	77.16
$\text{DMSO-d}_6$	2.50	39.52
$\text{Acetone-d}_6$	2.05	29.84

The following abbreviations are used to describe the observed multiplicities: s (singlet), d (doublet), t (triplet), q (quartet), p (pentet), h (hexet), hept (heptet), m (multiplet) or analogous representations. The coupling constants  $J$  are reported in Hertz (Hz). Analysis of the recorded spectra was carried out using MestReNova 10 software.

### Mass Spectrometry

Electron ionization (EI) and EI high resolution mass spectra (HRMS) were measured on a time-of-flight mass spectrometer AccuTOF from JOEL. Electrospray ionization (ESI) mass spectra were recorded on an Io-Trap mass spectrometer LCQ from Finnigan, a quadrupole time-of-flight maXis from Bruker Daltonic or on a time-of-flight mass spectrometer microTOF from Bruker Daltonic. ESI-HRMS spectra were recorded on a Bruker Apex IV or Bruker Daltonic 7T, fourier transform ion cyclotron resonance (FTICR) mass spectrometer. The ratios of mass to charge ( $m/z$ ) are indicated, intensities relative to the base peak ( $I = 100$ ) are written in parentheses.

### Hydrogenations

Hydrogenation reactions were conducted using a H-Cube® flow system from Thales Nano. Hydrogen was generated by electrolysis of water. The employed catalysts ruthenium on charcoal, Raney-Nickel, Raney-Cobalt and platinum on silica were packed in cartridges and obtained from Thales Nano or Sigma Aldrich.

### Ozonolysis

Ozone was generated on a Fischer Model 502 ozone generator attached to an oxygen gas cylinder using the indicated current and flow.

### Solvents

Solvents for column chromatography were purified via distillation under reduced pressure prior to their use. All solvents for reactions involving moisture-sensitive reagents were dried, distilled and stored under inert atmosphere (Ar or N<sub>2</sub>) according to following standard procedures.<sup>[167]</sup>

Solvents purified by solvent purification system (SPS-800) from M. Braun: Dichloromethane, toluene, diethylether, tetrahydrofurane, dimethylformamide.

Solvents dried and distilled over sodium using benzophenone as indicator: *t*-Amylalcohol, *o*-,*m*-,*p*-xylene, 1,4-dioxane, *n*-Bu<sub>2</sub>O, methanol.

Solvents dried and distilled over CaH<sub>2</sub>: 1,2-Dichloroethane, 1,3-dimethyltetrahydropyrimidin-2(1*H*)-one, *N*-methyl-2-pyrrolidone,  $\gamma$ -valerolactone

Water was degassed before its use applying repeated freeze-pump-thaw cycles.

### Reagents

Chemicals obtained from commercial sources (with a purity of >95%) were used without further purification. The following compounds were known and synthesized according to previously described literature protocols:

(pyrimidyl-2-yl)-1*H*-indoles **15**,<sup>[122]</sup> 2-(2-methyl-1*H*-pyrrol-1-yl)pyrimidine **146**,<sup>[168]</sup> (pyridine-2-yl)-1*H*-ferrocene **154**,<sup>[127]</sup> alkenyl acetates **134**,<sup>[117c, 169]</sup> alkenyl carbamates **150**,<sup>[124d]</sup> alkenyl carbonate **151**,<sup>[124b]</sup> alkeyl phosphates **149**,<sup>[124a]</sup> crotyl acetate (**171b**),<sup>[170]</sup> allyl carbonate **176**, carbamate **175**,<sup>[171]</sup> sulfamate **178** and phosphate **179**,<sup>[124a]</sup> [Cp\*Co(CO)I<sub>2</sub>] and [Cp\*Co(C<sub>6</sub>H<sub>6</sub>)](PF<sub>6</sub>)<sub>2</sub>,<sup>[51]</sup> nitrones **128**,<sup>[172]</sup> bisaryl alkynes **35**,<sup>[173]</sup> aryl alkyl alkynes **35**<sup>[174]</sup>, amides **76**<sup>[58, 63e, 175]</sup> and acids **196**.<sup>[63e, 176]</sup>

The following compounds were kindly synthesized and provided by the persons named below.

**Maria J. González:** Alkynes **35g**, **35i**, **35k**.

**Frederik Kramm:** Amides **76b**, **76e**, **76f**.

**Jie (Jack) Li:** Amides **76d**, **76g**

**Josef Mathys:** [Cp\*Co(CO)I<sub>2</sub>].

**Karsten Rauch:** [RuCl<sub>2</sub>(*p*-cymene)]<sub>2</sub>, [Ru(O<sub>2</sub>CMes)<sub>2</sub>(*p*-cymene)], Phenyl Pyridine **14f**.

**Sven C. Richter:** Alkenyl Acetates **134e**, **134k**, **134l**.

**Nicolas Sauermann:** Indoles **14e**, **14g**, **14h**, **14i**.

**Hui Wang:** Nitroene **129a**.

**Svenja Warratz:** [Ru(*t*-BuCN)<sub>6</sub>][BF<sub>4</sub>]<sub>2</sub>, [Ru(MeCN)<sub>6</sub>][BF<sub>4</sub>]<sub>2</sub>, [Ru(*t*-BuCN)<sub>6</sub>][Al(hfip)<sub>4</sub>], phenyl pyrimidine **14b**.

**Alexandra Schischko:** Aryl bromide **24s**,

## 5.2 General Procedures

### General Procedure A: Cobalt-Catalyzed Alkenylation with Enol Derivatives

To a solution of heteroarene **14**, **15** or **146** (0.50 mmol, 1.0 equiv), the enol derivative **134**, **149-151** (0.75 mmol, 1.5 equiv), CoI<sub>2</sub> (15.7 mg, 0.05 mmol, 10 mol %) and IPrHCl (**13**) (21.2 mg, 0.05 mmol, 10 mol %) in DMPU (1.5 mL), CyMgCl (1.0 M in 2-MeTHF, 1 mL, 1.00 mmol, 2.0 equiv) was added dropwise. The mixture was stirred for 16 h at 23 °C. After completion of the reaction, saturated aq. NH<sub>4</sub>Cl solution (5 mL) was added and the mixture was extracted with MTBE (4 x 5 mL). Drying over Na<sub>2</sub>SO<sub>4</sub>, evaporation of the solvents and purification by column chromatography on silica gel yielded the products **39**, **40** or **147**.

### General Procedure B: Cleavage of the Pyrimidyl Group

Pyrimidyl indole **40** (0.30 mmol, 1.0 equiv) and NaOEt (40.8 mg, 0.60 mmol, 2.0 equiv) were dissolved in DMSO (3 mL) and stirred at 100 °C for 24 h. After cooling to ambient temperature, the reaction mixture was diluted with EtOAc (10 mL) and washed with H<sub>2</sub>O (2 x 20 mL). The aqueous phase was extracted with EtOAc (2 x 20 mL) and the combined organic layers dried over Na<sub>2</sub>SO<sub>4</sub>. Evaporation of the solvent and purification by column chromatography on silica gave the indole **170**.

**General Procedure C: Cobalt-Catalyzed C–H Allylation with Allyl Acetates**

To a solution of heteroarene **14**, **15**, or **146** (0.50 mmol, 1.0 equiv), [Cp\*Co(CO)I<sub>2</sub>] (11.9 mg, 0.03 mmol, 5.0 mol %), AgSbF<sub>6</sub> (17.2 mg, 0.05 mmol, 10 mol %) and KOAc (4.9 mg, 0.05 mmol, 10 mol %) in DCE (1.5 mL) allyl acetate (**171a**) (100 mg, 1.00 mmol, 2.0 equiv) was added. The mixture was stirred for 16 h at 80 °C. After completion of the reaction, saturated aq. NH<sub>4</sub>Cl solution (5 mL) was added at ambient temperature and the mixture was extracted with MTBE (4 x 5 mL). Drying over Na<sub>2</sub>SO<sub>4</sub>, evaporation of the solvent and purification by column chromatography on silica gel or further preparative HPLC using *n*-hexane/EtOAc yielded the products **172-174**.

**General Procedure D: Cobalt-Catalyzed C–H/N–O Functionalization**

A suspension of nitrene **129** (0.50 mmol, 1.0 equiv), alkyne **35** (0.75 mmol, 1.5 equiv), [Cp\*Co(CO)I<sub>2</sub>] (12.1 mg, 0.03 mmol, 5.0 mol %), AgSbF<sub>6</sub> (34.4 mg, 0.10 mmol, 20 mol %), NaOAc (8.2 mg, 0.10 mmol, 20 mol %) or Piv-Leu-OH (22.1 mg, 0.10 mmol, 20 mol %) was stirred at 100 °C for 16 h under ambient air. After cooling to ambient temperature, the mixture was transferred into a round bottom flask with CH<sub>2</sub>Cl<sub>2</sub> (20 mL) and concentrated in *vacuo*. Purification by column chromatography on silica gel and optionally GPC afforded the desired product **130**.

**General Procedure E: Ruthenium(II)-Catalyzed C–C Arylation of Amides and Acids**

To a Schlenk tube charged with amide **76** or acid **196** (0.20 mmol, 1.0 equiv), aryl halide **24** (0.22–0.50 mmol, 1.1–2.5 equiv), [RuCl<sub>2</sub>(*p*-cymene)]<sub>2</sub> (3.1 mg, 5.0 μmol, 2.5 mol %), MesCO<sub>2</sub>H (3.3 mg, 20 μmol, 10 mol %) and K<sub>2</sub>CO<sub>3</sub> (55.3 mg, 0.40 mmol, 2.0 equiv) was added *o*-xylene (0.5 mL). The Schlenk tube was degassed and filled with N<sub>2</sub> three times and the mixture was stirred at 120 °C for 16 h. After cooling to ambient temperature, the solvent was removed under reduced pressure and purification of the residue by column chromatography on silica gel yielded the product **191**.

**General Procedure F: Ruthenium(II)-Catalyzed Hydroarylation of Acids:**

To a Schlenk tube charged with acid **196** (0.20 mmol, 1.0 equiv), alkene **46** (0.40 mmol, 2.0 equiv), [RuCl<sub>2</sub>(*p*-cymene)]<sub>2</sub> (3.1 mg, 5.0 μmol, 2.5 mol %), MesCO<sub>2</sub>H (3.3 mg, 20 μmol, 10 mol %) and K<sub>2</sub>CO<sub>3</sub> (55.3 mg, 0.40 mmol, 2.0 equiv) was added *o*-xylene (0.5 mL). The Schlenk tube was degassed and refilled with N<sub>2</sub> three times and the mixture was stirred at 120 °C for 16 h. Removal of the solvent under reduced pressure and purification of the residue by column chromatography on silica gel yielded the product **197**.

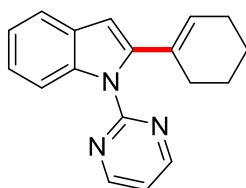


**General Procedure G: Ozonolysis of Pyrazoles**

A solution of pyrazole **191**, **203** (0.20 mmol, 1.0 equiv) in CH<sub>2</sub>Cl<sub>2</sub> (20 mL) was cooled to –78 °C. Ozone (Initial current: 250 mA, flow: 50 L/h) was passed through the solution for 20–40 min. Thereafter, the solution was allowed to warm up to ambient temperature, whereupon a solution of NaBH<sub>4</sub> (30.3 mg, 0.80 mmol, 4.0 equiv) in EtOH (10 mL) was added and the reaction was allowed to stir for 16 h. H<sub>2</sub>O (10 mL) and brine (10 mL) were added to the reaction mixture, the aqueous layer was extracted with CH<sub>2</sub>Cl<sub>2</sub> (20 mL), dried over Na<sub>2</sub>SO<sub>4</sub> and concentrated *in vacuo*. Purification by column chromatography on silica gel yielded the anilides **202**, **209**.

**General Procedure H: Ruthenium(II)-Catalyzed C–C Alkylation of Acids:**

To a Schlenk tube charged with acid **191** (0.50 mmol, 1.0 equiv), alkyl bromide **11** (1.50 mmol, 3.0 equiv), [RuCl<sub>2</sub>(*p*-cymene)]<sub>2</sub> (7.7 mg, 13 μmol, 2.5 mol %) MesCO<sub>2</sub>H (24.6 mg, 0.15 mmol, 30 mol %) and K<sub>2</sub>CO<sub>3</sub> (138 mg, 1.00 mmol, 2.0 equiv) was added *o*-xylene (1.0 mL). The Schlenk tube was degassed and filled with N<sub>2</sub> three times and the mixture was stirred at 120 °C for 16 h. Removal of the solvent under reduced pressure and purification of the residue by column chromatography on silica gel yielded the product **203**.

**5.3 Cobalt-Catalyzed C–H Alkenylation with Enol Derivatives****5.3.1 Experimental Procedures and Analytical Data****2-(Cyclohex-1-en-1-yl)-1-(pyrimidin-2-yl)-1*H*-indole (40aa)****40aa**

The general procedure **A** was followed using indole **15a** (97.6 mg, 0.50 mmol, 1.0 equiv) and enol acetate **134a** (106 mg, 0.75 mmol, 1.5 equiv). Purification by column chromatography (*n*-hexane/EtOAc: 9/1) yielded **40aa** (121 mg, 0.44 mmol, 88%) as a colorless solid.

The general procedure **A** was followed using indole **15a** (97.6 mg, 0.50 mmol, 1.0 equiv) and enol phosphate **149a** (176 mg, 0.75 mmol, 1.5 equiv). Purification by column

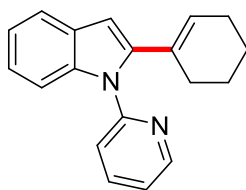
chromatography (*n*-hexane/EtOAc: 9/1) yielded **40aa** (106 mg, 0.39 mmol, 77%) as a colorless solid.

The general procedure **A** was followed using indole **15a** (97.6 mg, 0.50 mmol, 1.0 equiv) and enol carbamate **150a** (127 mg, 0.75 mmol, 1.5 equiv). Purification by column chromatography (*n*-hexane/EtOAc: 9/1) yielded **40aa** (120 mg, 0.44 mmol, 87%), as a colorless solid.

The general procedure **A** was followed using indole **40aa** (97.6 mg, 0.50 mmol, 1.0 equiv) and enol carbonate **151a** (128 mg, 0.75 mol, 1.5 equiv). Purification by column chromatography (*n*-hexane/EtOAc: 9/1) yielded **40aa** (77.1 mg, 0.28 mmol, 56%), as a colorless solid.

**M.p.:** 157–159 °C. **<sup>1</sup>H-NMR** (300 MHz, CDCl<sub>3</sub>):  $\delta$  = 8.66 (d, *J* = 4.2 Hz, 2H), 8.17–8.15 (m, 1H), 7.59–7.57 (m, 1H), 7.27–7.18 (m, 2H), 7.09 (t, *J* = 4.2 Hz, 1H), 6.57 (d, *J* = 0.7 Hz, 1H), 5.89–5.87 (m, 1H), 2.20–2.17 (m, 2H), 2.10–2.07 (m, 2H), 1.68–1.65 (m, 4H). **<sup>13</sup>C-NMR** (125 MHz, CDCl<sub>3</sub>):  $\delta$  = 158.2 (C<sub>q</sub>), 158.0 (CH), 143.3 (C<sub>q</sub>), 137.3 (C<sub>q</sub>), 131.7 (C<sub>q</sub>), 129.2 (C<sub>q</sub>), 127.0 (CH), 122.9 (CH), 121.8 (CH), 120.1 (CH), 117.2 (CH), 113.0 (CH), 106.0 (CH), 28.9 (CH<sub>2</sub>), 25.5 (CH<sub>2</sub>), 22.7 (CH<sub>2</sub>), 22.0 (CH<sub>2</sub>). **IR** (ATR): 2928, 1558, 1452, 1346, 1318, 794, 738, 717, 615, 463 cm<sup>-1</sup>. **MS** (ESI) *m/z* (relative intensity) 298 (35) [M+Na]<sup>+</sup>, 276 (100) [M+H]<sup>+</sup>, 247 (19), 219 (8). **HR-MS** (ESI) *m/z* calcd for C<sub>18</sub>H<sub>17</sub>N<sub>3</sub> [M+H]<sup>+</sup>: 276.1501, found: 276.1497.

#### 2-(Cyclohex-1-en-1-yl)-1-(pyridin-2-yl)-1*H*-indole (**40ba**)



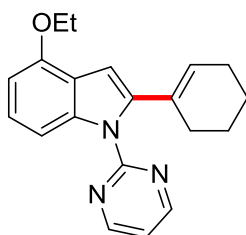
**40ba**

The general procedure **A** was followed using indole **15b** (97.1 mg, 0.50 mmol, 1.0 equiv) and enol acetate **134a** (106 mg, 0.75 mmol, 1.5 equiv). Purification by column chromatography (*n*-hexane/EtOAc: 12/1) yielded **40ba** (125 mg, 0.46 mmol, 91%) as a pale yellow solid.

**M.p.:** 109–111 °C. **<sup>1</sup>H-NMR** (300 MHz, CDCl<sub>3</sub>):  $\delta$  = 8.67–8.65 (m, 1H), 7.79 (ddd, *J* = 8.1, 7.5, 2.0 Hz, 1H), 7.57–7.61 (m, 2H), 7.29–7.28 (m, 1H), 7.27 (dd, *J* = 3.7, 1.0 Hz, 1H), 7.17–7.13 (m, 2H), 6.56 (d, *J* = 0.8 Hz, 1H), 5.81–5.79 (m, 1H), 2.11–2.06 (m, 4H), 1.63–1.58 (m, 4H). **<sup>13</sup>C-NMR** (125 MHz, CDCl<sub>3</sub>):  $\delta$  = 152.7 (C<sub>q</sub>), 149.0 (CH), 142.4 (C<sub>q</sub>), 138.0

(C<sub>q</sub>), 137.7 (CH), 130.0 (C<sub>q</sub>), 129.4 (CH), 128.5 (C<sub>q</sub>), 122.4 (CH), 121.4 (CH), 121.0 (CH), 120.9 (CH), 120.1 (CH), 111.1 (CH), 103.4 (CH), 28.3 (CH<sub>2</sub>), 25.6 (CH<sub>2</sub>), 22.6 (CH<sub>2</sub>), 21.9 (CH<sub>2</sub>). **IR** (ATR): 2929, 1585, 1473, 1344, 1321, 1048, 996, 748, 665, 608 cm<sup>-1</sup>. **MS** (ESI) *m/z* (relative intensity) 312 (25) [M+K]<sup>+</sup>, 275 (100) [M+H]<sup>+</sup>. **HR-MS** (ESI) *m/z* calcd for C<sub>19</sub>H<sub>18</sub>N<sub>2</sub> [M+H]<sup>+</sup>: 275.1543, found: 275.1544.

### 2-(Cyclohex-1-en-1-yl)-4-ethoxy-1-(pyrimidin-2-yl)-1*H*-indole (40ca)

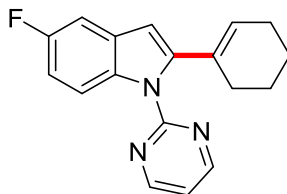


**40ca**

The general procedure **A** was followed using indole **15c** (118 mg, 0.50 mmol, 1.0 equiv) and enol acetate **134a** (105 mg, 0.75 mmol, 1.5 equiv). Purification by column chromatography (*n*-hexane/EtOAc: 15/1) yielded **40ca** (95.8 mg, 0.30 mmol, 60%) as a pale yellow solid.

**M.p.**: 105–107 °C. **<sup>1</sup>H-NMR** (300 MHz, CDCl<sub>3</sub>)  $\delta$  = 8.77 (d, *J* = 5.4 Hz, 2H), 7.71 (d, *J* = 8.3 Hz, 1H), 7.13–7.09 (m, 2H), 6.68 (d, *J* = 0.7 Hz, 1H), 6.61 (d, *J* = 8.3 Hz, 1H), 5.85–5.83 (m, 1H), 4.18 (q, *J* = 5.6 Hz, 2H), 2.14–2.12 (m, 2H), 2.05–2.04 (m, 2H), 1.64–1.61 (m, 4H), 1.47 (t, *J* = 5.6 Hz, 3H). **<sup>13</sup>C-NMR** (125 MHz CDCl<sub>3</sub>):  $\delta$  = 158.5 (C<sub>q</sub>), 158.1 (CH), 152.1 (C<sub>q</sub>), 141.8 (C<sub>q</sub>), 138.8 (C<sub>q</sub>), 131.8 (C<sub>q</sub>), 126.7 (CH), 123.7 (CH), 119.9 (C<sub>q</sub>), 117.3 (CH), 106.1 (CH), 103.2 (CH), 103.1 (CH), 63.6 (CH<sub>2</sub>), 29.0 (CH<sub>2</sub>), 25.6 (CH<sub>2</sub>), 22.8 (CH<sub>2</sub>), 15.0 (CH<sub>2</sub>), 12.3 (CH<sub>3</sub>). **IR** (ATR): 2918, 1561, 1451, 1422, 1345, 1319, 1253, 832, 806, 745 cm<sup>-1</sup>. **MS** (ESI) *m/z* (relative intensity) 342 (12) [M+Na]<sup>+</sup>, 320 (100) [M+H]<sup>+</sup>. **HR-MS** (ESI) *m/z* calcd for C<sub>20</sub>H<sub>21</sub>N<sub>3</sub>O [M+H]<sup>+</sup>: 320.1757, found: 320.1757.

### 2-(Cyclohex-1-en-1-yl)-5-fluoro-1-(pyrimidin-2-yl)-1*H*-indole (40da)

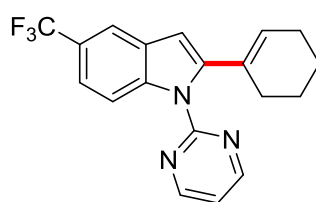


**40da**

The general procedure **A** was followed using indole **15d** (107 mg, 0.50 mmol, 1.0 equiv) and enol acetate **134a** (105 mg, 0.75 mmol, 1.5 equiv). Purification by column chromatography (*n*-hexane/EtOAc: 15/1) yielded **40da** (109 mg, 0.38 mmol, 75%) as a pale yellow solid.

**M.p.:** 141–142 °C. **<sup>1</sup>H-NMR** (300 MHz, CDCl<sub>3</sub>)  $\delta$  = 8.76 (d,  $J$  = 5.0 Hz, 2H), 8.08 (dd,  $J$  = 9.0, 5.0 Hz, 1H), 7.18 (dd,  $J$  = 9.0, 2.9 Hz, 1H), 7.13 (t,  $J$  = 5.0 Hz, 1H), 6.94 (ddd,  $J$  = 8.4, 2.9, 2.9 Hz, 1H), 6.48 (d,  $J$  = 0.7 Hz, 1H), 5.86–5.84 (m, 1H), 2.16–2.14 (m, 2H), 2.06–2.04 (m, 2H), 1.66–1.63 (m, 4H). **<sup>13</sup>C-NMR** (125 MHz, CDCl<sub>3</sub>):  $\delta$  = 159.0 (d,  $^1J_{\text{C-F}}$  = 237.5 Hz, C<sub>q</sub>), 158.2 (CH), 145.0 (C<sub>q</sub>), 133.8 (C<sub>q</sub>), 131.8 (C<sub>q</sub>), 131.7 (C<sub>q</sub>), 130.1 (d,  $^3J_{\text{C-F}}$  = 10.2 Hz, C<sub>q</sub>), 127.6 (CH), 117.4 (CH), 114.2 (d,  $^3J_{\text{C-F}}$  = 9.2 Hz, CH), 110.7 (d,  $^2J_{\text{C-F}}$  = 25.1 Hz, CH), 106.0 (CH), 105.4 (d,  $^2J_{\text{C-F}}$  = 23.5 Hz, CH), 29.2 (CH<sub>2</sub>), 25.8 (CH<sub>2</sub>), 23.0 (CH<sub>2</sub>), 22.3 (CH<sub>2</sub>). **<sup>19</sup>F-NMR** (282 MHz, CDCl<sub>3</sub>):  $\delta$  = –122.86. **IR** (ATR): 2924, 1574, 1424, 1351, 1278, 1250, 832, 804, 774, 742 cm<sup>–1</sup>. **MS** (ESI)  $m/z$  (relative intensity) 316 (16) [M+Na]<sup>+</sup>, 294 (100) [M+H]<sup>+</sup>. **HR-MS** (ESI)  $m/z$  calcd for C<sub>18</sub>H<sub>16</sub>FN<sub>3</sub> [M+H]<sup>+</sup>: 294.1401, found: 294.1401.

#### 2-(Cyclohex-1-en-1-yl)-1-(pyrimidin-2-yl)-5-(trifluoromethyl)-1*H*-indole (**40ea**)



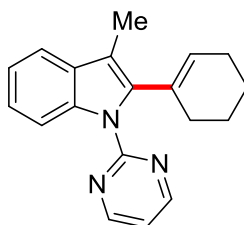
**40ea**

The general procedure **A** was followed using indole **15e** (132 mg, 0.50 mmol, 1.0 equiv) and enol acetate **134a** (105 mg, 0.75 mmol, 1.5 equiv). Purification by column chromatography (*n*-hexane/EtOAc: 15/1) yielded **40ea** (122 mg, 0.36 mmol, 71%) as a pale yellow oil.

**<sup>1</sup>H-NMR** (300 MHz, CDCl<sub>3</sub>)  $\delta$  = 8.81 (d,  $J$  = 4.3 Hz, 2H), 8.15 (dd,  $J$  = 7.3, 0.7 Hz, 1H), 7.83–7.81 (m, 1H), 7.43 (dd,  $J$  = 7.3, 1.9 Hz, 1H), 7.20 (t,  $J$  = 4.3 Hz, 1H), 6.58 (d,  $J$  = 0.7 Hz, 1H), 5.867–5.84 (m, 1H), 2.16–2.12 (m, 2H), 2.06–2.03 (m, 2H), 1.66–1.62 (m, 4H). **<sup>13</sup>C-NMR** (125 MHz, CDCl<sub>3</sub>):  $\delta$  = 158.3 (CH), 158.0 (C<sub>q</sub>), 145.0 (C<sub>q</sub>), 138.7 (C<sub>q</sub>), 131.3 (C<sub>q</sub>), 128.7 (C<sub>q</sub>), 128.2 (CH), 125.1 (q,  $^1J_{\text{C-F}}$  = 273.1 Hz, C<sub>q</sub>), 124.0 (q,  $^2J_{\text{C-F}}$  = 31.3 Hz, C<sub>q</sub>), 119.6 (q,  $^3J_{\text{C-F}}$  = 3.3 Hz, CH), 118.0 (CH), 117.7 (q,  $^3J_{\text{C-F}}$  = 3.3 Hz, CH), 113.2 (CH), 105.9 (CH), 29.1 (CH<sub>2</sub>), 26.0 (CH<sub>2</sub>), 22.7 (CH<sub>2</sub>), 21.4 (CH<sub>2</sub>). **<sup>19</sup>F-NMR** (282 MHz, CDCl<sub>3</sub>):  $\delta$  = –61.15. **IR** (ATR): 2929, 1564, 1449, 1333, 1278,

1157, 1057, 804  $\text{cm}^{-1}$ . **MS** (ESI)  $m/z$  (relative intensity) 344 (100)  $[\text{M}+\text{H}]^+$ , 321 (11). **HR-MS** (ESI)  $m/z$  calcd for  $\text{C}_{19}\text{H}_{16}\text{F}_3\text{N}_3$   $[\text{M}+\text{H}]^+$ : 344.1369, found: 344.1370.

**2-(Cyclohex-1-en-1-yl)-3-methyl-1-(pyrimidin-2-yl)-1H-indole (40fa)**

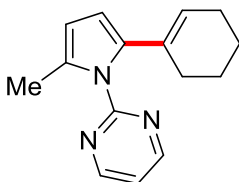


**40fa**

The general procedure **A** was followed using indole **15f** (104 mg, 0.50 mmol, 1.0 equiv) and enol acetate **134a** (105 mg, 0.75 mmol, 1.5 equiv). Purification by column chromatography (*n*-hexane/EtOAc: 18/1) yielded **40fa** (134 mg, 0.46 mmol, 93%) as a pale yellow solid.

**M.p.:** 166–168 °C.  **$^1\text{H-NMR}$**  (300 MHz,  $\text{CDCl}_3$ ):  $\delta$  = 8.72 (d,  $J$  = 4.4 Hz, 2H), 8.31–8.27 (m, 1H), 7.55–7.51 (m, 1H), 7.26–7.19 (m, 2H), 7.05 (t,  $J$  = 4.4 Hz, 1H), 5.79–5.77 (m, 1H), 2.28 (s, 3H), 2.24–2.20 (m, 2H), 2.02–1.98 (m, 2H), 1.68–1.66 (m, 4H).  **$^{13}\text{C-NMR}$**  (125 MHz,  $\text{CDCl}_3$ ):  $\delta$  = 158.2 ( $\text{C}_q$ ), 158.0 (CH), 138.7 ( $\text{C}_q$ ), 136.1 ( $\text{C}_q$ ), 131.4 ( $\text{C}_q$ ), 130.7 ( $\text{C}_q$ ), 128.5 (CH), 123.7 (CH), 123.2 (CH), 121.5 (CH), 118.5 (CH), 116.5 (CH), 113.3 ( $\text{C}_q$ ), 29.8 ( $\text{CH}_2$ ), 25.6 ( $\text{CH}_2$ ), 23.0 ( $\text{CH}_2$ ), 22.2 ( $\text{CH}_2$ ), 11.6 ( $\text{CH}_3$ ). **IR** (ATR): 2914, 1558, 1430, 1355, 1310, 1249, 1211, 1136, 1017, 792.  $\text{cm}^{-1}$ . **MS** (ESI)  $m/z$  (relative intensity) 290 (100)  $[\text{M}+\text{H}]^+$ , 238 (9), 210 (11). **HR-MS** (ESI)  $m/z$  calcd for  $\text{C}_{19}\text{H}_{19}\text{N}_3$   $[\text{M}+\text{H}]^+$ : 290.1652, found: 290.1654.

**2-[2-(Cyclohex-1-en-1-yl)-5-methyl-1H-pyrrol-1-yl]pyrimidine (147aa)**

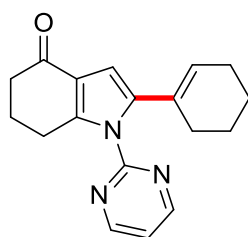


**147aa**

The general procedure **A** was followed using pyrimidyl pyrrole **146a** (80.3 mg, 0.50 mmol, 1.0 equiv) and enol acetate **134a** (105 mg, 0.75 mmol, 1.5 equiv). Purification by column chromatography (*n*-hexane/EtOAc: 6/1) yielded **147aa** (82.2 mg, 0.34 mmol, 69%) as a white solid.

**M.p.:** 92–94 °C. **<sup>1</sup>H-NMR** (300 MHz, CDCl<sub>3</sub>):  $\delta$  = 8.77 (d,  $J$  = 4.8 Hz, 2H), 7.20 (t, 4.8 Hz, 1H), 6.07 (d,  $J$  = 3.3 Hz, 1H), 5.94 (dd,  $J$  = 3.3, 1.0 Hz, 1H), 5.38–5.34 (m, 1H), 2.25 (d,  $J$  = 0.9 Hz, 3H), 2.00–1.93 (m, 4H), 1.58–1.50 (m, 4H). **<sup>13</sup>C-NMR** (125 MHz, CDCl<sub>3</sub>):  $\delta$  = 158.7 (C<sub>q</sub>), 158.0 (CH), 136.6 (C<sub>q</sub>), 130.7 (C<sub>q</sub>), 130.4 (C<sub>q</sub>), 124.4 (CH), 118.6 (CH), 108.3 (CH), 108.0 (CH), 28.6 (CH<sub>2</sub>), 25.5 (CH<sub>2</sub>), 22.8 (CH<sub>2</sub>), 22.1 (CH<sub>2</sub>), 13.7 (CH<sub>3</sub>). **IR** (ATR): 2930, 1572, 1557, 1514, 1417, 1247, 1210, 916, 824, 804 cm<sup>-1</sup>. **MS** (ESI)  $m/z$  (relative intensity) 262 (25) [M+Na]<sup>+</sup>, 240 (100) [M+H]<sup>+</sup>. **HR-MS** (ESI)  $m/z$  calcd for C<sub>15</sub>H<sub>17</sub>N<sub>3</sub> [M+H]<sup>+</sup>: 240.1495, found: 240.1497.

## 2-(Cyclohex-1-en-1-yl)-1-(pyrimidin-2-yl)-1,5,6,7-tetrahydro-4H-indol-4-one (147ba)

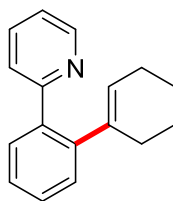


**147ba**

The general procedure **A** was followed using pyrrole **146b** (108 mg, 0.50 mmol, 1.0 equiv) and enol acetate **134a** (105 mg, 0.75 mmol, 1.5 equiv). Purification by column chromatography (*n*-hexane/EtOAc: 1/2) yielded **147ba** (78.3 mg, 0.27 mmol, 54%) as a white solid.

**M.p.:** 115–117 °C. **<sup>1</sup>H-NMR** (300 MHz, CDCl<sub>3</sub>):  $\delta$  = 8.79 (d,  $J$  = 4.8 Hz, 2H), 7.29 (t,  $J$  = 4.8 Hz, 1H), 6.50 (s, 1H), 5.48–5.44 (m, 1H), 2.85 (t,  $J$  = 6.2 Hz, 2H), 2.49 (dd,  $J$  = 7.7, 5.5 Hz, 2H), 2.10 (tt,  $J$  = 7.7, 5.5 Hz, 2H), 2.02–1.89 (m, 4H), 1.58–1.52 (m, 4H). **<sup>13</sup>C-NMR** (125 MHz, CDCl<sub>3</sub>):  $\delta$  = 194.3 (C<sub>q</sub>), 158.4 (CH), 157.4 (C<sub>q</sub>), 145.2 (C<sub>q</sub>), 138.3 (C<sub>q</sub>), 129.6 (C<sub>q</sub>), 126.9 (CH), 121.4 (C<sub>q</sub>), 119.3 (CH), 105.3 (CH), 37.9 (CH<sub>2</sub>), 28.7 (CH<sub>2</sub>), 25.6 (CH<sub>2</sub>), 23.8 (CH<sub>2</sub>), 23.7 (CH<sub>2</sub>), 22.7 (CH<sub>2</sub>), 21.9 (CH<sub>2</sub>). **IR** (ATR): 2926, 1655, 1571, 1413, 1313, 1214, 1176, 1134, 896, 834 cm<sup>-1</sup>. **MS** (ESI)  $m/z$  (relative intensity) 332 (80) [M+K]<sup>+</sup>, 316 (28) [M+Na]<sup>+</sup>, 294 (100) [M+H]<sup>+</sup>. **HR-MS** (ESI)  $m/z$  calcd for C<sub>18</sub>H<sub>19</sub>N<sub>3</sub>O [M+H]<sup>+</sup>: 294.1601, found: 294.1602.

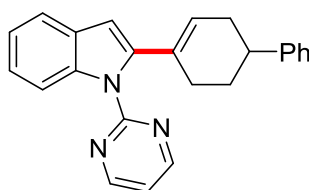
## 2-(2',3',4',5'-Tetrahydro-[1,1'-biphenyl]-2-yl)pyridine (39aa)

**39aa**

The general procedure **A** was followed using 2-phenyl pyridine (**14a**) (78.0 mg, 0.50 mmol, 1.0 equiv), enol acetate **134a** (105 mg, 0.75 mmol, 1.5 equiv) and ICyHCl (**23**) (12.7 mg, 0.05 mmol, 10 mol %) instead of **13**. Purification by column chromatography (*n*-hexane/EtOAc: 12/1) yielded **39aa** (63.2 mg, 0.27 mmol, 54%) as a white solid.

**M.p.:** 65–67 °C. **<sup>1</sup>H-NMR** (300 MHz, CDCl<sub>3</sub>):  $\delta$  = 8.66 (ddd,  $J$  = 4.9, 1.9, 1.0 Hz, 1H), 7.62 (ddd,  $J$  = 7.7, 1.8, 1.8 Hz, 1H), 7.60–7.53 (m, 1H), 7.48 (ddd,  $J$  = 7.9, 7.9, 1.1 Hz, 1H), 7.32 (dd,  $J$  = 5.7, 3.4 Hz, 2H), 7.25–7.20 (m, 1H), 7.17 (ddd,  $J$  = 7.5, 4.9, 1.2 Hz, 1H), 5.63 (tt,  $J$  = 3.7, 1.7 Hz, 1H), 2.09–2.01 (m, 2H), 1.90–1.84 (m, 2H), 1.57–1.49 (m, 4H). **<sup>13</sup>C-NMR** (125 MHz CDCl<sub>3</sub>):  $\delta$  = 159.8 (C<sub>q</sub>), 149.3 (CH), 143.4 (C<sub>q</sub>), 139.0 (C<sub>q</sub>), 138.6 (C<sub>q</sub>), 135.3 (CH), 130.0 (CH), 129.1 (CH), 128.2 (CH), 127.7 (CH), 126.9 (CH), 124.0 (CH), 121.4 (CH), 29.8 (CH<sub>2</sub>), 25.7 (CH<sub>2</sub>), 23.0 (CH<sub>2</sub>), 21.9 (CH<sub>2</sub>). **IR** (ATR): 2928, 2815, 1599, 1574, 1512, 1413, 1268, 1177, 1028, 674 cm<sup>-1</sup>. **MS** (ESI)  $m/z$  (relative intensity) 236 (100) [M+H]<sup>+</sup>. **HR-MS** (ESI)  $m/z$  calcd for C<sub>17</sub>H<sub>17</sub>N [M+H]<sup>+</sup>: 236.1434, found: 236.1436.

#### 1-(Pyrimidin-2-yl)-2-(1,2,3,6-tetrahydro-[1,1'-biphenyl]-4-yl)-1*H*-indole (40ab)

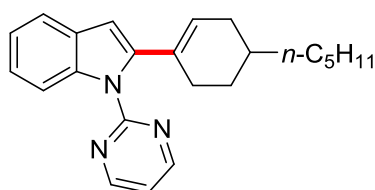
**40ab**

The general procedure **A** was followed using indole **15a** (97.6 mg, 0.50 mmol, 1.0 equiv) and enol acetate **134b** (162 mg, 0.75 mmol, 1.5 equiv). Purification by column chromatography (*n*-hexane/EtOAc: 9/1) yielded **40ab** (158 mg, 0.45 mmol, 90%) as a yellow solid.

**M.p.:** 144–146 °C. **<sup>1</sup>H-NMR** (300 MHz, CDCl<sub>3</sub>):  $\delta$  = 8.80 (d,  $J$  = 4.5 Hz, 2H), 8.18 (ddd,  $J$  = 7.5, 1.7, 0.8 Hz, 1H), 7.60–7.57 (m, 1H), 7.33–7.30 (m, 2H), 7.27–7.25 (m, 2H), 7.23–

7.18 (m, 3H), 7.14 (t,  $J = 4.5$  Hz, 1H), 6.60 (d,  $J = 0.8$  Hz, 1H), 5.97–5.96 (m, 1H), 2.94–2.87 (m, 1H), 2.51–2.44 (m, 1H), 2.36–2.27 (m, 2H), 2.21–2.17 (m, 1H), 1.99–1.94 (m, 1H), 1.89–1.82 (m, 1H).  **$^{13}\text{C-NMR}$**  (126 MHz,  $\text{CDCl}_3$ ):  $\delta = 158.4$  ( $\text{C}_q$ ), 158.2 (CH), 146.9 ( $\text{C}_q$ ), 142.8 ( $\text{C}_q$ ), 137.6 ( $\text{C}_q$ ), 131.9 ( $\text{C}_q$ ), 129.4 ( $\text{C}_q$ ), 128.5 (CH), 127.0 (CH), 126.5 (CH), 126.1 (CH), 123.2 (CH), 122.0 (CH), 120.4 (CH), 117.4 (CH), 113.3 (CH), 106.6 (CH), 39.8 (CH), 33.9 ( $\text{CH}_2$ ), 30.1 ( $\text{CH}_2$ ), 29.6 ( $\text{CH}_2$ ). **IR** (ATR): 2920, 2843, 221, 2213, 2010, 1559, 1450, 1420, 1344  $\text{cm}^{-1}$ . **MS** (ESI)  $m/z$  (relative intensity) 374 (33)  $[\text{M}+\text{Na}]^+$ , 352 (100)  $[\text{M}+\text{H}]^+$ , 323 (8), 285 (5), 231 (9), 223 (7). **HR-MS** (ESI)  $m/z$  calcd for  $\text{C}_{24}\text{H}_{21}\text{N}_3$   $[\text{M}+\text{H}]^+$ : 352.1808, found: 352.1808.

## 2-(4-Pentylcyclohex-1-en-1-yl)-1-(pyrimidin-2-yl)-1H-indole (40ac)



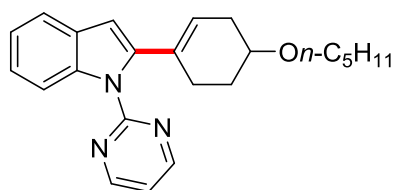
**40ac**

The general procedure **A** was followed using indole **15a** (97.6 mg, 0.50 mmol, 1.0 equiv) and enol acetate **134c** (158 mg, 0.75 mmol, 1.5 equiv). Purification by column chromatography (*n*-hexane/EtOAc: 11/1) yielded **40ac** (153 mg, 0.44 mmol, 89%) as a yellow oil.

The general procedure **A** was followed using indole **15a** (97.6 mg, 0.50 mmol, 1.0 equiv) and enol carbamate **150c** (180 mg, 0.75 mmol, 1.5 equiv). Purification by column chromatography (*n*-hexane/EtOAc: 11/1) yielded **40ac** (141 mg, 0.41 mmol, 82%) as a yellow oil.

**$^1\text{H-NMR}$**  (300 MHz,  $\text{CDCl}_3$ ):  $\delta = 8.77$  (d,  $J = 4.8$  Hz, 2H), 8.13 (ddd,  $J = 7.4, 1.8, 0.8$  Hz, 1H), 7.56–7.53 (m, 1H), 7.22–7.15 (m, 2H), 7.12 (t,  $J = 4.8$  Hz, 1H), 6.54 (d,  $J = 0.8$  Hz, 1H), 5.83–5.82 (m, 1H), 2.28–2.22 (m, 1H), 2.13–2.05 (m, 2H), 1.81–1.72 (m, 2H), 1.60–1.56 (m, 1H), 1.33–1.26 (m, 9H), 0.89 (t,  $J = 7.6$  Hz, 3H).  **$^{13}\text{C-NMR}$**  (126 MHz,  $\text{CDCl}_3$ ):  $\delta = 158.4$  ( $\text{C}_q$ ), 158.2 (CH), 143.2 ( $\text{C}_q$ ), 137.5 ( $\text{C}_q$ ), 131.7 ( $\text{C}_q$ ), 129.4 ( $\text{C}_q$ ), 126.8 (CH), 123.0 (CH), 121.9 (CH), 120.3 (CH), 117.4 (CH), 113.1 (CH), 106.2 (CH), 36.6 ( $\text{CH}_2$ ), 33.2 (CH), 32.7 ( $\text{CH}_2$ ), 32.4 ( $\text{CH}_2$ ), 29.3 ( $\text{CH}_2$ ), 29.1 ( $\text{CH}_2$ ), 26.9 ( $\text{CH}_2$ ), 22.9 ( $\text{CH}_2$ ), 14.4 ( $\text{CH}_3$ ). **IR** (ATR): 2962, 1561, 1517, 1450, 1416, 1345, 1259, 1212, 1016, 863  $\text{cm}^{-1}$ . **MS** (ESI)  $m/z$  (relative intensity) 346 (100)  $[\text{M}+\text{H}]^+$ , 326 (11), 303 (9), 271 (46), 249 (18). **HR-MS** (ESI)  $m/z$  calcd for  $\text{C}_{23}\text{H}_{27}\text{N}_3$   $[\text{M}+\text{H}]^+$ : 346.2278, found: 346.2278.

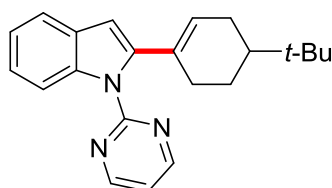


**2-[4-(Pentyloxy)cyclohex-1-en-1-yl]-1-(pyrimidin-2-yl)-1H-indole (40ad)****40ad**

The general procedure **A** was followed using indole **15a** (97.6 mg, 0.50 mmol, 1.0 equiv) and enol acetate **134d** (178 mg, 0.75 mmol, 1.5 equiv). Purification by column chromatography (*n*-hexane/EtOAc: 9/1) yielded **40ad** (153 mg, 0.42 mmol, 85%) as a yellow oil.

The general procedure **A** was followed using indole **15a** (97.6 mg, 0.50 mmol, 1.0 equiv) and enol carbamate **150d** (192 mg, 0.75 mmol, 1.5 equiv). Purification by column chromatography (*n*-hexane/EtOAc: 9/1) yielded **40ad** (143 mg, 0.40 mmol, 79%) as a yellow oil.

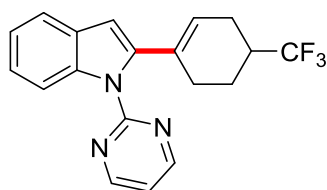
**<sup>1</sup>H-NMR** (300 MHz, CDCl<sub>3</sub>):  $\delta$  = 8.76 (d, *J* = 4.8 Hz, 2H), 8.17 (ddd, *J* = 8.3, 0.9, 0.9 Hz, 1H), 7.54 (ddd, *J* = 7.6, 1.5, 0.7 Hz, 1H), 7.22 (ddd, *J* = 8.3, 7.1, 1.4 Hz, 1H), 7.19–7.16 (m, 1H), 7.12 (t, *J* = 4.8 Hz, 1H), 6.53 (d, *J* = 0.8 Hz, 1H), 5.76–5.74 (m, 1H), 3.61–3.56 (m, 1H), 3.49–3.45 (m, 2H), 2.55–2.49 (m, 1H), 2.25–2.10 (m, 3H), 1.97–1.92 (m, 1H), 1.70–1.63 (m, 1H), 1.59–1.56 (m, 2H), 1.34–1.31 (m, 4H), 0.89 (t, *J* = 6.8 Hz, 3H). **<sup>13</sup>C-NMR** (125 MHz, CDCl<sub>3</sub>):  $\delta$  = 158.3 (C<sub>q</sub>), 158.1 (CH), 142.4 (C<sub>q</sub>), 137.4 (C<sub>q</sub>), 131.8 (C<sub>q</sub>), 129.3 (C<sub>q</sub>), 124.3 (CH), 123.1 (CH), 121.9 (CH), 120.3 (CH), 117.2 (CH), 113.3 (CH), 106.5 (CH), 74.0 (CH), 68.3 (CH<sub>2</sub>), 32.3 (CH<sub>2</sub>), 29.8 (CH<sub>2</sub>), 28.4 (CH<sub>2</sub>), 28.3 (CH<sub>2</sub>), 28.0 (CH<sub>2</sub>), 22.5 (CH<sub>2</sub>), 14.0 (CH<sub>3</sub>). **IR** (ATR): 2928, 2857, 1561, 1451, 1418, 1345, 1317, 1096, 795, 739 cm<sup>-1</sup>. **MS** (ESI) *m/z* (relative intensity) 384 (37) [M+Na]<sup>+</sup>, 362 (100) [M+H]<sup>+</sup>. **HR-MS** (ESI) *m/z* calcd for C<sub>23</sub>H<sub>27</sub>N<sub>3</sub>O [M+H]<sup>+</sup>: 362.2227, found: 362.2226.

**2-[4-(*tert*-Butyl)cyclohex-1-en-1-yl]-1-(pyrimidin-2-yl)-1H-indole (40ae)****40ae**

The general procedure **A** was followed using indole **15a** (97.6 mg, 0.50 mmol, 1.0 equiv) and enol acetate **134e** (148 mg, 0.75 mmol, 1.5 equiv). Purification by column chromatography (*n*-hexane/EtOAc: 12/1) yielded **40ae** (139 mg, 0.42 mmol, 84%) as a colorless solid.

**M.p.:** 148–150 °C. **<sup>1</sup>H-NMR** (300 MHz, CDCl<sub>3</sub>):  $\delta$  = 8.78 (d, *J* = 4.8 Hz, 2H), 8.12 (ddd, *J* = 8.4, 0.8, 0.8 Hz, 1H), 7.55 (d, *J* = 8.0 Hz, 1H), 7.25–7.14 (m, 2H), 7.12 (t, *J* = 4.8 Hz, 1H), 6.54 (d, *J* = 0.7 Hz, 1H), 5.91–5.86 (m, 1H), 2.22–2.08 (m, 3H), 1.99–1.89 (m, 1H), 1.83–1.75 (m, 1H), 1.36 (tdd, *J* = 11.1, 5.1, 2.2 Hz, 1H), 1.24 (tdd, *J* = 12.3, 9.8, 6.8 Hz, 1H), 0.88 (s, 9H). **<sup>13</sup>C-NMR** (125 MHz, CDCl<sub>3</sub>):  $\delta$  = 158.3 (C<sub>q</sub>), 158.1 (CH), 143.0 (C<sub>q</sub>), 137.4 (C<sub>q</sub>), 131.5 (C<sub>q</sub>), 129.3 (C<sub>q</sub>), 127.3 (CH), 123.0 (CH), 121.8 (CH), 120.2 (CH), 117.3 (CH), 113.0 (CH), 106.1 (CH), 43.7 (CH), 32.2 (CH<sub>2</sub>), 30.3 (CH<sub>2</sub>), 27.3 (CH<sub>2</sub>), 27.2 (CH<sub>3</sub>), 24.1 (C<sub>q</sub>). **IR** (ATR): 2955, 1561, 1452, 1420, 1347, 1320, 1260, 1216, 798, 743, 670, 623, 391 cm<sup>-1</sup>. **MS** (ESI) *m/z* (relative intensity) 370 (50) [M+K]<sup>+</sup>, 332 (100) [M+H]<sup>+</sup>. **HR-MS** (ESI) *m/z* calcd for C<sub>22</sub>H<sub>25</sub>N<sub>3</sub> [M+H]<sup>+</sup>: 322.2121, found: 322.2121.

#### 1-(Pyrimidin-2-yl)-2-[4-(trifluoromethyl)cyclohex-1-en-1-yl]-1*H*-indole (**40af**)



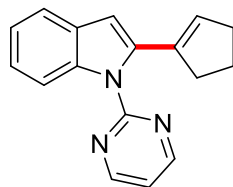
**40af**

The general procedure **A** was followed using indole **15a** (97.6 mg, 0.50 mmol, 1.0 equiv) and enol acetate **134f** (155 mg, 0.75 mmol, 1.5 equiv). Purification by column chromatography (*n*-hexane/EtOAc: 18/1) yielded **40af** (146 mg, 0.43 mmol, 86%) as a colorless oil.

**<sup>1</sup>H-NMR** (300 MHz, CDCl<sub>3</sub>)  $\delta$  = 8.77 (d, *J* = 4.8 Hz, 2H), 8.22 (dd, *J* = 8.0, 1.0 Hz, 1H), 7.56 (dd, *J* = 8.0, 1.0 Hz, 1H), 7.26–7.23 (m, 1H), 7.20 (ddd, *J* = 7.6, 1.3, 1.3 Hz, 1H), 7.14 (t, *J* = 4.8 Hz, 1H), 6.55 (d, *J* = 0.8 Hz, 1H), 5.83–5.81 (m, 1H), 2.43–2.33 (m, 2H), 2.30–2.21 (m, 3H), 2.03–1.98 (m, 1H), 1.68–1.59 (m, 1H). **<sup>13</sup>C-NMR** (125 MHz, CDCl<sub>3</sub>):  $\delta$  = 158.3 (C<sub>q</sub>), 158.2 (CH), 141.8 (C<sub>q</sub>), 137.4 (C<sub>q</sub>), 132.1 (C<sub>q</sub>), 129.4 (C<sub>q</sub>), 129.2 (q, <sup>1</sup>*J*<sub>C-F</sub> = 278 Hz, C<sub>q</sub>), 123.4 (CH), 123.3 (CH), 122.1 (CH), 120.4 (CH), 117.3 (CH), 113.5 (CH), 106.9 (CH), 38.3 (q, <sup>2</sup>*J*<sub>C-F</sub> = 30.5 Hz, CH), 28.2 (CH<sub>2</sub>), 24.6 (q, <sup>3</sup>*J*<sub>C-F</sub> = 2.6 Hz, CH<sub>2</sub>), 21.7 (q, <sup>3</sup>*J*<sub>C-F</sub> = 2.6 Hz, CH<sub>2</sub>). **<sup>19</sup>F-NMR** (282 MHz, CDCl<sub>3</sub>):  $\delta$  = -74.07. **IR** (ATR): 2928, 1562, 1423, 1347, 1271, 1248, 1166, 801, 746 cm<sup>-1</sup>. **MS** (ESI) *m/z* (relative intensity)

344 (38)  $[M+H]^+$ , 339 (100), 324 (8). **HR-MS** (ESI)  $m/z$  calcd for  $C_{19}H_{16}F_3N_3$   $[M+H]^+$ : 344.1369, found: 344.1377.

**2-(Cyclopent-1-en-1-yl)-1-(pyrimidin-2-yl)-1H-indole (40ag)**

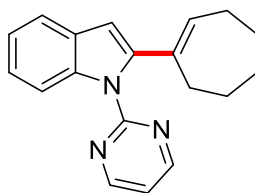


**40ag**

The general procedure **A** was followed using indole **15a** (97.6 mg, 0.50 mmol, 1.0 equiv) and enol acetate **134g** (94.6 mg, 0.75 mmol, 1.5 equiv). Purification by column chromatography (*n*-hexane/EtOAc: 15/1) yielded **40ag** (10.5 mg, 0.04 mmol, 8%) as a colorless solid.

**M.p.:** 124–126 °C.  **$^1H$ -NMR** (300 MHz,  $CDCl_3$ )  $\delta$  = 8.81 (d,  $J$  = 4.5 Hz, 2H), 7.94 (d,  $J$  = 8.1 Hz, 1H), 7.56 (d,  $J$  = 8.1 Hz, 1H), 7.22–7.14 (m, 3H), 6.65 (d,  $J$  = 0.7 Hz, 1H), 5.57–5.55 (m, 1H), 2.54–2.50 (m, 2H), 2.46–2.43 (m, 2H), 1.94 (tt,  $J$  = 7.6, 6.8 Hz, 2H).  **$^{13}C$ -NMR** (125 MHz,  $CDCl_3$ )  $\delta$  = 158.4 ( $C_q$ ), 158.3 (CH), 138.2 ( $C_q$ ), 137.6 ( $C_q$ ), 126.4 ( $C_q$ ), 129.1 ( $C_q$ ), 128.8 (CH), 123.3 (CH), 121.8 (CH), 120.4 (CH), 117.8 (CH), 112.3 (CH), 106.9 (CH), 35.2 ( $CH_2$ ), 33.4 ( $CH_2$ ), 23.5 ( $CH_2$ ). **IR** (ATR): 2211, 1597, 1499, 1288, 1250, 1132, 1034, 940, 820, 758  $cm^{-1}$ . **MS** (ESI)  $m/z$  (relative intensity) 262 (100)  $[M+H]^+$ . **HR-MS** (ESI)  $m/z$  calcd for  $C_{17}H_{15}N_3$   $[M+H]^+$ : 262.1339, found: 262.1339.

**2-(Cyclohept-1-en-1-yl)-1-(pyrimidin-2-yl)-1H-indole (40ah)**



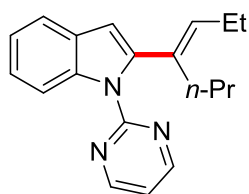
**40ah**

The general procedure **A** was followed using indole **15a** (97.6 mg, 0.50 mmol, 1.0 equiv) and enol acetate **134h** (116 mg, 0.75 mmol, 1.5 equiv). Purification by column chromatography (*n*-hexane/EtOAc: 15/1) yielded **40ah** (50.0 mg, 0.18 mmol, 35%) as a colorless solid.

**M.p.:** 161–165 °C.  **$^1H$ -NMR** (300 MHz,  $CDCl_3$ )  $\delta$  = 8.78 (d,  $J$  = 4.8 Hz, 2H), 8.19–8.17 (m, 1H), 7.53–7.50 (m, 1H), 7.22–7.15 (m, 2H), 7.12 (t,  $J$  = 4.8 Hz, 1H), 6.52 (d,  $J$  = 0.7

Hz, 1H), 6.18 (t,  $J = 6.0$  Hz, 1H), 2.30–2.26 (m, 2H), 2.21–2.18 (m, 2H), 1.76–1.72 (m, 2H), 1.57–1.54 (m, 2H), 1.49–1.45 (m, 2H).  $^{13}\text{C-NMR}$  (125 MHz,  $\text{CDCl}_3$ )  $\delta = 158.3$  ( $\text{C}_q$ ), 158.2 (CH), 144.5 ( $\text{C}_q$ ), 138.9 ( $\text{C}_q$ ), 131.1 ( $\text{C}_q$ ), 129.4 ( $\text{C}_q$ ), 128.5 (CH), 123.0 (CH), 121.9 (CH), 120.1 (CH), 117.1 (CH), 113.4 (CH), 106.7 (CH), 34.0 ( $\text{CH}_2$ ), 33.5 ( $\text{CH}_2$ ), 29.2 ( $\text{CH}_2$ ), 26.7 ( $\text{CH}_2$ ), 26.6 ( $\text{CH}_2$ ). **IR** (ATR): 2921, 1561, 1453, 1424, 1347, 1318, 1253, 1030, 797, 745  $\text{cm}^{-1}$ . **MS** (ESI)  $m/z$  (relative intensity) 312, (19)  $[\text{M}+\text{Na}]^+$ , 290 (100)  $[\text{M}+\text{H}]^+$ . **HR-MS** (ESI)  $m/z$  calcd for  $\text{C}_{19}\text{H}_{19}\text{N}_3$   $[\text{M}+\text{H}]^+$ : 290.1652, found: 262.1653.

**(*E*)-2-(Hept-3-en-4-yl)-1-(pyrimidin-2-yl)-1*H*-indole (40ai)**

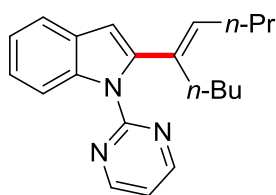


**40ai**

The general procedure **A** was followed using indole **15a** (97.6 mg, 0.50 mmol, 1.0 equiv) and enol acetate **134i** (117 mg, 0.75 mmol, 1.5 equiv,  $E/Z = 34/66$ ). Purification by column chromatography ( $n$ -hexane/EtOAc: 15/1) yielded **40ai** (72.8 mg, 0.25 mmol, 50%) as a red oil. The (*E*)-configuration was determined NOE NMR.

$^1\text{H-NMR}$  (300 MHz,  $\text{CDCl}_3$ ):  $\delta = 8.75$  (d,  $J = 5.7$  Hz, 2H), 8.14 (d,  $J = 8.2$  Hz, 1H), 7.57 (ddd,  $J = 7.5, 1.5, 0.7$  Hz, 1H), 7.23–7.18 (m, 2H), 7.10 (t,  $J = 5.7$  Hz, 1H), 6.55 (d,  $J = 0.8$  Hz, 1H), 5.57 (t,  $J = 7.0$  Hz, 1H), 2.20–2.13 (m, 4H), 1.36 (dq,  $J = 7.0, 6.7$  Hz, 2H), 0.98 (t,  $J = 6.8$  Hz, 3H), 0.89 (t,  $J = 6.9$  Hz, 3H).  $^{13}\text{C-NMR}$  (125 MHz,  $\text{CDCl}_3$ ):  $\delta = 158.4$  ( $\text{C}_q$ ), 158.1 (CH), 143.3 ( $\text{C}_q$ ), 137.4 ( $\text{C}_q$ ), 133.1 ( $\text{C}_q$ ), 132.6 (CH), 129.3 ( $\text{C}_q$ ), 122.8 (CH), 121.7 (CH), 120.0 (CH), 117.2 (CH), 113.0 (CH), 106.9 (CH), 33.0 ( $\text{CH}_2$ ), 21.8 ( $\text{CH}_2$ ), 21.5 ( $\text{CH}_2$ ), 14.1 ( $\text{CH}_3$ ), 14.0 ( $\text{CH}_3$ ). **IR** (ATR): 2958, 1561, 1452, 1420, 1347, 804, 745  $\text{cm}^{-1}$ . **MS** (ESI)  $m/z$  (relative intensity) 314 (27)  $[\text{M}+\text{Na}]^+$ , 292 (100)  $[\text{M}+\text{H}]^+$ , 250 (8), 196 (7). **HR-MS** (ESI)  $m/z$  calcd for  $\text{C}_{19}\text{H}_{21}\text{N}_3$   $[\text{M}+\text{H}]^+$ : 292.1808, found: 292.1811.

**(*E*)-2-(Non-4-en-5-yl)-1-(pyrimidin-2-yl)-1*H*-indole (40aj)**

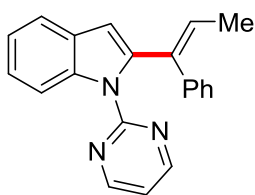


**40aj**

The general procedure **A** was followed using indole **15a** (97.6 mg, 0.50 mmol, 1.0 equiv) and enol acetate **134j** (138 mg, 0.75 mmol, 1.5 equiv, *E/Z* = 37/63). Purification by column chromatography (*n*-hexane/EtOAc: 14/1) yielded **40aj** (89.5 mg, 0.28 mmol, 56%) as a red oil. The (*E*)- configuration was determined NOE NMR.

**<sup>1</sup>H-NMR** (300 MHz, CDCl<sub>3</sub>):  $\delta$  = 8.75 (d, *J* = 4.3 Hz, 2H), 8.11–8.08 (m, 1H), 7.56–7.52 (m, 1H), 7.22–7.15 (m, 2H), 7.11 (t, *J* = 4.3 Hz, 1H), 6.53 (d, *J* = 0.7 Hz, 1H), 5.57 (t, *J* = 7.8 Hz, 1H), 2.17–2.09 (m, 4H), 1.45–1.17 (m, 6H), 0.91 (t, *J* = 7.9 Hz, 3H), 0.79 (t, *J* = 7.4 Hz, 3H). **<sup>13</sup>C-NMR** (125 MHz, CDCl<sub>3</sub>):  $\delta$  = 158.4 (C<sub>q</sub>), 158.1 (CH), 143.5 (C<sub>q</sub>), 137.4 (C<sub>q</sub>), 134.1 (C<sub>q</sub>), 130.8 (CH), 129.3 (C<sub>q</sub>), 122.6 (CH), 121.8 (CH), 120.8 (CH), 117.2 (CH), 113.0 (CH), 106.9 (CH), 30.9 (CH<sub>2</sub>), 30.8 (CH<sub>2</sub>), 30.2 (CH<sub>2</sub>), 22.7 (CH<sub>2</sub>), 22.6 (CH<sub>2</sub>), 13.9 (CH<sub>3</sub>), 13.8 (CH<sub>3</sub>). **IR** (ATR): 2920, 1560, 1451, 1418, 1345, 1316, 1251, 1213, 794, 738 cm<sup>-1</sup>. **MS** (ESI) *m/z* (relative intensity) 342 (17) [M+Na]<sup>+</sup>, 320 (100) [M+H]<sup>+</sup>, 264 (7). **HR-MS** (ESI) *m/z* calcd for C<sub>21</sub>H<sub>25</sub>N<sub>3</sub> [M+H]<sup>+</sup>: 320.2121, found: 320.2123.

**(*E*)-2-(1-Phenylprop-1-en-1-yl)-1-(pyrimidin-2-yl)-1*H*-indole (40ak)**



**40ak**

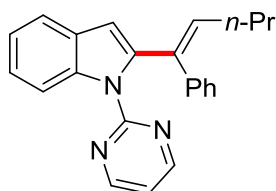
The general procedure **A** was followed using indole **15a** (97.6 mg, 0.50 mmol, 1.0 equiv) and enol acetate **134k** (133 mg, 0.75 mmol, 1.5 equiv, *E/Z* = 27/73). Purification by column chromatography (*n*-hexane/EtOAc: 10/1) yielded **40ak** (124 mg, 0.40 mmol, 80%) as a yellow oil. (*E*)- configuration was determined NOE NMR.

The general procedure **A** was followed using indole **15a** (97.6 mg, 0.50 mmol, 1.0 equiv) and enol acetate **134k** (133 mg, 0.75 mmol, 1.5 equiv, *E/Z* = 16/84). Purification by column chromatography (*n*-hexane/EtOAc: 10/1) yielded **40ak** (122 mg, 0.39 mmol, 78%) as a yellow oil..

The general procedure **A** was followed using indole **15a** (97.6 mg, 0.50 mmol, 1.0 equiv) and enol acetate **134k** (133 mg, 0.75 mmol, 1.5 equiv, *E/Z* = 5/95). Purification by column chromatography (*n*-hexane/EtOAc: 10/1) yielded **40ak** (102 mg, 0.33 mmol, 65%) as a yellow oil.

**<sup>1</sup>H-NMR** (300 MHz, CDCl<sub>3</sub>):  $\delta$  = 8.51 (d,  $J$  = 4.8 Hz, 2H), 8.04 (d,  $J$  = 7.1 Hz, 1H), 7.63 (d,  $J$  = 7.1 Hz, 1H), 7.25–7.19 (m, 3H), 7.09–7.05 (m, 3H), 7.01–6.98 (m, 1H), 6.85 (t,  $J$  = 4.8 Hz, 1H), 6.78 (d,  $J$  = 0.8 Hz, 1H), 6.32 (q,  $J$  = 11.0 Hz, 1H), 1.93 (d,  $J$  = 11.0 Hz, 3H). **<sup>13</sup>C-NMR** (125 MHz, CDCl<sub>3</sub>):  $\delta$  = 157.8 (CH), 157.4 (C<sub>q</sub>), 142.6 (C<sub>q</sub>), 138.2 (C<sub>q</sub>), 137.3 (C<sub>q</sub>), 135.5 (C<sub>q</sub>), 129.7 (CH), 128.9 (C<sub>q</sub>), 127.3 (CH), 126.5 (CH), 126.1 (CH), 123.2 (CH), 121.8 (CH), 120.3 (CH), 116.8 (CH), 112.9 (CH), 108.7 (CH), 15.4 (CH<sub>3</sub>). **IR** (ATR): 2930, 2028, 1565, 1494, 1449, 1354, 1257, 1145, 1084, 1050 cm<sup>-1</sup>. **MS** (ESI)  $m/z$  (relative intensity) 334 (24) [M+Na]<sup>+</sup>, 312 (100) [M+H]<sup>+</sup>, 284 (21). **HR-MS** (ESI)  $m/z$  calcd for C<sub>21</sub>H<sub>17</sub>N<sub>3</sub> [M+H]<sup>+</sup>: 312.1495, found: 312.1495. The analytical data corresponds with those reported in literature.<sup>[41a]</sup>

**(*E*)-2-(1-Phenylpent-1-en-1-yl)-1-(pyrimidin-2-yl)-1*H*-indole (40al)**

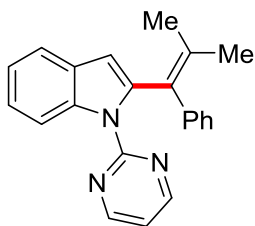


**40al**

The general procedure **A** was followed using indole **15a** (97.6 mg, 0.50 mmol, 1.0 equiv) and enol acetate **134l** (153 mg, 0.75 mmol, 1.5 equiv, *E/Z* = 29/71). Purification by column chromatography (*n*-hexane/EtOAc: 10/1) yielded **40al** (91.6 mg, 0.27 mmol, 54%) as a yellow oil. (*E*)- configuration was determined NOE NMR.

**<sup>1</sup>H-NMR** (300 MHz, CDCl<sub>3</sub>):  $\delta$  = 8.54 (d,  $J$  = 4.8 Hz, 2H), 8.02–7.98 (m, 1H), 7.61–7.58 (m, 1H), 7.22–7.18 (m, 2H), 7.09–6.99 (m, 5H), 6.88 (t,  $J$  = 4.0 Hz, 1H), 6.74 (d,  $J$  = 0.7 Hz, 1H), 6.13 (t,  $J$  = 4.8 Hz, 1H), 2.28 (dt,  $J$  = 7.0, 5.6 Hz, 2H), 1.47 (tq,  $J$  = 6.4, 5.6 Hz, 2H), 0.89 (t,  $J$  = 6.4 Hz, 3H). **<sup>13</sup>C-NMR** (125 MHz, CDCl<sub>3</sub>):  $\delta$  = 157.8 (CH), 157.6 (C<sub>q</sub>), 142.7 (C<sub>q</sub>), 138.7 (C<sub>q</sub>), 137.4 (C<sub>q</sub>), 134.6 (C<sub>q</sub>), 132.3 (CH), 129.7 (CH), 128.9 (C<sub>q</sub>), 128.3 (CH), 126.5 (CH), 123.3 (CH), 121.9 (CH), 120.3 (CH), 116.9 (CH), 112.9 (CH), 108.7 (CH), 31.3 (CH<sub>2</sub>), 23.1 (CH<sub>2</sub>), 13.8 (CH<sub>3</sub>). **IR** (ATR): 2947, 2865, 1572, 1426, 1321, 1253, 1150, 1074, 849, 777 cm<sup>-1</sup>. **MS** (ESI)  $m/z$  (relative intensity) 362 (27) [M+Na]<sup>+</sup>, 340 (100) [M+H]<sup>+</sup>, 320 (14), 284 (56), 258 (7), 214 (4), 198 (6). **HR-MS** (ESI)  $m/z$  calcd for C<sub>23</sub>H<sub>21</sub>N<sub>3</sub> [M+H]<sup>+</sup>: 340.1808, found: 340.1808.

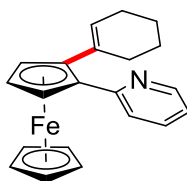
**2-(2-Methyl-1-phenylprop-1-en-1-yl)-1-(pyrimidin-2-yl)-1*H*-indole (40am)**

**40am**

The general procedure **A** was followed using indole **15a** (97.6 mg, 0.50 mmol, 1.0 equiv) and enol acetate **134m** (143 mg, 0.75 mmol, 1.5 equiv). Purification by column chromatography (*n*-hexane/EtOAc: 10/1) yielded **40am** (16.5 mg, 0.05 mmol, 10%) as a yellow oil.

**<sup>1</sup>H-NMR** (300 MHz, CDCl<sub>3</sub>)  $\delta$  = 8.61 (d, *J* = 4.3 Hz, 2H), 8.07–8.04 (m, 1H), 7.60–7.57 (m, 1H), 7.22–7.17 (m, 2H), 7.09–7.07 (m, 4H), 7.03–6.96 (m, 2H), 6.60 (d, *J* = 0.7 Hz, 1H), 1.88 (s, 3H), 1.84 (s, 3H). **<sup>13</sup>C-NMR** (125 MHz, CDCl<sub>3</sub>):  $\delta$  = 157.8 (CH), 157.6 (C<sub>q</sub>), 141.0 (C<sub>q</sub>), 140.7 (C<sub>q</sub>), 136.4 (C<sub>q</sub>), 134.3 (CH), 130.1 (CH), 129.3 (C<sub>q</sub>), 129.0 (C<sub>q</sub>), 126.4 (CH), 122.9 (CH), 121.6 (CH), 120.2 (CH), 116.9 (CH), 113.2 (CH), 108.7 (CH), 91.4 (C<sub>q</sub>), 23.4 (CH<sub>3</sub>), 22.2 (CH<sub>3</sub>). **IR** (ATR): 2985, 1685, 1518, 1431, 1371, 1273, 1134, 1024, 849, 538 cm<sup>-1</sup>. **MS** (ESI) *m/z* (relative intensity) 348 (21) [M+Na]<sup>+</sup>, 326 (58) [M+H]<sup>+</sup>, 308 (100). **HR-MS** (ESI) *m/z* calcd for C<sub>22</sub>H<sub>19</sub>N<sub>3</sub> [M+H]<sup>+</sup>: 326.1652, found: 326.1652.

#### 1-(2-Pyridin-2-yl)-2-cyclohex-1-enylferrocene (**158a**)

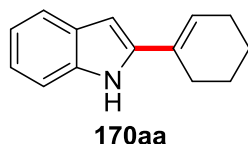
**158a**

The general procedure **A** was followed using pyridyl ferrocene (**154**) (132 mg, 0.50 mmol, 1.0 equiv), enol acetate **134a** (105 mg, 0.75 mmol, 1.5 equiv) and ICyHCl (**23**) (12.7 mg, 0.05 mmol, 10 mol %) instead of **13**. Purification by column chromatography (*n*-hexane/EtOAc: 5/1) yielded **158a** (84.0 mg, 0.24 mmol, 48%) as a dark red solid.

**M.p.**: 115–117 °C. **<sup>1</sup>H-NMR** (500 MHz, CDCl<sub>3</sub>):  $\delta$  = 8.48 (ddd, *J* = 4.9, 1.8, 0.9 Hz, 1H), 7.66 (ddd, *J* = 8.0, 8.0, 1.1 Hz, 1H), 7.55 (ddd, *J* = 8.0, 7.4, 1.9 Hz, 1H), 7.07 (ddd, *J* = 7.4, 4.9, 1.2 Hz, 1H), 5.86–5.76 (m, 1H), 4.80 (dd, *J* = 2.5, 1.7 Hz, 1H), 4.32–4.26 (m, 2H), 4.09 (s, 5H), 2.28–2.19 (m, 2H), 2.09–2.02 (m, 2H), 1.73–1.63 (m, 4H).

**$^{13}\text{C}$ -NMR** (125 MHz  $\text{CDCl}_3$ ):  $\delta$  = 159.6 ( $\text{C}_q$ ), 148.8 (CH), 135.0 (CH), 133.4 ( $\text{C}_q$ ), 127.0 (CH), 124.1 (CH), 120.6 (CH), 91.6 ( $\text{C}_q$ ), 83.0 ( $\text{C}_q$ ), 70.4 (CH), 70.2 (CH), 69.3 (CH), 67.5 (CH), 30.5 ( $\text{CH}_2$ ), 26.0 ( $\text{CH}_2$ ), 23.4 ( $\text{CH}_2$ ), 22.3 ( $\text{CH}_2$ ). **IR** (ATR): 2926, 1586, 1561, 1484, 1412, 1106, 1000, 815, 785, 744  $\text{cm}^{-1}$ . **MS** (ESI)  $m/z$  (relative intensity) 344 (100)  $[\text{M}+\text{H}]^+$ . **HR-MS** (ESI)  $m/z$  calcd for  $\text{C}_{21}\text{H}_{21}\text{FeN}$   $[\text{M}+\text{H}]^+$ : 344.1096, found: 344.1098.

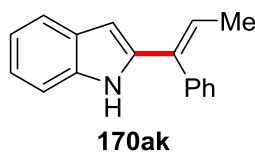
## 2-(Cyclohex-1-en-1-yl)-1*H*-indole (170aa)



The general procedure **B** was followed using pyrimidyl indole **40aa** (82.6 mg, 0.30 mmol). Purification by column chromatography (*n*-hexane/EtOAc: 20/1) yielded **170aa** (51.1 mg, 0.26 mmol, 85%) as a colorless solid.

**M.p.**: 137–139 °C.  **$^1\text{H}$ -NMR** (300 MHz,  $\text{CDCl}_3$ ):  $\delta$  = 8.08 ( $s_{\text{br}}$ , 1H), 7.57 (d,  $J$  = 7.5 Hz, 1H), 7.31 (d,  $J$  = 7.8, 1H), 7.20–7.11 (m, 1H), 7.11–7.03 (m, 1H), 6.46 (s, 1H), 6.17–6.10 (m, 1H), 2.56–2.42 (m, 2H), 2.42–2.14 (m, 2H), 1.92–1.76 (m, 2H), 1.76–1.65 (m, 2H).  **$^{13}\text{C}$ -NMR** (125 MHz,  $\text{CDCl}_3$ ):  $\delta$  = 139.5 ( $\text{C}_q$ ), 136.2 ( $\text{C}_q$ ), 129.2 ( $\text{C}_q$ ), 129.0 ( $\text{C}_q$ ), 122.7 (CH), 122.0 (CH), 120.4 (CH), 119.8 (CH), 110.5 (CH), 98.8 (CH), 26.3 ( $\text{CH}_2$ ), 25.7 ( $\text{CH}_2$ ), 22.8 ( $\text{CH}_2$ ), 22.5 ( $\text{CH}_2$ ). **IR** (ATR): 3415, 2923, 2855, 1453, 1412, 1340, 1289, 921, 787, 745  $\text{cm}^{-1}$ . **MS** (ESI)  $m/z$  (relative intensity) 196 (100)  $[\text{M}-\text{H}]^-$ . **HR-MS** (ESI)  $m/z$  calcd for  $\text{C}_{14}\text{H}_{15}\text{N}$   $[\text{M}-\text{H}]^-$ : 196.1132, found: 196.1132. The analytical data corresponds with those reported in literature.<sup>[177]</sup>

## (*E*)-2-(1-Phenylprop-1-en-1-yl)-1*H*-indole (170ak)



The general procedure **B** was followed using pyrimidyl indole **40ak** (93.4 mg, 0.30 mmol). Purification by column chromatography (*n*-hexane/EtOAc: 10/1) yielded **170ak** (56.0 mg, 0.24 mmol, 80%) as a yellow solid.

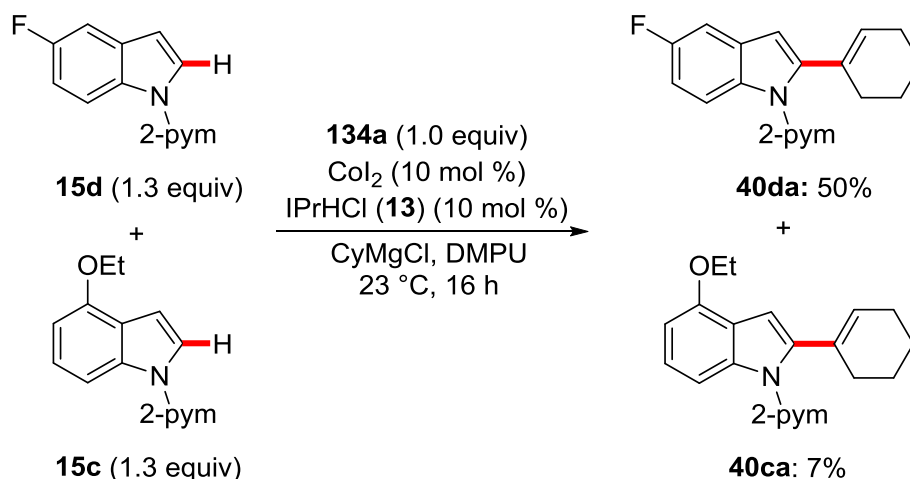
**M.p.**: 155–157 °C.  **$^1\text{H}$ -NMR** (300 MHz  $\text{CDCl}_3$ ):  $\delta$  = 7.90 ( $s_{\text{br}}$ , 1H), 7.48 (dd,  $J$  = 7.9, 1.0 Hz, 1H), 7.44–7.39 (m, 2H), 7.38–7.35 (m, 1H), 7.31–7.23 (m, 3H), 7.10 (ddd,  $J$  = 8.2, 7.1, 1.2 Hz, 1H), 7.03 (ddd,  $J$  = 8.1, 7.1, 1.0 Hz, 1H), 6.27 (q,  $J$  = 7.1 Hz, 1H), 6.25 (s, 1H), 1.75 (d,  $J$  = 7.1 Hz, 3H).  **$^{13}\text{C}$ -NMR** (125 MHz,  $\text{CDCl}_3$ ):  $\delta$  = 139.7 ( $\text{C}_q$ ), 137.9



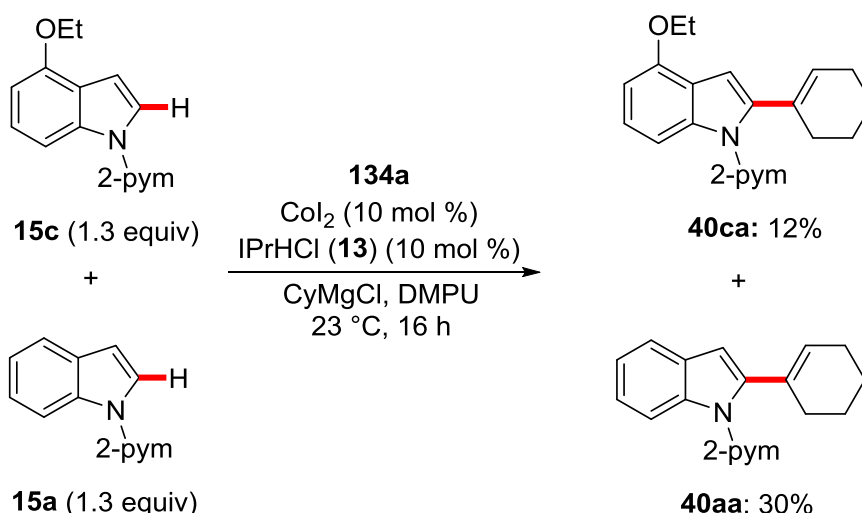
(C<sub>q</sub>), 136.2 (C<sub>q</sub>), 134.6 (C<sub>q</sub>), 129.9 (CH), 128.8 (C<sub>q</sub>), 128.4 (CH), 127.5 (CH), 122.6 (CH), 122.0 (CH), 120.3 (CH), 119.9 (CH), 110.5 (CH), 101.0 (CH), 15.1 (CH<sub>3</sub>). **IR** (ATR): 3418, 2967, 2745, 1488, 1311, 1218, 1130, 1069, 844, 763, 717, 672, 621, 532 cm<sup>-1</sup>. **MS** (ESI) *m/z* (relative intensity) 232 (100) [M–H]<sup>–</sup>. **HR-MS** (ESI) *m/z* calcd for C<sub>17</sub>H<sub>15</sub>N [M–H]<sup>–</sup>: 232.1132, found: 232.1139.

### 5.3.2 Mechanistic Studies

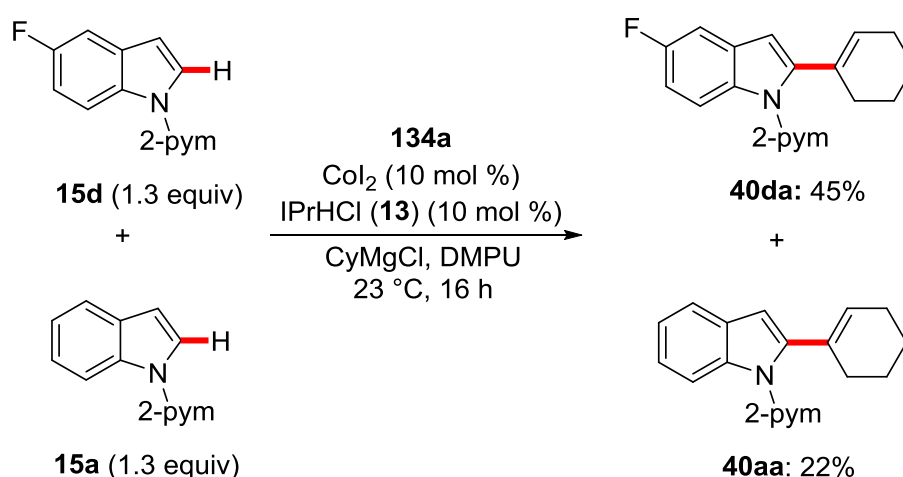
#### Intermolecular Competition Experiments



To a solution of 5-fluoro-1-(pyrimidin-2-yl)-1*H*-indole (**15d**) (107 mg, 0.50 mmol, 1.30 equiv), 4-ethoxy-1-(pyrimidin-2-yl)-1*H*-indole (**15c**) (120 mg, 0.50 mmol, 1.30 equiv), acetate **134a** (70.7 mg, 0.38 mmol, 1.0 equiv), CoI<sub>2</sub> (15.7 mg, 0.05 mmol, 10 mol%) and IPrHCl (**13**) (21.2 mg, 0.05 mmol, 10 mol %) in DMPU (1.5 mL), CyMgCl (1.0 M in MeTHF, 1.0 mmol, 2.7 equiv) was added drop wise. The mixture was stirred for 16 h at 23 °C. After completion of the reaction, saturated aq. NH<sub>4</sub>Cl solution (5 mL) was added and the mixture was extracted with MTBE (4 × 5 mL). Drying over Na<sub>2</sub>SO<sub>4</sub>, evaporation of the solvent and purification by column chromatography on silica gel (*n*-hexane/EtOAc 12:1) yielded the products **40da** (72.8 mg, 0.25 mmol, 50%) and **40ca** (10.8 mg, 33.8 μmol, 7%).

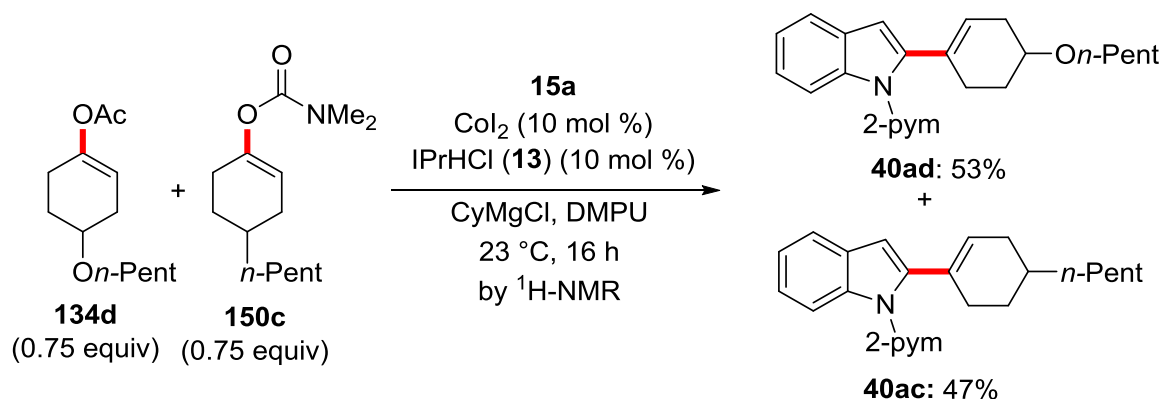


To a solution of 4-ethoxy-1-(pyrimidin-2-yl)-1*H*-indole (**15c**) (120 mg, 0.50 mmol, 1.30 equiv), 1-(pyrimidin-2-yl)-1*H*-indole (**15a**) (97.6 mg, 0.50 mmol, 1.3 equiv), acetate **134a** (70.7 mg, 0.38 mmol, 1.0 equiv),  $\text{Col}_2$  (15.7 mg, 0.05 mmol, 10 mol%) and IPrHCl (**13**) (21.2 mg, 0.05 mmol, 10 mol %) in DMPU (1.5 mL), CyMgCl (1.0 M in MeTHF, 1.0 mmol, 2.7 equiv) was added drop wise. The mixture was stirred for 16 h at 23 °C. After completion of the reaction, saturated aq.  $\text{NH}_4\text{Cl}$  solution (5 mL) was added and the mixture was extracted with MTBE (4 × 5 mL). Drying over  $\text{Na}_2\text{SO}_4$ , evaporation of the solvent and purification by column chromatography on silica gel (*n*-hexane/EtOAc 12:1) yielded the products **40ca** (19.2 mg, 60.0  $\mu\text{mol}$ , 12%) and **40aa** (41.3 mg, 150  $\mu\text{mol}$ , 30%).

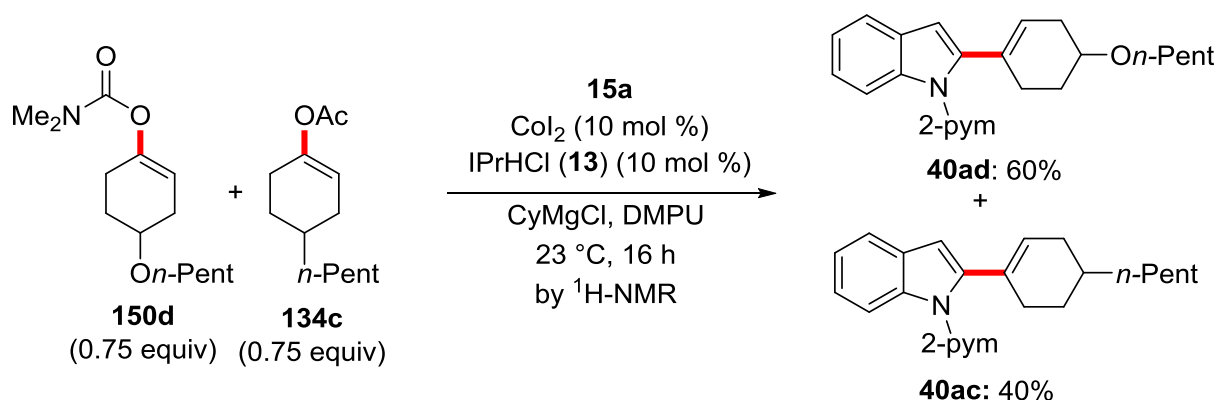


To a solution of 5-fluoro-1-(pyrimidin-2-yl)-1*H*-indole (**15d**) (107 mg, 0.50 mmol, 1.30 equiv), 1-(pyrimidin-2-yl)-1*H*-indole (**15a**) (97.6 mg, 0.50 mmol, 1.3 equiv), acetate **134a** (70.7 mg, 0.38 mmol, 1.0 equiv),  $\text{Col}_2$  (15.7 mg, 0.05 mmol, 10 mol%) and IPrHCl (**13**) (21.2 mg, 0.05 mmol, 10 mol %) in DMPU (1.5 mL), CyMgCl (1.0 M in MeTHF, 1.0 mmol, 2.7 equiv) was added drop wise. The mixture was stirred for 16 h at 23 °C. After

completion of the reaction, saturated aq.  $\text{NH}_4\text{Cl}$  solution (5 mL) was added and the mixture was extracted with MTBE (4 × 5 mL). Drying over  $\text{Na}_2\text{SO}_4$ , evaporation of the solvent and purification by column chromatography on silica gel (*n*-hexane/EtOAc 20:1) yielded the product **40da** (66.0 mg, 0.23 mmol, 45%) and **40aa** (30.3 mg, 0.11 mmol, 22%).

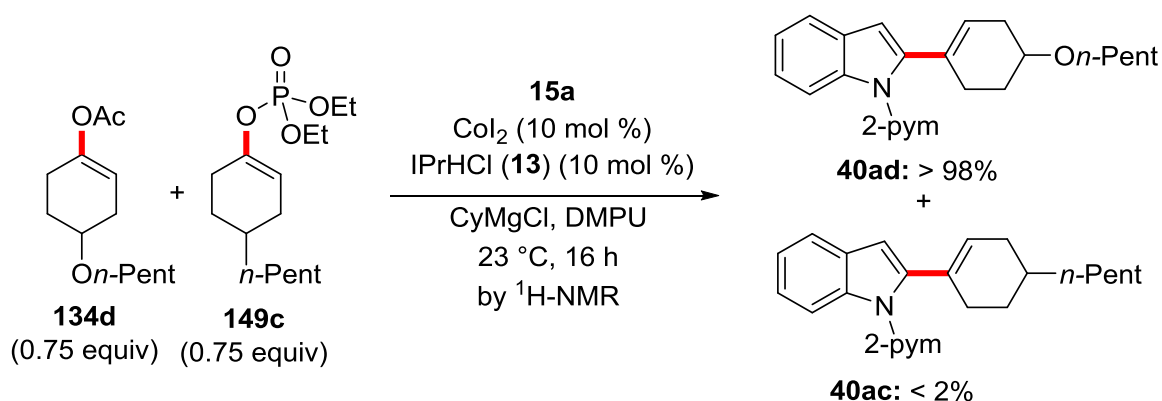


To a solution of 1-(pyrimidin-2-yl)-1*H*-indole (**15a**) (97.6 mg, 0.5 mmol, 1.0 equiv) 4-(pentyloxy)cyclohex-1-en-1-yl acetate (**134d**) (85.1 mg, 0.38 mmol, 0.75 equiv), 4-pentylcyclohex-1-en-1-yl dimethylcarbamate (**150c**) (90.2 mg, 0.38 mmol, 0.75 equiv),  $\text{CoI}_2$  (15.7 mg, 0.05 mmol, 10 mol %) and  $\text{IPrHCl}$  (**13**) (21.2 mg, 0.05 mmol, 10 mol %) in DMPU (1.5 mL),  $\text{CyMgCl}$  (1.0 M in MeTHF, 1.0 mmol, 2.0 equiv) was added dropwise. The mixture was stirred for 16 h at 23 °C. After completion of the reaction, saturated aq.  $\text{NH}_4\text{Cl}$  solution (5 mL) was added and the mixture was extracted with MTBE (4 × 5 mL). Drying over  $\text{Na}_2\text{SO}_4$ , evaporation of the solvent and purification by column chromatography on silica gel using *n*-hexane/EtOAc (12:1) gave a mixture of **40ad** (53%) and **40ac** (47%) according to  $^1\text{H-NMR}$  analysis.

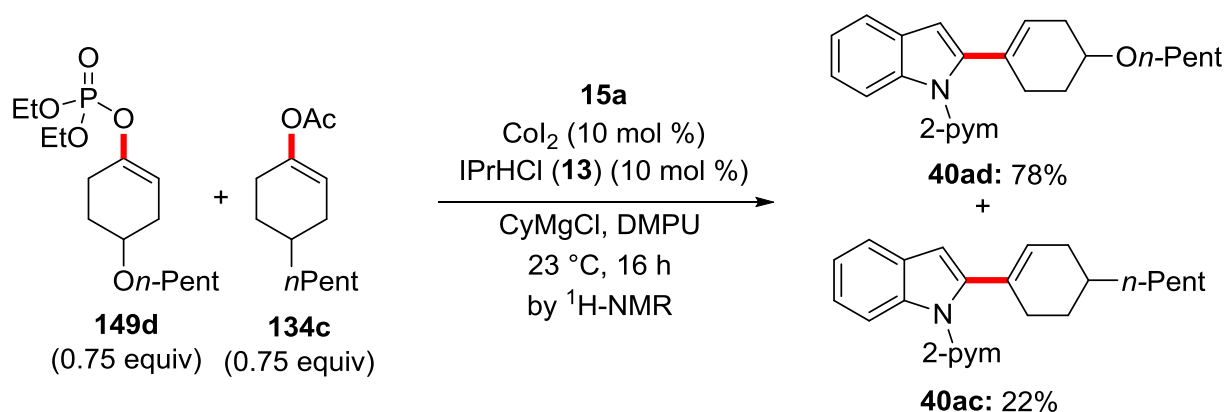


To a solution of 1-(pyrimidin-2-yl)-1*H*-indole (**15a**) (97.6 mg, 0.50 mmol, 1.0 equiv) 4-(pentyloxy)cyclohex-1-en-1-yl dimethylcarbamate (**150d**) (96.2 mg, 0.38 mmol,

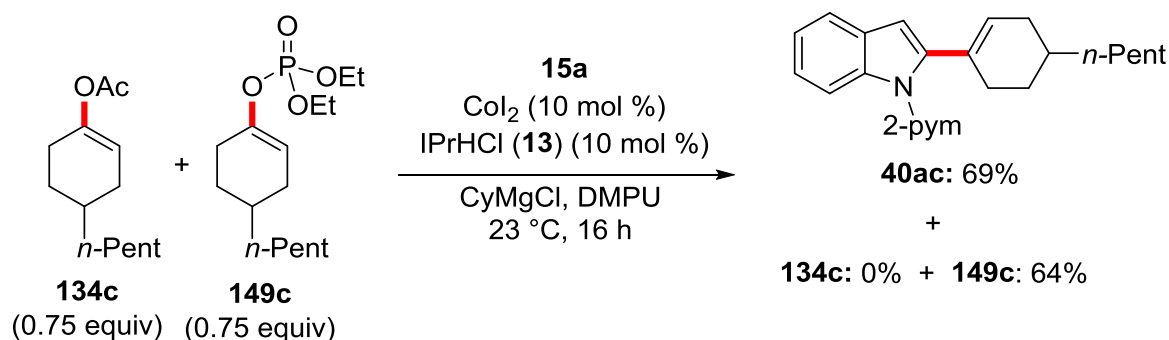
0.75 equiv), 4-pentylcyclohex-1-en-1-yl acetate (**134c**) (79.2 mg, 0.38 mmol, 0.75 equiv),  $\text{CoI}_2$  (15.7 mg, 0.05 mmol, 10 mol %) and  $\text{IPrHCl}$  (**13**) (21.2 mg, 0.05 mmol, 10 mol %) in DMPU (1.5 mL),  $\text{CyMgCl}$  (1.0 M in MeTHF, 1.0 mmol, 2.0 equiv) was added dropwise. The mixture was stirred for 16 h at 23 °C. After completion of the reaction, saturated aq.  $\text{NH}_4\text{Cl}$  solution (5 mL) was added and the mixture was extracted with MTBE (4 × 5 mL). Drying over  $\text{Na}_2\text{SO}_4$ , evaporation of the solvent and purification by column chromatography on silica gel using (*n*-hexane/EtOAc 12:1) gave a mixture of **40ad** (60%) and **40ac** (40%) according to  $^1\text{H}$ -NMR analysis.



To a solution of 1-(pyrimidin-2-yl)-1*H*-indole (**15a**) (97.6 mg, 0.50 mmol, 1.0 equiv) 4-(pentyloxy)cyclohex-1-en-1-yl acetate (**134d**) (85.5 mg, 0.38 mmol, 0.75 equiv), diethyl (4-pentylcyclohex-1-en-1-yl) phosphate (**149c**) (114.6 mg, 0.38 mmol, 0.75 equiv),  $\text{CoI}_2$  (15.7 mg, 0.05 mmol, 10 mol %) and  $\text{IPrHCl}$  (**13**) (21.2 mg, 0.05 mmol, 10 mol %) in DMPU (1.5 mL),  $\text{CyMgCl}$  (1.0 M in MeTHF, 1.0 mmol, 2.0 equiv) was added dropwise. The mixture was stirred for 16 h at 23 °C. After completion of the reaction, saturated aq.  $\text{NH}_4\text{Cl}$  solution (5 mL) was added and the mixture was extracted with MTBE (4 × 5 mL). Drying over  $\text{Na}_2\text{SO}_4$ , evaporation of the solvent and purification by column chromatography on silica gel (*n*-hexane/EtOAc 12:1) gave only **40ad** (92.2 mg, 0.26 mmol, 51%).

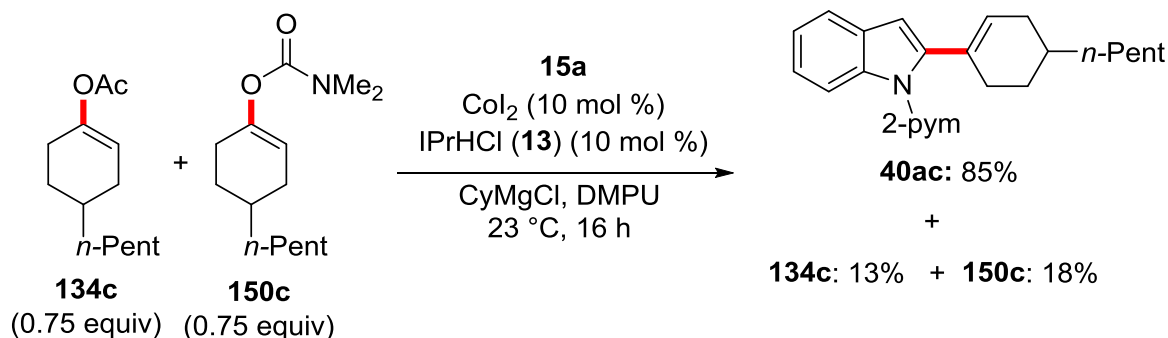


To a solution of 1-(pyrimidin-2-yl)-1*H*-indole (**15a**) (97.6 mg, 0.50 mmol, 1.0 equiv), diethyl 4-(pentyloxy)cyclohex-1-en-1-yl phosphate (**149d**) (125.2 mg, 0.38 mmol, 0.75 equiv), 4-pentylcyclohex-1-en-1-yl acetate (**134c**) (79.2 mg, 0.38 mmol, 0.75 equiv),  $\text{Col}_2$  (15.7 mg, 0.05 mmol, 10 mol %) and IPrHCl (**13**) (21.2 mg, 0.05 mmol, 10 mol %) in DMPU (1.5 mL), CyMgCl (1.0 M in MeTHF, 1.0 mmol, 2.0 equiv) was added dropwise. The mixture was stirred for 16 h at 23 °C. After completion of the reaction, saturated aq.  $\text{NH}_4\text{Cl}$  solution (5 mL) was added and the mixture was extracted with MTBE (4 × 5 mL). Drying over  $\text{Na}_2\text{SO}_4$ , evaporation of the solvent and purification by column chromatography on silica gel (*n*-hexane/EtOAc 12:1) gave mixture of **40ad** (78%) and **40ac** (22%) according to  $^1\text{H}$ -NMR analysis.



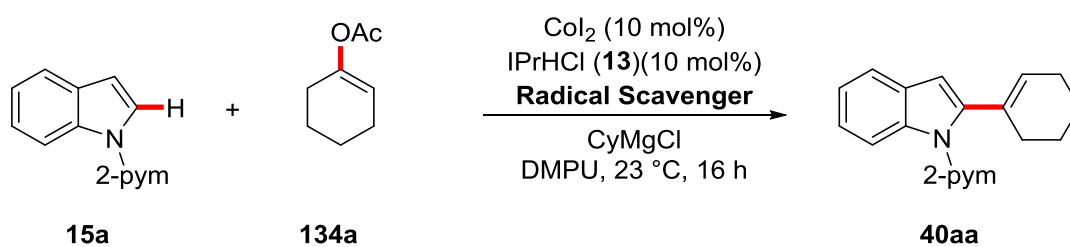
To a solution of 1-(pyrimidin-2-yl)-1*H*-indole (**15a**) (97.6 mg, 0.50 mmol, 1.0 equiv), 4-pentylcyclohex-1-en-1-yl acetate (**134c**) (79.2 mg, 0.38 mmol, 0.75 equiv), diethyl (4-pentylcyclohex-1-en-1-yl) phosphate (**149c**) (114.6 mg, 0.38 mmol, 0.75 equiv),  $\text{Col}_2$  (15.7 mg, 0.05 mmol, 10 mol %) and IPrHCl (**13**) (21.2 mg, 0.05 mmol, 10 mol %) in DMPU (1.5 mL), CyMgCl (1.0 M in MeTHF, 1.0 mmol, 2.0 equiv) was added dropwise. The mixture was stirred for 16 h at 23 °C. After completion of the reaction, saturated aq.  $\text{NH}_4\text{Cl}$  solution (5 mL) was added and the mixture was extracted with MTBE (4 × 5 mL). Drying over  $\text{Na}_2\text{SO}_4$ , evaporation of the solvent and purification by column

chromatography on silica gel (*n*-hexane/EtOAc 12:1) yielded the desired product **40ac** (120 mg, 345  $\mu$ mol, 22%) and unreacted **149c** (73.0 mg, 240  $\mu$ mol, 64%).



To a solution of 1-(pyrimidin-2-yl)-1*H*-indole (**15a**) (97.6 mg, 0.50 mmol, 1.0 equiv), 4-pentylcyclohex-1-en-1-yl acetate (**134c**) (79.2 mg, 0.38 mmol, 0.75 equiv), 4-pentylcyclohex-1-en-1-yl dimethylcarbamate (**150c**) (90.2 mg, 0.38 mmol, 0.75 equiv),  $\text{Col}_2$  (15.7 mg, 0.05 mmol, 10 mol %) and  $\text{IPrHCl}$  (**13**) (21.2 mg, 0.05 mmol, 10 mol %) in DMPU (1.5 mL),  $\text{CyMgCl}$  (1.0 M in MeTHF, 1.0 mL, 1.0 mmol, 2.0 equiv) was added dropwise. The mixture was stirred for 16 h at  $23^\circ\text{C}$ . After completion of the reaction, saturated aq.  $\text{NH}_4\text{Cl}$  solution (5 mL) was added and the mixture was extracted with MTBE (4  $\times$  5 mL). Drying over  $\text{Na}_2\text{SO}_4$ , evaporation of the solvent and purification by column chromatography on silica gel (*n*-hexane/EtOAc 12:1) yielded the desired product **40ac** (147 mg, 425  $\mu$ mol, 85%), unreacted **134c** (10.3 mg, 49  $\mu$ mol, 13%) and **150c** (16.2 mg, 68  $\mu$ mol, 18%).

### Reactions with Radical Scavengers



Entry	Radical Scavenger	Equiv	Yield
1	---		88%
2	TEMPO	0.1	86%
3	TEMPO	1.0	24%

4

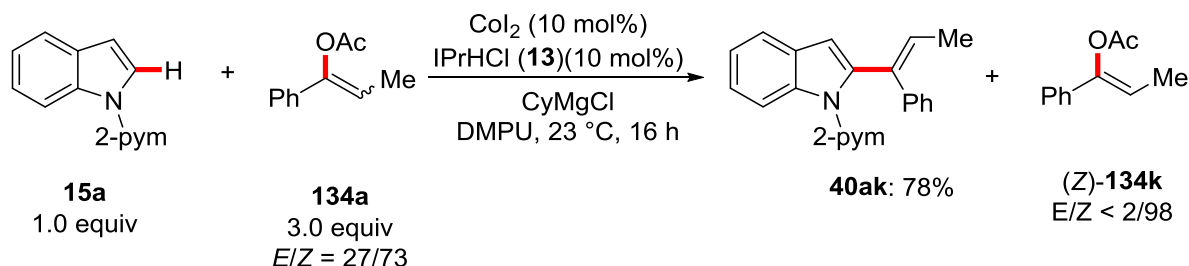
Styrene

1.0

42%

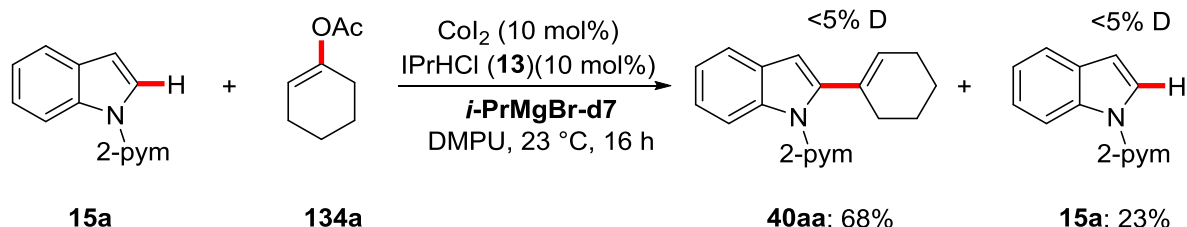
The general procedure **A** was followed using indole **15a** (97.6 mg, 0.50 mmol, 1.0 equiv), enol acetate **134a** (106 mg, 0.75 mmol, 1.5 equiv) and a radical scavenger (0.1 or 1.0 equiv). Purification by column chromatography (*n*-hexane/EtOAc: 9/1) yielded **40aa** in the indicated yields.

### Alkene Isomerization



The general procedure **A** was followed using indole **15a** (97.6 mg, 0.50 mmol, 1.0 equiv) and enol acetate **134k** (266 mg, 1.50 mmol, 3.0 equiv, *E/Z* = 27/73). Purification by column chromatography (*n*-hexane/EtOAc: 10/1) yielded **40ak** (121 mg, 0.39 mmol, 78%) and reisolated enol acetate **134k** (127 mg, 0.72 mmol, 48%, *E/Z* < 2/98).

### Experiment with Deuterium-Labeled Compound

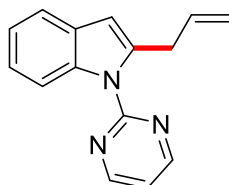


To a solution of indole **15a** (97.6 mg, 0.50 mmol, 1.0 equiv), enol acetate **134a** (105 mg, 0.75 mmol, 1.5 equiv),  $\text{CoI}_2$  (15.7 mg, 0.05 mmol, 10 mol %) and IPrHCl (**13**) (21.2 mg, 0.05 mmol, 10 mol %) in DMPU (1.5 mL), *i*-PrMgBr- $\text{d}_7$  (1.0 M in THF, 1.0 mL, 1.0 mmol, 2.0 equiv) was added dropwise. The mixture was stirred for 16 h at 23 °C. After completion of the reaction, saturated aq.  $\text{NH}_4\text{Cl}$  solution (5 mL) was added and the mixture was extracted with MTBE (4 × 5 mL). Drying over  $\text{Na}_2\text{SO}_4$ , evaporation of the solvent and purification by column chromatography on silica gel (*n*-hexane/EtOAc 18:1) yielded the alkenylated indole **40aa** (93.6 mg, 0.34 mmol, 68%) and reisolated **15a** (22.4 mg, 0.12 mmol, 23%). No deuterium incorporation could be observed by  $^1\text{H}$  NMR spectroscopy.

## 5.4 Cobalt-Catalyzed Allylation with Allyl Acetates

### 5.4.1 Experimental Procedures and Analytical Data

#### 2-Allyl-1-(pyrimidin-2-yl)-1*H*-indole (**172aa**)



**172aa**

The general procedure **C** was followed using indole **15a** (97.1 mg, 0.50 mmol, 1.0 equiv). Purification by column chromatography (*n*-hexane/EtOAc: 10/1) yielded **172aa** (113 mg, 0.48 mmol, 96%) as a colorless oil.

The general procedure **C** was followed using indole **15a** (97.1 mg, 0.50 mmol, 1.0 equiv) and allyl carbonate **176a** (117 mg, 1.00 mmol, 2.0 equiv) instead of allyl acetate (**171a**). Purification by column chromatography (*n*-hexane/EtOAc: 10/1) yielded **172aa** (103 mg, 0.44 mmol, 88%) as a colorless oil.

The general procedure **C** was followed using indole **15a** (97.1 mg, 0.50 mmol, 1.0 equiv) and allyl carbamate **175a** (130 mg, 1.00 mmol, 2.0 equiv) instead of allyl acetate (**171a**). Purification by column chromatography (*n*-hexane/EtOAc: 10/1) yielded **172aa** (106 mg, 0.45 mmol, 90%) as a colorless oil.

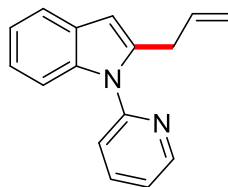
The general procedure **C** was followed using indole **15a** (97.1 mg, 0.50 mmol, 1.0 equiv) and allyl sulfamate **178a** (137 mg, 1.00 mmol, 2.0 equiv) instead of allyl acetate (**171a**). Purification by column chromatography (*n*-hexane/EtOAc: 10/1) yielded **172aa** (9.4 mg, 0.04 mmol, 8%) as a colorless oil.

**<sup>1</sup>H-NMR** (300 MHz, CDCl<sub>3</sub>)  $\delta$  = 8.75 (d, *J* = 4.8 Hz, 2H), 8.30–8.27 (m, 1H), 7.56 (ddd, *J* = 7.4, 1.6, 0.7 Hz, 1H), 7.29–7.18 (m, 2H), 7.07 (t, *J* = 4.8 Hz, 1H), 6.52 (q, *J* = 1.0 Hz, 1H), 6.02 (ddt, *J* = 17.1, 10.1, 6.5 Hz, 1H), 5.08 (ddt, *J* = 17.0, 1.6 Hz, 1.6 Hz, 1H), 5.05 (ddt, *J* = 10.1, 1.6, 1.3 Hz, 1H), 3.98 (dq, *J* = 6.5, 1.3 Hz, 2H). **<sup>13</sup>C-NMR** (125 MHz, CDCl<sub>3</sub>)  $\delta$  = 158.2 (C<sub>q</sub>), 158.1 (CH), 139.8 (C<sub>q</sub>), 137.2 (C<sub>q</sub>), 135.7 (CH), 129.3 (C<sub>q</sub>), 122.7 (CH), 121.9 (CH), 119.9 (CH), 117.1 (CH), 116.5 (CH<sub>2</sub>), 113.9 (CH), 106.5 (CH), 34.1 (CH<sub>2</sub>). **IR** (ATR): 3045, 1557, 1419, 1347, 1202, 990, 797, 739, 630 cm<sup>-1</sup>. **ESI-MS**: *m/z* (relative intensity): 258 (12), [M+Na]<sup>+</sup>, 236 (100) [M+H]. **HR-MS** (ESI): *m/z* calcd for C<sub>15</sub>H<sub>13</sub>N<sub>3</sub>



$[M+H]^+$ : 236.1182, found: 236.1184. The analytical data correspond with those reported in literature.<sup>[59]</sup>

### 2-Allyl-1-(Pyridin-2-yl)-1*H*-indole (172ba)

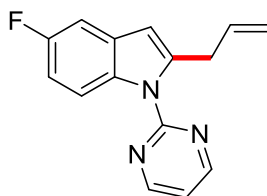


**172ba**

The general procedure **C** was followed using indole **15b** (97.2 mg, 0.50 mmol, 1.0 equiv). Purification by column chromatography (*n*-hexane/EtOAc: 10/1) yielded **172ba** (89.5 mg, 0.38 mmol, 76%) as a colorless solid.

**M.p.:** 79–81 °C. **<sup>1</sup>H-NMR** (300 MHz, CDCl<sub>3</sub>)  $\delta$  = 8.67 (ddd,  $J$  = 4.9, 2.0, 0.9 Hz, 1H), 7.87 (ddd,  $J$  = 8.0, 7.4, 2.0 Hz, 1H), 7.62 (ddd,  $J$  = 6.0, 3.1, 0.7 Hz, 1H), 7.46 (ddd,  $J$  = 8.0, 1.0, 1.0 Hz, 1H), 7.40 (ddd,  $J$  = 6.1, 3.2, 0.8 Hz, 1H), 7.31 (ddd,  $J$  = 7.5, 4.9, 1.0 Hz, 1H), 7.20–7.15 (m, 2H), 6.51 (q,  $J$  = 0.9 Hz, 1H), 5.93 (ddt,  $J$  = 16.8, 10.3, 6.5 Hz, 1H), 5.00 (ddt,  $J$  = 16.9, 1.8, 1.3 Hz, 1H), 4.99 (ddt,  $J$  = 10.2, 1.8, 1.8 Hz, 1H), 3.69 (dt,  $J$  = 6.5, 1.5 Hz, 2H). **<sup>13</sup>C-NMR** (125 MHz, CDCl<sub>3</sub>)  $\delta$  = 151.5 (C<sub>q</sub>), 149.6 (CH), 139.2 (C<sub>q</sub>), 138.3 (CH), 137.4 (C<sub>q</sub>), 134.9 (CH), 128.7 (C<sub>q</sub>), 122.1 (CH), 121.9 (CH), 121.1 (CH), 120.8 (CH), 120.2 (CH), 116.7 (CH<sub>2</sub>), 110.2 (CH), 103.3 (CH), 32.8 (CH<sub>2</sub>). **IR** (ATR): 3049, 1578, 1553, 1470, 1455, 1436, 1352, 908, 745, 601 cm<sup>-1</sup>. **ESI-MS:**  $m/z$  (relative intensity): 273 (12)  $[M+K]^+$ , 257 (16)  $[M+Na]^+$ , 235 (100)  $[M+H]^+$ . **HR-MS** (ESI):  $m/z$  calcd for C<sub>16</sub>H<sub>14</sub>N<sub>2</sub>  $[M+H]^+$ : 235.1230, found: 235.1235. The analytical data correspond with those reported in the literature.<sup>[164a]</sup>

### 2-Allyl-5-fluoro-1-(pyrimidin-2-yl)-1*H*-indole (172da)

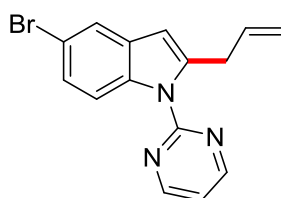


**172da**

The general procedure **C** was followed using indole **15d** (107 mg, 0.50 mmol, 1.0 equiv). Purification by column chromatography (*n*-hexane/EtOAc: 10/1) yielded **172da** (119 mg, 0.47 mmol, 94%) as a colorless solid.

**M.p.:** 65–67 °C. **<sup>1</sup>H-NMR** (300 MHz, CDCl<sub>3</sub>)  $\delta$  = 8.77 (dd,  $J$  = 4.8, 0.5 Hz, 2H), 8.23 (ddd,  $J$  = 9.1, 4.7, 0.6 Hz, 1H), 7.18 (ddd,  $J$  = 9.0, 2.6, 0.5 Hz, 1H), 7.14 (td,  $J$  = 4.8, 0.5 Hz, 1H), 6.95 (ddd,  $J$  = 9.2, 2.6, 2.6 Hz, 1H), 6.45 (d,  $J$  = 1.0 Hz, 1H), 5.97 (ddt,  $J$  = 17.0, 10.1, 6.5 Hz, 1H), 5.06 (ddt,  $J$  = 17.0, 1.6, 1.6 Hz, 1H), 5.03 (ddt,  $J$  = 10.1, 1.6, 1.6 Hz, 1H), 3.97 (dq,  $J$  = 6.6, 1.3 Hz, 2H). **<sup>13</sup>C-NMR** (125 MHz, CDCl<sub>3</sub>)  $\delta$  = 159.1 (d,  $^1J_{\text{C-F}}$  = 237.0 Hz, C<sub>q</sub>), 158.2 (CH), 158.2 (C<sub>q</sub>), 141.7 (C<sub>q</sub>), 135.4 (CH), 133.6 (C<sub>q</sub>), 130.1 (d,  $^3J_{\text{C-F}}$  = 10.1 Hz, C<sub>q</sub>), 117.3 (CH), 116.8 (CH<sub>2</sub>), 115.1 (d,  $^3J_{\text{C-F}}$  = 9.0 Hz, CH), 110.4 (d,  $^2J_{\text{C-F}}$  = 25.0 Hz, CH), 106.4 (CH), 105.1 (d,  $^2J_{\text{C-F}}$  = 23.6 Hz, CH), 34.4 (CH<sub>2</sub>). **<sup>19</sup>F-NMR** (282 MHz, CDCl<sub>3</sub>)  $\delta$  = -122.89 (td,  $J$  = 9.2, 4.7 Hz). **IR** (ATR): 3080, 2922, 1558, 1442, 1348, 1204, 927, 897, 809, 635 cm<sup>-1</sup>. **ESI-MS:**  $m/z$  (relative intensity): 276 (19) [M+Na]<sup>+</sup>, 254 (100) [M+H]<sup>+</sup>. **HR-MS** (ESI):  $m/z$  calcd for C<sub>15</sub>H<sub>12</sub>FN<sub>3</sub> [M+H]<sup>+</sup>: 254.1088, found: 254.1088. The analytical data correspond with those reported in the literature.<sup>[178]</sup>

### 2-Allyl-5-bromo-1-(pyrimidin-2-yl)-1H-indole (172ga)

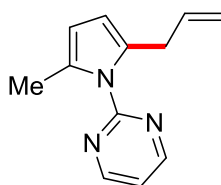


**172ga**

The general procedure **C** was followed using indole **15g** (138 mg, 0.50 mmol, 1.0 equiv). Purification by column chromatography (*n*-hexane/EtOAc: 10/1) yielded **172ga** (150 mg, 0.47 mmol, 95%) as a colorless solid.

**M.p.:** 77–79 °C. **<sup>1</sup>H-NMR** (300 MHz, CDCl<sub>3</sub>)  $\delta$  = 8.78 (d,  $J$  = 4.8 Hz, 2H), 8.15 (ddd,  $J$  = 8.9, 0.6, 0.6 Hz, 1H), 7.65 (dd,  $J$  = 2.1, 0.5 Hz, 1H), 7.30 (dd,  $J$  = 8.9, 2.0 Hz, 1H), 7.16 (t,  $J$  = 4.8 Hz, 1H), 6.42 (d,  $J$  = 0.9 Hz, 1H), 5.98 (ddt,  $J$  = 17.1, 10.1, 6.5 Hz, 1H), 5.06 (ddt,  $J$  = 17.1, 1.6 Hz, 1.6 Hz, 1H), 5.02 (ddt,  $J$  = 10.1, 1.5, 1.5 Hz, 1H), 3.96 (dq,  $J$  = 6.5, 1.3 Hz, 2H). **<sup>13</sup>C-NMR** (125 MHz, CDCl<sub>3</sub>)  $\delta$  = 158.3 (CH), 158.1 (C<sub>q</sub>), 141.3 (C<sub>q</sub>), 135.9 (C<sub>q</sub>), 135.3 (CH), 131.9 (C<sub>q</sub>), 125.5 (CH), 122.5 (CH), 117.5 (CH), 116.9 (CH<sub>2</sub>), 115.6 (CH), 115.1 (C<sub>q</sub>), 105.8 (CH), 34.2 (CH<sub>2</sub>). **IR** (ATR): 2931, 1571, 1557, 1441, 1196, 926, 857, 809, 780, 577 cm<sup>-1</sup>. **EI-MS:**  $m/z$  (relative intensity): 314 (100) [<sup>79</sup>BrM+H]<sup>+</sup>, 235 (73) [M-<sup>79</sup>Br+H]<sup>+</sup>. **HR-MS** (ESI):  $m/z$  calcd for C<sub>15</sub>H<sub>12</sub><sup>79</sup>BrN<sub>3</sub> [M+H]<sup>+</sup>: 314.0287, found: 314.0287. The analytical data correspond with those reported in the literature.<sup>[178]</sup>

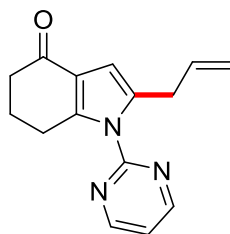
### 2-(2-Allyl-5-methyl-1H-pyrrol-1-yl)pyrimidine (173aa)

**173aa**

The general procedure **C** was followed using pyrrole **146a** (80.7 mg, 0.50 mmol, 1.0 equiv). Purification by column chromatography (*n*-hexane/EtOAc: 10/1) yielded **173aa** (84.3 mg, 0.42 mmol, 84%) as a yellow oil.

**<sup>1</sup>H-NMR** (300 MHz, CDCl<sub>3</sub>)  $\delta$  = 8.75 (d, *J* = 4.8 Hz, 2H), 7.17 (t, *J* = 4.8 Hz, 1H), 5.96 (d, *J* = 3.2 Hz, 1H), 5.94 (dd, *J* = 3.2, 0.9 Hz, 1H), 5.80 (ddt, *J* = 17.6, 9.5, 6.5 Hz, 1H), 4.87 (ddt, *J* = 17.6, 1.4, 1.4 Hz, 1H), 4.82 (ddt, *J* = 9.5, 1.5, 1.4 Hz, 1H), 3.58 (d, *J* = 6.6 Hz, 2H), 2.34 (s, 3H). **<sup>13</sup>C-NMR** (125 MHz, CDCl<sub>3</sub>)  $\delta$  = 158.2 (CH), 158.1 (C<sub>q</sub>), 136.4 (CH), 131.9 (C<sub>q</sub>), 130.4 (C<sub>q</sub>), 118.2 (CH), 115.4 (CH<sub>2</sub>), 108.7 (CH), 108.7 (CH), 32.8 (CH<sub>2</sub>), 14.4 (CH<sub>3</sub>). **IR** (ATR): 2922, 1638, 1558, 1421, 911, 813, 760 cm<sup>-1</sup>. **ESI-MS**: *m/z* (relative intensity): 200 [M+H]<sup>+</sup>. **HR-MS** (ESI): *m/z* calcd for C<sub>12</sub>H<sub>13</sub>N<sub>3</sub> [M+H]<sup>+</sup>: 200.1182, found: 200.1184.

#### 2-Allyl-1-(pyrimidin-2-yl)-1,5,6,7-tetrahydro-4*H*-indol-4-one (173ba)

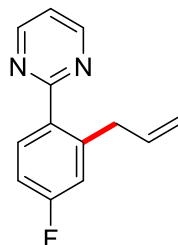
**173ba**

The general procedure **C** was followed using pyrrole **146b** (107 mg, 0.50 mmol, 1.0 equiv). Purification by column chromatography (*n*-hexane/EtOAc: 5/1) yielded **173ba** (116 mg, 0.46 mmol, 92%) as a colorless solid.

**M.p.:** 104–106 °C. **<sup>1</sup>H-NMR** (300 MHz, CDCl<sub>3</sub>)  $\delta$  = 8.78 (dd, *J* = 4.9, 0.7 Hz, 2H), 7.28 (t, *J* = 4.9 Hz, 1H), 6.43 (d, *J* = 1.0 Hz, 1H), 5.76 (ddt, *J* = 16.8, 10.4, 6.5 Hz, 1H), 4.87 (ddt, *J* = 10.3, 1.4, 1.4 Hz, 1H), 4.85 (ddt, *J* = 16.8, 1.6, 1.4 Hz, 1H), 3.59 (dq, *J* = 6.5, 1.2 Hz, 2H), 2.95 (t, *J* = 6.2 Hz, 2H), 2.48 (dd, *J* = 7.1, 5.7 Hz, 2H), 2.09 (tt, *J* = 6.4 Hz, 2H). **<sup>13</sup>C-NMR** (125 MHz, CDCl<sub>3</sub>)  $\delta$  = 194.9 (C<sub>q</sub>), 158.9 (CH), 157.0 (C<sub>q</sub>), 145.5 (C<sub>q</sub>), 135.2 (CH), 134.2 (C<sub>q</sub>), 121.6 (C<sub>q</sub>), 119.2 (CH), 116.4 (CH<sub>2</sub>), 106.2 (CH), 37.9 (CH<sub>2</sub>), 32.4 (CH<sub>2</sub>), 24.2 (CH<sub>2</sub>), 24.0 (CH<sub>2</sub>). **IR** (ATR): 2935, 1640, 1559, 1417, 1406, 1168, 994, 898, 823, 734

$\text{cm}^{-1}$ . **ESI-MS**:  $m/z$  (relative intensity): 292 (60)  $[\text{M}+\text{K}]^+$ , 276 (51)  $[\text{M}+\text{Na}]^+$ , 254 (100)  $[\text{M}+\text{H}]^+$ . **HR-MS** (ESI):  $m/z$  calcd for  $\text{C}_{15}\text{H}_{15}\text{N}_3\text{O}$   $[\text{M}+\text{H}]^+$ : 254.1288, found: 254.1288.

### 2-(2-Allyl-4-fluorophenyl)pyrimidine (174ba)

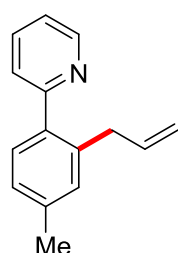


**174ba**

The general procedure **C** was followed using phenyl pyrimidine **14b** (87.2 mg, 0.50 mmol, 1.0 equiv). Purification by column chromatography (*n*-hexane/EtOAc: 95/5) yielded **174ba** (61.6 mg, 0.29 mmol, 57%) as a colorless oil.

**$^1\text{H-NMR}$**  (300 MHz,  $\text{CDCl}_3$ )  $\delta$  = 8.79 (d,  $J$  = 5.5 Hz 2H), 7.80 (dd,  $J$  = 8.9, 5.5 Hz, 1H), 7.19 (t,  $J$  = 5.4 Hz, 1H), 7.03–6.98 (m, 2H), 5.88 (ddt,  $J$  = 17.2, 10.5, 6.5 Hz, 1H), 4.97 (ddt,  $J$  = 17.2, 1.7, 1.7 Hz, 1H), 4.95 (ddt,  $J$  = 10.5, 1.7, 1.7 Hz, 1H), 3.75 (d,  $J$  = 6.5 Hz, 2H).  **$^{13}\text{C-NMR}$**  (125 MHz,  $\text{CDCl}_3$ )  $\delta$  = 166.7 ( $\text{C}_q$ ), 163.3 (d,  $^1J_{\text{C-F}}$  = 250.7 Hz,  $\text{C}_q$ ), 156.9 (CH), 142.2 (d,  $^3J_{\text{C-F}}$  = 12.1 Hz,  $\text{C}_q$ ), 136.9 (CH), 134.1 (d,  $^4J_{\text{C-F}}$  = 3.0 Hz,  $\text{C}_q$ ), 132.8 (d,  $^3J_{\text{C-F}}$  = 9.1 Hz, CH), 118.6 (CH), 117.0 (d,  $^2J_{\text{C-F}}$  = 25.1 Hz, CH), 115.9 ( $\text{CH}_2$ ), 113.3 (d,  $^2J_{\text{C-F}}$  = 21.8 Hz, CH), 37.9 ( $\text{CH}_2$ ).  **$^{19}\text{F-NMR}$**  (282 MHz,  $\text{CDCl}_3$ )  $\delta$  = -112.41. **IR** (ATR): 2977, 1555, 1412, 1222, 966, 802, 768, 578  $\text{cm}^{-1}$ . **ESI-MS**:  $m/z$  (relative intensity): 215 (100)  $[\text{M}+\text{H}]^+$ . **HR-MS** (ESI):  $m/z$  calcd for  $\text{C}_{13}\text{H}_{11}\text{FN}_2$   $[\text{M}+\text{H}]^+$ : 215.0979, found: 215.0979.

### 2-(2-Allyl-4-methylphenyl)pyridine (174ca)

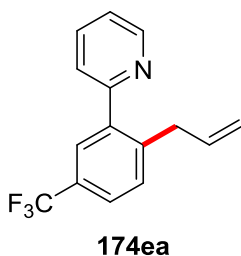


**174ca**

The general procedure **C** was followed using phenyl pyridine **14c** (84.6 mg, 0.50 mmol, 1.0 equiv). Purification by column chromatography (*n*-hexane/EtOAc: 20/1) yielded **174ca** (36.6 mg, 0.18 mmol, 35%) as a colorless oil.

**<sup>1</sup>H-NMR** (500 MHz, CDCl<sub>3</sub>)  $\delta$  = 8.67 (ddd,  $J$  = 4.9, 1.9, 1.0 Hz, 1H), 7.71 (ddd,  $J$  = 7.7, 7.7, 1.8 Hz, 1H), 7.38 (ddd,  $J$  = 7.8, 1.1, 1.1 Hz, 1H), 7.29 (d,  $J$  = 8.4 Hz, 1H), 7.22 (ddd,  $J$  = 7.6, 4.9, 1.2 Hz, 1H), 7.13–7.10 (m, 2H), 5.88 (ddt,  $J$  = 16.7, 10.1, 6.5 Hz, 1H), 4.96 (ddt,  $J$  = 10.0, 1.5, 1.5 Hz, 1H), 4.90 (ddt,  $J$  = 17.1, 1.8, 1.8 Hz, 1H), 3.48 (dt,  $J$  = 6.5, 1.5 Hz, 2H), 2.38 (s, 3H). **<sup>13</sup>C-NMR** (126 MHz, CDCl<sub>3</sub>):  $\delta$  = 160.1 (C<sub>q</sub>), 149.3 (CH), 138.3 (C<sub>q</sub>), 137.9 (CH), 137.8 (C<sub>q</sub>), 137.6 (C<sub>q</sub>), 136.2 (CH), 130.9 (CH), 130.0 (CH), 127.2 (CH), 124.3 (CH), 121.6 (CH), 115.6 (CH<sub>2</sub>), 37.6 (CH<sub>2</sub>), 21.4 (CH<sub>3</sub>). **IR** (ATR): 3061, 1567, 1408, 1221, 1166, 1120, 966, 854, 802, 748 cm<sup>-1</sup>. **ESI-MS**:  $m/z$  (relative intensity): 210 (100) [M+H]<sup>+</sup>. **HR-MS** (ESI):  $m/z$  calcd for C<sub>15</sub>H<sub>15</sub>N [M+H]<sup>+</sup>: 210.1277, found: 210.1281.

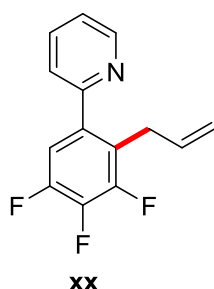
### 2-[2-Allyl-5-(trifluoromethyl)phenyl]pyridine (174ea)



The general procedure **C** was followed using phenyl pyridine **14e** (111 mg, 0.50 mmol, 1.0 equiv). Purification by column chromatography (*n*-hexane/EtOAc: 10/1) yielded **174ea** (80.8 mg, 0.31 mmol, 61%) as a colorless oil.

**<sup>1</sup>H-NMR** (300 MHz, CDCl<sub>3</sub>)  $\delta$  = 8.71 (ddd,  $J$  = 4.9, 1.8, 0.9 Hz, 1H), 7.77 (ddd,  $J$  = 7.7, 7.7, 1.8 Hz, 1H), 7.67 (d,  $J$  = 1.9 Hz, 1H), 7.60 (dd,  $J$  = 8.2, 1.1 Hz, 1H), 7.46–7.39 (m, 2H), 7.29 (ddd,  $J$  = 7.6, 4.9, 1.2 Hz, 1H), 5.86 (ddt,  $J$  = 16.7, 10.1, 6.5 Hz, 1H), 5.01 (ddt,  $J$  = 10.1, 1.5, 1.5 Hz, 1H), 4.91 (ddt,  $J$  = 16.7, 1.7, 1.5 Hz, 1H), 3.54 (d,  $J$  = 6.5 Hz, 2H). **<sup>13</sup>C-NMR** (125 MHz, CDCl<sub>3</sub>)  $\delta$  = 158.6 (C<sub>q</sub>), 149.5 (CH), 142.0 (C<sub>q</sub>), 141.0 (C<sub>q</sub>), 136.6 (CH), 136.5 (CH), 130.9 (CH), 128.3 (q, <sup>2</sup> $J_{C-F}$  = 32.5 Hz, C<sub>q</sub>), 126.9 (q, <sup>3</sup> $J_{C-F}$  = 3.8 Hz, CH), 125.2 (q, <sup>3</sup> $J_{C-F}$  = 3.8 Hz, CH), 124.3 (q, <sup>1</sup> $J_{C-F}$  = 272.1 Hz, C<sub>q</sub>), 124.2 (CH), 122.5 (CH), 116.6 (CH<sub>2</sub>), 37.4 (CH<sub>2</sub>). **<sup>19</sup>F-NMR** (282 MHz, CDCl<sub>3</sub>):  $\delta$  = -62.75. **IR** (ATR): 3082, 1588, 1336, 1260, 1166, 1120, 1077, 907, 794, 748 cm<sup>-1</sup>. **ESI-MS**:  $m/z$  (relative intensity): 264 (100) [M+H]<sup>+</sup>, 235 (6) [M-C<sub>2</sub>H<sub>4</sub>]<sup>+</sup>. **HR-MS** (ESI):  $m/z$  calcd for C<sub>15</sub>H<sub>12</sub>F<sub>3</sub>N [M+H]<sup>+</sup>: 264.0995, found: 264.0997. The analytical data correspond with those reported in literature.<sup>[179]</sup>

### 2-(2-Allyl-3,4,5-trifluorophenyl)pyridine (174fa)

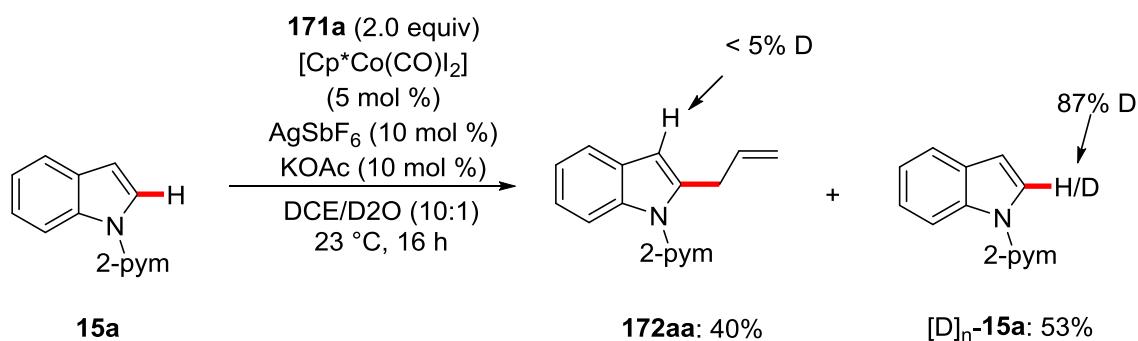


The general procedure **C** was followed using phenyl pyridine **14f** (105 mg, 0.50 mmol, 1.0 equiv). Purification by column chromatography (*n*-hexane/EtOAc: 20/1) and HPLC (*n*-hexane/EtOAc: 50/1 → 12:1) yielded **174fa** (76.2 mg, 0.31 mmol, 62%) as a colorless oil.

**<sup>1</sup>H-NMR** (500 MHz, CDCl<sub>3</sub>)  $\delta$  = 8.68 (ddd,  $J$  = 4.9, 1.8, 1.0 Hz, 1H), 7.75 (ddd,  $J$  = 7.7, 7.7, 1.8 Hz, 1H), 7.38 (ddd,  $J$  = 7.8, 1.0, 1.0 Hz, 1H), 7.30 (ddd,  $J$  = 7.6, 4.9, 1.1 Hz, 1H), 7.07 (ddd,  $J$  = 10.5, 7.2, 2.2 Hz, 1H), 5.84 (ddtd,  $J$  = 17.1, 10.2, 6.0, 0.6 Hz, 1H), 4.97 (ddt,  $J$  = 10.1, 1.5, 1.5 Hz, 1H), 4.83 (ddt,  $J$  = 17.1, 2.6, 1.7 Hz, 1H), 3.46 (dd,  $J$  = 6.1, 2.0 Hz, 2H). **<sup>13</sup>C-NMR** (125 MHz, CDCl<sub>3</sub>):  $\delta$  = 156.9 (C<sub>q</sub>), 150.2 (ddd,  $^1J_{C-F}$  = 248.1 Hz,  $^2J_{C-F}$  = 9.1 Hz,  $^3J_{C-F}$  = 3.6 Hz, C<sub>q</sub>), 149.6 (CH), 149.3 (ddd,  $^1J_{C-F}$  = 248.5 Hz,  $^2J_{C-F}$  = 10.1 Hz,  $^3J_{C-F}$  = 4.2 Hz, C<sub>q</sub>), 139.9 (dt,  $^1J_{C-F}$  = 253.4 Hz,  $^2J_{C-F}$  = 15.3 Hz, C<sub>q</sub>), 136.6 (CH), 136.5 (dd,  $^3J_{C-F}$  = 4.4, 2.6 Hz, C<sub>q</sub>), 135.3 (CH), 124.0 (CH), 123.0 (dd,  $^2J_{C-F}$  = 12.9 Hz,  $^3J_{C-F}$  = 3.2 Hz, C<sub>q</sub>), 122.8 (CH), 116.0 (CH<sub>2</sub>), 113.6 (dd,  $^2J_{C-F}$  = 17.9 Hz,  $^3J_{C-F}$  = 3.5 Hz, CH), 30.0 (d,  $^3J_{C-F}$  = 4.1 Hz, CH<sub>2</sub>). **<sup>19</sup>F-NMR** (282 MHz, CDCl<sub>3</sub>):  $\delta$  = -136.88 (ddd,  $J$  = 20.7, 6.2, 2.7 Hz), -137.88 (ddd,  $J$  = 21.0, 10.6, 6.8 Hz), -160.87 (td,  $J$  = 20.7, 7.3 Hz). **IR** (ATR): 3006, 2920, 1586, 1466, 1427, 910, 825, 788, 775, 748. cm<sup>-1</sup>. **ESI-MS**:  $m/z$  (relative intensity): 250 (100) [M+H]<sup>+</sup>. **HR-MS** (ESI):  $m/z$  calcd for C<sub>14</sub>H<sub>10</sub>F<sub>3</sub>N [M+H]<sup>+</sup>: 250.0838, found: 250.0843.

## 5.4.2 Mechanistic Studies

### H/D Exchange Experiment



To a solution of *N*-pyrimidyl indole (**15a**) (97.1 mg, 0.50 mmol, 1.0 equiv), [Cp\*Co(CO)I<sub>2</sub>] (11.9 mg, 0.03 mmol, 5.0 mol %), AgSbF<sub>6</sub> (17.2 mg, 0.05 mmol, 10 mol %) and KOAc (4.9 mg, 0.05 mmol, 10 mol %) in DCE (1.0 mL) and D<sub>2</sub>O (0.1 mL) allyl acetate (**171a**) (101 mg, 1.00 mmol, 2.0 equiv) was added. The mixture was stirred for 16 h at 80 °C. After completion of the reaction, saturated aq. NH<sub>4</sub>Cl solution (5 mL) was added at ambient temperature and the mixture was extracted with MTBE (4 x 5 mL). Drying over Na<sub>2</sub>SO<sub>4</sub>, evaporation of the solvent and purification by column chromatography on silica gel using (*n*-hexane/EtOAc: 12/1) yielded the product **172aa** (47.1 mg, 0.20 mmol, 40%) and deuterated starting material [D]<sub>n</sub>-**15a** (52.0 mg, 0.27 mmol, 53%). The amount of deuteration was determined by <sup>1</sup>H-NMR spectroscopy.

### C–H Allylation of Allyl Acetate (**171a**) and Carbonate **176a**

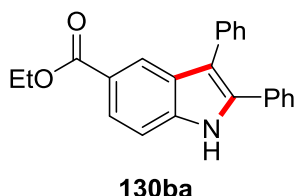
Two parallel reactions of 2-pyrimidyl indole (97.1 mg, 0.50 mmol, 1.0 equiv), allyl acetate (**171a**) (101 mg, 1.00 mmol, 2.0 equiv) or allyl carbonate **176a** (117 mg, 1.00 mmol, 2.0 equiv), [Cp\*Co(CO)I<sub>2</sub>] (11.9 mg, 0.03 mmol, 5.0 mol %), AgSbF<sub>6</sub> (17.2 mg, 0.05 mmol, 10 mol %), KOAc (4.9 mg, 0.05 mmol, 10 mol %) and *n*-dodecane (20 µL) in DCE (1.5 mL) were placed in a 25 mL Schlenk tube and stirred at 120 °C under an atmosphere of nitrogen. Periodic aliquots (20 µL) were removed by a syringe and the conversions were determined by gas chromatography.

Time	Conversion / %	
	with allyl acetate ( <b>171a</b> )	with allyl carbonate <b>176a</b>
5	5	2
10	14	8
15	34	26
20	47	35
30	56	50
60	67	66
120	75	77
180	90	90
240	96	92

## 5.5 Cobalt-Catalyzed C–H/N–O Functionalization

### 5.5.1 Experimental Procedures and Analytical Data

#### Ethyl 2,3-diphenyl-1*H*-indole-5-carboxylate (**130ba**)

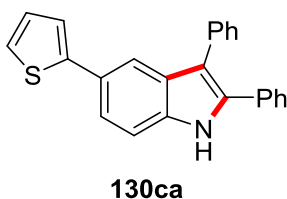


The general procedure **D** was followed using nitron **129b** (150 mg, 0.50 mmol, 1.0 equiv), diphenylacetylene (**35a**) (134 mg, 0.75 mmol, 1.5 equiv) and Piv-Leu-OH (22.1 mg, 0.10 mmol, 20 mol %). Purification by column chromatography (*n*-hexane/EtOAc: 20/1) yielded **130ba** (104 mg, 0.31 mmol, 61%) as an off-white solid.

The general procedure **D** was followed using nitron **129b** (150 mg, 0.50 mmol, 1.0 equiv), diphenylacetylene (**35a**) (134 mg, 0.75 mmol, 1.5 equiv) and NaOAc (8.2 mg, 0.10 mmol, 20 mol %). Purification by column chromatography (*n*-hexane/CH<sub>2</sub>Cl<sub>2</sub>: 3/1) yielded **130ba** (113 mg, 0.33 mmol, 67%) as an off-white solid.

**M.p.:** 178–180 °C. **<sup>1</sup>H-NMR** (500 MHz, DMSO-*d*<sub>6</sub>)  $\delta$  = 11.98 (s, 1H), 8.15 (d, *J* = 1.6 Hz, 1H), 7.82 (dd, *J* = 8.5, 1.6 Hz, 1H), 7.53 (d, *J* = 8.5 Hz, 1H), 7.48–7.42 (m, 4H), 7.38–7.32 (m, 6H), 4.29 (q, *J* = 7.1 Hz, 2H), 1.30 (t, *J* = 7.1 Hz, 3H). **<sup>13</sup>C-NMR** (125 MHz, DMSO-*d*<sub>6</sub>)  $\delta$  = 166.3 (C<sub>q</sub>), 138.4 (C<sub>q</sub>), 135.5 (C<sub>q</sub>), 134.3 (C<sub>q</sub>), 131.6 (C<sub>q</sub>), 129.6 (CH), 128.5 (CH), 128.3 (CH), 127.9 (CH), 127.6 (CH), 127.5 (C<sub>q</sub>), 126.3 (CH), 122.7 (CH), 121.3 (C<sub>q</sub>), 120.8 (CH), 114.3 (C<sub>q</sub>), 111.1 (CH), 60.0 (CH<sub>2</sub>), 14.2 (CH<sub>3</sub>). **IR** (ATR): 3310, 1684, 1306, 1235, 1102, 1083, 756, 694, 654, 608 cm<sup>-1</sup>. **MS** (ESI) *m/z* (relative intensity) 364 (100) [M+Na]<sup>+</sup>, 342 (20) [M+H]<sup>+</sup>. **HR-MS** (ESI) *m/z* calcd for C<sub>23</sub>H<sub>19</sub>NO<sub>2</sub> [M+Na]<sup>+</sup>: 364.1308, found: 364.1301.

#### 2,3-Diphenyl-5-(thiophen-2-yl)-1*H*-indole (**130ca**)



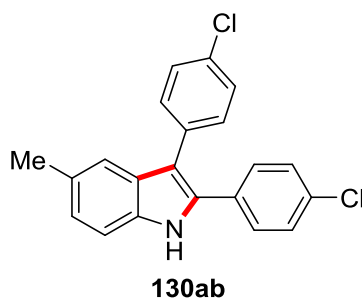


The general procedure **D** was followed using nitron **129c** (155 mg, 0.50 mmol, 1.0 equiv), diphenylacetylene (**35a**) (134 mg, 0.75 mmol, 1.5 equiv) and Piv-Leu-OH (22.1 mg, 0.10 mmol, 20 mol %). Purification by column chromatography (*n*-hexane/EtOAc: 30/1) and GPC yielded **130ca** (135 mg, 0.39 mmol, 77%) as an off-white solid.

The general procedure **D** was followed using nitron **129c** (155 mg, 0.50 mmol, 1.0 equiv), diphenylacetylene (**35a**) (134 mg, 0.75 mmol, 1.5 equiv) and NaOAc (8.2 mg, 0.10 mmol, 20 mol %). Purification by column chromatography (*n*-hexane/EtOAc: 30/1) and GPC yielded **130ca** (144 mg, 0.39 mmol, 82%) as an off-white solid.

**M.p.:** 186–188 °C. **<sup>1</sup>H-NMR** (500 MHz, DMSO-*d*<sub>6</sub>)  $\delta$  = 11.71 (s, 1H), 7.69 (d, *J* = 1.2 Hz, 1H), 7.50 (d, *J* = 1.3 Hz, 2H), 7.48–7.46 (m, 2H), 7.44–7.35 (m, 8H), 7.33–7.29 (m, 2H), 7.08 (dd, *J* = 5.1, 3.5 Hz, 1H). **<sup>13</sup>C-NMR** (75 MHz, DMSO-*d*<sub>6</sub>)  $\delta$  = 145.3 (C<sub>q</sub>), 135.7 (CH), 135.1 (C<sub>q</sub>), 134.9 (C<sub>q</sub>), 132.2 (C<sub>q</sub>), 129.8 (CH), 128.7 (CH), 128.5 (CH), 128.4 (C<sub>q</sub>), 128.3 (C<sub>q</sub>), 128.1 (CH), 127.7 (C<sub>q</sub>), 126.3 (CH), 126.0 (CH), 124.0 (CH), 122.1 (CH), 120.6 (CH), 115.3 (CH), 113.6 (C<sub>q</sub>), 112.1 (CH). **IR** (ATR): 3399, 798, 761, 703, 693, 630, 608, 515, 494, 431 cm<sup>-1</sup>. **MS** (ESI) *m/z* (relative intensity) 386 (3) [M+Cl]<sup>-</sup>, 350 (100) [M-H]<sup>-</sup>. **HR-MS** (ESI) *m/z* calcd for C<sub>24</sub>H<sub>17</sub>NS [M-H]<sup>-</sup>: 350.1009, found: 350.1009.

### 2,3-Bis(4-chlorophenyl)-5-methyl-1*H*-indole (**130ab**)

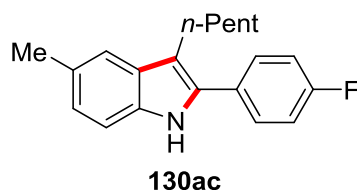


The general procedure **D** was followed using nitron **129a** (121 mg, 0.50 mmol, 1.0 equiv), alkyne **35b** (185 mg, 0.75 mmol, 1.5 equiv) and Piv-Leu-OH (22.1 mg, 0.10 mmol, 20 mol %). Purification by column chromatography (*n*-hexane/CH<sub>2</sub>Cl<sub>2</sub>: 3/1) yielded **130ab** (99.2 mg, 0.28 mmol, 56%) as a pale yellow solid.

The general procedure **D** was followed using nitron **129a** (121 mg, 0.50 mmol, 1.0 equiv), alkyne **35b** (185 mg, 0.75 mmol, 1.5 equiv) and NaOAc (8.2 mg, 0.10 mmol, 20 mol %). Purification by column chromatography (*n*-hexane/CH<sub>2</sub>Cl<sub>2</sub>: 3/1) yielded **130ab** (93.5 mg, 0.27 mmol, 53%) as a pale yellow solid.

**M.p.:** 131–132 °C. **<sup>1</sup>H-NMR** (300 MHz, CDCl<sub>3</sub>)  $\delta$  = 8.08 (s, 1H), 7.40 (s, 1H), 7.39–7.31 (m, 9H), 7.08 (d,  $J$  = 9.4 Hz, 1H), 2.43 (s, 3H). **<sup>13</sup>C-NMR** (125 MHz, CDCl<sub>3</sub>)  $\delta$  = 134.2 (C<sub>q</sub>), 133.6 (C<sub>q</sub>), 133.3 (C<sub>q</sub>), 133.1 (C<sub>q</sub>), 132.1 (C<sub>q</sub>), 131.2 (CH), 130.9 (C<sub>q</sub>), 130.1 (C<sub>q</sub>), 129.2 (CH), 128.9 (CH), 128.8 (CH), 128.6 (C<sub>q</sub>), 124.7 (CH), 118.9 (CH), 113.8 (C<sub>q</sub>), 110.6 (CH), 21.6 (CH<sub>3</sub>). **IR** (ATR): 3452, 3390, 1498, 1471, 1086, 1013, 833, 784, 529, 504 cm<sup>-1</sup>. **MS** (ESI)  $m/z$  (relative intensity) 352 (60) [M+H]<sup>+</sup>, 351 (20), 350 (100) [M-H]<sup>-</sup>. **HR-MS** (ESI)  $m/z$  calcd for C<sub>21</sub>H<sub>15</sub>Cl<sub>2</sub>N [M-H]<sup>-</sup>: 350.0509, found: 350.0508.

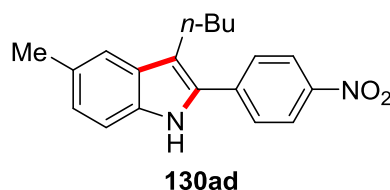
### 2-(4-Fluorophenyl)-5-methyl-3-*n*-pentyl-1*H*-indole (130ac)



The general procedure **D** was followed using nitroene **129a** (121 mg, 0.50 mmol, 1.0 equiv), alkyne **35c** (143 mg, 0.75 mmol, 1.5 equiv) and Piv-Leu-OH (22.1 mg, 0.10 mmol, 20 mol %). Purification by column chromatography (*n*-hexane/EtOAc: 10/1) and GPC yielded **130ac** (114 mg, 0.39 mmol, 77%) as a pale yellow solid.

**M.p.:** 118–120 °C. **<sup>1</sup>H-NMR** (300 MHz, DMSO-*d*<sub>6</sub>)  $\delta$  = 10.98 (s, 1H), 7.65–7.58 (m, 2H), 7.35 (d,  $J$  = 8.9 Hz, 2H), 7.31 (d,  $J$  = 1.8 Hz, 1H), 7.24 (d,  $J$  = 8.1 Hz, 1H), 6.92 (dd,  $J$  = 8.2, 1.6 Hz, 1H), 2.78 (t,  $J$  = 7.8 Hz, 2H), 2.39 (s, 3H), 1.62 (p,  $J$  = 7.2 Hz, 2H), 1.35–1.25 (m, 4H), 0.83 (t,  $J$  = 7.1 Hz, 3H). **<sup>13</sup>C-NMR** (75 MHz, DMSO-*d*<sub>6</sub>)  $\delta$  = 161.3 (d,  $^1J_{C-F}$  = 245 Hz, C<sub>q</sub>), 134.3 (C<sub>q</sub>), 132.9 (C<sub>q</sub>), 129.5 (d,  $^3J_{C-F}$  = 8.1 Hz, CH), 128.9 (C<sub>q</sub>), 127.0 (C<sub>q</sub>), 123.0 (CH), 119.9 (C<sub>q</sub>), 118.1 (CH), 115.6 (d,  $^2J_{C-F}$  = 21.5 Hz, CH), 111.7 (C<sub>q</sub>), 110.8 (CH), 31.4 (CH<sub>3</sub>), 30.3 (CH<sub>2</sub>), 24.0 (CH<sub>2</sub>), 22.0 (CH<sub>3</sub>), 21.3 (CH<sub>2</sub>), 13.9 (CH<sub>2</sub>). **<sup>19</sup>F-NMR** (282 MHz, DMSO-*d*<sub>6</sub>):  $\delta$  = 115.01. **IR** (ATR): 3381, 2923, 2857, 1506, 1441, 1225, 838, 797, 516, 477 cm<sup>-1</sup>. **MS** (ESI)  $m/z$  (relative intensity) 350 (24), 334 (34) [M+K]<sup>+</sup>, 312 (100), 295 (6) [M]<sup>+</sup>. **HR-MS** (ESI)  $m/z$  calcd for C<sub>20</sub>H<sub>22</sub>FN [M]<sup>+</sup>: 295.1731, found: 295.1727. The connectivity was determined by NOESY-NMR spectroscopy.

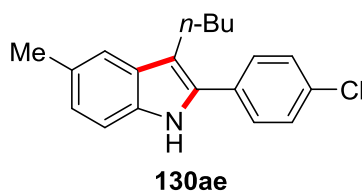
### 3-*n*-Butyl-5-methyl-2-(4-nitrophenyl)-1*H*-indole (130ad)



The general procedure **D** was followed using nitron **129a** (121 mg, 0.50 mmol, 1.0 equiv), alkyne **35d** (152 mg, 0.75 mmol, 1.5 equiv) and Piv-Leu-OH (22.1 mg, 0.10 mmol, 20 mol %). Purification by column chromatography (*n*-hexane/EtOAc: 30/1) and GPC yielded **130ad** (84.2 mg, 0.27 mmol, 54%) as a yellow solid.

**M.p.:** 126–128 °C. **<sup>1</sup>H-NMR** (300 MHz, DMSO-*d*<sub>6</sub>)  $\delta$  = 11.23 (s, 1H), 8.34 (d, *J* = 8.9 Hz, 2H), 7.87 (d, *J* = 8.9 Hz, 2H), 7.37 (d, *J* = 1.6 Hz, 1H), 7.29 (d, *J* = 8.2 Hz, 1H), 7.00 (dd, *J* = 8.4, 1.5 Hz, 1H), 2.89 (dd, *J* = 8.7, 6.8 Hz, 2H), 2.40 (s, 3H), 1.62 (tt, *J* = 8.0, 6.2 Hz, 2H), 1.39 (tt, *J* = 8.0, 7.3 Hz, 2H), 0.90 (t, *J* = 7.3 Hz, 3H). **<sup>13</sup>C-NMR** (75 MHz, DMSO-*d*<sub>6</sub>)  $\delta$  = 145.5 (C<sub>q</sub>), 139.7 (C<sub>q</sub>), 135.1 (C<sub>q</sub>), 131.3 (C<sub>q</sub>), 128.3 (C<sub>q</sub>), 127.7 (CH), 127.5 (C<sub>q</sub>), 124.5 (CH), 123.9 (CH), 118.5 (CH), 115.2 (C<sub>q</sub>), 111.1 (CH), 32.6 (CH<sub>2</sub>), 23.9 (CH<sub>2</sub>), 22.0 (CH<sub>2</sub>), 21.2 (CH<sub>3</sub>), 13.7 (CH<sub>3</sub>). **IR** (ATR): 3313, 1684, 1306, 1234, 1106, 755, 693, 654, 608, 590 cm<sup>-1</sup>. **MS** (ESI) *m/z* (relative intensity) 356.2 (25), 331.2 (100) [M+Na]<sup>+</sup>. **HR-MS** (ESI) *m/z* calcd for C<sub>19</sub>H<sub>20</sub>N<sub>2</sub>O<sub>2</sub> [M+Na]<sup>+</sup>: 331.1417, found: 331.1410. The connectivity was determined by NOESY-NMR spectroscopy.

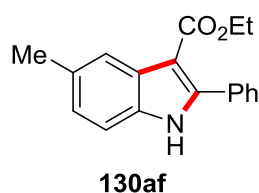
### 3-Butyl-5-methyl-2-(4-chlorophenyl)-1*H*-indole (**130ae**)



The general procedure **D** was followed using nitron **129a** (121 mg, 0.50 mmol, 1.0 equiv), alkyne **35e** (144 mg, 0.75 mmol, 1.5 equiv) and Piv-Leu-OH (22.1 mg, 0.10 mmol, 20 mol %). Purification by column chromatography (*n*-hexane/CH<sub>2</sub>Cl<sub>2</sub>: 3/1) and GPC yielded **130ae** (101 mg, 0.34 mmol, 68%) as a pale yellow solid.

**M.p.:** 143–145 °C. **<sup>1</sup>H-NMR** (300 MHz, CDCl<sub>3</sub>)  $\delta$  = 7.81 (s, 1H), 7.53–7.31 (m, 5H), 7.23 (d, *J* = 6.2 Hz, 1H), 7.02 (dd, *J* = 8.2, 1.6 Hz, 1H), 2.81 (t, *J* = 8.0 Hz, 2H), 2.47 (s, 3H), 1.74–1.60 (m, 2H), 1.47–1.33 (m, 2H), 0.92 (t, *J* = 7.3 Hz, 3H). **<sup>13</sup>C-NMR** (75 MHz, CDCl<sub>3</sub>):  $\delta$  = 134.3 (C<sub>q</sub>), 133.2 (C<sub>q</sub>), 132.9 (C<sub>q</sub>), 132.1 (C<sub>q</sub>), 129.4 (C<sub>q</sub>), 129.0 (CH), 128.9 (CH), 128.8 (C<sub>q</sub>), 124.0 (CH), 119.0 (CH), 114.2 (C<sub>q</sub>), 110.5 (CH), 33.2 (CH<sub>2</sub>), 24.33 (CH<sub>2</sub>), 22.9 (CH<sub>2</sub>), 21.6 (CH<sub>3</sub>), 14.0 (CH<sub>3</sub>). **IR** (ATR): 3379, 2949, 1469, 1439, 1312, 1246, 1093, 835, 798, 504 cm<sup>-1</sup>. **MS** (ESI) *m/z* (relative intensity) 296 (100) [<sup>35</sup>ClM-H]<sup>-</sup>. **HR-MS** (ESI) *m/z* calcd for C<sub>19</sub>H<sub>20</sub><sup>35</sup>ClN [M-H]<sup>-</sup>: 296.1212, found: 296.1215. The connectivity was determined by NOESY-NMR spectroscopy.

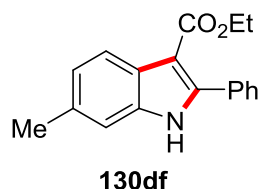
### Ethyl 5-methyl-2-phenyl-1*H*-indole-3-carboxylate (**130af**)



The general procedure **D** was followed using nitrone **129a** (121 mg, 0.50 mmol, 1.0 equiv), alkyne **35f** (131 mg, 0.75 mmol, 1.5 equiv) and Piv-Leu-OH (22.1 mg, 0.10 mmol, 20 mol %). Purification by column chromatography (*n*-hexane/EtOAc: 10/1) and GPC yielded **130af** (86.6 mg, 0.31 mmol, 63%) as a colorless solid.

**M.p.:** 145–147 °C. **<sup>1</sup>H-NMR** (300 MHz, DMSO-*d*<sub>6</sub>)  $\delta$  = 11.97 (s, 1H), 7.86 (d, *J* = 1.0 Hz, 1H), 7.68–7.65 (m, 2H), 7.52–7.45 (m, 3H), 7.33 (d, *J* = 8.2 Hz, 1H), 7.44 (dd, *J* = 8.2, 1.1 Hz, 1H), 4.19 (q, *J* = 7.1 Hz, 2H), 2.43 (s, 3H), 1.21 (t, *J* = 7.1 Hz, 3H). **<sup>13</sup>C-NMR** (125 MHz, DMSO-*d*<sub>6</sub>)  $\delta$  = 164.5 (C<sub>q</sub>), 144.3 (C<sub>q</sub>), 133.9 (C<sub>q</sub>), 132.0 (C<sub>q</sub>), 129.9 (C<sub>q</sub>), 129.8 (CH), 128.6 (CH), 127.7 (CH), 127.5 (C<sub>q</sub>), 124.0 (CH), 120.8 (CH), 111.4 (CH), 102.4 (C<sub>q</sub>), 58.8 (CH<sub>2</sub>), 21.4 (CH<sub>3</sub>), 14.1 (CH<sub>3</sub>). **IR** (ATR): 3232, 1652, 1476, 1451, 1268, 1218, 1145, 1049, 777, 696 cm<sup>-1</sup>. **MS** (ESI) *m/z* (relative intensity) 302 (100) [M+Na]<sup>+</sup>, 280 (6) [M+H]<sup>+</sup>, 234 (3) [M-OEt]<sup>+</sup>. **HR-MS** (ESI) *m/z* calcd for C<sub>18</sub>H<sub>17</sub>NO<sub>2</sub> [M+Na]<sup>+</sup>: 302.1151, found: 302.1159. The connectivity was determined by NOESY-NMR spectroscopy. The analytical data were in accordance with those reported in the literature.<sup>[180]</sup>

#### Ethyl 6-methyl-2-phenyl-1*H*-indole-3-carboxylate (**130df**)

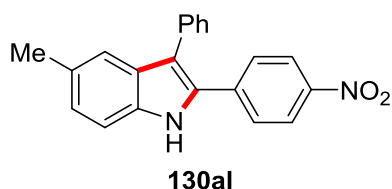


The general procedure **D** was followed using nitrone **129d** (121 mg, 0.50 mmol, 1.0 equiv), alkyne **35f** (131 mg, 0.75 mmol, 1.5 equiv) and Piv-Leu-OH (22.1 mg, 0.10 mmol, 20 mol %). Purification by column chromatography (*n*-hexane/EtOAc: 10/1) and GPC yielded **130df** (94.9 mg, 0.34 mmol, 68%) as a colorless solid.

**M.p.:** 144–146 °C. **<sup>1</sup>H-NMR** (300 MHz, DMSO-*d*<sub>6</sub>)  $\delta$  = 11.94 (s, 1H), 7.92 (d, *J* = 8.2 Hz, 1H), 7.94–7.91 (m, 2H), 7.51–7.45 (m, 3H), 7.23 (d, *J* = 1.4 Hz, 1H), 7.02 (dd, *J* = 8.2, 1.6 Hz, 1H), 4.18 (q, *J* = 7.1 Hz, 2H), 2.42 (s, 3H), 1.22 (t, *J* = 7.1 Hz, 3H). **<sup>13</sup>C-NMR** (75 MHz, DMSO-*d*<sub>6</sub>)  $\delta$  = 164.5 (C<sub>q</sub>), 143.9 (C<sub>q</sub>), 135.9 (C<sub>q</sub>), 132.0 (C<sub>q</sub>), 131.7 (C<sub>q</sub>), 129.9 (CH), 128.7 (CH), 127.7 (CH), 125.1 (C<sub>q</sub>), 123.1 (CH), 120.9 (CH), 111.5 (CH), 102.7 (C<sub>q</sub>), 58.9 (CH<sub>2</sub>), 21.3 (CH<sub>3</sub>), 14.2 (CH<sub>3</sub>). **IR** (ATR): 3251, 1661, 1452, 1269, 1214, 1123,

1046, 805, 766, 688  $\text{cm}^{-1}$ . **MS** (ESI)  $m/z$  (relative intensity) 318 (3)  $[\text{M}+\text{K}]^+$ , 302 (100)  $[\text{M}+\text{Na}]^+$ , 280 (27)  $[\text{M}+\text{H}]^+$ . **HR-MS** (ESI)  $m/z$  calcd for  $\text{C}_{18}\text{H}_{17}\text{NO}_2$   $[\text{M}+\text{H}]^+$ : 280.1332, found: 280.1332. The connectivity was determined by NOESY-NMR spectroscopy. The analytical data were in accordance with those reported in the literature.<sup>[180]</sup>

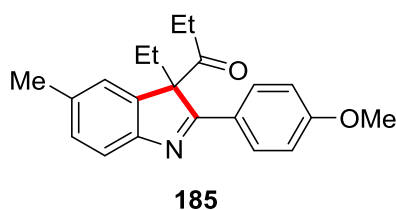
#### 5-Methyl-2-(4-nitrophenyl)-3-phenyl-1*H*-indole (130ag)



The general procedure **D** was followed using nitron **129a** (121 mg, 0.50 mmol, 1.0 equiv), alkyne **30g** (175 mg, 0.75 mmol, 1.5 equiv) and Piv-Leu-OH (22.1 mg, 0.10 mmol, 20 mol %). Purification by column chromatography (*n*-hexane/EtOAc: 10/1) and GPC yielded **130ag** (105 mg, 0.32 mmol, 64%) as a red solid.

**M.p.:** 153–155 °C. **<sup>1</sup>H-NMR** (500 MHz,  $\text{DMSO}-d_6$ )  $\delta$  = 11.68 (s, 1H), 8.19 (d,  $J$  = 9.0 Hz, 2H), 7.66 (d,  $J$  = 9.1 Hz, 2H), 7.47–7.42 (m, 2H), 7.37–7.33 (m, 4H), 7.25 (d,  $J$  = 1.4 Hz, 1H), 7.66 (dd,  $J$  = 8.3, 1.5 Hz, 1H), 2.36 (s, 3H). **<sup>13</sup>C-NMR** (75 MHz,  $\text{DMSO}-d_3$ )  $\delta$  = 145.8 ( $\text{C}_q$ ), 139.1 ( $\text{C}_q$ ), 135.1 ( $\text{C}_q$ ), 134.6 ( $\text{C}_q$ ), 131.4 ( $\text{C}_q$ ), 129.8 (CH), 128.8 (CH), 128.8 ( $\text{C}_q$ ), 128.3 (CH), 128.2 ( $\text{C}_q$ ), 126.6 (CH), 124.9 (CH), 123.6 (CH), 118.5 (CH), 115.9 ( $\text{C}_q$ ), 111.5 (CH), 21.1 ( $\text{CH}_3$ ). **IR** (ATR): 3266, 1595, 1504, 1336, 1107, 1008, 849, 754, 705, 439  $\text{cm}^{-1}$ . **MS** (ESI)  $m/z$  (relative intensity) 351 (100)  $[\text{M}+\text{Na}]^+$ , 329 (12)  $[\text{M}+\text{H}]^+$ . **HR-MS** (ESI)  $m/z$  calcd for  $\text{C}_{21}\text{H}_{16}\text{N}_2\text{O}_2$   $[\text{M}+\text{Na}]^+$ : 351.1104, found: 351.1095. The connectivity was determined by NOESY-NMR spectroscopy.

#### 1-[3-Ethyl-2-(4-methoxyphenyl)-5-methyl-3*H*-indol-3-yl]propan-1-one (185)



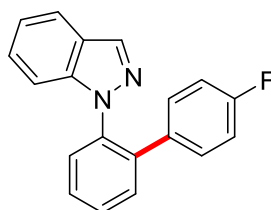
The general procedure **D** was followed using nitron **129a** (121 mg, 0.50 mmol, 1.0 equiv), 3-hexyne (**35h**) (61.6 mg, 0.75 mmol, 1.5 equiv) and Piv-Leu-OH (22.1 mg, 0.10 mmol, 20 mol %). Purification by column chromatography (*n*-hexane/EtOAc: 10/1) and GPC yielded **185** (74.1 mg, 0.23 mmol, 46%) as a colorless solid.

**M.p.:** 69–98 °C. **<sup>1</sup>H-NMR** (300 MHz, CDCl<sub>3</sub>)  $\delta$  = 7.87 (d,  $J$  = 8.9 Hz, 2H), 7.60 (d,  $J$  = 7.9 Hz, 1H), 7.24 (ddd,  $J$  = 8.0, 1.7, 0.8 Hz, 1H), 6.99 (d,  $J$  = 0.8 Hz, 1H), 6.96 (d,  $J$  = 9.0 Hz, 2H), 3.86 (s, 3H), 2.53–2.27 (m, 2H), 2.40 (s, 3H), 2.03–1.75 (m, 2H), 0.8 (t,  $J$  = 7.2 Hz, 3H), 0.24 (t,  $J$  = 7.4 Hz, 3H). **<sup>13</sup>C-NMR** (75 MHz, CDCl<sub>3</sub>)  $\delta$  = 207.3 (C<sub>q</sub>), 175.8 (C<sub>q</sub>), 162.2 (C<sub>q</sub>), 155.0 (C<sub>q</sub>), 139.1 (C<sub>q</sub>), 136.3 (C<sub>q</sub>), 129.9 (CH), 129.7 (CH), 125.7 (C<sub>q</sub>), 122.7 (CH), 120.4 (CH), 114.6 (CH), 75.4 (C<sub>q</sub>), 55.6 (CH<sub>3</sub>), 31.3 (CH<sub>3</sub>), 26.6 (CH<sub>2</sub>), 21.7 (CH<sub>2</sub>), 8.3 (CH<sub>3</sub>), 7.3 (CH<sub>3</sub>). **IR** (ATR): 2967, 3935, 1706, 1603, 1505, 1459, 1254, 1174, 1033, 836 cm<sup>-1</sup>. **MS** (ESI)  $m/z$  (relative intensity) 344 (100) [M+Na]<sup>+</sup>, 322 (41) [M+H]<sup>+</sup>, 306 (70) [M-Me]<sup>+</sup>. **HR-MS** (ESI)  $m/z$  calcd for C<sub>21</sub>H<sub>23</sub>NO<sub>2</sub> [M+Na]<sup>+</sup>: 344.1621, found: 344.1624.

## 5.6 Ruthenium(II)-Catalyzed C–C Arylation of Amides and Acids

### 5.6.1 Experimental Procedures and Analytical Data

#### 1-(4'-Fluoro-[1,1'-biphenyl]-2-yl)-1*H*-indazole (191aa)



**191aa**

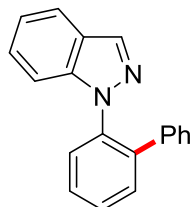
The general procedure **E** was followed using amide **76a** (62.7 mg, 0.20 mmol, 1.0 equiv) and aryl chloride **24a** (52.2 mg, 0.40 mmol, 2.0 equiv). Purification by column chromatography (*n*-hexane/EtOAc: 10/1) yielded **191aa** (45.0 mg, 0.16 mmol, 78%) as a colorless solid.

The general procedure **E** was followed using acid **196a** (47.7 mg, 0.20 mmol, 1.0 equiv) and aryl chloride **24a** (52.2 mg, 0.40 mmol, 2.0 equiv). Purification by column chromatography (*n*-hexane/EtOAc: 10/1) yielded **191aa** (44.4 mg, 0.15 mmol, 77%) as a colorless solid.

**M.p.:** 96–98 °C. **<sup>1</sup>H-NMR** (600 MHz, CDCl<sub>3</sub>):  $\delta$  = 8.11 (d,  $J$  = 1.0 Hz, 1H), 7.70 (ddd,  $J$  = 8.1, 8.1, 1.1 Hz, 1H), 7.59–7.51 (m, 4H), 7.19 (ddd,  $J$  = 8.2, 6.8, 1.1 Hz, 1H), 7.10 (ddd,  $J$  = 7.8, 6.8, 0.9 Hz, 1H), 7.05–6.98 (m, 3H), 6.83–6.76 (m, 2H). **<sup>13</sup>C-NMR** (125 MHz, CDCl<sub>3</sub>):  $\delta$  = 162.0 (d,  $^1J_{C-F}$  = 245.8 Hz, C<sub>q</sub>), 140.1 (C<sub>q</sub>), 138.2 (C<sub>q</sub>), 137.1 (C<sub>q</sub>), 134.9 (CH), 134.7 (d,  $^4J_{C-F}$  = 3.4 Hz, C<sub>q</sub>), 131.1 (CH), 129.8 (d,  $^3J_{C-F}$  = 8.1 Hz, CH), 129.0 (CH), 128.5 (CH), 128.5 (CH), 126.6 (CH), 124.2 (C<sub>q</sub>), 121.0 (CH), 120.8 (CH), 115.2 (d,  $^2J_{C-F}$  =

21.4 Hz, CH), 110.0 (CH). **<sup>19</sup>F-NMR** (471 MHz, CDCl<sub>3</sub>):  $\delta$  = -115.1–(-115.0) (m). **IR** (ATR): 2903, 1714, 1393, 1272, 1055, 937, 878, 756, 687, 623 cm<sup>-1</sup>. **MS** (ESI) *m/z* (relative intensity): 311 (74) [M+Na]<sup>+</sup>, 289 (100) [M+H]<sup>+</sup>. **HR-MS** (ESI): *m/z* calcd for C<sub>19</sub>H<sub>13</sub>FN<sub>2</sub>, [M+H]<sup>+</sup> 289.1136, found 289.1140.

#### 1-([1,1'-Biphenyl]-2-yl)-1*H*-indazole (191ab)

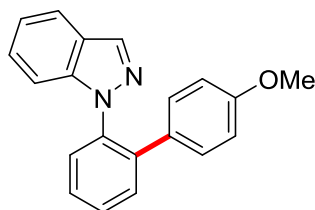


**191ab**

The general procedure **E** was followed using amide **76a** (62.7 mg, 0.20 mmol, 1.0 equiv) and bromobenzene (**24b**) (62.8 mg, 0.40 mmol, 2.0 equiv). Purification by column chromatography (*n*-hexane/EtOAc: 12/1) yielded **191ab** (43.8 mg, 0.16 mmol, 81%) as a colorless oil.

**<sup>1</sup>H-NMR** (600 MHz, CDCl<sub>3</sub>):  $\delta$  = 8.10 (d, *J* = 1.0 Hz, 1H), 7.68 (ddd, *J* = 8.0, 1.1, 1.1 Hz, 1H), 7.62 (dd, *J* = 2.6, 0.8 Hz, 1H), 7.60–7.49 (m, 3H), 7.17 (ddd, *J* = 8.3, 6.9, 1.2 Hz, 1H), 7.12–7.08 (m, 3H), 7.11–6.98 (m, 3H), 7.06 (ddd, *J* = 3.9, 1.2, 1.2 Hz, 1H). **<sup>13</sup>C-NMR** (76 MHz, CDCl<sub>3</sub>):  $\delta$  = 140.2 (C<sub>q</sub>), 139.2 (C<sub>q</sub>), 138.8 (C<sub>q</sub>), 137.2 (C<sub>q</sub>), 134.9 (CH), 131.3 (CH), 129.0 (CH), 128.5 (CH), 128.5 (CH), 128.3 (CH), 128.2 (CH), 127.3 (CH), 126.6 (CH), 124.2 (C<sub>q</sub>), 121.0 (CH), 120.8 (CH), 110.2 (CH). **IR** (ATR): 1484, 1438, 1198, 982, 773, 734, 697, 637, 583, 429 cm<sup>-1</sup>. **MS** (ESI) *m/z* (relative intensity): 293 (2) [M+Na]<sup>+</sup>, 271 (100) [M+H]<sup>+</sup>. **HR-MS** (ESI): *m/z* calcd for C<sub>19</sub>H<sub>14</sub>N<sub>2</sub>, [M+H]<sup>+</sup> 271.1230, found 271.1231. The analytical data correspond with those reported in the literature.<sup>[147d]</sup>

#### 1-(4'-Methoxy-[1,1'-biphenyl]-2-yl)-1*H*-indazole (191ad)



**191ad**

The general procedure **E** was followed using amide **76a** (62.7 mg, 0.20 mmol, 1.0 equiv) and 4-bromoanisole (**24d**) (74.8 mg, 0.40 mmol, 2.0 equiv). Purification by column

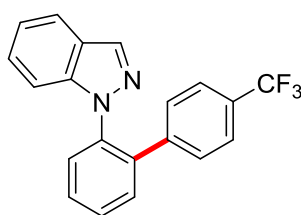
chromatography (*n*-hexane/EtOAc: 8/1) yielded **191ad** (51.1 mg, 0.17 mmol, 85%) as a colorless solid.

The general procedure **E** was followed using amide **76a** (62.7 mg, 0.20 mmol, 1.0 equiv) and 4-chloroanisole (**24d'**) (57.0 mg, 0.40 mmol, 2.0 equiv). Purification by column chromatography (*n*-hexane/EtOAc: 8/1) yielded **191ad** (47.4 mg, 0.16 mmol, 79%) as a colorless solid.

The general procedure **E** was followed using acid **196a** (47.7 mg, 0.20 mmol, 1.0 equiv) and 4-bromoanisole (**24d**) (74.8 mg, 0.40 mmol, 2.0 equiv). Purification by column chromatography (*n*-hexane/EtOAc: 8/1) yielded **191ad** (53.4 mg, 0.18 mmol, 89%) as a colorless solid.

**M.p.:** 107–109 °C. **<sup>1</sup>H-NMR** (400 MHz, CDCl<sub>3</sub>):  $\delta$  = 8.12 (d, *J* = 1.0 Hz, 1H), 7.69 (ddd, *J* = 8.0, 1.0, 1.0 Hz, 1H), 7.59–7.56 (m, 1H), 7.55–7.52 (m, 2H), 7.50–7.46 (m, 1H), 7.18 (ddd, *J* = 8.4, 6.9, 1.1 Hz, 1H), 7.08 (ddd, *J* = 7.9, 6.9, 1.0 Hz, 1H), 7.03 (ddd, *J* = 8.4, 1.0, 1.0 Hz, 1H), 6.96 (d, *J* = 8.9 Hz, 2H), 6.64 (d, *J* = 8.8 Hz, 2H), 3.68 (s, 3H). **<sup>13</sup>C-NMR** (101 MHz, CDCl<sub>3</sub>):  $\delta$  = 158.9 (C<sub>q</sub>), 140.2 (C<sub>q</sub>), 138.9 (C<sub>q</sub>), 137.1 (C<sub>q</sub>), 134.8 (CH), 131.2 (CH), 129.3 (CH), 129.0 (CH), 129.0 (C<sub>q</sub>), 128.5 (CH), 128.0 (CH), 126.6 (CH), 124.2 (C<sub>q</sub>), 121.0 (CH), 120.8 (CH), 113.6 (CH), 110.3 (CH), 55.2 (CH<sub>3</sub>). **IR** (ATR): 1487, 1242, 1177, 1034, 982, 830, 774, 740, 632, 554 cm<sup>-1</sup>. **MS** (ESI) *m/z* (relative intensity): 339 (12) [M+K]<sup>+</sup>, 323 (100) [M+Na]<sup>+</sup>, 301 (66) [M+H]<sup>+</sup>. **HR-MS** (ESI): *m/z* calcd for C<sub>20</sub>H<sub>16</sub>N<sub>2</sub>O, [M+H]<sup>+</sup> 301.1335, found 301.1334.

#### 1-{4'-(Trifluoromethyl)-[1,1'-biphenyl]-2-yl}-1*H*-indazole (**191ae**)



**191ae**

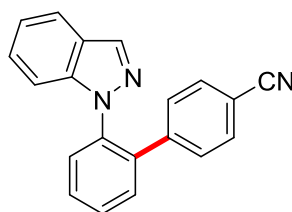
The general procedure **E** was followed using amide **76a** (62.7 mg, 0.20 mmol, 1.0 equiv) and aryl bromide **24e** (90.1 mg, 0.40 mmol, 2.0 equiv). Purification by column chromatography (*n*-hexane/EtOAc: 15/1) yielded **191ae** (59.6 mg, 0.18 mmol, 88%) as a colorless solid.

**M.p.:** 101–103 °C. **<sup>1</sup>H-NMR** (300 MHz, CDCl<sub>3</sub>):  $\delta$  = 8.08 (d, *J* = 1.0 Hz, 1H), 7.71 (ddd, *J* = 8.0, 1.1, 1.1 Hz, 1H), 7.62–7.58 (m, 4H), 7.37 (d, *J* = 8.0 Hz, 2H), 7.23 (ddd, *J* = 8.2,



7.0, 1.2 Hz, 1H), 7.15 (d,  $J = 8.1$  Hz, 2H), 7.13–7.11 (m, 1H), 7.10–7.07 (m, 1H).  **$^{13}\text{C}$ -NMR** (126 MHz,  $\text{CDCl}_3$ ):  $\delta = 142.4$  ( $\text{C}_q$ ), 140.2 ( $\text{C}_q$ ), 137.8 ( $\text{C}_q$ ), 137.2 ( $\text{C}_q$ ), 135.1 (CH), 132.0 (CH), 129.3 (q,  $^2J_{\text{C-F}} = 32.4$  Hz,  $\text{C}_q$ ), 129.2 (CH), 129.1 (CH), 128.5 (CH), 128.4 (CH), 126.9 (CH), 125.2 (q,  $^3J_{\text{C-F}} = 3.6$  Hz, CH), 124.3 ( $\text{C}_q$ ), 124.1 (q,  $^1J_{\text{C-F}} = 273.2$  Hz,  $\text{C}_q$ ), 121.2 (CH), 121.0 (CH), 109.9 (CH).  **$^{19}\text{F}$ -NMR** (282 MHz,  $\text{CDCl}_3$ ):  $\delta = -62.61$ . **IR** (ATR): 1322, 1118, 1067, 1019, 840, 772, 762, 737, 608, 427  $\text{cm}^{-1}$ . **MS** (ESI)  $m/z$  (relative intensity): 361 (2)  $[\text{M}+\text{Na}]^+$ , 339 (100)  $[\text{M}+\text{H}]^+$ . **HR-MS** (ESI):  $m/z$  calcd for  $\text{C}_{20}\text{H}_{13}\text{F}_3\text{N}_2$ ,  $[\text{M}+\text{H}]^+$  339.1104, found 339.1103.

### 2'-(1*H*-Indazol-1-yl)-[1,1'-biphenyl]-4-carbonitrile (**191af**)

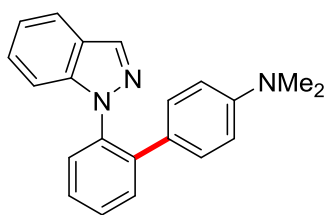


**191af**

The general procedure **E** was followed using amide **76a** (62.7 mg, 0.20 mmol, 1.0 equiv) and aryl bromide **24f** (72.8 mg, 0.40 mmol, 2.0 equiv),  $[\text{RuCl}_2(p\text{-cymene})]_2$  (6.1 mg, 10  $\mu\text{mol}$ , 5.0 mol %) and  $\text{MesCO}_2\text{H}$  (6.6 mg, 40 mol, 20 mol %). Purification by column chromatography (*n*-hexane/EtOAc: 10/1) yielded **191af** (37.2 mg, 0.13 mmol, 63%) as a yellow oil.

**$^1\text{H}$ -NMR** (300 MHz,  $\text{CDCl}_3$ ):  $\delta = 8.07$  (d,  $J = 1.0$  Hz, 1H), 7.71 (ddd,  $J = 8.0, 1.0, 1.0$  Hz, 1H), 7.63–7.56 (m, 4H), 7.39 (d,  $J = 8.7$  Hz, 2H), 7.22 (ddd,  $J = 8.3, 6.9, 1.2$  Hz, 1H), 7.15–7.12 (m, 2H), 7.11–7.09 (m, 1H), 7.06 (ddd,  $J = 8.4, 1.0, 1.0$  Hz, 1H).  **$^{13}\text{C}$ -NMR** (75 MHz,  $\text{CDCl}_3$ ):  $\delta = 143.7$  ( $\text{C}_q$ ), 140.2 ( $\text{C}_q$ ), 137.4 ( $\text{C}_q$ ), 137.2 ( $\text{C}_q$ ), 135.3 (CH), 132.1 (CH), 131.1 (CH), 129.7 (CH), 129.3 (CH), 129.0 (CH), 128.5 (CH), 127.1 (CH), 124.4 ( $\text{C}_q$ ), 121.4 (CH), 121.1 (CH), 118.8 ( $\text{C}_q$ ), 110.1 ( $\text{C}_q$ ), 109.8 (CH). **IR** (ATR): 2957, 2923, 2321, 1487, 1260, 1083, 1015, 797, 777, 741  $\text{cm}^{-1}$ . **MS** (ESI)  $m/z$  (relative intensity): 318 (44)  $[\text{M}+\text{Na}]^+$ , 296 (100)  $[\text{M}+\text{H}]^+$ . **HR-MS** (ESI):  $m/z$  calcd for  $\text{C}_{20}\text{H}_{13}\text{N}_3$ ,  $[\text{M}+\text{H}]^+$  296.1182, found 296.1184.

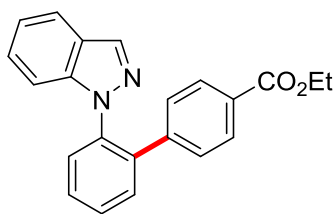
### 2'-(1*H*-Indazol-1-yl)-*N,N*-dimethyl-[1,1'-biphenyl]-4-amine (**191ag**)

**191ag**

The general procedure **E** was followed using amide **76a** (62.7 mg, 0.20 mmol, 1.0 equiv) and aryl bromide **24g** (80.0 mg, 0.40 mmol, 2.0 equiv). Purification by column chromatography (*n*-hexane/EtOAc: 8/1) yielded **191ag** (37.0 mg, 0.12 mmol, 59%) as a colorless solid.

**M.p.:** 118–120 °C. **<sup>1</sup>H-NMR** (300 MHz, CDCl<sub>3</sub>):  $\delta$  = 8.13 (d, *J* = 0.9 Hz, 1H), 7.70 (ddd, *J* = 8.0, 1.1, 1.1 Hz, 1H), 7.58 (ddd, *J* = 7.3, 1.7, 0.8 Hz, 1H), 7.54–7.47 (m, 2H), 7.46–7.39 (m, 1H), 7.18 (ddd, *J* = 8.1, 7.1, 1.2 Hz, 1H), 7.10–7.04 (m, 2H), 6.91 (d, *J* = 8.9 Hz, 2H), 6.46 (d, *J* = 8.8 Hz, 2H), 2.83 (s, 6H). **<sup>13</sup>C-NMR** (75 MHz, CDCl<sub>3</sub>):  $\delta$  = 149.6 (C<sub>q</sub>), 140.2 (C<sub>q</sub>), 139.4 (C<sub>q</sub>), 136.9 (C<sub>q</sub>), 134.7 (CH), 131.0 (CH), 129.0 (CH), 128.9 (CH), 128.6 (CH), 127.3 (CH), 126.6 (C<sub>q</sub>), 126.5 (CH), 124.2 (C<sub>q</sub>), 120.8 (CH), 120.7 (CH), 112.3 (CH), 110.5 (CH), 40.5 (CH<sub>3</sub>). **IR** (ATR): 1611, 1489, 1359, 1195, 811, 776, 764, 754, 429, 386 cm<sup>-1</sup>. **MS** (ESI) *m/z* (relative intensity): 649 (11) [2M+Na]<sup>+</sup>, 336 (100) [M+Na]<sup>+</sup>, 314 (74) [M+H]<sup>+</sup>. **HR-MS** (ESI): *m/z* calcd for C<sub>21</sub>H<sub>19</sub>N<sub>3</sub>, [M+H]<sup>+</sup> 314.1652, found 314.1652.

#### Ethyl 2'-(1*H*-indazol-1-yl)-[1,1'-biphenyl]-4-carboxylate (**191ah**)

**191ah**

The general procedure **E** was followed using amide **76a** (62.7 mg, 0.20 mmol, 1.0 equiv) and aryl chloride **24h** (73.9 mg, 0.40 mmol, 2.0 equiv). Purification by column chromatography (*n*-hexane/EtOAc: 8/1) yielded **191ah** (55.5 mg, 0.16 mmol, 81%) as colorless crystals.

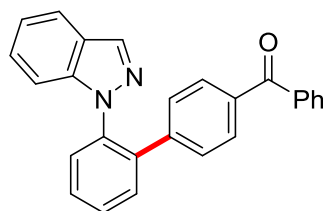
The general procedure **E** was followed using acid **196a** (47.7 mg, 0.20 mmol, 1.0 equiv) and aryl chloride **24h** (73.9 mg, 0.40 mmol, 2.0 equiv). Purification by column

chromatography (*n*-hexane/EtOAc: 8/1) yielded **191ah** (54.1 mg, 0.16 mmol, 79%) as colorless crystals.

The general procedure **E** was followed using alcohol **116a** (42.9 mg, 0.20 mmol, 1.0 equiv) and aryl chloride **24h** (73.9 mg, 0.40 mmol, 2.0 equiv). Purification by column chromatography (*n*-hexane/EtOAc: 8/1) yielded **191ah** (65.0 mg, 0.19 mmol, 95%) as colorless crystals.

**M.p.:** 123–125 °C. **<sup>1</sup>H-NMR** (400 MHz, CDCl<sub>3</sub>):  $\delta$  = 8.08 (d, *J* = 0.9 Hz, 1H), 7.79 (d, *J* = 8.7 Hz, 2H), 7.68 (ddd, *J* = 8.1, 1.0, 1.0 Hz, 1H), 7.62–7.55 (m, 4H), 7.19 (ddd, *J* = 8.2, 6.9, 1.2 Hz, 1H), 7.12–7.08 (m, 1H), 7.10 (d, *J* = 8.7 Hz, 2H), 7.06 (ddd, *J* = 8.6, 1.0, 1.0 Hz, 1H), 4.30 (q, *J* = 7.1 Hz, 2H), 1.33 (t, *J* = 7.1 Hz, 3H). **<sup>13</sup>C-NMR** (101 MHz, CDCl<sub>3</sub>):  $\delta$  = 166.4 (C<sub>q</sub>), 143.4 (C<sub>q</sub>), 140.2 (C<sub>q</sub>), 138.2 (C<sub>q</sub>), 137.2 (C<sub>q</sub>), 135.1 (CH), 131.2 (CH), 129.6 (CH), 129.2 (C<sub>q</sub>), 129.2 (CH), 129.1 (CH), 128.3 (CH), 128.2 (CH), 126.9 (CH), 124.3 (C<sub>q</sub>), 121.2 (CH), 121.0 (CH), 110.0 (CH), 61.0 (CH<sub>2</sub>), 14.4 (CH<sub>3</sub>). **IR** (ATR): 1709, 1269, 1198, 1024, 855, 774, 739, 703, 430 cm<sup>-1</sup>. **MS** (ESI) *m/z* (relative intensity): 707 (39) [2M+Na]<sup>+</sup>, 381 (4) [M+K]<sup>+</sup>, 365 (100) [M+Na]<sup>+</sup>, 343 (42) [M+H]<sup>+</sup>. **HR-MS** (ESI): *m/z* calcd for C<sub>22</sub>H<sub>18</sub>N<sub>2</sub>O<sub>2</sub>, [M+H]<sup>+</sup> 343.1441, found 343.1438.

**{2'-(1*H*-Indazol-1-yl)-[1,1'-biphenyl]-4-yl}(phenyl)methanone (191ai)**



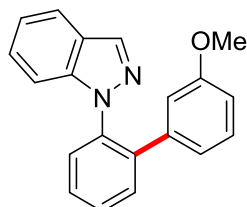
**191ai**

The general procedure **E** was followed using amide **76a** (62.7 mg, 0.20 mmol, 1.0 equiv) and 4-bromobenzophenone (**24i**) (104 mg, 0.40 mmol, 2.0 equiv). Purification by column chromatography (*n*-hexane/EtOAc: 15/1) yielded **191ai** (59.2 mg, 0.16 mmol, 79%) as colorless crystals.

**M.p.:** 141–143 °C. **<sup>1</sup>H-NMR** (400 MHz, CDCl<sub>3</sub>):  $\delta$  = 8.10 (d, *J* = 1.0 Hz, 1H), 7.70 (ddd, *J* = 8.0, 1.0, 1.0 Hz, 1H), 7.66–7.58 (m, 6H), 7.57–7.53 (m, 1H), 7.53 (d, *J* = 8.6 Hz, 2H), 7.45–7.40 (m, 2H), 7.20 (dd, *J* = 7.7, 1.2 Hz, 1H), 7.13 (d, *J* = 8.6 Hz, 2H), 7.12–7.08 (m, 1H), 7.05 (ddd, *J* = 8.4, 0.9, 0.9 Hz, 1H). **<sup>13</sup>C-NMR** (101 MHz, CDCl<sub>3</sub>):  $\delta$  = 196.4 (C<sub>q</sub>), 143.0 (C<sub>q</sub>), 140.2 (C<sub>q</sub>), 138.1 (C<sub>q</sub>), 137.7 (C<sub>q</sub>), 137.3 (C<sub>q</sub>), 136.2 (C<sub>q</sub>), 135.2 (CH), 132.4 (CH), 131.1 (CH), 130.1 (CH), 130.0 (CH), 129.3 (CH), 129.2 (CH), 128.5 (CH), 128.3 (CH), 128.1 (CH), 126.8 (CH), 124.4 (C<sub>q</sub>), 121.2 (CH), 121.0 (CH), 110.1 (CH). **IR** (ATR):

2922, 1497, 1260, 1068, 1006, 982, 837, 800, 742, 696  $\text{cm}^{-1}$ . **MS** (ESI)  $m/z$  (relative intensity): 749 (4)  $[2\text{M}+\text{H}]^+$ , 397 (5)  $[\text{M}+\text{Na}]^+$ , 375 (100)  $[\text{M}+\text{H}]^+$ . **HR-MS** (ESI):  $m/z$  calcd for  $\text{C}_{26}\text{H}_{18}\text{N}_2\text{O}$ ,  $[\text{M}+\text{H}]^+$  375.1492, found 375.1496.

### 1-(3'-Methoxy-[1,1'-biphenyl]-2-yl)-1*H*-indazole (191al)

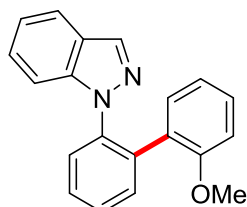


191al

The general procedure **E** was followed using amide **76a** (62.7 mg, 0.20 mmol, 1.0 equiv) and 3-chloroanisole **24l** (57.1 mg, 0.40 mmol, 2.0 equiv). Purification by column chromatography (*n*-hexane/EtOAc: 10/1) yielded **191al** (41.4 mg, 0.14 mmol, 69%) as a colorless oil.

**<sup>1</sup>H-NMR** (300 MHz,  $\text{CDCl}_3$ ):  $\delta$  = 8.11 (d,  $J$  = 1.0 Hz, 1H), 7.68 (ddd,  $J$  = 8.0, 1.1, 1.1 Hz, 1H), 7.64–7.51 (m, 4H), 7.18 (ddd,  $J$  = 8.1, 7.0, 1.2 Hz, 1H), 7.09 (dd,  $J$  = 6.9, 1.1 Hz, 1H), 7.08 – 7.02 (m, 2H), 6.71 (ddd,  $J$  = 7.6, 1.6, 1.0 Hz, 1H), 6.65 (ddd,  $J$  = 8.3, 2.6, 1.0 Hz, 1H), 6.48 (dd,  $J$  = 2.6, 1.6 Hz, 1H), 3.46 (s, 3H). **<sup>13</sup>C-NMR** (75 MHz,  $\text{CDCl}_3$ ):  $\delta$  = 159.0 ( $\text{C}_q$ ), 140.1 ( $\text{C}_q$ ), 139.8 ( $\text{C}_q$ ), 139.0 ( $\text{C}_q$ ), 136.9 ( $\text{C}_q$ ), 134.5 (CH), 130.9 (CH), 129.1 (CH), 128.9 (CH), 128.4 (CH), 128.3 (CH), 126.4 (CH), 124.0 ( $\text{C}_q$ ), 121.0 (CH), 120.5 (CH), 120.5 (CH), 113.6 (CH), 112.8 (CH), 110.0 (CH), 54.9 ( $\text{CH}_3$ ). **IR** (ATR): 1482, 1209, 1020, 982, 848, 776, 757, 733, 697, 638  $\text{cm}^{-1}$ . **MS** (ESI)  $m/z$  (relative intensity): 623 (8)  $[2\text{M}+\text{Na}]^+$ , 323 (59)  $[\text{M}+\text{Na}]^+$ , 301 (100)  $[\text{M}+\text{H}]^+$ , 284 (6)  $[\text{M}-\text{CH}_2]^+$ . **HR-MS** (ESI):  $m/z$  calcd for  $\text{C}_{20}\text{H}_{16}\text{N}_2\text{O}$ ,  $[\text{M}+\text{H}]^+$  301.1335, found 301.1339.

### 1-(2'-Methoxy-[1,1'-biphenyl]-2-yl)-1*H*-indazole (191am)



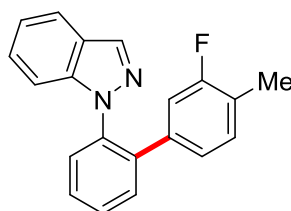
191am

The general procedure **E** was followed using amide **76a** (62.7 mg, 0.20 mmol, 1.0 equiv) and 2-bromoanisole **24m** (74.8 mg, 0.40 mmol, 2.0 equiv). Purification by column

chromatography (*n*-hexane/EtOAc: 10/1) yielded **191am** (45.1 mg, 0.15 mmol, 75%) as a colorless oil.

**<sup>1</sup>H-NMR** (400 MHz, CDCl<sub>3</sub>):  $\delta$  = 7.96 (d, *J* = 0.9 Hz, 1H), 7.65 (ddd, *J* = 8.1, 1.0, 1.0 Hz, 1H), 7.61–7.51 (m, 4H), 7.27 (ddd, *J* = 8.5, 1.0, 1.0 Hz, 1H), 7.21 (ddd, *J* = 8.5, 6.7, 1.1 Hz, 1H), 7.14–7.09 (m, 2H), 7.07 (ddd, *J* = 7.9, 6.7, 1.0 Hz, 1H), 6.81 (ddd, *J* = 7.4, 1.1, 1.1 Hz, 1H), 6.59 (dd, *J* = 8.7, 1.1 Hz, 1H), 3.17 (s, 3H). **<sup>13</sup>C-NMR** (101 MHz, CDCl<sub>3</sub>):  $\delta$  = 156.2 (C<sub>q</sub>), 140.0 (C<sub>q</sub>), 138.3 (C<sub>q</sub>), 136.0 (C<sub>q</sub>), 134.2 (CH), 132.5 (CH), 131.0 (CH), 128.9 (CH), 128.3 (CH), 128.2 (CH), 128.0 (C<sub>q</sub>), 127.2 (CH), 126.2 (CH), 124.0 (C<sub>q</sub>), 120.8 (CH), 120.6 (CH), 120.5 (CH), 110.5 (CH), 110.2 (CH), 54.9 (CH<sub>3</sub>). **IR** (ATR): 1506, 1463, 1251, 1005, 744, 729, 637, 429 cm<sup>-1</sup>. **MS** (ESI) *m/z* (relative intensity): 623 (17) [2M+Na]<sup>+</sup>, 323 (100) [M+Na]<sup>+</sup>, 301 (71) [M+H]<sup>+</sup>. **HR-MS** (ESI): *m/z* calcd for C<sub>20</sub>H<sub>16</sub>N<sub>2</sub>O, [M+H]<sup>+</sup> 301.1335, found 301.1337.

#### 1-(3'-Fluoro-4'-methyl-[1,1'-biphenyl]-2-yl)-1*H*-indazole (**191an**)



**191an**

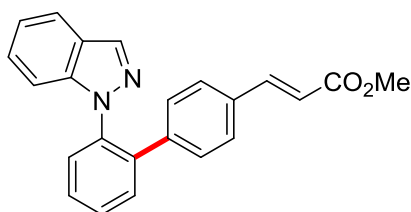
The general procedure **E** was followed using amide **76a** (62.7 mg, 0.20 mmol, 1.0 equiv) and aryl chloride **24n** (57.9 mg, 0.40 mmol, 2.0 equiv). Purification by column chromatography (*n*-hexane/EtOAc: 9/1) yielded **191an** (40.0 mg, 0.13 mmol, 66%) as a colorless oil.

The general procedure **E** was followed using acid **196a** (47.7 mg, 0.20 mmol, 1.0 equiv) and aryl chloride **24n** (57.9 mg, 0.40 mmol, 2.0 equiv). Purification by column chromatography (*n*-hexane/EtOAc: 9/1) yielded **191an** (42.9 mg, 0.13 mmol, 71%) as a colorless oil.

**<sup>1</sup>H-NMR** (300 MHz, CDCl<sub>3</sub>):  $\delta$  = 7.98 (d, *J* = 0.9 Hz, 1H), 7.65 (ddd, *J* = 8.1, 1.0, 1.0 Hz, 1H), 7.60–7.51 (m, 3H), 7.49–7.38 (m, 1H), 7.23 (ddd, *J* = 8.5, 6.6, 1.2 Hz, 1H), 7.16 (ddd, *J* = 8.5, 1.0, 1.0 Hz, 1H), 7.09 (ddd, *J* = 7.9, 6.6, 1.2 Hz, 1H), 6.99–6.85 (m, 1H), 6.84–6.75 (m, 2H), 1.91 (d, *J* = 2.6 Hz, 3H). **<sup>13</sup>C-NMR** (75 MHz, CDCl<sub>3</sub>):  $\delta$  = 162.2 (d, <sup>1</sup>*J*<sub>C-F</sub> = 243.6 Hz, C<sub>q</sub>), 140.8 (d, <sup>3</sup>*J*<sub>C-F</sub> = 4.8 Hz, C<sub>q</sub>), 140.1 (C<sub>q</sub>), 138.1 (C<sub>q</sub>), 137.8 (d, <sup>4</sup>*J*<sub>C-F</sub> = 2.8 Hz, C<sub>q</sub>), 134.9 (CH), 132.0 (CH), 128.8 (CH), 128.4 (CH), 127.7 (CH), 126.6 (CH), 126.2 (d, <sup>3</sup>*J*<sub>C-F</sub> = 9.1 Hz, CH), 125.4 (d, <sup>4</sup>*J*<sub>C-F</sub> = 3.2 Hz, CH), 124.2 (C<sub>q</sub>), 123.5 (d, <sup>2</sup>*J*<sub>C-F</sub> =

17.2 Hz, C<sub>q</sub>), 121.1 (CH), 121.0 (CH), 113.9 (d,  $^2J_{\text{C-F}} = 22.9$  Hz, CH), 110.0 (CH), 12.3 (d,  $^3J_{\text{C-F}} = 4.9$  Hz, CH<sub>3</sub>). **<sup>19</sup>F-NMR** (282 MHz, CDCl<sub>3</sub>):  $\delta = -116.0$ . IR (ATR): 1501, 1415, 1199, 1007, 860, 771, 741, 712, 692, 631 cm<sup>-1</sup>. **MS** (ESI)  $m/z$  (relative intensity): 627 (11) [2M+Na]<sup>+</sup>, 235 (73) [M+Na]<sup>+</sup>, 303 (100) [M+H]<sup>+</sup>, 286 (4) [M-CH<sub>2</sub>]<sup>+</sup>. **HR-MS** (ESI):  $m/z$  calcd for C<sub>20</sub>H<sub>15</sub>N<sub>2</sub>F, [M+H]<sup>+</sup> 303.1292, found 303.1293.

**Methyl (E)-3-{2'-(1*H*-indazol-1-yl)-[1,1'-biphenyl]-4-yl}acrylate (191ap)**

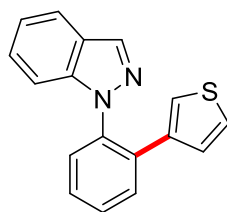


**191ap**

The general procedure **E** was followed using amide **76a** (62.7 mg, 0.20 mmol, 1.0 equiv) and aryl bromide **24p** (96.4 mg, 0.40 mmol, 2.0 equiv). Purification by column chromatography (*n*-hexane/EtOAc: 6/1) yielded **191ap** (49.6 mg, 0.14 mmol, 70%) as a colorless solid.

**M.p.:** 161–163 °C. **<sup>1</sup>H-NMR** (400 MHz, CDCl<sub>3</sub>):  $\delta = 8.09$  (d,  $J = 1.0$  Hz, 1H), 7.69 (ddd,  $J = 8.0, 1.0, 1.0$  Hz, 1H), 7.61–7.51 (m, 5H), 7.26 (d,  $J = 8.1$  Hz, 2H), 7.19 (ddd,  $J = 8.2, 6.9, 1.1$  Hz, 1H), 7.11–7.08 (m, 1H), 7.07 (ddd,  $J = 2.9, 1.0, 1.0$  Hz, 1H), 7.04 (d,  $J = 8.3$  Hz, 2H), 6.30 (d,  $J = 16.0$  Hz, 1H), 3.76 (s, 3H). **<sup>13</sup>C-NMR** (101 MHz, CDCl<sub>3</sub>):  $\delta = 167.4$  (C<sub>q</sub>), 144.3 (CH), 140.9 (C<sub>q</sub>), 140.2 (C<sub>q</sub>), 138.3 (C<sub>q</sub>), 137.2 (C<sub>q</sub>), 135.0 (CH), 133.2 (C<sub>q</sub>), 131.1 (CH), 129.1 (CH), 128.9 (CH), 128.7 (CH), 128.4 (CH), 128.1 (CH), 126.8 (CH), 124.3 (C<sub>q</sub>), 121.2 (CH), 120.9 (CH), 117.8 (CH), 110.0 (CH), 51.7 (CH<sub>3</sub>). IR (ATR): 1712, 1633, 1169, 982, 830, 775, 750, 462, 425, 406 cm<sup>-1</sup>. **MS** (ESI)  $m/z$  (relative intensity): 731 (12) [2M+Na]<sup>+</sup>, 393 (2) [M+K]<sup>+</sup>, 377 (25) [M+Na]<sup>+</sup>, 355 (100) [M+H]<sup>+</sup>. **HR-MS** (ESI):  $m/z$  calcd for C<sub>23</sub>H<sub>18</sub>N<sub>2</sub>O<sub>2</sub>, [M+H]<sup>+</sup> 355.1441, found 355.1449.

**1-[2-(Thiophen-3-yl)phenyl]-1*H*-indazole (191aq)**



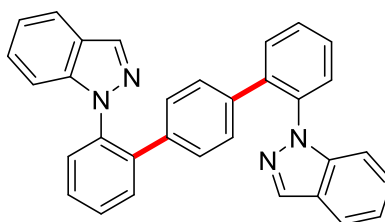
**191aq**

The general procedure **E** was followed using amide **76a** (62.7 mg, 0.20 mmol, 1.0 equiv) and 3-bromothiophene (**24q**) (32.6 mg, 0.40 mmol, 2.0 equiv). Purification by column chromatography (*n*-hexane/EtOAc: 15/1 → 7/1) yielded **191aq** (33.8 mg, 0.12 mmol, 61%) as a colorless oil.

The general procedure **E** was followed using acid **196a** (47.7 mg, 0.20 mmol, 1.0 equiv) and 3-bromothiophene (**24q**) (32.6 mg, 0.40 mmol, 2.0 equiv). Purification by column chromatography (*n*-hexane/EtOAc: 15/1 → 7/1) yielded **191aq** (37.6 mg, 0.14 mmol, 68%) as a colorless oil.

**<sup>1</sup>H-NMR** (400 MHz, CDCl<sub>3</sub>): δ = 8.15 (d, *J* = 1.0 Hz, 1H), 7.71 (ddd, *J* = 8.0, 1.0, 1.0 Hz, 1H), 7.69–7.62 (m, 1H), 7.54–7.49 (m, 2H), 7.47 (ddd, *J* = 8.2, 6.4, 1.7 Hz, 1H), 7.17 (ddd, *J* = 8.3, 6.9, 1.2 Hz, 1H), 7.09 (ddd, *J* = 7.9, 6.9, 1.0 Hz, 1H), 7.01–6.95 (m, 2H), 6.89 (dd, *J* = 3.0, 1.3 Hz, 1H), 6.54 (dd, *J* = 5.0, 1.3 Hz, 1H). **<sup>13</sup>C-NMR** (101 MHz, CDCl<sub>3</sub>): δ = 140.3 (C<sub>q</sub>), 138.7 (C<sub>q</sub>), 137.0 (C<sub>q</sub>), 135.0 (CH), 134.2 (C<sub>q</sub>), 130.5 (CH), 129.2 (CH), 128.8 (CH), 128.4 (CH), 127.4 (CH), 126.7 (CH), 125.4 (CH), 124.3 (C<sub>q</sub>), 122.9 (CH), 121.1 (CH), 120.9 (CH), 110.2 (CH). **IR** (ATR): 2954, 2922, 2852, 1498, 1463, 1197, 983, 738, 633, 429 cm<sup>-1</sup>. **MS** (ESI) *m/z* (relative intensity): 572 (6) [2M+Na]<sup>+</sup>, 299 (53) [M+Na]<sup>+</sup>, 277 (100) [M+H]<sup>+</sup>. **HR-MS** (ESI): *m/z* calcd for C<sub>17</sub>H<sub>12</sub>N<sub>2</sub>S, [M+H]<sup>+</sup> 277.0794, found 277.0798.

### 2,2''-Di(1*H*-indazol-1-yl)-1,1':4',1''-terphenyl (**191ar**)



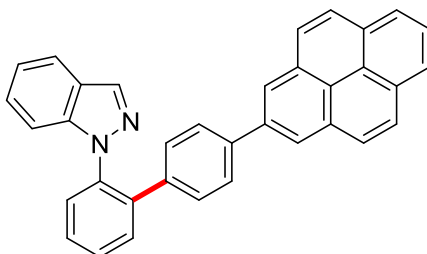
**191ar**

The general procedure **E** was followed using amide **76a** (62.7 mg, 0.20 mmol, 2.0 equiv) and 1,4-dibromobenzene (**24r**) (23.6 mg, 0.10 mmol, 1.0 equiv). Purification by column chromatography (*n*-hexane/EtOAc: 8/1) yielded **191ar** (37.7 mg, 0.08 mmol, 80%) as a colorless solid.

**M.p.:** 191–193 °C. **<sup>1</sup>H-NMR** (300 MHz, CDCl<sub>3</sub>): δ = 7.93 (d, *J* = 1.0 Hz, 2H), 7.74–7.61 (m, 2H), 7.55–7.39 (m, 8H), 7.18–7.03 (m, 4H), 7.03–6.90 (m, 2H), 6.78 (s, 4H). **<sup>13</sup>C-NMR** (76 MHz, CDCl<sub>3</sub>): δ = 140.2 (C<sub>q</sub>), 138.8 (C<sub>q</sub>), 137.7 (C<sub>q</sub>), 137.1 (C<sub>q</sub>), 134.8 (CH), 131.3 (CH), 128.9 (CH), 128.4 (CH), 128.3 (CH), 128.1 (CH), 126.8 (CH), 124.2 (C<sub>q</sub>), 121.0 (CH), 120.8 (CH), 110.1 (CH). **IR** (ATR): 1458, 1999, 983, 852, 840, 775, 741,

633, 576, 434  $\text{cm}^{-1}$ . **MS** (ESI)  $m/z$  (relative intensity): 947 (22)  $[2\text{M}+\text{Na}]^+$ , 925 (15)  $[2\text{M}+\text{H}]^+$ , 485 (100)  $[\text{M}+\text{Na}]^+$ , 463 (78)  $[\text{M}+\text{H}]^+$ . **HR-MS** (ESI):  $m/z$  calcd for  $\text{C}_{32}\text{H}_{22}\text{N}_4$ ,  $[\text{M}+\text{H}]^+$  463.1917, found 463.1916.

### 1-{4'-(Pyren-2-yl)-[1,1'-biphenyl]-2-yl}-1*H*-indazole (191as)



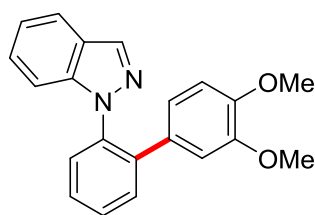
**191as**

The general procedure **E** was followed using amide **76a** (62.7 mg, 0.20 mmol, 1.0 equiv) and aryl bromide **24s** (143 mg, 0.40 mmol, 2.0 equiv). Purification by column chromatography (*n*-hexane/EtOAc: 15/1  $\rightarrow$  8/1) yielded **191as** (65.8 mg, 0.14 mmol, 70%) as a red solid.

**M.p.:** 219–221  $^{\circ}\text{C}$ .  **$^1\text{H-NMR}$**  (600 MHz,  $\text{CDCl}_3$ ):  $\delta$  = 8.22 (d,  $J$  = 1.0 Hz, 1H), 8.18 (dd,  $J$  = 7.6, 1.0 Hz, 1H), 8.17–8.14 (m, 2H), 8.07 (d,  $J$  = 1.4 Hz, 2H), 8.01 (dd,  $J$  = 7.6, 7.6 Hz, 1H), 7.96 (d,  $J$  = 9.3 Hz, 1H), 7.85 (d,  $J$  = 7.9 Hz, 1H), 7.79–7.76 (m, 2H), 7.74 (d,  $J$  = 9.2 Hz, 1H), 7.70 (dd,  $J$  = 7.7, 1.4 Hz, 1H), 7.64 (ddd,  $J$  = 7.4, 7.4 1.6 Hz, 1H), 7.60 (ddd,  $J$  = 7.5, 7.5, 1.6 Hz, 1H), 7.34 (d,  $J$  = 8.3 Hz, 2H), 7.24 (ddd,  $J$  = 8.6, 6.6, 1.1 Hz, 1H), 7.20 (d,  $J$  = 8.5 Hz, 2H), 7.17 (ddd,  $J$  = 8.2, 6.8, 0.8 Hz, 1H), 7.10 (ddd,  $J$  = 8.4, 0.9, 0.9 Hz, 1H).  **$^{13}\text{C-NMR}$**  (126 MHz,  $\text{CDCl}_3$ ):  $\delta$  = 140.1 (Cq), 138.7 (Cq), 137.7 (Cq), 137.5 (Cq), 137.3 (Cq), 135.1 (CH), 131.6 (Cq), 131.1 (CH), 131.0 (Cq), 130.6 (Cq), 130.5 (CH), 129.1 (CH), 128.6 (CH), 128.5 (Cq), 128.2 (CH), 127.5 (CH), 127.4 (CH), 126.6 (CH), 126.1 (CH), 125.3 (CH), 125.0 (Cq), 124.9 (Cq), 124.9 (CH), 124.6 (CH), 121.0 (CH), 120.9 (CH), 110.5 (CH). **IR** (ATR): 1496, 1464, 1416, 1199, 905, 839, 773, 763, 748, 723  $\text{cm}^{-1}$ . **MS** (ESI)  $m/z$  (relative intensity): 963 (12)  $[2\text{M}+\text{Na}]^+$ , 941 (24)  $[2\text{M}+\text{H}]^+$ , 493 (11)  $[\text{M}+\text{Na}]^+$ , 471 (100)  $[\text{M}+\text{H}]^+$ . **HR-MS** (ESI):  $m/z$  calcd for  $\text{C}_{35}\text{H}_{22}\text{N}_2$ ,  $[\text{M}+\text{H}]^+$  471.1856, found 471.1850.

### 1-{3',4'-Dimethoxy-[1,1'-biphenyl]-2-yl}-1*H*-indazole (191av)



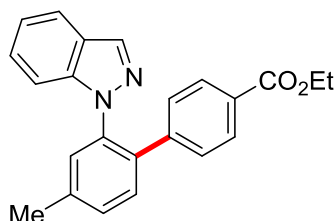
**191av**

The general procedure **E** was followed using amide **76a** (62.7 mg, 0.20 mmol, 1.0 equiv) and aryl bromide **24v** (86.8 mg, 0.40 mmol, 2.0 equiv). Purification by column chromatography (*n*-hexane/EtOAc: 6/1 → 2/1) yielded **191av** (17.8 mg, 0.05 mmol, 27%) as a colorless solid.

The general procedure **E** was followed using acid **196a** (47.7 mg, 0.20 mmol, 1.0 equiv) and aryl chloride **24v** (69.0 mg, 0.40 mmol, 2.0 equiv). Purification by column chromatography (*n*-hexane/EtOAc: 6/1 → 2/1) yielded **191av** (37.0 mg, 0.11 mmol, 56%) as a colorless solid.

**M.p.:** 110–112 °C. **<sup>1</sup>H-NMR** (400 MHz, CDCl<sub>3</sub>): δ = 8.11 (d, *J* = 1.0 Hz, 1H), 7.68 (ddd, *J* = 8.1, 8.1, 1.0 Hz, 1H), 7.62–7.59 (m, 1H), 7.57–7.52 (m, 2H), 7.52–7.46 (m, 1H), 7.17 (ddd, *J* = 8.4, 6.9, 1.1 Hz, 1H), 7.07 (ddd, *J* = 7.9, 6.9, 1.0, 1H), 7.04 (ddd, *J* = 8.4, 1.0, 1.0 Hz, 1H), 6.82 (dd, *J* = 8.3, 2.1, 1H), 6.71 (d, *J* = 8.3 Hz, 1H), 6.28 (d, *J* = 2.1 Hz, 1H), 3.77 (s, 3H), 3.36 (s, 3H). **<sup>13</sup>C-NMR** (101 MHz, CDCl<sub>3</sub>): δ = 148.4 (C<sub>q</sub>), 148.4 (C<sub>q</sub>), 140.5 (C<sub>q</sub>), 139.2 (C<sub>q</sub>), 137.0 (C<sub>q</sub>), 134.7 (CH), 131.4 (C<sub>q</sub>), 131.0 (CH), 129.2 (CH), 128.8 (CH), 128.1 (CH), 126.7 (CH), 124.2 (C<sub>q</sub>), 121.1 (CH), 120.8 (CH), 120.7 (CH), 111.1 (CH), 111.1 (CH), 110.1 (CH), 55.8 (CH<sub>3</sub>), 55.4 (CH<sub>3</sub>). **IR** (ATR): 2833, 1519, 1486, 1461, 1244, 1188, 858, 782, 745, 635 cm<sup>-1</sup>. **MS** (ESI) *m/z* (relative intensity): 353 (100) [M+Na]<sup>+</sup>, 331 (54) [M+H]<sup>+</sup>. **HR-MS** (ESI): *m/z* calcd for C<sub>21</sub>H<sub>18</sub>N<sub>2</sub>O<sub>2</sub>, [M+Na]<sup>+</sup> 353.1260, found 353.1260.

#### Ethyl 2'-(1*H*-indazol-1-yl)-4'-methyl-[1,1'-biphenyl]-4-carboxylate (**191bh**)

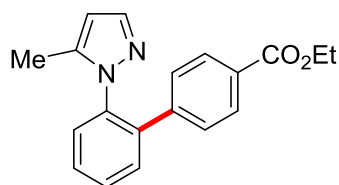
**191bh**

The general procedure **E** was followed using amide **76b** (65.5 mg, 0.20 mmol, 1.0 equiv) and aryl chloride **24h** (73.8 mg, 0.40 mmol, 2.0 equiv). Purification by column

chromatography (*n*-hexane/EtOAc: 7/1) yielded **191bh** (51.3 mg, 0.14 mmol, 72%) as a colorless oil.

**<sup>1</sup>H-NMR** (500 MHz, CDCl<sub>3</sub>): δ = 8.09 (d, *J* = 0.9 Hz, 1H), 7.76 (d, *J* = 8.4 Hz, 2H), 7.68 (ddd, *J* = 8.1, 1.0, 1.0 Hz, 1H), 7.49 (d, *J* = 7.7 Hz, 1H), 7.39 (s, 1H), 7.38 (dd, *J* = 8.5, 1.7 Hz, 1H), 7.16 (ddd, *J* = 8.2, 6.9, 1.1 Hz, 1H), 7.10–7.05 (m, 3H), 7.01 (dd, *J* = 8.4, 1.0 Hz, 1H), 4.29 (q, *J* = 7.1 Hz, 2H), 2.48 (s, 3H), 1.33 (t, *J* = 7.1 Hz, 3H). **<sup>13</sup>C-NMR** (126 MHz, CDCl<sub>3</sub>): δ = 166.5 (C<sub>q</sub>), 143.5 (C<sub>q</sub>), 140.1 (C<sub>q</sub>), 139.5 (C<sub>q</sub>), 137.0 (C<sub>q</sub>), 135.2 (C<sub>q</sub>), 135.0 (CH), 131.0 (CH), 123.0 (CH), 129.6 (CH), 129.0 (CH), 129.0 (C<sub>q</sub>), 128.2 (CH), 126.8 (CH), 124.3 (C<sub>q</sub>), 121.1 (CH), 121.0 (CH), 110.1 (CH), 61.0 (CH<sub>2</sub>), 21.2 (CH<sub>3</sub>), 14.4 (CH<sub>3</sub>). **IR** (ATR): 1713, 1610, 1494, 1274, 1229, 1176, 1102, 1006, 776, 741 cm<sup>-1</sup>. **MS** (ESI) *m/z* (relative intensity): 735 (4) [2M+Na]<sup>+</sup>, 379 (17) [M+Na]<sup>+</sup>, 357 (100) [M+H]<sup>+</sup>. **HR-MS** (ESI): *m/z* calcd for C<sub>23</sub>H<sub>20</sub>N<sub>2</sub>O<sub>2</sub>, [M+H]<sup>+</sup> 357.1598, found 357.1606.

#### Ethyl 2'-(5-methyl-1*H*-pyrazol-1-yl)-[1,1'-biphenyl]-4-carboxylate (**191ch**)

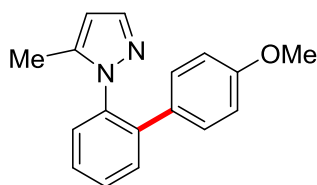


**191ch**

The general procedure **E** was followed using amide **76c** (55.5 mg, 0.20 mmol, 1.0 equiv) and aryl chloride **24h** (73.8 mg, 0.40 mmol, 2.0 equiv). Purification by column chromatography (*n*-hexane/EtOAc: 8/1) yielded **191ch** (51.5 mg, 0.17 mmol, 84%) as a colorless oil.

**<sup>1</sup>H-NMR** (400 MHz, CDCl<sub>3</sub>): δ = 7.92 (d, *J* = 8.7 Hz, 2H), 7.58–7.50 (m, 3H), 7.52–7.49 (m, 1H), 7.47 (ddd, *J* = 7.6, 1.5, 1.2 Hz, 1H), 7.14 (d, *J* = 8.7 Hz, 2H), 5.97 (ddd, *J* = 1.6, 1.6, 0.8 Hz, 1H), 4.35 (q, *J* = 7.2 Hz, 2H), 1.72 (s, 3H), 1.38 (t, *J* = 7.1 Hz, 3H). **<sup>13</sup>C-NMR** (126 MHz, CDCl<sub>3</sub>): δ = 166.5 (C<sub>q</sub>), 143.0 (C<sub>q</sub>), 139.9 (C<sub>q</sub>), 139.9 (CH), 138.5 (C<sub>q</sub>), 137.6 (C<sub>q</sub>), 130.5 (CH), 129.7 (CH), 129.6 (CH), 129.5 (C<sub>q</sub>), 129.1 (CH), 129.0 (CH), 128.5 (CH), 106.0 (CH), 61.1 (CH<sub>2</sub>), 14.5 (CH<sub>3</sub>), 11.3 (CH<sub>3</sub>). **IR** (ATR): 1712, 1491, 1286, 1124, 1108, 920, 773, 761, 740, 705 cm<sup>-1</sup>. **MS** (ESI) *m/z* (relative intensity): 635 (7) [2M+Na]<sup>+</sup>, 329 (100) [M+Na]<sup>+</sup>, 307 (13) [M+H]<sup>+</sup>. **HR-MS** (ESI): *m/z* calcd for C<sub>19</sub>H<sub>18</sub>N<sub>2</sub>O<sub>2</sub>, [M+H]<sup>+</sup> 307.1441, found 307.1442.

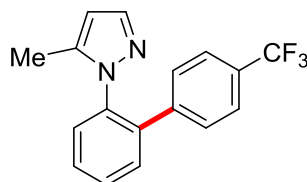
#### 1-(4'-Methoxy-[1,1'-biphenyl]-2-yl)-5-methyl-1*H*-pyrazole (**191cd**)

**191cd**

The general procedure **E** was followed using amide **76c** (55.5 mg, 0.20 mmol, 1.0 equiv) and 4-chloroanisole (**24d**) (57.0 mg, 0.40 mmol, 2.0 equiv). Purification by column chromatography (*n*-hexane/EtOAc: 10/1) yielded **191cd** (43.1 mg, 0.16 mmol, 80%) as a pale yellow oil.

**<sup>1</sup>H-NMR** (400 MHz, CDCl<sub>3</sub>):  $\delta$  = 7.55 (dd, *J* = 1.8, 0.6 Hz, 1H), 7.51–7.46 (m, 2H), 7.45–7.39 (m, 2H), 6.99 (d, *J* = 8.9 Hz, 2H), 6.78 (d, *J* = 8.9 Hz, 2H), 5.97 (ddd, *J* = 1.8, 0.8, 0.8 Hz, 1H), 3.77 (s, 3H), 1.71 (d, *J* = 0.6 Hz, 3H). **<sup>13</sup>C-NMR** (101 MHz, CDCl<sub>3</sub>):  $\delta$  = 159.1 (C<sub>q</sub>), 139.9 (C<sub>q</sub>), 139.6 (CH), 139.1 (C<sub>q</sub>), 137.4 (C<sub>q</sub>), 130.8 (C<sub>q</sub>), 130.3 (CH), 129.6 (CH), 129.4 (CH), 128.8 (CH), 127.8 (CH), 113.9 (CH), 105.7 (CH), 55.2 (CH<sub>3</sub>), 11.2 (CH<sub>3</sub>). **IR** (ATR): 1484, 1240, 1101, 1052, 914, 855, 741, 739, 711, 704 cm<sup>-1</sup>. **MS** (ESI) *m/z* (relative intensity): 287 (4) [M+Na]<sup>+</sup>, 265 (100) [M+H]<sup>+</sup>. **HR-MS** (ESI): *m/z* calcd for C<sub>17</sub>H<sub>16</sub>N<sub>2</sub>O, [M+H]<sup>+</sup> 265.1335, found 265.1336.

#### 5-Methyl-1-{4'-(trifluoromethyl)-[1,1'-biphenyl]-2-yl}-1H-pyrazole (**191ce**)

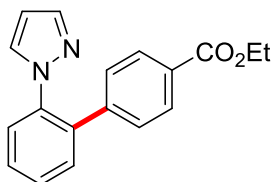
**191ce**

The general procedure **E** was followed using amide **76c** (55.5 mg, 0.20 mmol, 1.0 equiv) and aryl chloride **24e** (72.2 mg, 0.40 mmol, 2.0 equiv). Purification by column chromatography (*n*-hexane/EtOAc: 10/1) yielded **191ce** (43.5 mg, 0.14 mmol, 72%) as a colorless oil.

**<sup>1</sup>H-NMR** (400 MHz, CDCl<sub>3</sub>):  $\delta$  = 7.58–7.53 (m, 1H), 7.54 (d, *J* = 8.0 Hz, 2H), 7.52–7.51 (m, 2H), 7.50–7.46 (m, 2H), 7.19 (d, *J* = 8.0 Hz, 2H), 5.99 (dq, *J* = 1.6, 0.8 Hz, 1H), 1.74 (d, *J* = 0.6 Hz, 3H). **<sup>13</sup>C-NMR** (101 MHz, CDCl<sub>3</sub>):  $\delta$  = 142.1 (C<sub>q</sub>), 139.9 (CH), 139.9 (C<sub>q</sub>), 138.1 (C<sub>q</sub>), 137.6 (C<sub>q</sub>), 130.5 (CH), 129.7 (CH), 129.6 (q, <sup>2</sup>*J*<sub>C-F</sub> = 32.3, C<sub>q</sub>), 129.2 (CH), 129.0 (CH), 128.8 (CH), 125.4 (q, <sup>3</sup>*J*<sub>C-F</sub> = 3.8 Hz, CH), 124.3 (q, <sup>1</sup>*J*<sub>C-F</sub> = 273 Hz, C<sub>q</sub>), 106.1 (CH), 11.2 (CH<sub>3</sub>). **<sup>19</sup>F-NMR** (282 MHz, CDCl<sub>3</sub>):  $\delta$  = -62.55. **IR** (ATR): 1479, 1214,

1155, 1100, 1048, 944, 806, 786, 724, 673  $\text{cm}^{-1}$ . **MS** (ESI)  $m/z$  (relative intensity): 325 (1)  $[\text{M}+\text{Na}]^+$ , 303 (100)  $[\text{M}+\text{H}]^+$ . **HR-MS** (ESI):  $m/z$  calcd for  $\text{C}_{17}\text{H}_{13}\text{N}_2\text{F}_3$ ,  $[\text{M}+\text{H}]^+$  303.1104, found 303.1107.

#### Ethyl 2'-(1*H*-pyrazol-1-yl)-[1,1'-biphenyl]-4-carboxylate (**191dh**)

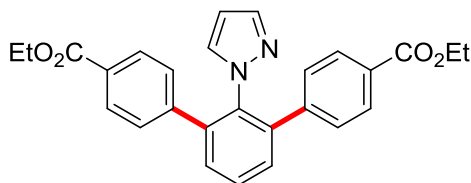


**191dh**

The general procedure **E** was followed using amide **76d** (52.6 mg, 0.20 mmol, 1.0 equiv) and aryl chloride **24h** (40.7 mg, 0.22 mmol, 1.1 equiv). Purification by column chromatography (*n*-hexane/EtOAc: 9/1) yielded **191dh** (38.6 mg, 0.13 mmol, 66%) as a colorless oil.

**<sup>1</sup>H-NMR** (400 MHz,  $\text{CDCl}_3$ ):  $\delta$  = 7.96 (d,  $J$  = 8.7 Hz, 2H), 7.62 (dd,  $J$  = 1.9, 0.6 Hz, 1H), 7.61–7.58 (m, 1H), 7.53–7.46 (m, 3H), 7.17 (d,  $J$  = 8.7 Hz, 2H), 7.09 (dd,  $J$  = 2.4, 0.6 Hz, 1H), 6.20 (dd,  $J$  = 2.4, 1.8 Hz, 1H), 4.37 (q,  $J$  = 7.1 Hz, 2H), 1.38 (t,  $J$  = 7.1 Hz, 3H). **<sup>13</sup>C-NMR** (101 MHz,  $\text{CDCl}_3$ ):  $\delta$  = 166.4 ( $\text{C}_q$ ), 143.3 ( $\text{C}_q$ ), 140.6 (CH), 138.7 ( $\text{C}_q$ ), 136.0 ( $\text{C}_q$ ), 131.3 (CH), 131.0 (CH), 129.8 (CH), 129.6 ( $\text{C}_q$ ), 129.1 (CH), 128.6 (CH), 128.6 (CH), 126.9 (CH), 106.8 (CH), 61.1 ( $\text{CH}_2$ ), 14.5 ( $\text{CH}_3$ ). **IR** (ATR): 1714, 1393, 1274, 1126, 1112, 1100, 1021, 758, 705, 623  $\text{cm}^{-1}$ . **MS** (ESI)  $m/z$  (relative intensity): 607 (7)  $[2\text{M}+\text{Na}]^+$ , 315 (100)  $[\text{M}+\text{Na}]^+$ , 293 (7)  $[\text{M}+\text{H}]^+$ . **HR-MS** (ESI):  $m/z$  calcd for  $\text{C}_{18}\text{H}_{16}\text{N}_2\text{O}_2$ ,  $[\text{M}+\text{Na}]^+$  315.1104, found 315.1107. The analytical data correspond with those reported in the literature.<sup>[181]</sup>

#### Diethyl 2'-(1*H*-pyrazol-1-yl)-[1,1':3',1''-terphenyl]-4,4''-dicarboxylate (**191dh'**)

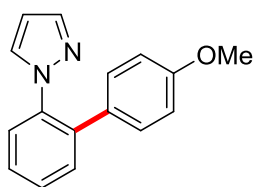


**191dh'**

The general procedure **E** was followed using amide **76d** (52.6 mg, 0.20 mmol, 1.0 equiv) and aryl chloride **24h** (92.3 mg, 0.50 mmol, 2.5 equiv). Purification by column chromatography (*n*-hexane/EtOAc: 5/1) yielded **191dh'** (52.9 mg, 0.12 mmol, 60%) as a colorless solid.

**M.p.:** 146–148 °C. **<sup>1</sup>H-NMR** (300 MHz, CDCl<sub>3</sub>):  $\delta$  = 7.90 (dd,  $J$  = 8.2, 2.0 Hz, 4H), 7.59 (dd,  $J$  = 8.8, 6.3 Hz, 1H), 7.52 (d,  $J$  = 6.3 Hz, 1H), 7.51 (d,  $J$  = 8.8 Hz, 1H), 7.35 (dd,  $J$  = 1.8, 0.6 Hz, 1H), 7.15 (dd,  $J$  = 8.2, 2.0 Hz, 4H), 7.03 (dd,  $J$  = 2.4, 0.6 Hz, 1H), 6.05 (dd,  $J$  = 2.4, 1.8 Hz, 1H), 4.33 (q,  $J$  = 7.1 Hz, 4H), 1.35 (t,  $J$  = 7.1 Hz, 6H). **<sup>13</sup>C-NMR** (125MHz, CDCl<sub>3</sub>):  $\delta$  = 166.3 (C<sub>q</sub>), 143.0 (C<sub>q</sub>), 139.8 (CH), 139.6 (C<sub>q</sub>), 136.4 (C<sub>q</sub>), 132.3 (CH), 130.5 (CH), 129.4 (C<sub>q</sub>), 129.3 (CH), 129.3 (CH), 128.2 (CH), 106.6 (CH), 61.0 (CH<sub>2</sub>), 14.3 (CH<sub>3</sub>). **IR** (ATR): 2995, 1699, 1472, 1279, 1099, 772 cm<sup>-1</sup>. **MS** (EI)  $m/z$  (relative intensity) 440 (60) [M]<sup>+</sup>, 439 (100) [M-H]<sup>+</sup>. **HR-MS** (ESI)  $m/z$  calcd for C<sub>27</sub>H<sub>24</sub>N<sub>2</sub>O<sub>4</sub> [M+H]<sup>+</sup> 441.1814, found 441.1812. The analytical data correspond with those reported in the literature.<sup>[181]</sup>

**1-{4'-Methoxy-[1,1'-biphenyl]-2-yl}-1H-pyrazole (191dd)**

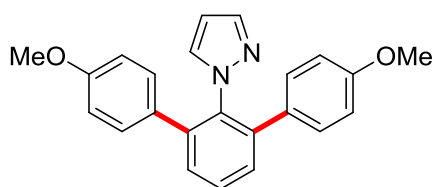


**191dd**

The general procedure **E** was followed using amide **76d** (52.6 mg, 0.20 mmol, 1.0 equiv) and 4-chloroanisole (**24d**) (31.4 mg, 0.22 mmol, 1.1 equiv). Purification by column chromatography (*n*-hexane/EtOAc: 8/1) yielded **191dd** (28.0 mg, 0.11 mmol, 56%) as a colorless oil.

**<sup>1</sup>H-NMR** (400 MHz, CDCl<sub>3</sub>):  $\delta$  = 7.64 (dd,  $J$  = 1.8, 0.6 Hz, 1H), 7.64–7.53 (m, 1H), 7.46–7.40 (m, 3H), 7.10 (dd,  $J$  = 2.4, 0.6 Hz, 1H), 7.02 (d,  $J$  = 9.0 Hz, 2H), 6.82 (d,  $J$  = 9.0 Hz, 2H), 6.20 (ddd,  $J$  = 2.4, 1.8, 0.5 Hz, 1H), 3.80 (s, 3H). **<sup>13</sup>C-NMR** (75 MHz, CDCl<sub>3</sub>):  $\delta$  = 159.2 (C<sub>q</sub>), 140.3 (CH), 138.7 (C<sub>q</sub>), 136.6 (C<sub>q</sub>), 131.5 (CH), 131.0 (CH), 131.0 (C<sub>q</sub>), 129.8 (CH), 128.4 (CH), 128.1 (CH), 126.8 (CH), 114.1 (CH), 106.5 (CH), 55.4 (CH<sub>3</sub>). **IR** (ATR): 2881, 1484, 1202, 1091, 1040, 914, 846, 740, 711, 704 cm<sup>-1</sup>. **MS** (ESI)  $m/z$  (relative intensity): 273 (44) [M+Na]<sup>+</sup>, 251 (100) [M+H]<sup>+</sup>. **HR-MS** (ESI):  $m/z$  calcd for C<sub>16</sub>H<sub>14</sub>N<sub>2</sub>O, [M+H]<sup>+</sup> 251.1179, found 251.1185.

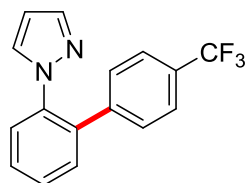
**1-{4,4''-Dimethoxy-[1,1':3',1''-terphenyl]-2'-yl}-1H-pyrazole (191dd')**

**191dd'**

The general procedure **E** was followed using amide **76d** (52.6 mg, 0.20 mmol, 1.0 equiv) and 4-chloroanisole (**24d**) (71.3 mg, 0.50 mmol, 2.5 equiv). Purification by column chromatography (*n*-hexane/EtOAc: 4/1) yielded **191dd'** (49.1 mg, 0.14 mmol, 69%) as a colorless solid.

**M.p.:** 122–124 °C. **<sup>1</sup>H-NMR** (300 MHz, CDCl<sub>3</sub>):  $\delta$  = 7.50 (dd, *J* = 8.3, 6.5 Hz, 1H), 7.45–7.41 (m, 1H), 7.40 (d, *J* = 8.3 Hz, 1H), 7.39 (d, *J* = 6.5 Hz, 1H), 7.06 (d, *J* = 2.3 Hz, 1H), 6.99 (d, *J* = 8.8 Hz, 4H), 6.73 (d, *J* = 8.8 Hz, 4H), 6.09–6.07 (m, 1H), 3.70 (s, 6H). **<sup>13</sup>C-NMR** (101 MHz, CDCl<sub>3</sub>):  $\delta$  = 158.8 (C<sub>q</sub>), 140.1 (C<sub>q</sub>), 139.2 (CH), 136.2 (C<sub>q</sub>), 132.4 (CH), 131.1 (CH), 129.6 (C<sub>q</sub>), 129.3 (CH), 129.0 (CH), 113.6 (CH), 106.1 (CH), 55.2 (CH<sub>3</sub>). **IR** (ATR): 1609, 1520, 1466, 1277, 1240, 1183, 1040, 1029, 844, 801 cm<sup>-1</sup>. **MS** (ESI) *m/z* (relative intensity): 379 (12) [M+Na]<sup>+</sup>, 357 (100) [M+H]<sup>+</sup>. **HR-MS** (ESI): *m/z* calcd for C<sub>23</sub>H<sub>20</sub>N<sub>2</sub>O<sub>2</sub>, [M+H]<sup>+</sup> 357.1589, found 357.1597. The analytical data correspond with those reported in the literature.<sup>[181]</sup>

#### 1-{4'-(Trifluoromethyl)-[1,1'-biphenyl]-2-yl}-1*H*-pyrazole (**191de**)

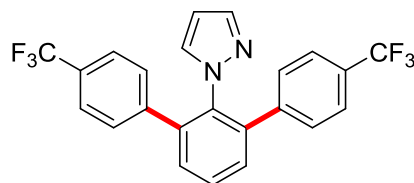
**191de**

The general procedure **E** was followed using amide **76d** (52.6 mg, 0.20 mmol, 1.0 equiv) and aryl chloride **24e** (39.7 mg, 0.22 mmol, 1.1 equiv). Purification by column chromatography (*n*-hexane/EtOAc: 10/1) yielded **191de** (40.9 mg, 0.14 mmol, 71%) as a colorless oil.

**<sup>1</sup>H-NMR** (400 MHz, CDCl<sub>3</sub>):  $\delta$  = 7.63 (dd, *J* = 1.9, 0.6 Hz, 1H), 7.64–7.57 (m, 1H), 7.56–7.51 (m, 3H), 7.50 (d, *J* = 2.1 Hz, 1H), 7.49–7.45 (m, 1H), 7.22 (d, *J* = 8.0 Hz, 2H), 7.12 (dd, *J* = 2.4, 0.7 Hz, 1H), 6.24 (dd, *J* = 2.4, 1.8 Hz, 1H). **<sup>13</sup>C-NMR** (101 MHz, CDCl<sub>3</sub>):  $\delta$  = 142.4 (C<sub>q</sub>), 140.7 (CH), 138.8 (C<sub>q</sub>), 135.7 (C<sub>q</sub>), 131.3 (CH), 131.0 (CH), 129.7 (q, <sup>2</sup>*J*<sub>C-F</sub> = 33.1 Hz, C<sub>q</sub>), 129.3 (CH), 128.9 (CH), 128.7 (CH), 127.1 (CH), 125.5 (q, <sup>3</sup>*J*<sub>C-F</sub> = 3.8 Hz,

CH), 124.3 (q,  $^1J_{\text{C-F}} = 272.7$  Hz, C<sub>q</sub>), 106.9 (CH).  **$^{19}\text{F}$ -NMR** (376 MHz, CDCl<sub>3</sub>):  $\delta = -62.55$ . **IR** (ATR): 1447, 1350, 1241, 1139, 1155, 1102, 964, 722, 702, 658 cm<sup>-1</sup>. **MS** (ESI)  $m/z$  (relative intensity): 311 (16) [M+Na]<sup>+</sup>, 289 (100) [M+H]<sup>+</sup>. **HR-MS** (ESI):  $m/z$  calcd for C<sub>16</sub>H<sub>11</sub>F<sub>3</sub>N<sub>2</sub>, [M+H]<sup>+</sup> 289.0947, found 289.0950.

**1-{4,4''-bis(Trifluoromethyl)-[1,1':3',1''-terphenyl]-2'-yl}-1H-pyrazole (191de')**

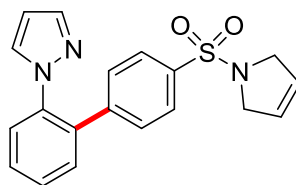


**191de'**

The general procedure **E** was followed using amide **76d** (52.6 mg, 0.20 mmol, 1.0 equiv) and aryl chloride **24e** (90.3 mg, 0.50 mmol, 2.5 equiv). Purification by column chromatography (*n*-hexane/EtOAc: 9/1) yielded **191de'** (53.4 mg, 0.12 mmol, 62%) as a colorless solid.

**M.p.:** 110–112 °C.  **$^1\text{H}$ -NMR** (400 MHz, CDCl<sub>3</sub>):  $\delta = 7.64$  (dd,  $J = 8.4, 6.9$  Hz, 1H), 7.54 (dd,  $J = 7.7, 0.7$  Hz, 2H), 7.50 (d,  $J = 8.1$  Hz, 4H), 7.39 (dd,  $J = 1.9, 0.6$  Hz, 1H), 7.23 (d,  $J = 8.0$  Hz, 4H), 7.06 (dd,  $J = 2.4, 0.6$  Hz, 1H), 6.10 (dd,  $J = 2.4, 1.9$  Hz, 1H).  **$^{13}\text{C}$ -NMR** (101 MHz, CDCl<sub>3</sub>):  $\delta = 142.2$  (C<sub>q</sub>), 140.2 (CH), 139.4 (C<sub>q</sub>), 136.6 (C<sub>q</sub>), 132.5 (CH), 130.8 (CH), 129.7 (q,  $^2J_{\text{C-F}} = 32.5$  Hz, C<sub>q</sub>), 129.7 (CH), 128.7 (CH), 125.2 (q,  $^3J_{\text{C-F}} = 3.8$  Hz, CH), 124.2 (q,  $^1J_{\text{C-F}} = 272$  Hz, C<sub>q</sub>), 107.0 (CH).  **$^{19}\text{F}$ -NMR** (376 MHz, CDCl<sub>3</sub>):  $\delta = -62.58$ . **IR** (ATR): 3301, 1706, 1543, 1251, 1040, 705 cm<sup>-1</sup>. **MS** (ESI)  $m/z$  (relative intensity): 455 (30) [M+Na]<sup>+</sup>, 433 (100) [M+H]<sup>+</sup>. **HR-MS** (ESI):  $m/z$  calcd for C<sub>23</sub>H<sub>14</sub>F<sub>6</sub>N<sub>2</sub>, [M+H]<sup>+</sup> 433.1139, found 433.1140.

**1-{4'-[(2,5-Dihydro-1H-pyrrol-1-yl)sulfonyl]-[1,1'-biphenyl]-2-yl}-1H-pyrazole (191dt)**

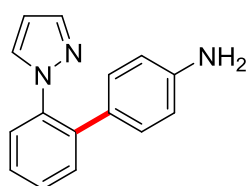


**191dt**

The general procedure **E** was followed using amide (**76d**) (52.6 mg, 0.20 mmol, 1.0 equiv) and aryl chloride **24t** (53.6 mg, 0.22 mmol, 1.1 equiv). Purification by column chromatography (*n*-hexane/EtOAc: 9/1 → 4/1) yielded **191dt** (59.0 mg, 0.17 mmol, 84%) as a colorless solid.

**M.p.:** 159–161 °C. **<sup>1</sup>H-NMR** (400 MHz, CDCl<sub>3</sub>):  $\delta$  = 7.73 (d,  $J$  = 8.7 Hz, 2H), 7.62–7.59 (m, 2H), 7.55–7.50 (m, 2H), 7.47 (ddd,  $J$  = 6.9, 2.7, 0.6 Hz, 1H), 7.23 (d,  $J$  = 8.7 Hz, 2H), 7.10 (dd,  $J$  = 2.4, 0.7 Hz, 1H), 6.21 (dd,  $J$  = 2.4, 1.9 Hz, 1H), 5.68 (s, 2H), 4.12 (s, 4H). **<sup>13</sup>C-NMR** (101 MHz, CDCl<sub>3</sub>):  $\delta$  = 143.3 (C<sub>q</sub>), 140.7 (CH), 138.8 (C<sub>q</sub>), 136.3 (C<sub>q</sub>), 135.4 (C<sub>q</sub>), 131.3 (CH), 130.9 (CH), 129.5 (CH), 129.3 (CH), 128.8 (CH), 127.6 (CH), 127.0 (CH), 125.6 (CH), 107.0 (CH), 55.0 (CH<sub>2</sub>). **IR** (ATR): 1395, 1340, 116, 1094, 1055, 757, 702, 650, 611, 580 cm<sup>-1</sup>. **MS** (ESI)  $m/z$  (relative intensity): 1076 (5) [3M+Na]<sup>+</sup>, 725 (26) [2M+Na]<sup>+</sup>, 374 (97) [M+Na]<sup>+</sup>, 352 (100) [M+H]<sup>+</sup>, 219 (5) [M-SO<sub>2</sub>C<sub>4</sub>H<sub>6</sub>N]<sup>+</sup>. **HR-MS** (ESI):  $m/z$  calcd for C<sub>19</sub>H<sub>17</sub>N<sub>3</sub>O<sub>2</sub>S, [M+H]<sup>+</sup> 352.1114, found 352.1119.

**2'-(1*H*-Pyrazol-1-yl)-[1,1'-biphenyl]-4-amine (191du)**



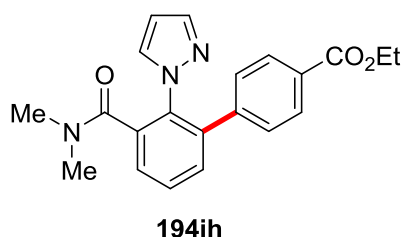
**191du**

The general procedure **E** was followed using amide **76d** (52.6 mg, 0.20 mmol, 1.0 equiv) and 4-chloroaniline (**24u**) (28.1 mg, 0.22 mmol, 1.1 equiv). Purification by column chromatography (*n*-hexane/EtOAc: 8/1) yielded **191du** (35.8 mg, 0.15 mmol, 76%) as an off-white solid.

**M.p.:** 120–122 °C. **<sup>1</sup>H-NMR** (400 MHz, CDCl<sub>3</sub>):  $\delta$  = 7.64 (dd,  $J$  = 1.8, 0.7 Hz, 1H), 7.61–7.53 (m, 1H), 7.45–7.37 (m, 3H), 7.13 (dd,  $J$  = 2.4, 0.7 Hz, 1H), 6.88 (d,  $J$  = 8.6 Hz, 2H), 6.58 (d,  $J$  = 8.6 Hz, 2H), 6.20 (dd,  $J$  = 2.4, 1.8 Hz, 1H), 3.68 (s<sub>br</sub>, 2H). **<sup>13</sup>C-NMR** (101 MHz, CDCl<sub>3</sub>):  $\delta$  = 145.9 (C<sub>q</sub>), 140.2 (CH), 138.5 (C<sub>q</sub>), 136.7 (C<sub>q</sub>), 131.5 (CH), 130.9 (CH), 129.6 (CH), 128.7 (C<sub>q</sub>), 128.3 (CH), 127.6 (CH), 126.7 (CH), 115.1 (CH), 106.3 (CH). **IR** (ATR): 3184, 2166, 2060, 1985, 1653, 1044, 759, 469, 430, 386 cm<sup>-1</sup>. **MS** (ESI)  $m/z$  (relative intensity): 493 (6) [2M+Na]<sup>+</sup>, 258 (32) [M+Na]<sup>+</sup>, 236 (100) [M+H]<sup>+</sup>, 219 (6) [M-NH<sub>2</sub>]<sup>+</sup>. **HR-MS** (ESI):  $m/z$  calcd for C<sub>15</sub>H<sub>13</sub>N<sub>3</sub>, [M+H]<sup>+</sup> 236.1182, found 236.1184.

**Ethyl 3'-(dimethylcarbamoyl)-2'-(1*H*-pyrazol-1-yl)-[1,1'-biphenyl]-4-carboxylate (194ih)**

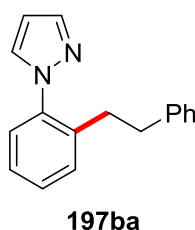




The general procedure **E** was followed using amide **76i** (43.1 mg, 0.20 mmol, 1.0 equiv) and aryl chloride **24h** (73.9 mg, 0.40 mmol, 2.0 equiv). Purification by column chromatography (*n*-hexane/EtOAc: 3/1) yielded **194ih** (67.6 mg, 0.19 mmol, 93%) as a colorless solid.

**M.p.:** 133–135 °C. **<sup>1</sup>H-NMR** (500 MHz, CDCl<sub>3</sub>):  $\delta$  = 7.89 (dd, *J* = 8.2, 2.0 Hz, 2H), 7.52 (dd, *J* = 7.8, 7.1 Hz, 1H), 7.51 (dd, *J* = 7.8, 2.0 Hz, 1H), 7.46 (dd, *J* = 1.8, 0.6 Hz, 1H), 7.39 (dd, *J* = 7.1, 2.0 Hz, 1H), 7.35 (dd, *J* = 2.4, 0.6 Hz, 1H), 7.0 (dd, *J* = 8.2, 2.0 Hz, 2H), 6.19 (dd, *J* = 2.4, 1.8 Hz, 1H), 4.33 (q, *J* = 7.1 Hz, 2H), 2.87 (s, 3H), 2.74 (s, 3H), 1.35 (t, *J* = 7.1 Hz, 3H). **<sup>13</sup>C-NMR** (125 MHz, CDCl<sub>3</sub>):  $\delta$  = 168.4 (C<sub>q</sub>), 166.2 (C<sub>q</sub>), 142.6 (C<sub>q</sub>), 140.4 (CH), 138.3 (C<sub>q</sub>), 138.3 (C<sub>q</sub>), 135.8 (C<sub>q</sub>), 135.0 (C<sub>q</sub>), 132.1 (CH), 131.2 (CH), 129.5 (CH), 129.1 (CH), 128.1 (CH), 126.8 (CH), 106.7 (CH), 61.0 (CH<sub>2</sub>), 38.9 (CH<sub>3</sub>), 34.5 (CH<sub>3</sub>), 14.3 (CH<sub>3</sub>). **IR** (ATR): 2988, 1715, 1630, 1270, 1160, 769 cm<sup>-1</sup>. **MS** (EI) *m/z* (relative intensity): 363 (30) [M]<sup>+</sup>, 362 (70) [M-H]<sup>+</sup>, 319 (100) [M-NMe<sub>2</sub>]<sup>+</sup>, 291 (100) [M-C(O)NMe<sub>2</sub>]<sup>+</sup>, 263 (10), 245 (15). **HR-MS** (ESI): *m/z* calcd for C<sub>21</sub>H<sub>21</sub>N<sub>3</sub>O<sub>3</sub>, [M+H]<sup>+</sup> 364.1661, found 364.1659.

#### 1-(2-Phenethylphenyl)-1*H*-pyrazole (**197ba**)

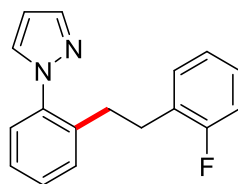


The general procedure **F** was followed using acid **196b** (37.6 mg, 0.20 mmol, 1.0 equiv) and styrene (**46a**) (41.7 mg, 0.40 mmol, 2.0 equiv). Purification by column chromatography (*n*-hexane/EtOAc: 10/1) yielded **197ba** (36.9 mg, 0.15 mmol, 74%) as a colorless oil.

**<sup>1</sup>H-NMR** (300 MHz, CDCl<sub>3</sub>):  $\delta$  = 7.67 (dd, *J* = 1.9, 0.7 Hz, 1H), 7.39 (dd, *J* = 2.3, 0.7 Hz, 1H), 7.31–7.24 (m, 2H), 7.24–7.20 (m, 2H), 7.18–7.11 (m, 2H), 7.08 (ddd, *J* = 7.2, 1.6, 1.4 Hz, 1H), 6.97–6.93 (m, 2H), 6.35 (dd, *J* = 2.3, 1.9 Hz, 1H), 2.83–2.74 (m, 2H), 2.68–

2.58 (m, 2H). **<sup>13</sup>C-NMR** (75 MHz, CDCl<sub>3</sub>):  $\delta$  = 141.7 (C<sub>q</sub>), 140.4 (CH), 139.9 (C<sub>q</sub>), 138.1 (C<sub>q</sub>), 130.8 (CH), 130.7 (CH), 128.8 (CH), 128.6 (CH), 128.4 (CH), 127.0 (CH), 126.9 (CH), 126.0 (CH), 106.4 (CH), 37.2 (CH<sub>2</sub>), 34.0 (CH<sub>2</sub>). **IR** (ATR): 1494, 1454, 1419, 938, 772, 760, 741, 698, 625, 516 cm<sup>-1</sup>. **MS** (ESI) *m/z* (relative intensity): 271 (100) [M+Na]<sup>+</sup>, 249 (42) [M+H]<sup>+</sup>. **HR-MS** (ESI): *m/z* calcd for C<sub>17</sub>H<sub>16</sub>N<sub>2</sub>, [M+H]<sup>+</sup> 249.1386, found 249.1387.

#### 1-[2-(2-Fluorophenethyl)phenyl]-1*H*-pyrazole (197bb)

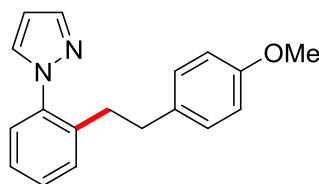


197bb

The general procedure **F** was followed using acid **196b** (37.6 mg, 0.20 mmol, 1.0 equiv) and alkene **46b** (48.9 mg, 0.40 mmol, 2.0 equiv). Purification by column chromatography (*n*-hexane/EtOAc: 10/1) yielded **197bb** (45.3 mg, 0.17 mmol, 85%) as a colorless oil.

**<sup>1</sup>H-NMR** (400 MHz, CDCl<sub>3</sub>):  $\delta$  = 7.75 (dd, *J* = 1.8, 0.7 Hz, 1H), 7.51 (dd, *J* = 2.3, 0.7 Hz, 1H), 7.40–7.28 (m, 4H), 7.14 (dddd, *J* = 8.0, 5.7, 5.2, 3.4 Hz, 1H), 7.02–6.95 (m, 3H), 6.44 (dd, *J* = 2.4, 1.8 Hz, 1H), 2.93–2.81 (m, 2H), 2.83–2.70 (m, 2H). **<sup>13</sup>C-NMR** (126 MHz, CDCl<sub>3</sub>):  $\delta$  = 161.1 (d, <sup>1</sup>*J*<sub>C-F</sub> = 244.7 Hz, C<sub>q</sub>), 140.4 (CH), 139.9 (C<sub>q</sub>), 137.7 (C<sub>q</sub>), 130.8 (d, <sup>3</sup>*J*<sub>C-F</sub> = 6.1 Hz, CH), 130.7 (CH), 128.7 (CH), 128.3 (d, <sup>2</sup>*J*<sub>C-F</sub> = 16.0 Hz, C<sub>q</sub>), 127.7 (d, <sup>3</sup>*J*<sub>C-F</sub> = 8.0 Hz, CH), 127.0 (CH), 126.7 (CH), 123.9 (CH), 123.9 (CH), 115.2 (d, <sup>2</sup>*J*<sub>C-F</sub> = 22.1 Hz, CH), 106.4 (CH), 32.5 (CH<sub>2</sub>), 30.5 (d, <sup>3</sup>*J*<sub>C-F</sub> = 2.2 Hz, CH<sub>2</sub>). **<sup>19</sup>F-NMR** (282 MHz, CDCl<sub>3</sub>):  $\delta$  = -119.06 (ddd, *J* = 9.8, 7.7, 5.1 Hz). **IR** (ATR): 1517, 1491, 1455, 1394, 1228, 1044, 938, 748, 624, 498 cm<sup>-1</sup>. **MS** (ESI) *m/z* (relative intensity): 555 (2) [2M+Na]<sup>+</sup>, 289 (100) [M+Na]<sup>+</sup>, 267 (92) [M+H]<sup>+</sup>. **HR-MS** (ESI): *m/z* calcd for [C<sub>17</sub>H<sub>15</sub>N<sub>2</sub>F] [M+H]<sup>+</sup> 267.1292, found 267.1293.

#### 1-[2-(4-Methoxyphenethyl)phenyl]-1*H*-pyrazole (197bc)

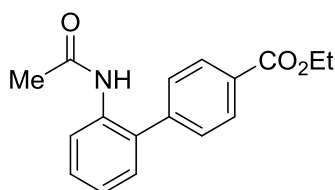


197bc

The general procedure **F** was followed using acid **196b** (37.6 mg, 0.20 mmol, 1.0 equiv) and alkene **46c** (53.7 mg, 0.40 mmol, 2.0 equiv). Purification by column chromatography (*n*-hexane/EtOAc: 8/1) yielded **197bc** (31.1 mg, 0.11 mmol, 56%) as a colorless solid.

**M.p.:** 71–73 °C. **<sup>1</sup>H-NMR** (300 MHz, CDCl<sub>3</sub>):  $\delta$  = 7.76 (ddd,  $J$  = 1.9, 0.6, 0.6 Hz, 1H), 7.49 (ddd,  $J$  = 2.4, 0.6, 0.6 Hz, 1H), 7.40–7.29 (m, 4H), 6.97 (d,  $J$  = 8.8 Hz, 2H), 6.79 (d,  $J$  = 8.7 Hz, 2H), 6.45 (ddd,  $J$  = 2.4, 1.8, 0.5 Hz, 1H), 3.77 (s, 3H), 2.88–2.80 (m, 2H), 2.74–2.62 (m, 2H). **<sup>13</sup>C-NMR** (75 MHz, CDCl<sub>3</sub>):  $\delta$  = 157.9 (C<sub>q</sub>), 140.3 (CH), 139.9 (C<sub>q</sub>), 138.1 (C<sub>q</sub>), 133.8 (C<sub>q</sub>), 130.8 (CH), 130.7 (CH), 129.4 (CH), 128.8 (CH), 126.9 (CH), 126.7 (CH), 113.8 (CH), 106.3 (CH), 55.3 (CH<sub>3</sub>), 36.3 (CH<sub>2</sub>), 34.2 (CH<sub>2</sub>). **IR** (ATR): 1510, 1394, 1241, 1177, 1034, 938, 821, 750, 624, 526 cm<sup>-1</sup>. **MS** (ESI)  $m/z$  (relative intensity): 296 (6) [M+NH<sub>4</sub>]<sup>+</sup>, 279 (100) [M+H]<sup>+</sup>. **HR-MS** (ESI):  $m/z$  calcd for C<sub>18</sub>H<sub>18</sub>N<sub>2</sub>O, [M+H]<sup>+</sup> 279.1492, found 279.1495.

#### Ethyl 2'-acetamido-[1,1'-biphenyl]-4-carboxylate (**202ch**)

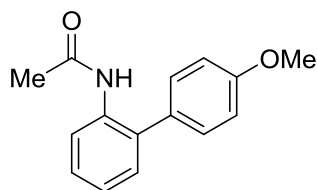


**202ch**

The general procedure **G** was followed using pyrazole **191ch** (61.3 mg, 0.20 mmol, 1.0 equiv) with a reaction time of 40 min. Purification by column chromatography (*n*-hexane/EtOAc: 1/1) yielded **202ch** (32.3 mg, 0.11 mmol, 57%) as a yellow solid.

**M.p.:** 168–170 °C. **<sup>1</sup>H-NMR** (300 MHz, CDCl<sub>3</sub>):  $\delta$  = 8.18 (d,  $J$  = 8.0 Hz, 1H), 8.14 (d,  $J$  = 8.3 Hz, 2H), 7.45 (d,  $J$  = 8.3 Hz, 2H), 7.39 (ddd,  $J$  = 8.4, 6.9, 2.2 Hz, 1H), 7.25–7.17 (m, 2H), 7.06 (s<sub>br</sub>, 1H), 4.41 (q,  $J$  = 7.1 Hz, 2H), 2.02 (s, 3H), 1.42 (t,  $J$  = 7.1 Hz, 3H). **<sup>13</sup>C-NMR** (76 MHz, CDCl<sub>3</sub>):  $\delta$  = 168.3 (C<sub>q</sub>), 166.1 (C<sub>q</sub>), 142.9 (C<sub>q</sub>), 134.4 (C<sub>q</sub>), 131.7 (C<sub>q</sub>), 130.2 (CH), 130.0 (C<sub>q</sub>), 129.9 (CH), 129.2 (CH), 129.0 (CH), 124.7 (CH), 122.4 (CH), 61.2 (CH<sub>2</sub>), 24.4 (CH<sub>3</sub>), 14.3 (CH<sub>3</sub>). **IR** (ATR): 3241, 2753, 2488, 1730, 1700, 1156, 1031, 970 cm<sup>-1</sup>. **MS** (ESI)  $m/z$  (relative intensity): 589 (15) [2M+Na]<sup>+</sup>, 567 (5) [2M+H]<sup>+</sup>, 306 (100) [M+Na]<sup>+</sup>, 284 (47) [M+H]<sup>+</sup>, 238 (35) [M-OEt]<sup>+</sup>. **HR-MS** (ESI):  $m/z$  calcd for C<sub>17</sub>H<sub>17</sub>NO<sub>3</sub>, [M+H]<sup>+</sup> 284.1281, found 284.1277.

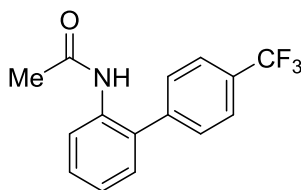
#### *N*-{4'-Methoxy-[1,1'-biphenyl]-2-yl}acetamide (**202cd**)

**202cd**

The general procedure **G** was followed using pyrazole **191cd** (52.9 mg, 0.20 mmol, 1.0 equiv) with a reaction time of 20 min. Purification by column chromatography (*n*-hexane/EtOAc: 1/1) yielded **202cd** (30.0 mg, 0.12 mmol, 62%) as a yellow oil.

**<sup>1</sup>H-NMR** (300 MHz, CDCl<sub>3</sub>):  $\delta$  = 8.17 (d,  $J$  = 8.2 Hz, 1H), 7.27 (ddd,  $J$  = 7.8, 2.1, 0.4 Hz, 1H), 7.22 (d,  $J$  = 8.7 Hz, 2H), 7.17–7.04 (m, 3H), 6.94 (d,  $J$  = 8.7 Hz, 2H), 3.80 (s, 3H), 1.95 (s, 3H). **<sup>13</sup>C-NMR** (75 MHz, CDCl<sub>3</sub>):  $\delta$  = 168.3 (C<sub>q</sub>), 159.5 (C<sub>q</sub>), 135.0 (C<sub>q</sub>), 132.0 (C<sub>q</sub>), 130.5 (CH), 130.4 (C<sub>q</sub>), 130.3 (CH), 128.2 (CH), 124.4 (CH), 121.6 (CH), 114.6 (CH), 55.5 (CH<sub>3</sub>), 24.8 (CH<sub>3</sub>). **IR** (ATR): 3355, 2929, 2838, 1687, 1510, 1240, 1032 cm<sup>-1</sup>. **MS** (ESI)  $m/z$  (relative intensity): 264 (100) [M+Na]<sup>+</sup>, 242 (24) [M+H]<sup>+</sup>. **HR-MS** (ESI):  $m/z$  calcd for C<sub>15</sub>H<sub>15</sub>NO<sub>2</sub>, [M+H]<sup>+</sup> 272.1176, found 272.1177. The analytical data correspond with those reported in the literature.<sup>[182]</sup>

#### ***N*-{4'-(Trifluoromethyl)-[1,1'-biphenyl]-2-yl}acetamide (202ce)**

**202ce**

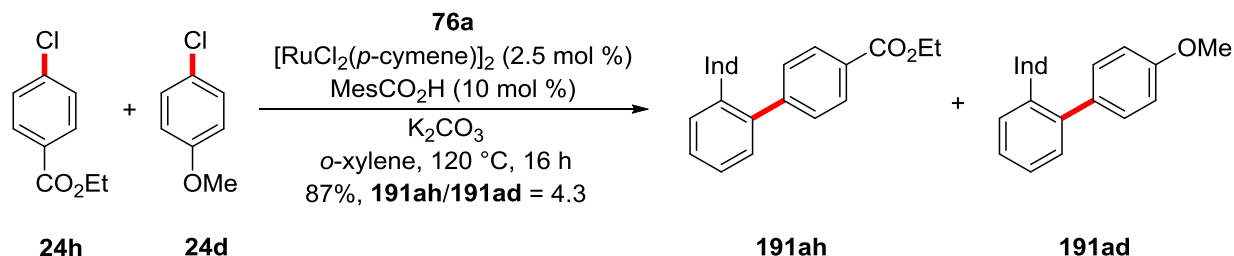
The general procedure **G** was followed using pyrazole **191ce** (60.5 mg, 0.20 mmol, 1.0 equiv) with a reaction time of 40 min. Purification by column chromatography (*n*-hexane/EtOAc: 1/1) yielded **202ce** (21.2 mg, 0.08 mmol, 38%) as a colorless solid.

**M.p.:** 118–119 °C. **<sup>1</sup>H-NMR** (300 MHz, CDCl<sub>3</sub>):  $\delta$  = 8.17 (d,  $J$  = 8.3 Hz, 1H), 7.74 (d,  $J$  = 8.0 Hz, 2H), 7.51 (d,  $J$  = 8.0 Hz, 2H), 7.41 (ddd,  $J$  = 8.5, 6.3, 2.7 Hz, 1H), 7.25–7.20 (m, 2H), 6.96 (s<sub>br</sub>, 1H), 2.04 (s, 3H). **<sup>13</sup>C-NMR** (76 MHz, CDCl<sub>3</sub>):  $\delta$  = 168.5 (C<sub>q</sub>), 142.2 (C<sub>q</sub>), 134.6 (C<sub>q</sub>), 131.6 (C<sub>q</sub>), 130.2 (q,  $^2J_{C-F}$  = 32.8 Hz, C<sub>q</sub>), 130.1 (CH), 129.8 (CH), 129.3 (CH), 126.1 (q,  $^3J_{C-F}$  = 3.8 Hz, CH), 125.1 (CH), 124.1 (q,  $^1J_{C-F}$  = 272 Hz, C<sub>q</sub>), 122.9 (CH), 24.6 (CH<sub>3</sub>). **<sup>19</sup>F-NMR** (282 MHz, CDCl<sub>3</sub>):  $\delta$  = -62.60. **IR** (ATR): 3228, 2711, 2351, 1720, 1652, 1254, 954, 771 cm<sup>-1</sup>. **MS** (ESI)  $m/z$  relative intensity): 581 (16) [2M+Na]<sup>+</sup>, 559 (2) [2M+H]<sup>+</sup>, 302 (64) [M+Na]<sup>+</sup>, 280 (100) [M+H]<sup>+</sup>. **HR-MS** (ESI):  $m/z$  calcd for C<sub>15</sub>H<sub>12</sub>F<sub>3</sub>NO,

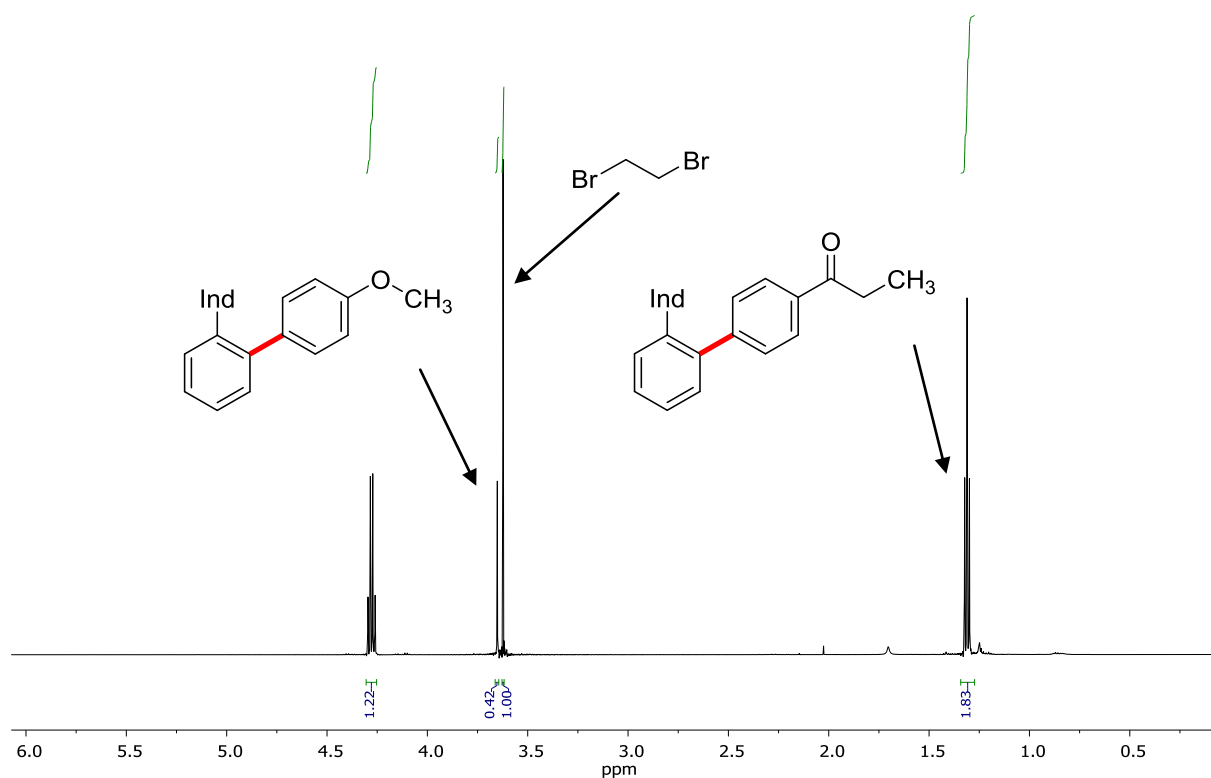
$[M+H]^+$  280.0944, found 280.0947. The analytical data correspond with those reported in the literature.<sup>[183]</sup>

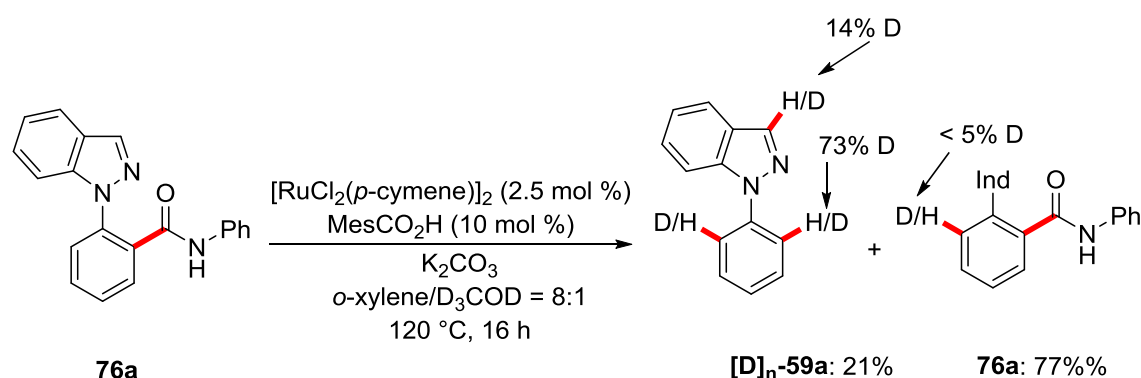
### 5.6.2 Mechanistic Studies

#### Intermolecular Competition Experiment between Aryl Chlorides **24h** and **24d**.



The general procedure **E** was followed using amide **76a** (62.7 mg, 0.20 mmol, 1.00 equiv), aryl chloride **24h** (36.9 mg, 0.20 mmol, 1.0 equiv) and aryl chloride **24d** (28.5 mg, 0.20 mmol, 1.00 equiv). Purification by column chromatography (*n*-hexane/EtOAc: 8/1) yielded a mixture of **191ah** (142 μmol, 71%) and **191ad** (32.5 μmol, 16%). The conversion was determined by <sup>1</sup>H-NMR spectroscopy using 1,2-dibromoethane (10.9 mg, 58.0 μmol) as an internal standard.

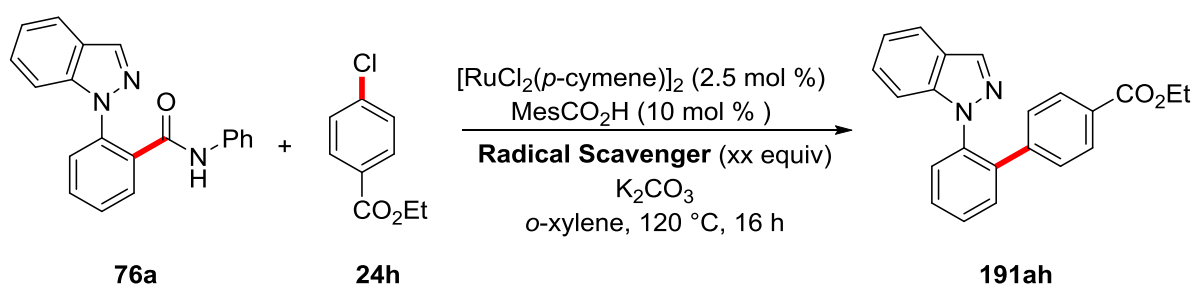


Organometallic  $\sigma$ -C–C Activation

To a Schlenk tube charged with amide **76a** (62.7 mg, 0.20 mmol, 1.0 equiv),  $[\text{RuCl}_2(p\text{-cymene})]_2$  (3.1 mg, 5.0  $\mu\text{mol}$ , 2.5 mol %),  $\text{MesCO}_2\text{H}$  (3.3 mg, 20  $\mu\text{mol}$ , 10 mol %) and  $\text{K}_2\text{CO}_3$  (55.3 mg, 0.40 mmol, 2.0 equiv) was added  $o$ -xylene (1.0 mL) and  $\text{CD}_3\text{OD}$  (0.2 mL). The Schlenk tube was degassed and filled with  $\text{N}_2$  for three times and the mixture was stirred at  $120\text{ }^\circ\text{C}$  for 16 h. Removal of the solvent under reduced pressure and purification of the residue by column chromatography on silica gel ( $n$ -Hexane/EtOAc: 5/1) yielded **[D]<sub>n</sub>-59a** (8.2 mg, 42  $\mu\text{mol}$ , 21%) and reisolated **76a** (48.3 mg, 154  $\mu\text{mol}$ , 77%). The amount of deuteration was determined by  $^1\text{H}$ -NMR spectroscopy.

## Reaction with Radical Scavengers

The general procedure **E** was followed using amide **76a** (62.7 mg, 0.20 mmol, 1.0 equiv), aryl chloride **24h** (73.9 mg, 0.40 mmol, 2.0 equiv) and a radical scavenger (0.1 or 1.0 equiv). Purification by column chromatography ( $n$ -hexane/EtOAc: 8/1) gave the product **191ah** in the indicated yields.



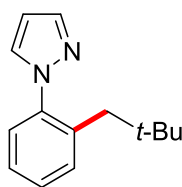
Entry	Radical Scavenger	Equiv	Isolated Yield
1	---	---	81%

2	BHT	0.1	79%
3	BHT	1.0	53%
4	TEMPO	0.1	36%
5	TEMPO	1.0	---

## 5.7 Ruthenium(II)-Catalyzed C–C Alkylation of Acids

### 5.7.1 Experimental Procedures and Analytical Data

#### 1-(2-Neopentylphenyl)-1*H*-pyrazole (203ba)

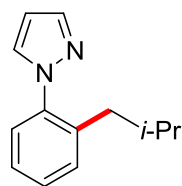


**203ba**

The general procedure **H** was followed using acid **196b** (94.1 mg, 0.50 mmol, 1.0 equiv) and neopentyl bromide (**11a**) (227 mg, 1.50 mmol, 3.0 equiv). Purification by column chromatography (*n*-hexane/EtOAc: 12/1) yielded **203ba** (103 mg, 0.48 mmol, 95%) as a colorless oil.

**<sup>1</sup>H-NMR** (300 MHz, CDCl<sub>3</sub>):  $\delta$  = 7.63 (dd, *J* = 1.8, 0.7 Hz, 1H), 7.51 (dd, *J* = 2.4, 0.7 Hz, 1H), 7.25–7.22 (m, 2H), 7.25–7.15 (m, 2H), 6.34 (dd, *J* = 2.4, 1.9 Hz, 1H), 2.68 (s, 2H), 0.61 (s, 9H). **<sup>13</sup>C-NMR** (75 MHz, CDCl<sub>3</sub>):  $\delta$  = 140.6 (C<sub>q</sub>), 140.1 (CH), 135.7 (C<sub>q</sub>), 133.2 (CH), 131.1 (CH), 127.8 (CH), 127.0 (CH), 126.8 (CH), 106.3 (CH), 44.1 (CH<sub>2</sub>), 32.2 (C<sub>q</sub>), 29.5 (CH<sub>3</sub>). **IR** (ATR): 2951, 2865, 1517, 1394, 1364, 1044, 940, 749, 718, 625 cm<sup>-1</sup>. **MS** (ESI) *m/z* (relative intensity): 215 (100) [M+H]<sup>+</sup>. **HR-MS** (ESI): *m/z* calcd for C<sub>14</sub>H<sub>18</sub>N<sub>2</sub>, [M+H]<sup>+</sup> 215.1543, found 215.1547. The analytical data correspond with those reported in the literature.<sup>[184]</sup>

#### 1-(2-Isobutylphenyl)-1*H*-pyrazole (203bb)

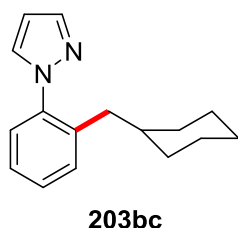


**203bb**

The general procedure **H** was followed using acid **196b** (94.1 mg, 0.50 mmol, 1.0 equiv) and isobutyl bromide (**11b**) (206 mg, 1.50 mmol, 3.0 equiv). Purification by column chromatography (*n*-hexane/EtOAc: 10/1) yielded **203bb** (80.1 mg, 0.40 mmol, 80%) as a colorless oil.

**<sup>1</sup>H-NMR** (400 MHz, CDCl<sub>3</sub>):  $\delta$  = 7.69 (dd, *J* = 1.9, 0.7 Hz, 1H), 7.55 (dd, *J* = 2.4, 0.7 Hz, 1H), 7.37–7.28 (m, 1H), 7.29–7.24 (m, 3H), 6.40 (dd, *J* = 2.3, 1.9 Hz, 1H), 2.45 (d, *J* = 7.3 Hz, 2H), 1.66–1.47 (m, 1H), 0.74 (d, *J* = 6.6 Hz, 6H). **<sup>13</sup>C-NMR** (101 MHz, CDCl<sub>3</sub>):  $\delta$  = 140.2 (CH), 140.1 (C<sub>q</sub>), 138.0 (C<sub>q</sub>), 131.2 (CH), 130.9 (CH), 128.5 (CH), 126.9 (CH), 126.7 (CH), 106.2 (CH), 40.7 (CH<sub>2</sub>), 29.2 (CH), 22.5 (CH<sub>3</sub>). **IR** (ATR): 2955, 2867, 1517, 1455, 1394, 1108, 1044, 939, 749, 625 cm<sup>-1</sup>. **MS** (ESI) *m/z* (relative intensity): 223 (10) [M+Na]<sup>+</sup>, 201 (100) [M+H]<sup>+</sup>. **HR-MS** (ESI): *m/z* calcd for C<sub>13</sub>H<sub>16</sub>N<sub>2</sub>, [M+H]<sup>+</sup> 201.1386, found 201.1391.

#### 1-[2-(Cyclohexylmethyl)phenyl]-1*H*-pyrazole (**203bc**)

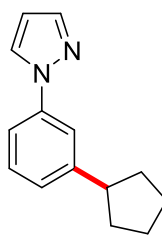


The general procedure **H** was followed using acid **196b** (94.1 mg, 0.50 mmol, 1.0 equiv) and alkyl bromide **11c** (266 mg, 1.50 mmol, 3.0 equiv). Purification by column chromatography (*n*-hexane/EtOAc: 10/1) yielded **203bc** (97.3 mg, 0.41 mmol, 81%) as a colorless oil.

**<sup>1</sup>H-NMR** (400 MHz, CDCl<sub>3</sub>):  $\delta$  = 7.69 (dd, *J* = 1.9, 0.7 Hz, 1H), 7.54 (dd, *J* = 2.4, 0.7 Hz, 1H), 7.32 (ddd, *J* = 7.8, 5.6, 2.7 Hz, 1H), 7.29–7.27 (m, 1H), 7.27–7.24 (m, 2H), 6.41 (dd, *J* = 2.3, 1.9 Hz, 1H), 2.44 (d, *J* = 7.1 Hz, 2H), 1.62–1.51 (m, 3H), 1.49 (ddt, *J* = 13.7, 3.7, 1.6 Hz, 2H), 1.23 (ttt, *J* = 10.8, 7.1, 3.5 Hz, 1H), 1.14 – 1.01 (m, 3H), 0.80–0.69 (m, 2H). **<sup>13</sup>C-NMR** (101 MHz, CDCl<sub>3</sub>):  $\delta$  = 140.2 (CH), 140.2 (C<sub>q</sub>), 137.7 (C<sub>q</sub>), 131.2 (CH), 131.0 (CH), 128.5 (CH), 126.9 (CH), 126.6 (CH), 106.2 (CH), 39.1 (CH<sub>2</sub>), 38.9 (CH), 33.2 (CH<sub>2</sub>), 26.5 (CH<sub>2</sub>), 26.3 (CH<sub>2</sub>). **IR** (ATR): 2921, 2850, 1516, 1498, 1449, 1394, 1043, 940, 748, 625 cm<sup>-1</sup>. **MS** (ESI) *m/z* (relative intensity): 263 (15) [M+Na]<sup>+</sup>, 241 (100) [M+H]<sup>+</sup>. **HR-MS** (ESI): *m/z* calcd for C<sub>16</sub>H<sub>20</sub>N<sub>2</sub>, [M+H]<sup>+</sup> 241.1699, found 241.1706.

#### 1-(3-Cyclopentylphenyl)-1*H*-pyrazole (**203bd**)

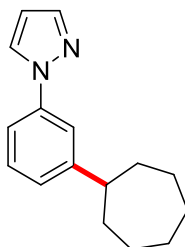


**203bd**

The general procedure **H** was followed using acid **196b** (94.1 mg, 0.50 mmol, 1.0 equiv) cyclopentyl bromide (**11d**) (224 mg, 1.50 mmol, 3.0 equiv). Purification by column chromatography (*n*-hexane/EtOAc: 14/1) yielded **203bd** (53.1 mg, 0.25 mmol, 50%) as a pale yellow oil. The connectivity was determined by 2D NMR spectroscopy.

**<sup>1</sup>H-NMR** (600 MHz, CDCl<sub>3</sub>):  $\delta$  = 7.92 (d, *J* = 2.4 Hz, 1H), 7.73 (d, *J* = 1.8 Hz, 1H), 7.62 (dd, *J* = 2.0, 2.0 Hz, 1H), 7.45 (ddd, *J* = 8.0, 2.2, 1.1 Hz, 1H), 7.35 (dd, *J* = 7.8, 7.8 Hz, 1H), 7.18 (ddd, *J* = 7.6, 1.3, 1.3 Hz, 1H), 6.46–6.45 (m, 1H), 3.06 (tt, *J* = 9.6, 7.5 Hz, 1H), 2.15–2.07 (m, 2H), 1.88–1.80 (m, 2H), 1.76–1.61 (m, 4H). **<sup>13</sup>C-NMR** (126 MHz, CDCl<sub>3</sub>):  $\delta$  = 148.3 (C<sub>q</sub>), 140.9 (CH), 140.2 (C<sub>q</sub>), 129.2 (CH), 126.9 (CH), 125.4 (CH), 118.4 (CH), 116.7 (CH), 107.5 (CH), 46.1 (CH), 34.8 (CH<sub>2</sub>), 25.7 (CH<sub>2</sub>). **IR** (ATR): 2951, 2867, 1608, 1590, 1519, 1393, 1043, 785, 747, 698 cm<sup>-1</sup>. **MS** (ESI) *m/z* (relative intensity): 213 (100) [M+H]<sup>+</sup>. **HR-MS** (ESI): *m/z* calcd for C<sub>14</sub>H<sub>16</sub>N<sub>2</sub>, [M+H]<sup>+</sup> 213.1386, found 213.1389.

#### 1-(3-Cycloheptylphenyl)-1H-pyrazole (**203be**)

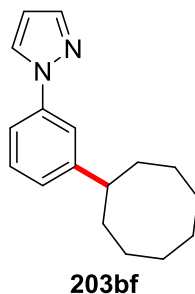
**203be**

The general procedure **H** was followed using acid **196b** (94.1 mg, 0.50 mmol, 1.0 equiv) and cycloheptyl bromide (**11e**) (266 mg, 1.50 mmol, 3.0 equiv). Purification by column chromatography (*n*-hexane/EtOAc: 15/1) yielded **203be** (87.7 mg, 0.37 mmol, 73%) as a pale yellow oil. The connectivity was determined by 2D NMR spectroscopy.

**<sup>1</sup>H-NMR** (300 MHz, CDCl<sub>3</sub>):  $\delta$  = 7.92 (dd, *J* = 2.5, 0.7 Hz, 1H), 7.72 (dd, *J* = 1.8, 0.6 Hz, 1H), 7.58 (dd, *J* = 2.0, 0.4 Hz, 1H), 7.44 (ddd, *J* = 8.0, 2.2, 1.1 Hz, 1H), 7.34 (ddd, *J* = 7.8, 0.5, 0.5 Hz, 1H), 7.12 (dddd, *J* = 7.6, 1.7, 1.1, 0.4 Hz, 1H), 6.45 (dd, *J* = 2.5, 1.8 Hz, 1H), 2.74 (tt, *J* = 10.4, 3.6 Hz, 1H), 2.01–1.90 (m, 2H), 1.87–1.48 (m, 10H). **<sup>13</sup>C-NMR** (75 MHz, CDCl<sub>3</sub>):  $\delta$  = 151.8 (C<sub>q</sub>), 141.0 (CH), 140.3 (C<sub>q</sub>), 129.4 (CH), 126.9 (CH), 125.0

(CH), 118.0 (CH), 116.5 (CH), 107.5 (CH), 47.2 (CH), 36.8 (CH<sub>2</sub>), 28.0 (CH<sub>2</sub>), 27.3 (CH<sub>2</sub>). **IR** (ATR): 2920, 2853, 1607, 1590, 1518, 1392, 1043, 784, 745, 698 cm<sup>-1</sup>. **MS** (ESI) *m/z* (relative intensity): 263 (14) [M+Na]<sup>+</sup>, 241 (100) [M+H]<sup>+</sup>. **HR-MS** (ESI): *m/z* calcd for C<sub>16</sub>H<sub>20</sub>N<sub>2</sub>, [M+H]<sup>+</sup> 241.1699, found 241.1705.

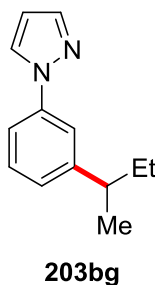
### 1-(3-Cyclooctylphenyl)-1*H*-pyrazole (203bf)



The general procedure **H** was followed using acid **196b** (94.1 mg, 0.50 mmol, 1.0 equiv) and cyclooctyl bromide (**11f**) (287 mg, 1.50 mmol, 3.0 equiv). Purification by column chromatography (*n*-hexane/EtOAc: 15/1) yielded **203bf** (70.0 mg, 0.28 mmol, 55%) as a yellow oil. The connectivity was determined by 2D NMR spectroscopy.

**<sup>1</sup>H-NMR** (300 MHz, CDCl<sub>3</sub>): δ = 7.92 (dd, *J* = 2.5, 0.7 Hz, 1H), 7.72 (dd, *J* = 1.8, 0.6 Hz, 1H), 7.57 (dd, *J* = 2.2, 1.7 Hz, 1H), 7.43 (ddd, *J* = 8.0, 2.2, 1.2 Hz, 1H), 7.35 (dd, *J* = 7.7, 7.7 Hz, 1H), 7.12 (dddd, *J* = 7.4, 1.7, 1.2, 0.5 Hz, 1H), 6.45 (dd, *J* = 2.5, 1.8 Hz, 1H), 2.91–2.78 (m, 1H), 1.95–1.73 (m, 6H), 1.71–1.49 (m, 8H). **<sup>13</sup>C-NMR** (75 MHz, CDCl<sub>3</sub>): δ = 152.3 (C<sub>q</sub>), 141.0 (CH), 140.3 (C<sub>q</sub>), 129.4 (CH), 127.0 (CH), 125.3 (CH), 118.3 (CH), 116.4 (CH), 107.5 (CH), 44.9 (CH), 34.8 (CH<sub>2</sub>), 27.0 (CH<sub>2</sub>), 26.5 (CH<sub>2</sub>), 26.2 (CH<sub>2</sub>). **IR** (ATR): 2917, 1606, 1591, 1518, 1392, 1043, 947, 783, 744, 698 cm<sup>-1</sup>. **MS** (ESI) *m/z* (relative intensity): 277 (2) [M+Na]<sup>+</sup>, 255 (100) [M+H]<sup>+</sup>. **HR-MS** (ESI): *m/z* calcd for C<sub>17</sub>H<sub>22</sub>N<sub>2</sub>, [M+H]<sup>+</sup> 255.1856, found 255.1858.

### 1-[3-(*sec*-Butyl)phenyl]-1*H*-pyrazole (203bg)

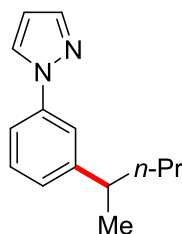


The general procedure **H** was followed using acid **196b** (94.1 mg, 0.50 mmol, 1.0 equiv) and 2-bromobutane (**11g**) (206 mg, 1.50 mmol, 3.0 equiv). Purification by column

chromatography (*n*-hexane/EtOAc: 12/1) yielded **203bg** (50.0 mg, 0.25 mmol, 50%) as a colorless oil. The connectivity was determined by 2D NMR spectroscopy.

**<sup>1</sup>H-NMR** (300 MHz, CDCl<sub>3</sub>):  $\delta$  = 7.92 (dd, *J* = 2.5, 0.6 Hz, 1H), 7.73 (dd, *J* = 1.8, 0.7 Hz, 1H), 7.56 (d, *J* = 1.9 Hz, 1H), 7.47 (ddd, *J* = 8.0, 2.2, 1.1 Hz, 1H), 7.36 (dd, *J* = 7.8, 7.8 Hz, 1H), 7.12 (dddd, *J* = 7.6, 1.4, 1.4, 0.5 Hz, 1H), 6.46 (dd, *J* = 2.5, 1.8 Hz, 1H), 2.68 (tq, *J* = 7.0 Hz, 1H), 1.64 (qd, *J* = 7.4, 7.0 Hz, 2H), 1.28 (d, *J* = 6.9 Hz, 3H), 0.85 (t, *J* = 7.4 Hz, 3H). **<sup>13</sup>C-NMR** (75 MHz, CDCl<sub>3</sub>):  $\delta$  = 149.6 (C<sub>q</sub>), 141.0 (CH), 140.4 (C<sub>q</sub>), 129.3 (CH), 127.0 (CH), 125.4 (CH), 118.4 (CH), 116.8 (CH), 107.5 (CH), 41.9 (CH), 31.2 (CH<sub>2</sub>), 21.9 (CH<sub>3</sub>), 12.4 (CH<sub>3</sub>). **IR** (ATR): 2961, 1591, 1519, 1392, 1042, 945, 787, 770, 744, 698 cm<sup>-1</sup>. **MS** (ESI) *m/z* (relative intensity): 223 (7) [M+Na]<sup>+</sup>, 201 (100) [M+H]<sup>+</sup>. **HR-MS** (ESI): *m/z* calcd for C<sub>13</sub>H<sub>16</sub>N<sub>2</sub>, [M+H]<sup>+</sup> 201.1386, found 201.1388.

### 1-[3-(Pentan-2-yl)phenyl]-1*H*-pyrazole (**203bh**)

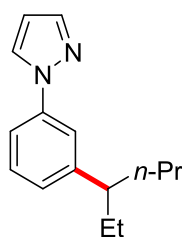


**203bh**

The general procedure **H** was followed using acid **196b** (94.1 mg, 0.50 mmol, 1.0 equiv) and 2-bromopentane (**11h**) (227 mg, 1.50 mmol, 3.0 equiv). Purification by column chromatography (*n*-hexane/EtOAc: 12/1) yielded **203bh** (64.3 mg, 0.30 mmol, 60%) as a colorless oil. The connectivity was determined by 2D NMR spectroscopy.

**<sup>1</sup>H-NMR** (300 MHz, CDCl<sub>3</sub>):  $\delta$  = 7.92 (dd, *J* = 2.5, 0.6 Hz, 1H), 7.73 (dd, *J* = 1.8, 0.6 Hz, 1H), 7.56 (dd, *J* = 2.0, 2.0 Hz, 1H), 7.46 (ddd, *J* = 8.0, 2.3, 1.2 Hz, 1H), 7.36 (dd, *J* = 7.8, 7.8 Hz, 1H), 7.12 (ddd, *J* = 7.4, 1.4, 1.4 Hz, 1H), 6.46 (dd, *J* = 2.5, 1.8 Hz, 1H), 2.78 (tq, *J* = 7.0 Hz, 1H), 1.69–1.50 (m, 2H), 1.31–1.17 (m, 2H), 1.27 (d, *J* = 6.9 Hz, 3H), 0.88 (t, *J* = 7.3 Hz, 3H). **<sup>13</sup>C-NMR** (75 MHz, CDCl<sub>3</sub>):  $\delta$  = 149.9 (C<sub>q</sub>), 141.0 (CH), 140.4 (C<sub>q</sub>), 129.4 (CH), 127.0 (CH), 125.4 (CH), 118.3 (CH), 116.8 (CH), 107.5 (CH), 40.7 (CH<sub>2</sub>), 40.0 (CH), 22.3 (CH<sub>3</sub>), 21.0 (CH<sub>2</sub>), 14.3 (CH<sub>3</sub>). **IR** (ATR): 2957, 1609, 1591, 1519, 1392, 1042, 948, 787, 743, 699 cm<sup>-1</sup>. **MS** (ESI) *m/z* (relative intensity): 237 (5) [M+Na]<sup>+</sup>, 215 (100) [M+H]<sup>+</sup>. **HR-MS** (ESI): *m/z* calcd for C<sub>14</sub>H<sub>18</sub>N<sub>2</sub>, [M+H]<sup>+</sup> 215.1543, found 215.1549. The analytical data correspond with those reported in the literature.<sup>[114c]</sup>

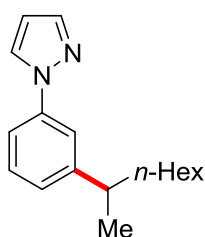
### 1-[3-(Hexan-3-yl)phenyl]-1*H*-pyrazole (**203bi**)

**203bi**

The general procedure **H** was followed using acid **196b** (94.1 mg, 0.50 mmol, 1.0 equiv) and 3-bromohexane (**11i**) (248 mg, 1.50 mmol, 3.0 equiv). Purification by column chromatography (*n*-hexane/EtOAc: 12/1) yielded **203bi** (67.4 mg, 0.30 mmol, 59%) as a yellow oil. The connectivity was determined by 2D NMR spectroscopy.

**<sup>1</sup>H-NMR** (300 MHz, CDCl<sub>3</sub>):  $\delta$  = 7.85 (dd,  $J$  = 2.5, 0.7 Hz, 1H), 7.65 (dd,  $J$  = 1.8, 0.6 Hz, 1H), 7.45 (dd,  $J$  = 2.2, 1.7 Hz, 1H), 7.39 (ddd,  $J$  = 8.0, 2.3, 1.1 Hz, 1H), 7.28 (dd,  $J$  = 7.8, 7.8 Hz, 1H), 7.00 (dddd,  $J$  = 7.6, 1.6, 1.1, 0.4 Hz, 1H), 6.39 (dd,  $J$  = 2.5, 1.8 Hz, 1H), 2.42 (tt,  $J$  = 9.1, 5.5 Hz, 1H), 1.70–1.43 (m, 4H), 1.17–1.04 (m, 2H), 0.78 (t,  $J$  = 7.3 Hz, 3H), 0.72 (t,  $J$  = 7.4 Hz, 3H). **<sup>13</sup>C-NMR** (75 MHz, CDCl<sub>3</sub>):  $\delta$  = 148.1 (C<sub>q</sub>), 141.0 (CH), 140.3 (C<sub>q</sub>), 129.2 (CH), 127.0 (CH), 126.1 (CH), 118.9 (CH), 116.8 (CH), 107.5 (CH), 47.9 (CH), 38.9 (CH<sub>2</sub>), 29.8 (CH<sub>2</sub>), 20.9 (CH<sub>2</sub>), 14.3 (CH<sub>3</sub>), 12.4 (CH<sub>3</sub>). **IR** (ATR): 2955, 1605, 1591, 1519, 1393, 1043, 946, 787, 746, 697 cm<sup>-1</sup>. **MS** (ESI)  $m/z$  (relative intensity): 251 (22) [M+Na]<sup>+</sup>, 229 (100) [M+H]<sup>+</sup>. **HR-MS** (ESI):  $m/z$  calcd for C<sub>15</sub>H<sub>20</sub>N<sub>2</sub>, [M+H]<sup>+</sup> 229.1699, found 229.1703.

#### 1-[3-(Octan-2-yl)phenyl]-1H-pyrazole (**203bj**)

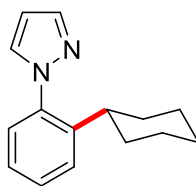
**203bj**

The general procedure **H** was followed using acid **196b** (94.1 mg, 0.50 mmol, 1.0 equiv) and 2-bromooctane (**11j**) (290 mg, 1.50 mmol, 3.0 equiv). Purification by column chromatography (*n*-hexane/EtOAc: 15/1) yielded **203bj** (91.0 mg, 0.36 mmol, 71%) as a yellow oil. The connectivity was determined by 2D NMR spectroscopy.

**<sup>1</sup>H-NMR** (300 MHz, CDCl<sub>3</sub>):  $\delta$  = 7.84 (dd,  $J$  = 2.5, 0.6 Hz, 1H), 7.65 (d,  $J$  = 1.6 Hz, 1H), 7.48 (dd,  $J$  = 2.0, 2.0 Hz, 1H), 7.38 (ddd,  $J$  = 8.0, 2.3, 1.1 Hz, 1H), 7.27 (dd,  $J$  = 7.8, 7.8

Hz, 1H), 7.03 (ddd,  $J = 7.6, 1.4, 1.4$  Hz, 1H), 6.37 (dd,  $J = 2.5, 1.8$  Hz, 1H), 2.67 (tq,  $J = 7.0$  Hz, 1H), 1.63–1.42 (m, 2H), 1.24–1.12 (m, 8H), 1.19 (d,  $J = 6.9$  Hz, 3H) 0.76 (t,  $J = 7.6$  Hz, 3H).  **$^{13}\text{C-NMR}$**  (75 MHz,  $\text{CDCl}_3$ ):  $\delta = 149.9$  ( $\text{C}_q$ ), 141.0 (CH), 140.4 ( $\text{C}_q$ ), 129.3 (CH), 127.0 (CH), 125.3 (CH), 118.3 (CH), 116.8 (CH), 107.5 (CH), 40.2 (CH), 38.5 ( $\text{CH}_2$ ), 31.9 ( $\text{CH}_2$ ), 29.5 ( $\text{CH}_2$ ), 27.8 ( $\text{CH}_2$ ), 22.8 ( $\text{CH}_2$ ), 22.4 ( $\text{CH}_3$ ), 14.2 ( $\text{CH}_3$ ). **IR** (ATR): 2950, 1600, 1591, 1519, 1392, 1040, 947, 787, 745, 699  $\text{cm}^{-1}$ . **MS** (ESI)  $m/z$  (relative intensity): 279 (27)  $[\text{M}+\text{Na}]^+$ , 257 (100)  $[\text{M}+\text{H}]^+$ . **HR-MS** (ESI):  $m/z$  calcd for  $\text{C}_{17}\text{H}_{24}\text{N}_2$ ,  $[\text{M}+\text{H}]^+$  257.2012, found 257.2009.

### 1-(2-Cyclohexylphenyl)-1*H*-pyrazole (203bk)

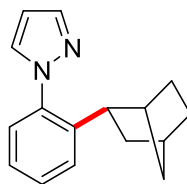


**203bk**

The general procedure **H** was followed using acid **196b** (94.1 mg, 0.50 mmol, 1.0 equiv) and cyclohexyl bromide (**11k**) (245 mg, 1.50 mmol, 3.0 equiv). Purification by column chromatography (*n*-hexane/EtOAc: 12/1) yielded **203bk** (84.9 mg, 0.38 mmol, 75%) as a colorless oil. The connectivity was determined by 2D NMR spectroscopy.

**$^1\text{H-NMR}$**  (300 MHz,  $\text{CDCl}_3$ ):  $\delta = 7.64$  (dd,  $J = 1.8, 0.7$  Hz, 1H), 7.47 (dd,  $J = 2.3, 0.7$  Hz, 1H), 7.36–7.30 (m, 2H), 7.21–7.16 (m, 2H), 6.36 (dd,  $J = 2.1, 2.1$  Hz, 1H), 2.36 (tt,  $J = 12.0, 3.1$  Hz, 1H), 1.76–1.56 (m, 5H), 1.42–1.24 (m, 2H), 1.22–1.07 (m, 3H).  **$^{13}\text{C-NMR}$**  (75 MHz,  $\text{CDCl}_3$ ):  $\delta = 144.2$  ( $\text{C}_q$ ), 140.2 (CH), 139.2 ( $\text{C}_q$ ), 131.2 (CH), 129.1 (CH), 127.3 (CH), 127.1 (CH), 126.3 (CH), 106.1 (CH), 38.4 (CH), 34.4 ( $\text{CH}_2$ ), 26.9 ( $\text{CH}_2$ ), 26.2 ( $\text{CH}_2$ ). **IR** (ATR): 2922, 2850, 1719, 1447, 1262, 1170, 1083, 912, 827, 741  $\text{cm}^{-1}$ . **MS** (ESI)  $m/z$  (relative intensity): 249 (2)  $[\text{M}+\text{Na}]^+$ , 227 (100)  $[\text{M}+\text{H}]^+$ . **HR-MS** (ESI):  $m/z$  calcd for  $\text{C}_{15}\text{H}_{18}\text{N}_2$ ,  $[\text{M}+\text{H}]^+$  227.1543, found 227.1548.

### 1-(*exo*-2-Norbornylphenyl)-1*H*-pyrazole (203bl)

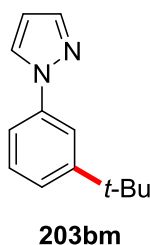


**203bl**

The general procedure **H** was followed using acid **196b** (94.1 mg, 0.50 mmol, 1.0 equiv) and *exo*-2-norbornyl bromide (**11l**) (263 mg, 1.50 mmol, 3.0 equiv). Purification by column chromatography (*n*-hexane/EtOAc: 20/1) yielded **203bl** (78.6 mg, 0.33 mmol, 66%) as a pale yellow oil. The connectivity was determined by 2D NMR spectroscopy. The connectivity was determined by 2D NMR spectroscopy.

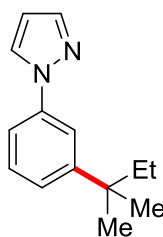
**<sup>1</sup>H-NMR** (500 MHz, CDCl<sub>3</sub>):  $\delta$  = 7.70 (d,  $J$  = 1.8 Hz, 1H), 7.53 (d,  $J$  = 2.3 Hz, 1H), 7.41 (d,  $J$  = 8.4 Hz, 1H), 7.36 (ddd,  $J$  = 8.0, 6.4, 2.3 Hz, 1H), 7.26–7.22 (m, 2H), 6.41 (dd,  $J$  = 2.1, 2.1 Hz, 1H), 2.67 (dd,  $J$  = 9.1, 5.7 Hz, 1H), 2.31 (s<sub>br</sub>, 1H), 2.25 (s<sub>br</sub>, 1H), 1.56 (dq,  $J$  = 9.9, 2.0 Hz, 1H), 1.50–1.42 (m, 3H), 1.36 (ddd,  $J$  = 12.1, 8.9, 2.4 Hz, 1H), 1.18 (ddd,  $J$  = 10.0, 2.5, 1.4 Hz, 1H), 1.16–1.06 (m, 2H). **<sup>13</sup>C-NMR** (75 MHz, CDCl<sub>3</sub>):  $\delta$  = 144.0 (C<sub>q</sub>), 140.3 (CH), 139.9 (C<sub>q</sub>), 131.2 (CH), 128.9 (CH), 127.3 (CH), 126.7 (CH), 126.1 (CH), 106.1 (CH), 42.6 (CH), 41.8 (CH), 39.6 (CH<sub>2</sub>), 37.0 (CH), 36.5 (CH<sub>2</sub>), 30.6 (CH<sub>2</sub>), 28.7 (CH<sub>2</sub>). **IR** (ATR): 2952, 2870, 1601, 1510, 1449, 1400, 1330, 1039, 941, 747 cm<sup>-1</sup>. **MS** (ESI)  $m/z$  (relative intensity): 261 (2) [M+Na]<sup>+</sup>, 239 (100) [M+H]<sup>+</sup>. **HR-MS** (ESI):  $m/z$  calcd for C<sub>16</sub>H<sub>18</sub>N<sub>2</sub>, [M+H]<sup>+</sup> 239.1543, found 239.1545. The analytical data correspond with those reported in the literature.<sup>[185]</sup>

#### 1-[3-(*tert*-Butyl)phenyl]-1*H*-pyrazole (**203bm**)



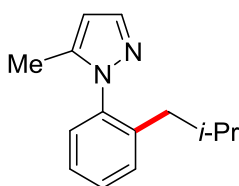
The general procedure **H** was followed using acid **196b** (94.1 mg, 0.50 mmol, 1.0 equiv) and *tert*-butyl bromide (**11m**) (206 mg, 1.50 mmol, 3.0 equiv). Purification by column chromatography (*n*-hexane/EtO Ac: 12/1) yielded **203bm** (66.1 mg, 0.33 mmol, 66%) as a colorless oil.

**<sup>1</sup>H-NMR** (300 MHz, CDCl<sub>3</sub>):  $\delta$  = 7.92 (dd,  $J$  = 2.5, 0.7 Hz, 1H), 7.76 (ddd,  $J$  = 2.0, 0.6, 0.6 Hz, 1H), 7.73 (dd,  $J$  = 1.8, 0.6 Hz, 1H), 7.45 (ddd,  $J$  = 7.6, 2.1, 1.6 Hz, 1H), 7.38 (ddd,  $J$  = 7.7, 7.7, 0.6 Hz, 1H), 7.33 (ddd,  $J$  = 7.7, 1.7, 1.7 Hz, 1H), 6.46 (dd,  $J$  = 2.5, 1.8 Hz, 1H), 1.38 (s, 9H). **<sup>13</sup>C-NMR** (75 MHz, CDCl<sub>3</sub>):  $\delta$  = 153.1 (C<sub>q</sub>), 141.0 (CH), 140.3 (C<sub>q</sub>), 129.1 (CH), 127.1 (CH), 123.8 (CH), 117.0 (CH), 116.6 (CH), 107.5 (CH), 35.1 (C<sub>q</sub>), 31.4 (CH<sub>3</sub>). **IR** (ATR): 2962, 1608, 1589, 1518, 1467, 1391, 1043, 947, 745, 698 cm<sup>-1</sup>. **MS** (ESI)  $m/z$  (relative intensity): 223 (16) [M+Na]<sup>+</sup>, 201 (100) [M+H]<sup>+</sup>. **HR-MS** (ESI):  $m/z$  calcd for C<sub>13</sub>H<sub>16</sub>N<sub>2</sub>, [M+H]<sup>+</sup> 201.1386, found 201.1393.

**1-[3-(*tert*-Pentyl)phenyl]-1*H*-pyrazole (203bn)****203bn**

The general procedure **H** was followed using acid **196b** (94.1 mg, 0.50 mmol, 1.0 equiv) and 2-bromo-2-methylbutane bromide (**11n**) (227 mg, 1.50 mmol, 3.0 equiv). Purification by column chromatography (*n*-hexane/EtOAc: 12/1) yielded **203bn** (58.9 mg, 0.28 mmol, 55%) as a colorless oil.

**<sup>1</sup>H-NMR** (300 MHz, CDCl<sub>3</sub>):  $\delta$  = 7.92 (dd,  $J$  = 2.4, 0.7 Hz, 1H), 7.73 (dd,  $J$  = 1.8, 0.7 Hz, 1H), 7.69 (dd,  $J$  = 2.0, 0.5 Hz, 1H), 7.45 (ddd,  $J$  = 7.9, 2.1, 1.3 Hz, 1H), 7.37 (ddd,  $J$  = 7.8, 7.8, 0.5 Hz, 1H), 7.28 (ddd,  $J$  = 7.6, 1.9, 1.3 Hz, 1H), 6.46 (dd,  $J$  = 2.5, 1.8 Hz, 1H), 1.70 (q,  $J$  = 7.4 Hz, 2H), 1.33 (s, 6H), 0.71 (t,  $J$  = 7.4 Hz, 3H). **<sup>13</sup>C-NMR** (75 MHz, CDCl<sub>3</sub>):  $\delta$  = 151.5 (C<sub>q</sub>), 141.0 (CH), 140.3 (C<sub>q</sub>), 129.0 (CH), 127.1 (CH), 124.5 (CH), 117.6 (CH), 116.6 (CH), 107.5 (CH), 38.4 (C<sub>q</sub>), 37.0 (CH<sub>2</sub>), 28.6 (CH<sub>3</sub>), 9.3 (CH<sub>3</sub>). **IR** (ATR): 2964, 1608, 1589, 1518, 1486, 1392, 1043, 788, 745, 700 cm<sup>-1</sup>. **MS** (ESI)  $m/z$  (relative intensity): 237 (16) [M+Na]<sup>+</sup>, 215 (100) [M+H]<sup>+</sup>. **HR-MS** (ESI):  $m/z$  calcd for C<sub>14</sub>H<sub>18</sub>N<sub>2</sub>, [M+H]<sup>+</sup> 215.1543, found 215.1549.

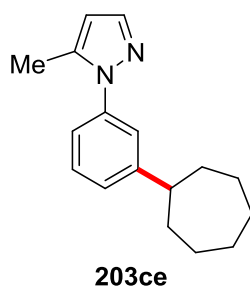
**1-(2-Isobutylphenyl)-5-methyl-1*H*-pyrazole (203cb)****203cb**

The general procedure **H** was followed using acid **196c** (101 mg, 0.50 mmol, 1.0 equiv) and 1-bromo-2-methylpropane (**11b**) (206 mg, 1.50 mmol, 3.0 equiv). Purification by column chromatography (*n*-hexane/EtOAc: 12/1) yielded **203cb** (87.9 mg, 0.41 mmol, 82%) as a yellow oil.

**<sup>1</sup>H-NMR** (300 MHz, CDCl<sub>3</sub>):  $\delta$  = 7.47 (d,  $J$  = 1.8 Hz, 1H), 7.30–7.24 (m, 1H), 7.23–7.19 (m, 1H), 7.16 (dd,  $J$  = 6.8, 2.2 Hz, 1H), 7.09 (ddd,  $J$  = 7.7, 1.5, 0.6 Hz, 1H), 6.06 (dq,  $J$  = 1.6, 0.7 Hz, 1H), 2.19 (d,  $J$  = 7.3 Hz, 2H), 2.00 (d,  $J$  = 0.6 Hz, 3H), 1.66–1.44 (m, 1H),

0.67 (d,  $J = 6.6$  Hz, 6H).  $^{13}\text{C-NMR}$  (75 MHz,  $\text{CDCl}_3$ ):  $\delta = 139.7$  ( $\text{C}_q$ ), 139.4 ( $\text{C}_q$ ), 139.2 (CH), 138.6 ( $\text{C}_q$ ), 130.9 (CH), 128.8 (CH), 127.9 (CH), 126.4 (CH), 105.1 (CH), 40.4 ( $\text{CH}_2$ ), 28.8 (CH), 22.5 ( $\text{CH}_3$ ), 11.5 ( $\text{CH}_3$ ). **IR** (ATR): 2956, 2868, 1500, 1455, 1392, 1202, 1017, 923, 767, 738  $\text{cm}^{-1}$ . **MS** (ESI)  $m/z$  (relative intensity): 237 (10)  $[\text{M}+\text{Na}]^+$ , 215 (100)  $[\text{M}+\text{H}]^+$ . **HR-MS** (ESI):  $m/z$  calcd for  $\text{C}_{14}\text{H}_{18}\text{N}_2$ ,  $[\text{M}+\text{H}]^+$  215.1543, found 289.1541.

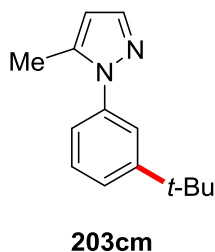
### 1-(3-Cycloheptylphenyl)-5-methyl-1H-pyrazole (203ce)



The general procedure **H** was followed using acid **196c** (101 mg, 0.50 mmol, 1.0 equiv) and cycloheptyl bromide (**11e**) (266 mg, 1.50 mmol, 3.0 equiv). Purification by column chromatography (*n*-hexane/EtOAc: 14/1) yielded **203ce** (97.9 mg, 0.39 mmol, 77%) as a yellow oil.

$^1\text{H-NMR}$  (300 MHz,  $\text{CDCl}_3$ ):  $\delta = 7.56$  (d,  $J = 1.8$  Hz, 1H), 7.33 (dd,  $J = 7.8, 7.8$  Hz, 1H), 7.30 (dd,  $J = 2.0, 2.0$  Hz, 1H), 7.26–7.14 (m, 2H), 6.17 (ddd,  $J = 1.6, 0.8, 0.8$  Hz, 1H), 2.73 (tt,  $J = 10.4, 3.6$  Hz, 1H), 2.33 (d,  $J = 0.8$  Hz, 3H), 2.02–1.89 (m, 2H), 1.86–1.74 (m, 2H), 1.74–1.49 (m, 8H).  $^{13}\text{C-NMR}$  (75 MHz,  $\text{CDCl}_3$ ):  $\delta = 151.2$  ( $\text{C}_q$ ), 139.8 ( $\text{C}_q$ ), 139.6 (CH), 138.5 ( $\text{C}_q$ ), 128.8 (CH), 126.0 (CH), 123.3 (CH), 121.9 (CH), 106.7 (CH), 46.9 (CH), 36.7 ( $\text{CH}_2$ ), 27.9 ( $\text{CH}_2$ ), 27.2 ( $\text{CH}_2$ ), 12.4 ( $\text{CH}_3$ ). **IR** (ATR): 2921, 2853, 1606, 1590, 1491, 1444, 1386, 921, 790, 703  $\text{cm}^{-1}$ . **MS** (ESI)  $m/z$  (relative intensity): 255 (100)  $[\text{M}+\text{H}]^+$ . **HR-MS** (ESI):  $m/z$  calcd for  $\text{C}_{17}\text{H}_{22}\text{N}_2$ ,  $[\text{M}+\text{H}]^+$  255.1856, found 255.1856.

### 1-[3-(*tert*-butyl)phenyl]-5-methyl-1H-pyrazole (203cm)



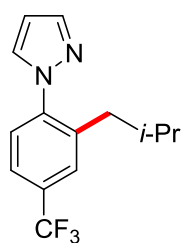
The general procedure **H** was followed using acid **196c** (101 mg, 0.50 mmol, 1.0 equiv) and *tert*-butyl bromide (**11m**) (206 mg, 1.50 mmol, 3.0 equiv). Purification by column



chromatography (*n*-hexane/EtOAc: 12/1) yielded **203cm** (65.4 mg, 0.31 mmol, 61%) as a yellow oil.

**<sup>1</sup>H-NMR** (300 MHz, CDCl<sub>3</sub>):  $\delta$  = 7.49 (d, *J* = 1.8 Hz, 1H), 7.38 (ddd, *J* = 1.8, 0.7, 0.7 Hz, 1H), 7.32 (ddd, *J* = 7.9, 1.9, 1.9 Hz, 1H), 7.28 (ddd, *J* = 7.9, 7.9, 0.7 Hz, 1H), 7.14 (ddd, *J* = 7.9, 2.1, 2.1 Hz, 1H), 6.10 (dq, *J* = 1.5, 0.7 Hz, 1H), 2.25 (t, *J* = 0.6 Hz, 3H), 1.26 (s, 9H). **<sup>13</sup>C-NMR** (75 MHz, CDCl<sub>3</sub>):  $\delta$  = 152.5 (C<sub>q</sub>), 139.7 (C<sub>q</sub>), 139.7 (CH), 138.7 (C<sub>q</sub>), 128.6 (CH), 124.7 (CH), 122.3 (CH), 122.0 (CH), 106.8 (CH), 34.9 (C<sub>q</sub>), 31.3 (CH<sub>3</sub>), 12.5 (CH<sub>3</sub>). **IR** (ATR): 2962, 1607, 1588, 1492, 1438, 1383, 922, 793, 774, 703 cm<sup>-1</sup>. **MS** (ESI) *m/z* (relative intensity): 237 (7) [M+Na]<sup>+</sup>, 215 (100) [M+H]<sup>+</sup>. **HR-MS** (ESI): *m/z* calcd for C<sub>14</sub>H<sub>18</sub>N<sub>2</sub>, [M+H]<sup>+</sup> 215.1543, found 215.1550.

### 1-[2-Isobutyl-4-(trifluoromethyl)phenyl]-1*H*-pyrazole (**203db**)

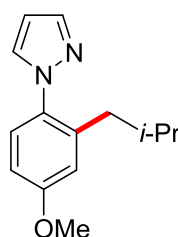


**203db**

The general procedure **H** was followed using acid **196d** (128 mg, 0.50 mmol, 1.0 equiv) and 1-bromo-2-methylpropane (**11b**) (206 mg, 1.50 mmol, 3.0 equiv). Purification by column chromatography (*n*-hexane/EtOAc: 9/1) yielded **203db** (118 mg, 0.44 mmol, 88%) as a colorless oil.

**<sup>1</sup>H-NMR** (300 MHz, CDCl<sub>3</sub>):  $\delta$  = 7.74 (dd, *J* = 1.9, 0.7 Hz, 1H), 7.60 (dd, *J* = 2.4, 0.7 Hz, 1H), 7.58–7.52 (m, 2H), 7.41 (ddd, *J* = 8.0, 0.9, 0.9 Hz, 1H), 6.46 (dd, *J* = 2.4, 1.9 Hz, 1H), 2.58 (d, *J* = 7.2 Hz, 2H), 1.73–1.48 (m, 1H), 0.77 (d, *J* = 6.6 Hz, 6H). **<sup>13</sup>C-NMR** (75 MHz, CDCl<sub>3</sub>):  $\delta$  = 142.8 (C<sub>q</sub>), 140.9 (CH), 138.7 (C<sub>q</sub>), 130.8 (CH), 130.5 (q, <sup>2</sup>*J*<sub>C-F</sub> = 32.5 Hz, C<sub>q</sub>), 128.4 (q, <sup>3</sup>*J*<sub>C-F</sub> = 3.7 Hz, CH), 127.1 (CH), 123.9 (q, <sup>1</sup>*J*<sub>C-F</sub> = 272 Hz, C<sub>q</sub>), 123.8 (q, <sup>3</sup>*J*<sub>C-F</sub> = 3.7 Hz, CH), 106.9 (CH), 40.7 (CH<sub>2</sub>), 29.2 (CH), 22.4 (CH<sub>3</sub>). **<sup>19</sup>F-NMR** (282 MHz, CDCl<sub>3</sub>):  $\delta$  = –62.58. **IR** (ATR): 2959, 1394, 1330, 1165, 1124, 1109, 1094, 938, 834, 750 cm<sup>-1</sup>. **MS** (ESI) *m/z* (relative intensity): 269 (100) [M+H]<sup>+</sup>. **HR-MS** (ESI): *m/z* calcd for C<sub>14</sub>H<sub>15</sub>F<sub>3</sub>N<sub>2</sub>, [M+H]<sup>+</sup> 269.1260, found 269.1262.

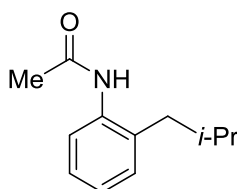
### 1-(2-Isobutyl-4-methoxyphenyl)-1*H*-pyrazole (**203eb**)

**203eb**

The general procedure **H** was followed using acid **196e** (109 mg, 0.50 mmol, 1.0 equiv) and 1-bromo-2-methylpropane (**11b**) (206 mg, 1.50 mmol, 3.0 equiv). Purification by column chromatography (*n*-hexane/EtOAc: 8/1) yielded **203eb** (104 mg, 0.45 mmol, 90%) as a yellow oil.

**<sup>1</sup>H-NMR** (400 MHz, CDCl<sub>3</sub>):  $\delta$  = 7.66 (dd, *J* = 1.9, 0.7 Hz, 1H), 7.49 (dd, *J* = 2.3, 0.7 Hz, 1H), 7.19 (dd, *J* = 8.3, 0.6 Hz, 1H), 6.80 (dd, *J* = 2.9, 0.6 Hz, 1H), 6.77 (dd, *J* = 8.4, 2.9 Hz, 1H), 6.38 (dd, *J* = 2.3, 1.9 Hz, 1H), 3.82 (s, 3H), 2.37 (d, *J* = 7.3 Hz, 2H), 1.68–1.49 (m, 1H), 0.76 (d, *J* = 6.6 Hz, 6H). **<sup>13</sup>C-NMR** (101 MHz, CDCl<sub>3</sub>):  $\delta$  = 159.4 (C<sub>q</sub>), 139.9 (CH), 139.7 (C<sub>q</sub>), 133.5 (C<sub>q</sub>), 131.1 (CH), 128.0 (CH), 116.2 (CH), 111.4 (CH), 105.6 (CH), 55.5 (CH<sub>3</sub>), 40.7 (CH<sub>2</sub>), 29.2 (CH), 22.5 (CH<sub>3</sub>). **IR** (ATR): 2955, 1518, 1464, 1244, 1161, 1041, 941, 822, 748, 613 cm<sup>-1</sup>. **MS** (ESI) *m/z* (relative intensity): 231 (100) [M+H]<sup>+</sup>, 215 (2) [M-Me]<sup>+</sup>. **HR-MS** (ESI): *m/z* calcd for C<sub>14</sub>H<sub>18</sub>N<sub>2</sub>O, [M+H]<sup>+</sup> 231.1492, found 231.1496.

#### ***N*-(2-Isobutylphenyl)acetamide (209cb)**

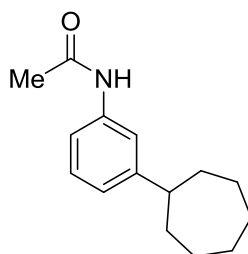
**209cb**

The general procedure **G** was followed using pyrazole **203cb** (42.9 mg, 0.20 mmol, 1.0 equiv) with a reaction time of 40 min. Purification by column chromatography (*n*-hexane/EtOAc: 2/1) yielded **209cb** (27.2 mg, 0.14 mmol, 71%) as a colorless solid.

**M.p.:** 90–92 °C **<sup>1</sup>H-NMR** (300 MHz, CDCl<sub>3</sub>):  $\delta$  = 7.73 (d, *J* = 8.0 Hz, 1H), 7.21 (ddd, *J* = 7.8, 7.4, 2.2 Hz, 1H), 7.16–7.06 (m, 2H), 6.97 (s<sub>br</sub>, 1H), 2.44 (d, *J* = 7.2 Hz, 2H), 2.18 (s, 3H), 1.91–1.80 (m, 1H), 0.93 (d, *J* = 6.6 Hz, 6H). **<sup>13</sup>C-NMR** (126 MHz, CDCl<sub>3</sub>):  $\delta$  = 168.4 (C<sub>q</sub>), 135.3 (C<sub>q</sub>), 133.0 (C<sub>q</sub>), 130.6 (CH), 126.8 (CH), 125.4 (CH), 124.4 (CH), 41.0 (CH<sub>2</sub>), 29.4 (CH), 24.5 (CH<sub>3</sub>), 22.8 (CH<sub>3</sub>). **IR** (ATR): 3297, 2955, 1654, 1527, 1447, 1364, 749,

739, 697, 546  $\text{cm}^{-1}$ . **MS** (ESI)  $m/z$  (relative intensity): 405 (11)  $[2\text{M}+\text{Ma}]^+$ , 215 (71)  $[\text{M}+\text{Na}]^+$ , 192 (100)  $[\text{M}+\text{H}]^+$ . **HR-MS** (ESI):  $m/z$  calcd for  $\text{C}_{12}\text{H}_{17}\text{NO}$ ,  $[\text{M}+\text{H}]^+$  192.1383, found 192.1380.

#### ***N*-(3-Cycloheptylphenyl)acetamide (209ce)**

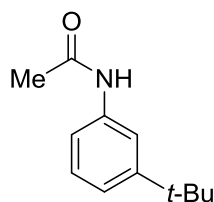


**209ce**

The general procedure **G** was followed using pyrazole **203ce** (50.9 mg, 0.20 mmol, 1.0 equiv) with a reaction time of 40 min. Purification by column chromatography (*n*-hexane/EtOAc: 2/1) yielded **209ce** (30.0 mg, 0.13 mmol, 65%) as a pale yellow solid.

**M.p.:** 118–120 °C.  **$^1\text{H-NMR}$**  (400 MHz,  $\text{CDCl}_3$ ):  $\delta$  = 7.42 ( $s_{\text{br}}$ , 1H), 7.34 (dd,  $J$  = 2.1, 1.9 Hz, 1H), 7.30 (ddd,  $J$  = 7.8, 2.1, 1.1 Hz, 1H), 7.20 (dd,  $J$  = 7.8, 7.8 Hz, 1H), 6.93 (ddd,  $J$  = 7.8, 2.9, 1.1 Hz, 1H), 2.63 (tt,  $J$  = 10.5, 3.6 Hz, 1H), 2.15 (s, 3H), 1.98–1.84 (m, 2H), 1.77 (ddq,  $J$  = 12.8, 6.5, 3.1 Hz, 2H), 1.71 – 1.47 (m, 8H).  **$^{13}\text{C-NMR}$**  (101 MHz,  $\text{CDCl}_3$ ):  $\delta$  = 168.5 ( $\text{C}_q$ ), 151.2 ( $\text{C}_q$ ), 138.0 ( $\text{C}_q$ ), 129.0 (CH), 122.8 (CH), 118.4 (CH), 117.3 (CH), 47.1 (CH), 36.8 ( $\text{CH}_2$ ), 28.0 ( $\text{CH}_2$ ), 27.3 ( $\text{CH}_2$ ), 24.7 ( $\text{CH}_3$ ). **IR** (ATR): 3298, 2923, 1656, 1529, 1446, 1366, 749, 739, 696, 537  $\text{cm}^{-1}$ . **MS** (ESI)  $m/z$  (relative intensity): 485 (52)  $[2\text{M}+\text{Na}]^+$ , 463 (9)  $[2\text{M}+\text{H}]^+$ , 254 (89)  $[\text{M}+\text{Na}]^+$ , 232 (100)  $[\text{M}+\text{H}]^+$ . **HR-MS** (ESI):  $m/z$  calcd for  $\text{C}_{15}\text{H}_{21}\text{NO}$ ,  $[\text{M}+\text{H}]^+$  232.1696, found 232.1700.

#### ***N*-[3-(*tert*-Butyl)phenyl]acetamide (209cm)**



**209cm**

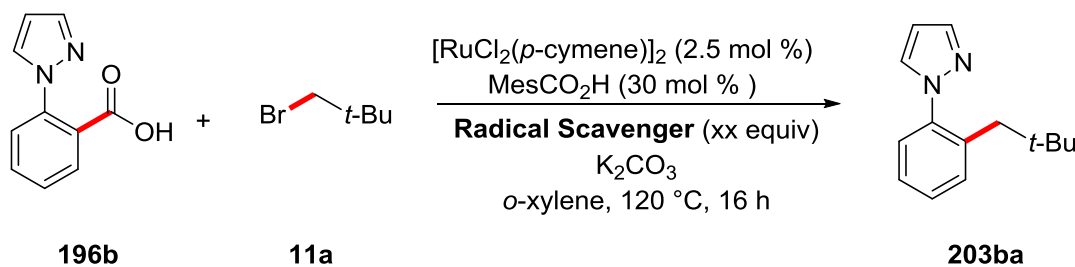
The general procedure **G** was followed using pyrazole **203cm** (42.9 mg, 0.20 mmol, 1.0 equiv) with a reaction time of 40 min. Purification by column chromatography (*n*-hexane/EtOAc: 2/1) yielded **209cm** (23.3 mg, 0.12 mmol, 61%) as a colorless solid.

**M.p.:** 97–99 °C. **<sup>1</sup>H-NMR** (300 MHz, CDCl<sub>3</sub>):  $\delta$  = 7.44 (dd,  $J$  = 1.9, 1.9 Hz, 1H), 7.40 (ddd,  $J$  = 8.0, 1.8, 1.3 Hz, 1H), 7.26 (s<sub>br</sub>, 1H), 7.25 (dd,  $J$  = 7.9, 7.9 Hz, 1H), 7.14 (ddd,  $J$  = 7.9, 1.9, 1.2 Hz, 1H), 2.17 (s, 3H), 1.31 (s, 9H). **<sup>13</sup>C-NMR** (75 MHz, CDCl<sub>3</sub>):  $\delta$  = 168.4 (C<sub>q</sub>), 152.3 (C<sub>q</sub>), 137.8 (C<sub>q</sub>), 128.8 (CH), 121.6 (CH), 117.4 (CH), 117.2 (CH), 34.9 (C<sub>q</sub>), 31.4 (CH<sub>3</sub>), 24.8 (CH<sub>3</sub>). **IR** (ATR): 3295, 2960, 1657, 1606, 1547, 1489, 1312, 1263, 787, 697 cm<sup>-1</sup>. **MS** (ESI)  $m/z$  (relative intensity): 405 (9) [2M+Na]<sup>+</sup>, 383 (2) [2M+H]<sup>+</sup>, 214 (38) [M+Na]<sup>+</sup>, 192 (100) [M+H]<sup>+</sup>. **HR-MS** (ESI):  $m/z$  calcd for C<sub>12</sub>H<sub>17</sub>NO, [M+H]<sup>+</sup> 192.1383, found 192.1383. The analytical data correspond with those reported in the literature.<sup>[186]</sup>

## 5.7.2 Mechanistic Studies

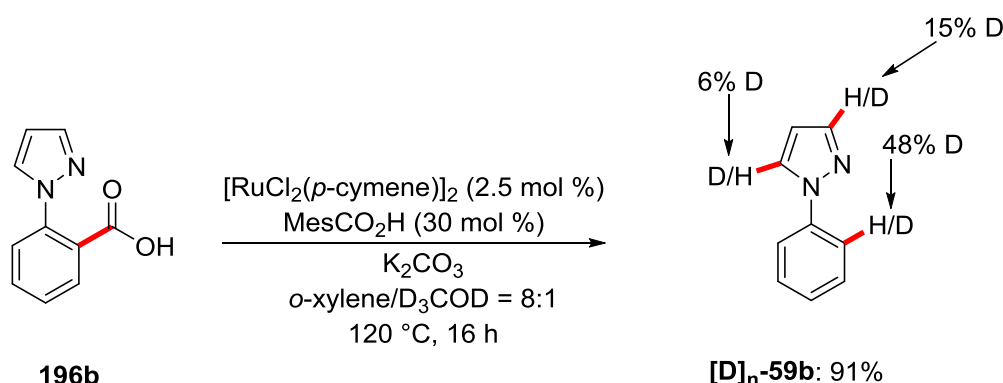
### Reaction with Radical Scavengers

The general procedure **H** was followed using acid **196b** (94.1 mg, 0.50 mmol, 1.0 equiv), neopentyl bromide (**11a**) (227 mg, 1.50 mmol, 3.0 equiv) and a radical scavenger (0.1 or 1.0 equiv). Purification by column chromatography (*n*-hexane/EtOAc: 12/1) gave the reaction product **203ba** in the indicated yields.

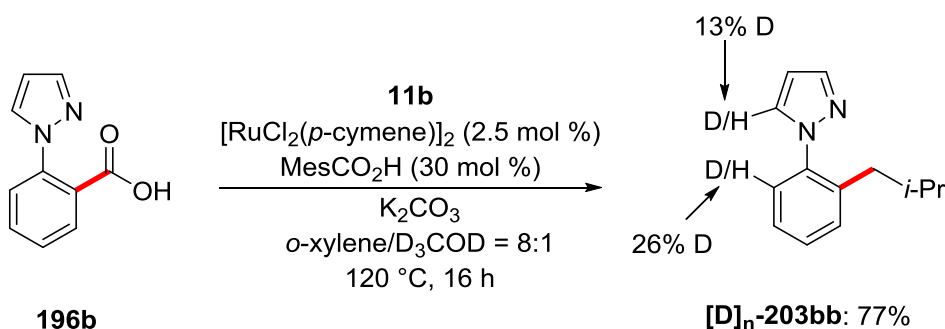


Entry	Radical Scavenger	Equiv	Isolated Yield
1	---	---	95%
2	BHT	0.1	90%
3	BHT	1.0	61%
4	TEMPO	0.1	22%
5	TEMPO	1.0	---
6	air	---	---

### Organometallic $\sigma$ -C–C Activation

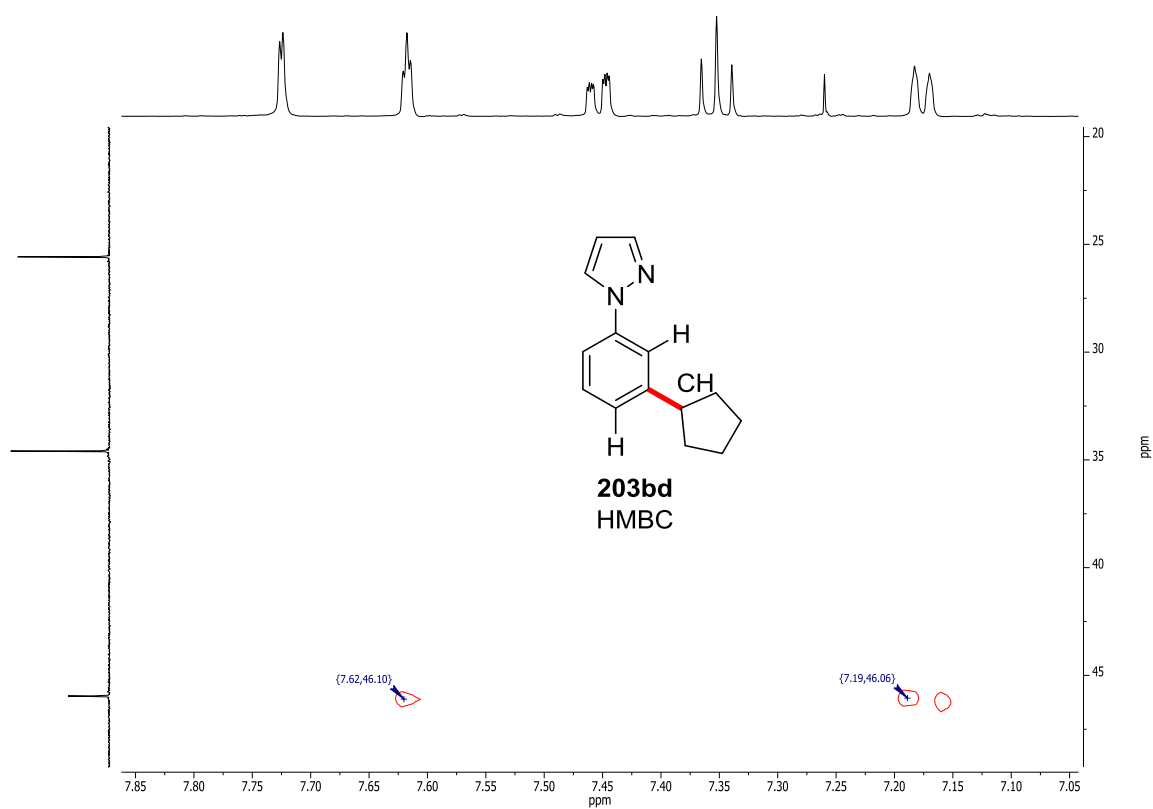
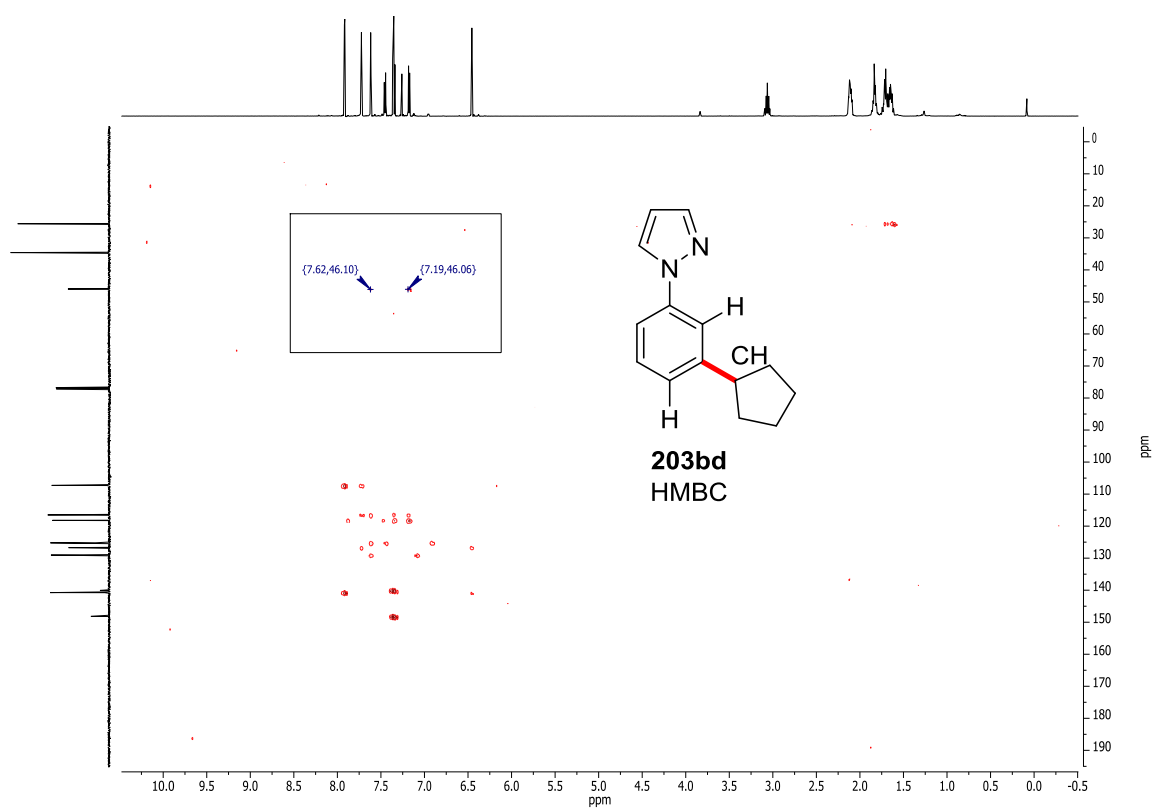


To a Schlenk tube charged with acid **196b** (94.1 mg, 0.50  $\mu\text{mol}$ , 1.0 equiv),  $[\text{RuCl}_2(\textit{p}\text{-cymene})]_2$  (7.7 mg, 13  $\mu\text{mol}$ , 2.5 mol %),  $\text{MesCO}_2\text{H}$  (24.6 mg, 150  $\mu\text{mol}$ , 30 mol %) and  $\text{K}_2\text{CO}_3$  (138 mg, 1.00 mmol, 2.0 equiv) was added *o*-xylene (1.0 mL) and  $\text{CD}_3\text{OD}$  (0.2 mL). The Schlenk tube was degassed and filled with  $\text{N}_2$  for three times and the mixture was stirred at 120  $^\circ\text{C}$  for 16 h. Removal of the solvent under reduced pressure and purification of the residue by column chromatography on silica gel (*n*-hexane/EtOAc: 10/1) yielded  $[\text{D}]_n\text{-59b}$  (66.3 mg, 0.46 mmol, 91%). The deuteration was determined by  $^1\text{H}$ -NMR spectroscopy.

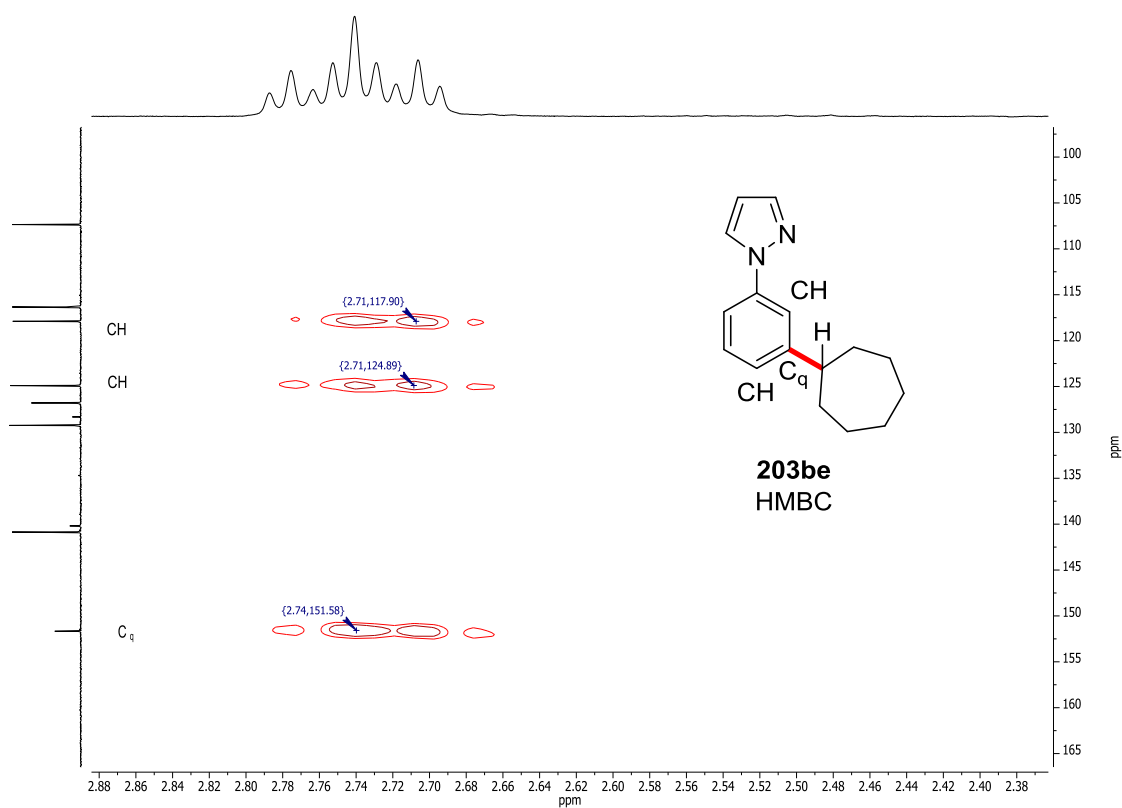
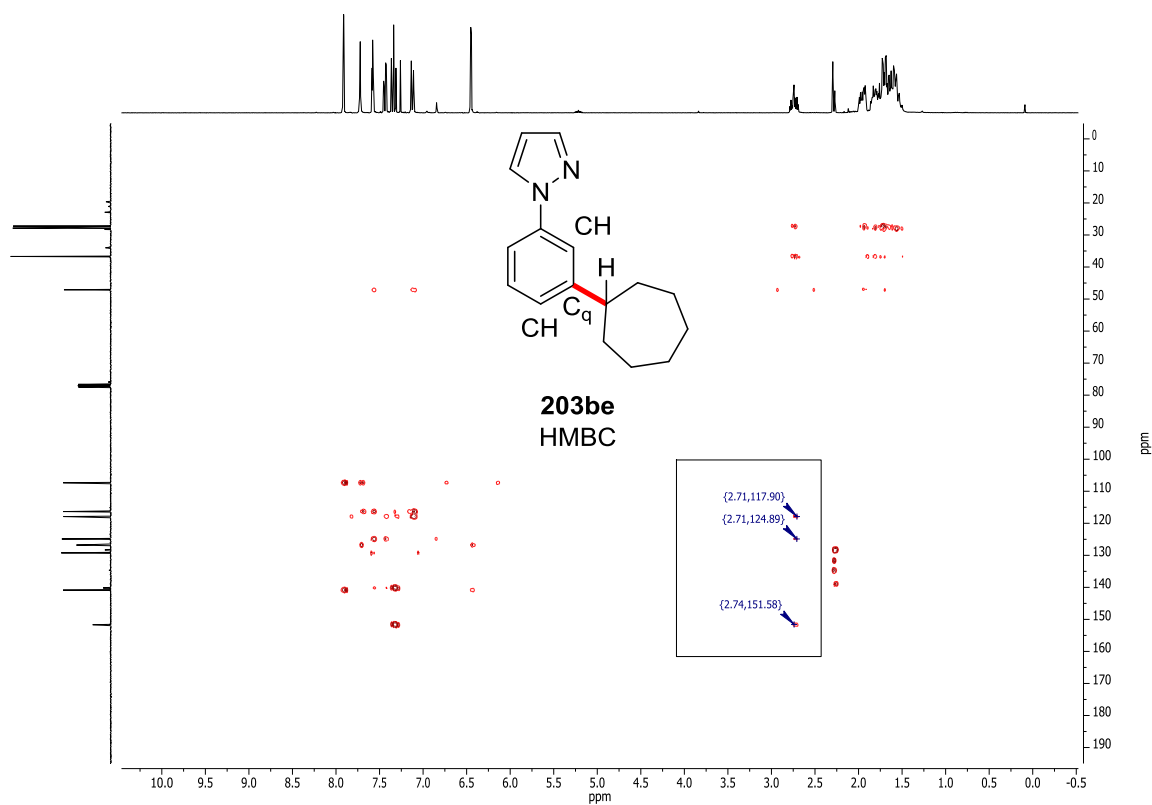


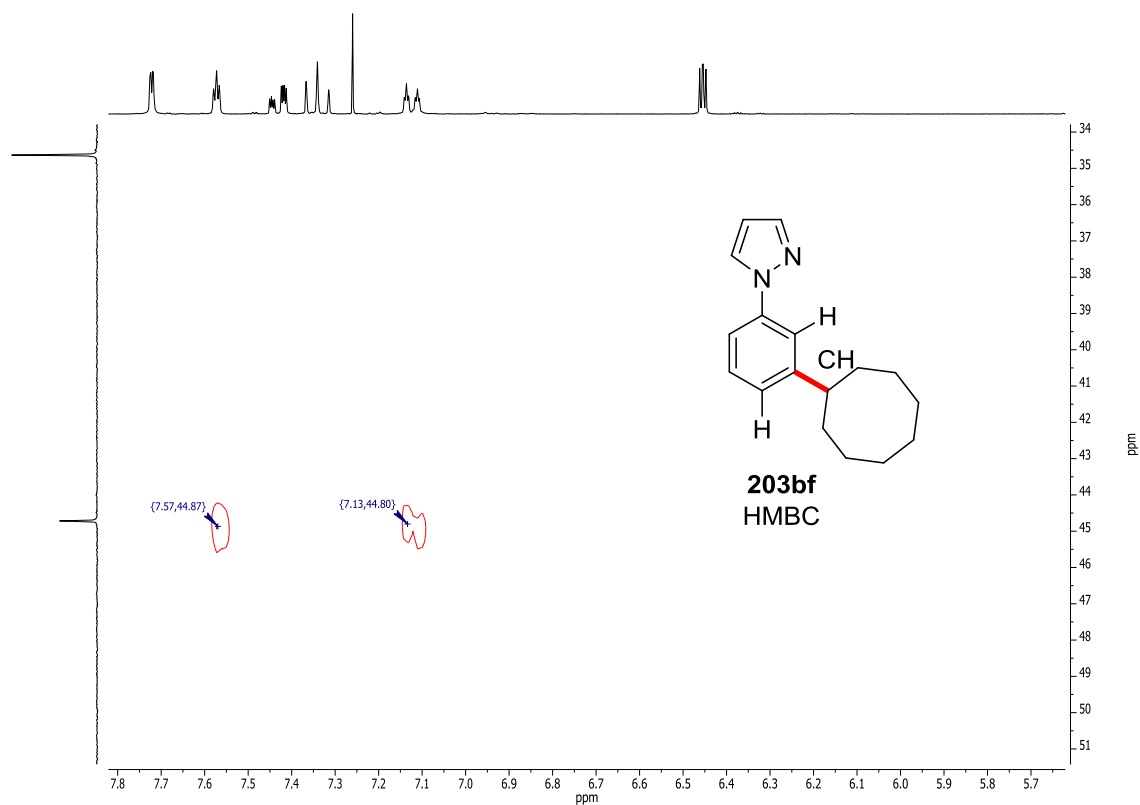
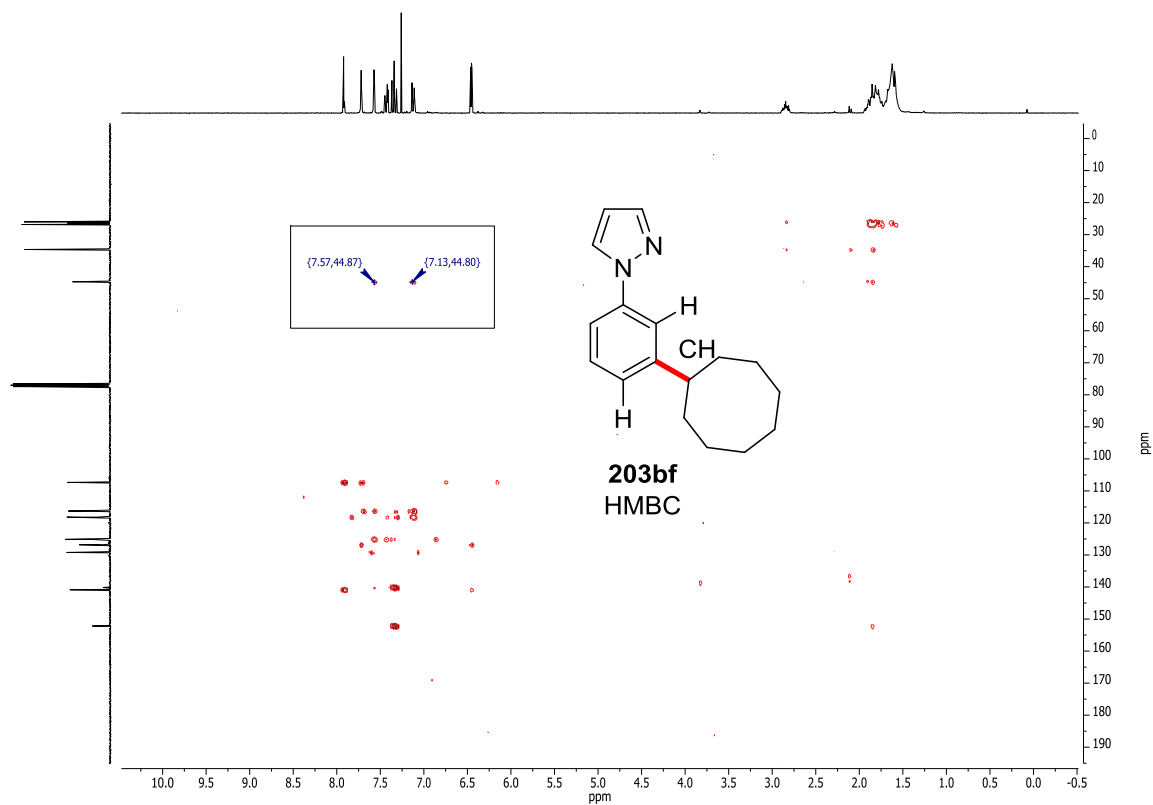
To a Schlenk tube charged with acid **196b** (94.1 mg, 0.50  $\mu\text{mol}$ , 1.0 equiv), 1-bromo-2-methylpropane (**11b**) (206 mg, 1.50 mmol, 3.0 equiv),  $[\text{RuCl}_2(\textit{p}\text{-cymene})]_2$  (7.7 mg, 13  $\mu\text{mol}$ , 2.5 mol %),  $\text{MesCO}_2\text{H}$  (24.6 mg, 150  $\mu\text{mol}$ , 30 mol %) and  $\text{K}_2\text{CO}_3$  (138 mg, 1.00 mmol, 2.0 equiv) was added *o*-xylene (1.0 mL) and  $\text{CD}_3\text{OD}$  (0.2 mL). The Schlenk tube was degassed and filled with  $\text{N}_2$  for three times and the mixture was stirred at 120  $^\circ\text{C}$  for 16 h. Removal of the solvent under reduced pressure and purification of the residue by column chromatography on silica gel (*n*-hexane/EtOAc: 10/1) yielded  $[\text{D}]_n\text{-203bb}$  (77.1 mg, 0.39 mmol, 77%). The deuteration was determined by  $^1\text{H}$ -NMR spectroscopy.

## 5.7.3 Selected 2D-NMR Spectra

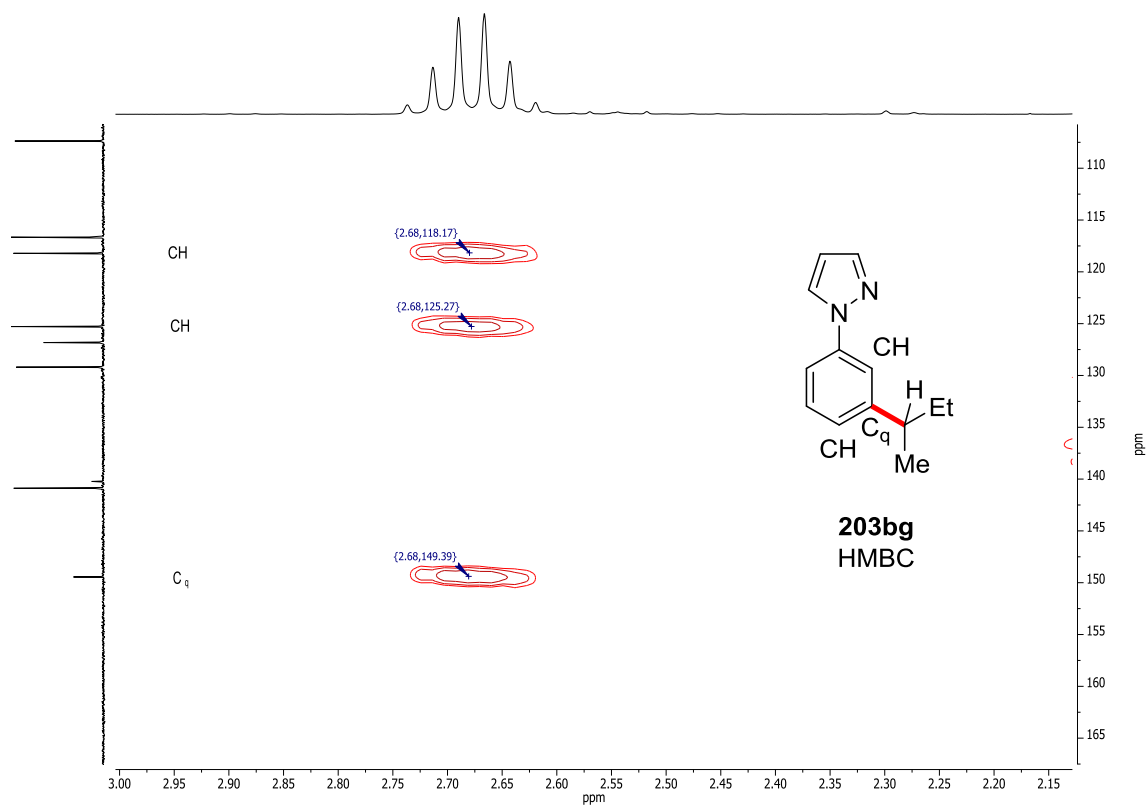
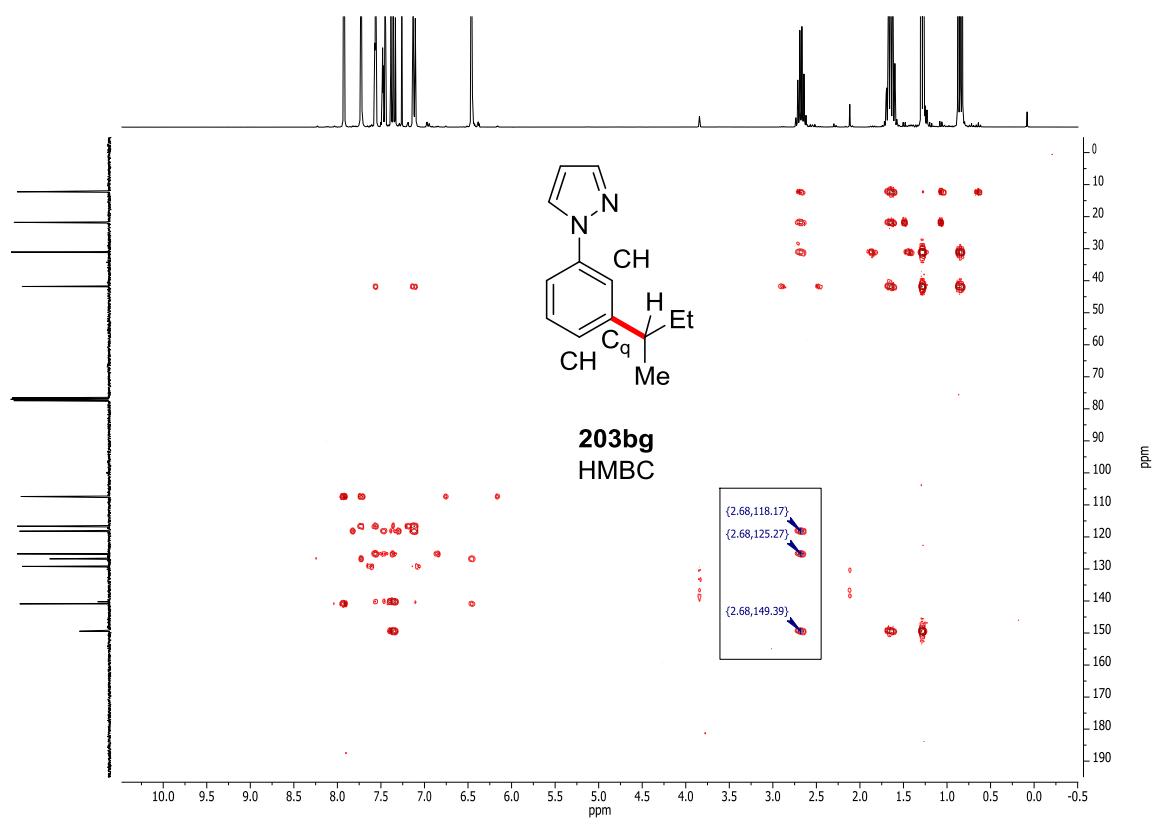


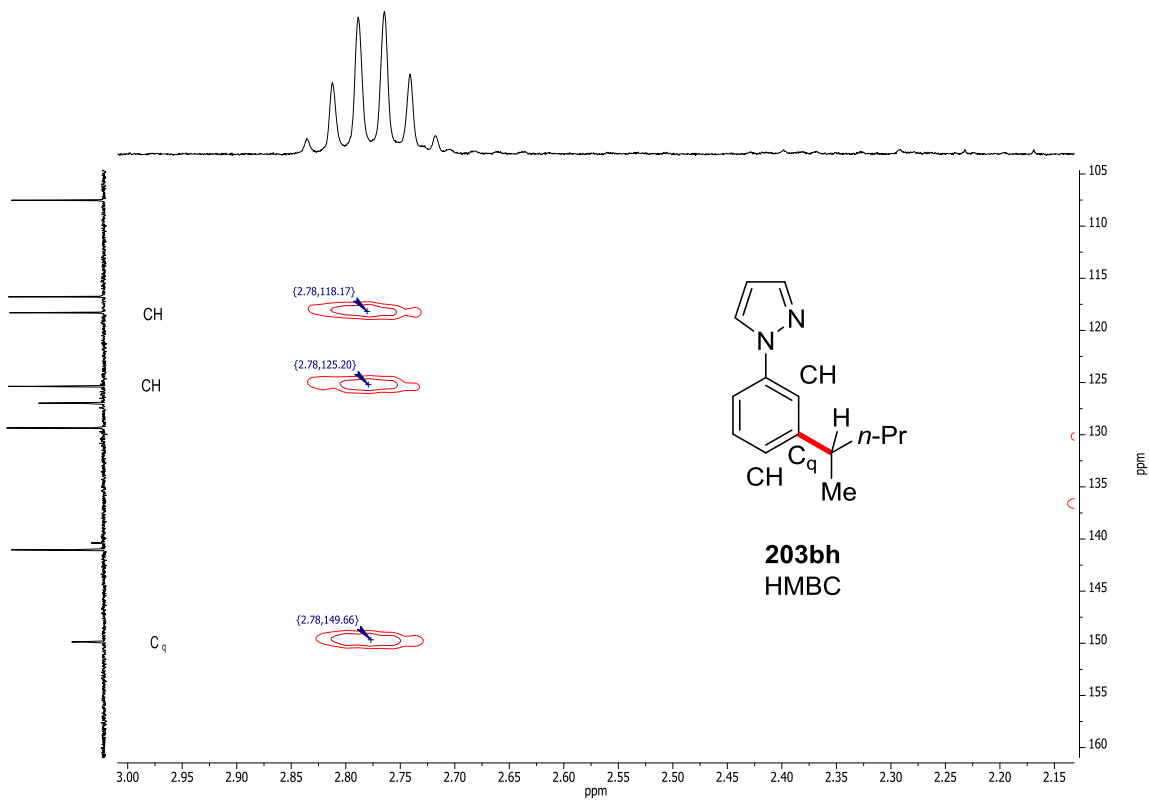
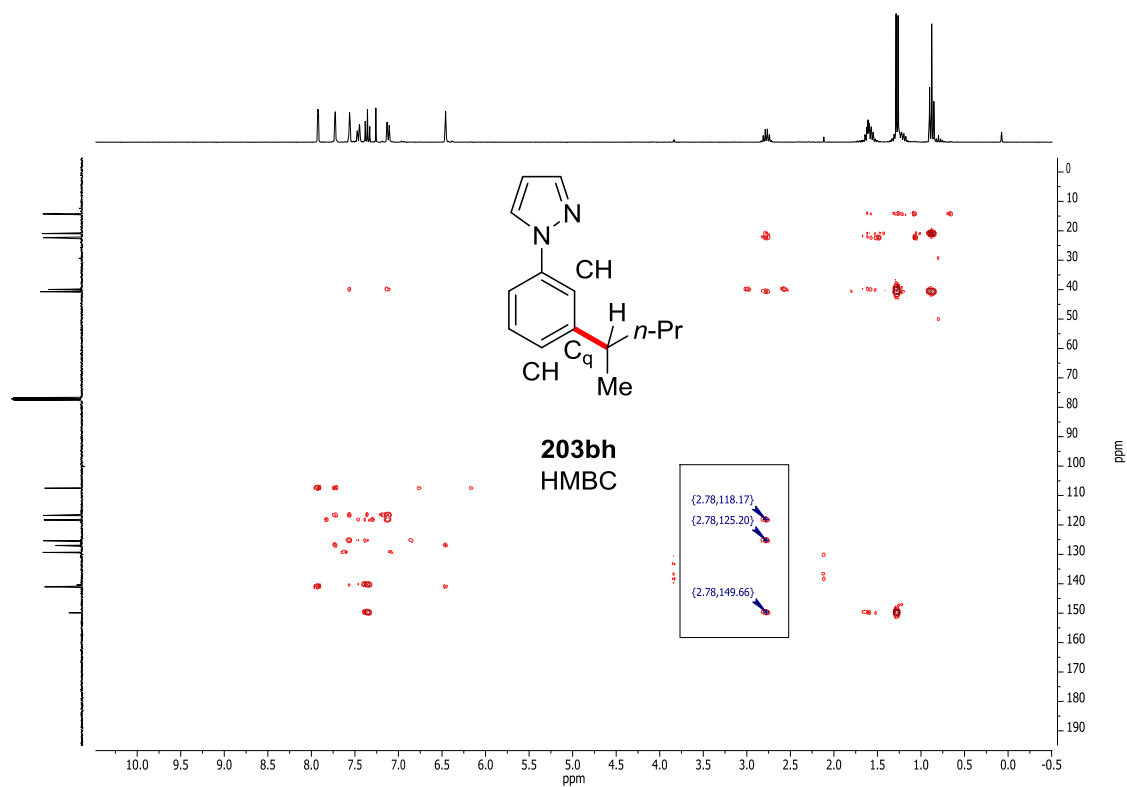
## 5.7 Ruthenium(II)-Catalyzed C–C Alkylation of Acids

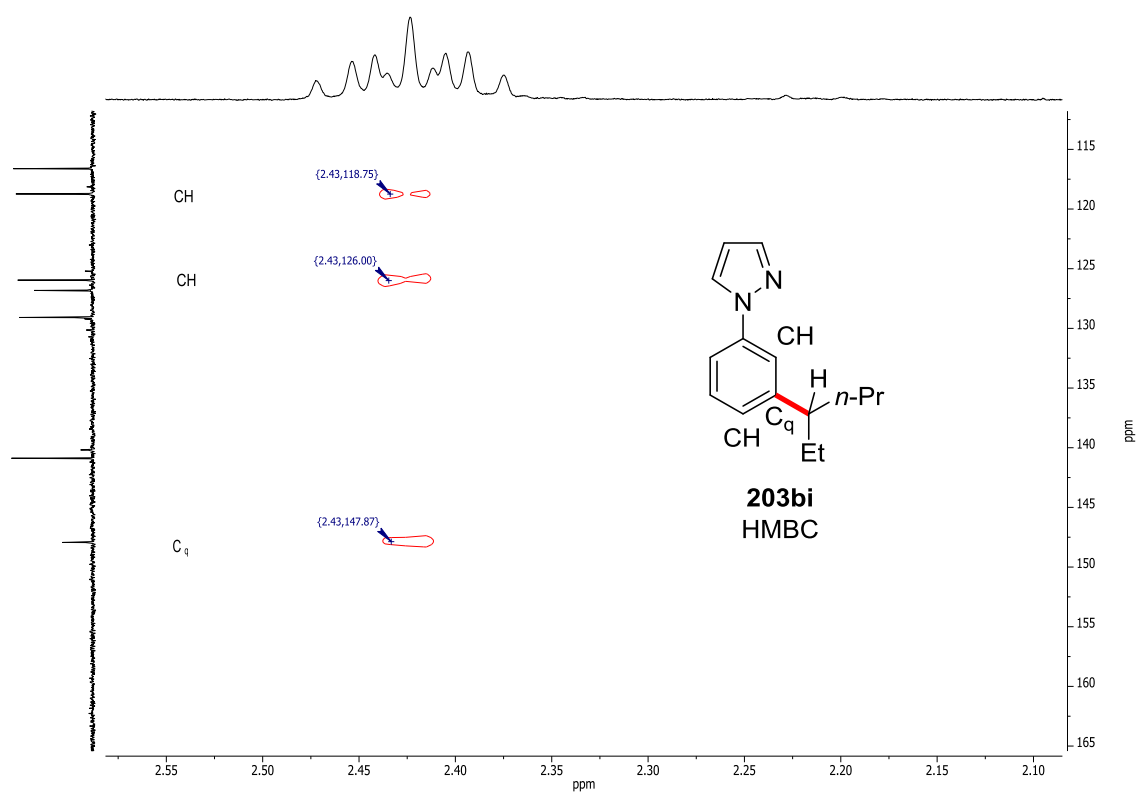
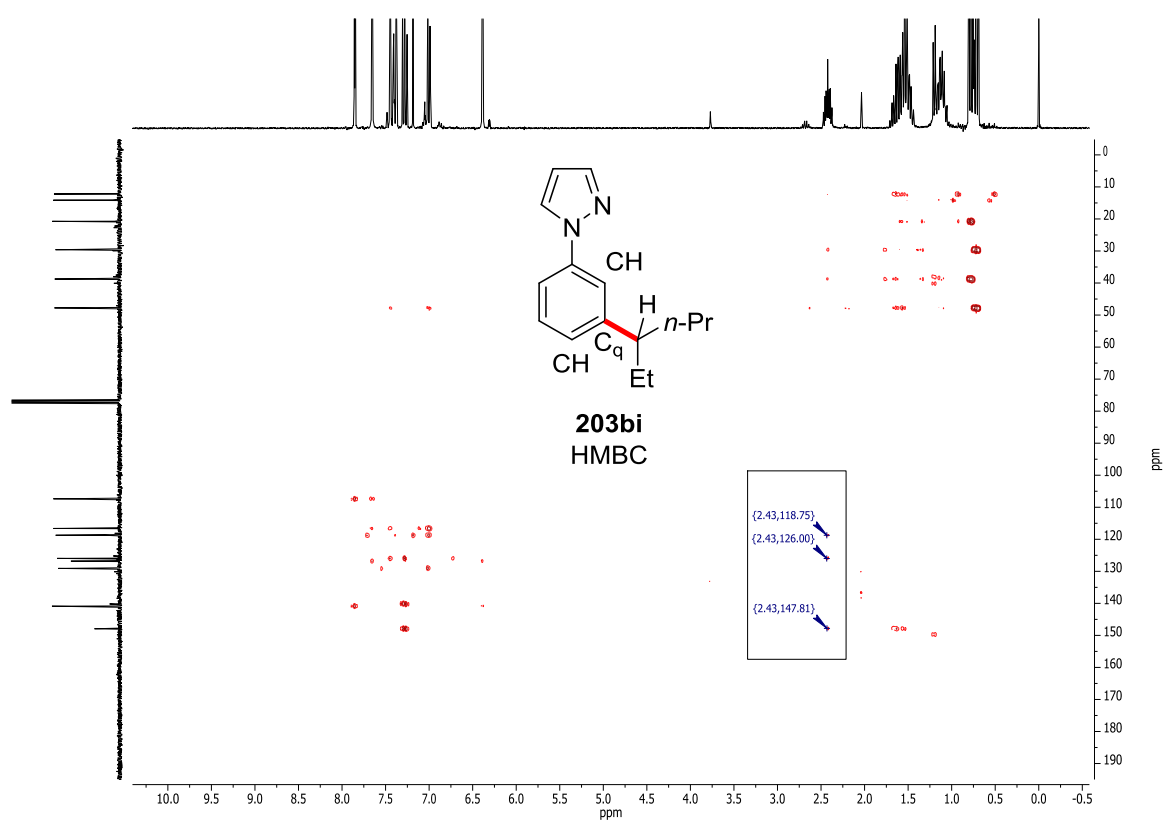


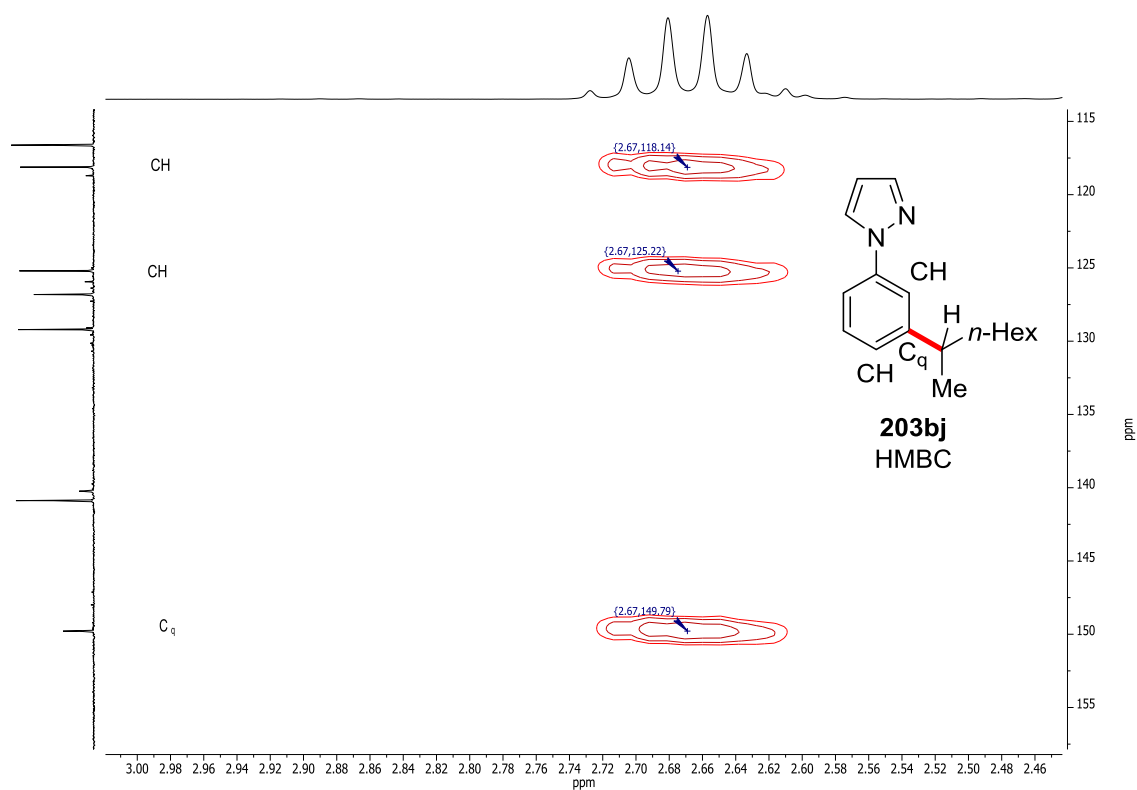
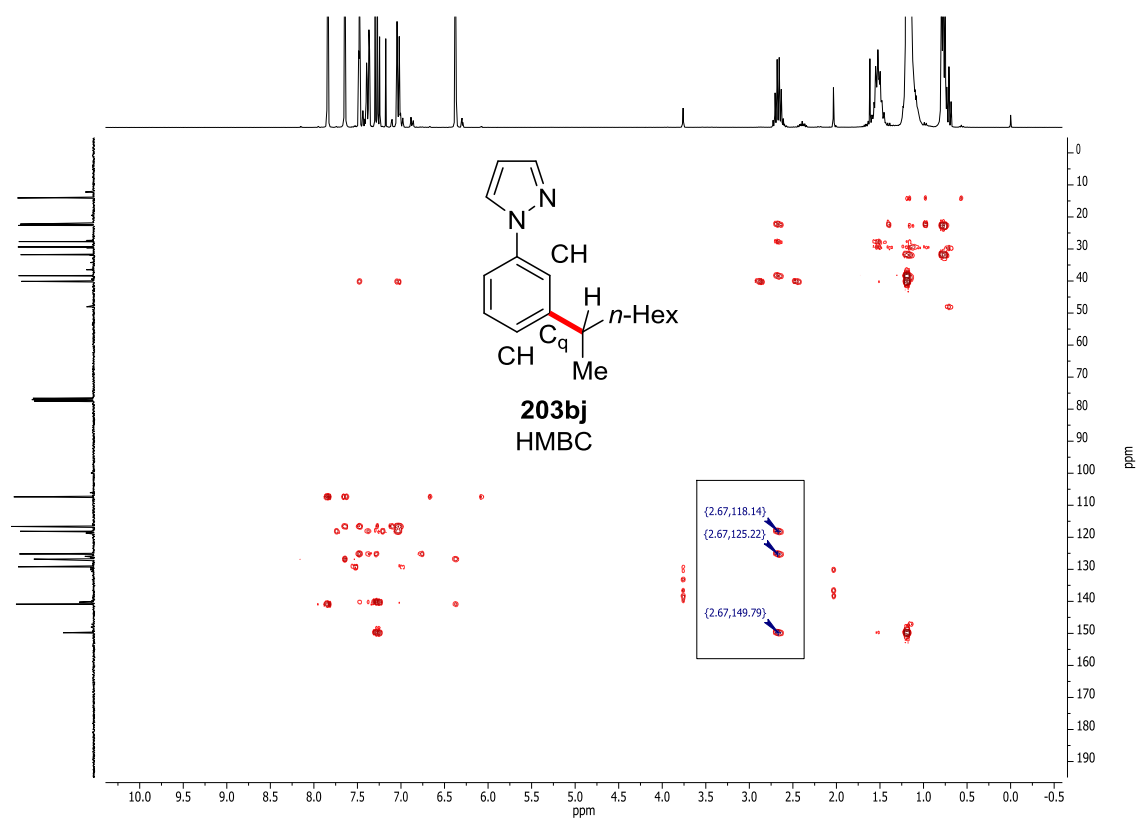


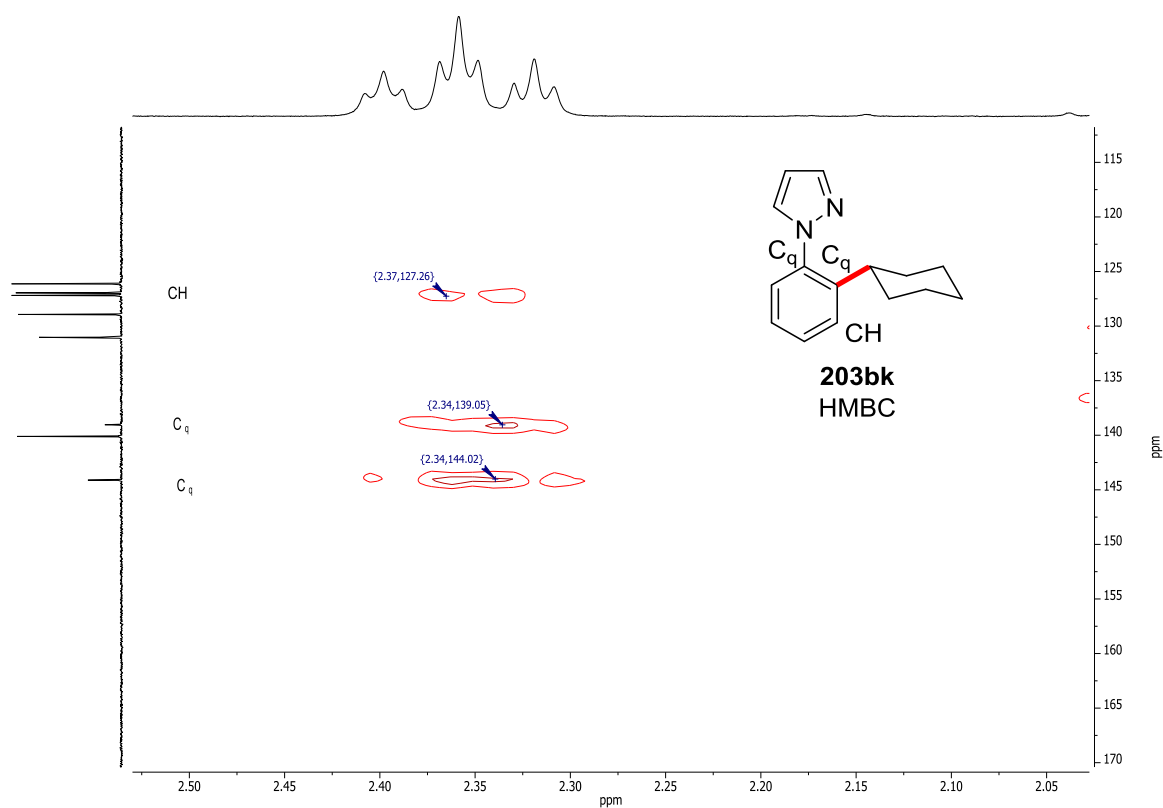
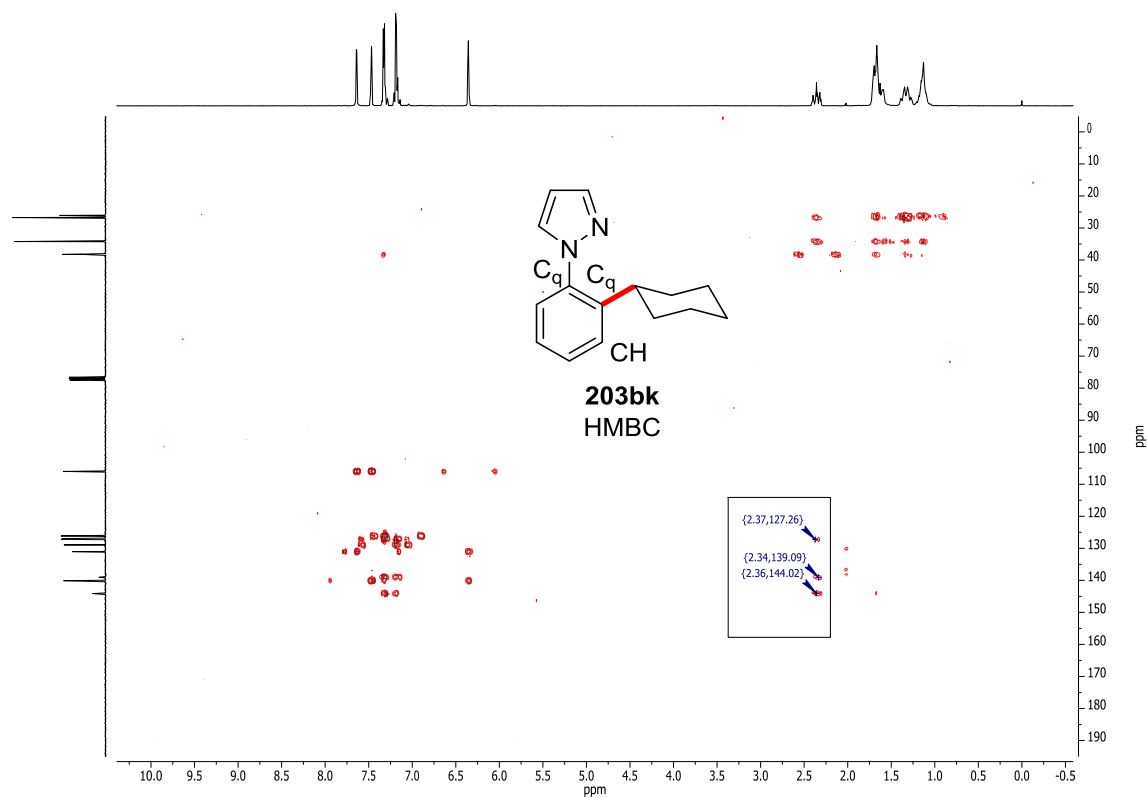


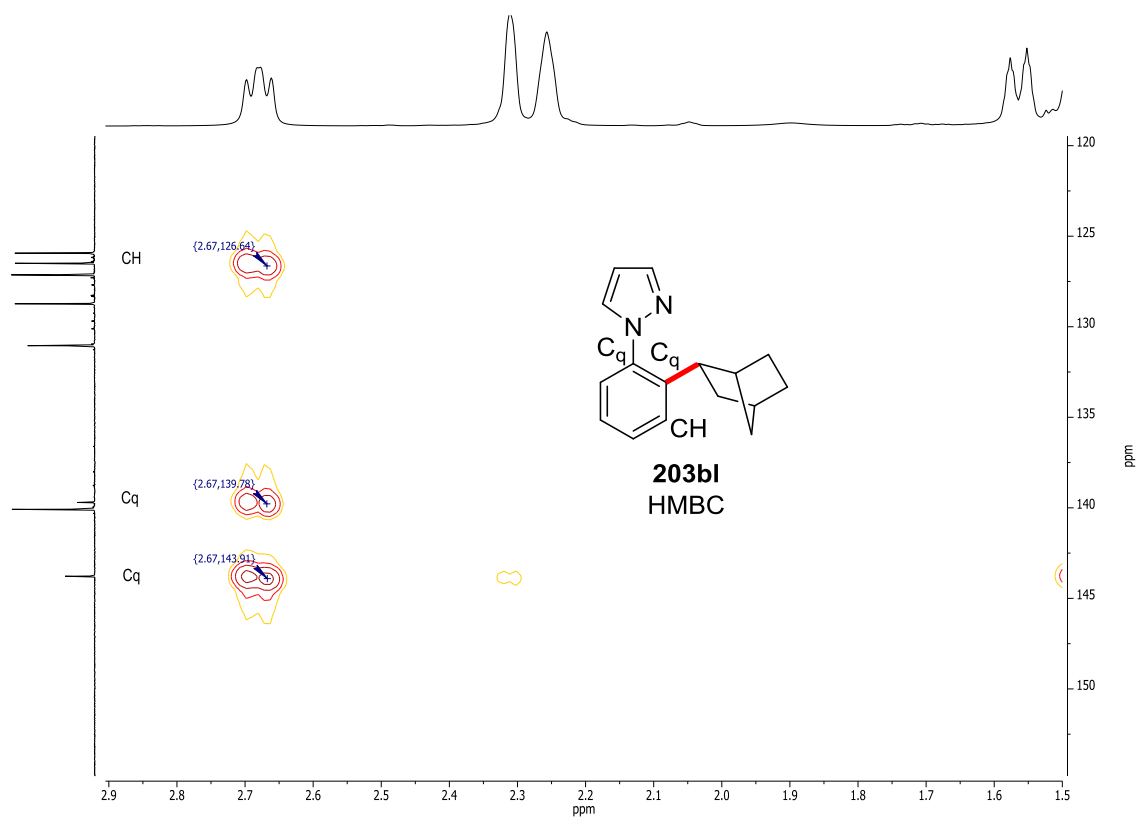
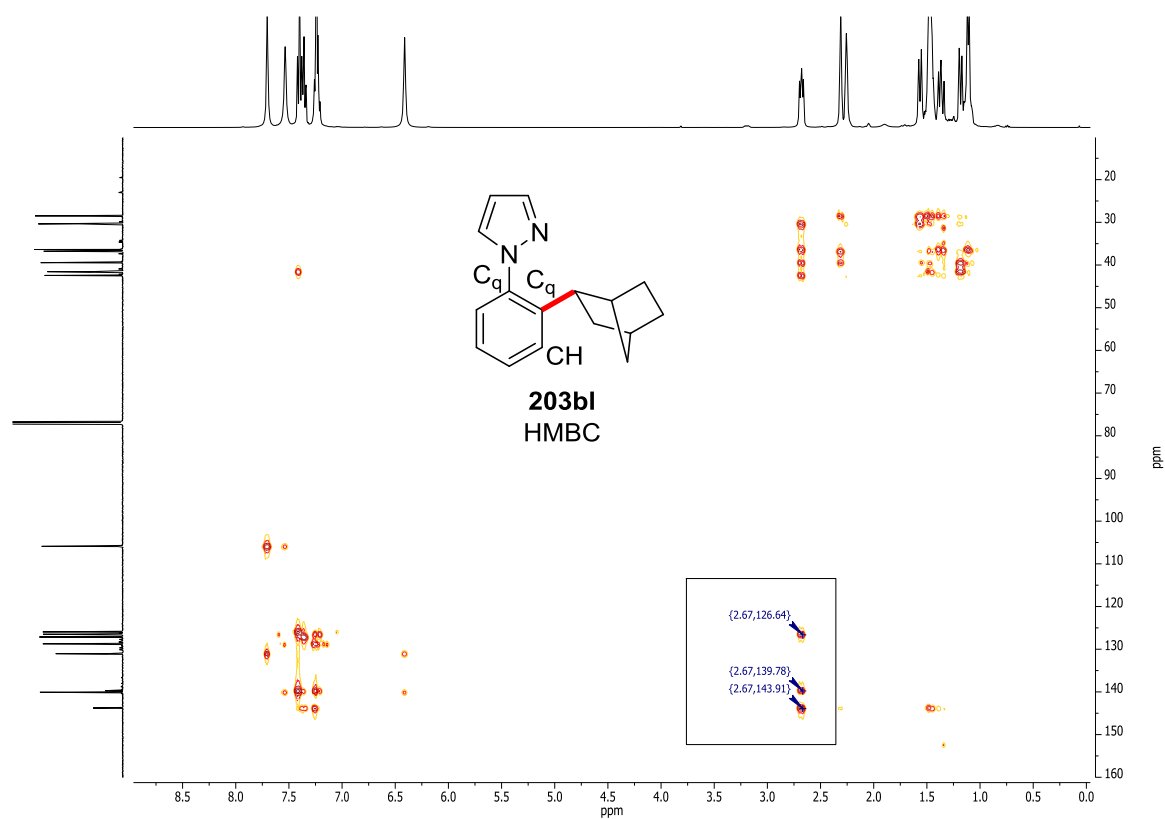












## 6 References

- [1] a) P. T. Anastas, M. M. Kirchhoff, *Acc. Chem. Res.* **2002**, 35, 686-694; b) *Green Chemistry, Theory and Practice* (Eds.: P. T. Anastas, J. C. Warner), Oxford Universal Press, Oxford, **1998**.
- [2] a) C.-Y. Lee, X. Chen, R. J. Romanelli, J. B. Segal, *J. Pharm. Policy Pract.* **2016**, 9, 26-32; b) R. A. Lionberger, *AAPS J.* **2008**, 10, 103-109.
- [3] I. Cepanec, *Synthesis of Biaryls*, Elsevier Science Ltd, Oxford, **2004**.
- [4] a) P. E. Fanta, *Synthesis* **1974**, 9-21; b) F. Ullmann, J. Bielecki, *Ber. Dtsch. Chem. Ges.* **1901**, 34, 2174-2185.
- [5] a) K. Tamao, K. Sumitani, M. Kumada, *J. Am. Chem. Soc.* **1972**, 94, 4374-4376; b) R. J. P. Corriu, J. P. Masse, *J. Chem. Soc., Chem. Commun.* **1972**, 144.
- [6] a) E. Negishi, A. O. King, N. Okukado, *J. Org. Chem.* **1977**, 42, 1821-1823; b) A. O. King, N. Okukado, E.-i. Negishi, *J. Chem. Soc., Chem. Commun.* **1977**, 683-684.
- [7] a) J. K. Stille, *Angew. Chem. Int. Ed. Engl.* **1986**, 25, 508-524; b) D. Milstein, J. K. Stille, *J. Am. Chem. Soc.* **1979**, 101, 4992-4998; c) D. Milstein, J. K. Stille, *J. Am. Chem. Soc.* **1978**, 100, 3636-3638; d) M. Kosugi, Y. Shimizu, T. Migita, *Chem. Lett.* **1977**, 6, 1423-1424; e) M. Kosugi, K. Sasazawa, Y. Shimizu, T. Migita, *Chem. Lett.* **1977**, 6, 301-302.
- [8] a) N. Miyaura, A. Suzuki, *Chem. Rev.* **1995**, 95, 2457-2483; b) N. Miyaura, K. Yamada, A. Suzuki, *Tetrahedron Lett.* **1979**, 20, 3437-3440; c) N. Miyaura, A. Suzuki, *J. Chem. Soc., Chem. Commun.* **1979**, 866-867.
- [9] a) T. Hiyama, *J. Organomet. Chem.* **2002**, 653, 58-61; b) Y. Hatanaka, T. Hiyama, *J. Org. Chem.* **1988**, 53, 918-920.
- [10] a) R. F. Heck, J. P. Nolley, *J. Org. Chem.* **1972**, 37, 2320-2322; b) T. Mizoroki, K. Mori, A. Ozaki, *Bull. Chem. Soc. Jpn.* **1971**, 44, 581.
- [11] a) K. Sonogashira, *J. Organomet. Chem.* **2002**, 653, 46-49; b) K. Sonogashira, Y. Tohda, N. Hagihara, *Tetrahedron Lett.* **1975**, 16, 4467-4470.
- [12] a) *Cross Coupling and Heck-Type Reactions* (Eds.: G. A. Molander, J. P. Wolfe, M. Larhed), Thieme, Stuttgart, **2013**. ; b) *Metal-Catalyzed Cross-Coupling Reactions and More* (Eds.: A. de Meijere, S. Bräse, M. Oestreich), Wiley-VCH, Weinheim, **2014**.
- [13] "The Noble Prize in Chemistry 2010 - Press Release". Nobel Media AB 2013. Web. 19 Jun 2017.  
[http://www.nobelprize.org/nobel\\_prizes/chemistry/laureates/2010/press.html](http://www.nobelprize.org/nobel_prizes/chemistry/laureates/2010/press.html)
- [14] Selected reviews: a) J. Wencel-Delord, F. Glorius, *Nat Chem* **2013**, 5, 369-375; b) L. Ackermann, *Chem. Rev.* **2011**, 111, 1315-1345; c) D. Balcells, E. Clot, O. Eisenstein, *Chem. Rev.* **2010**, 110, 749-823; d) X. Chen, K. M. Engle, D.-H. Wang, J.-Q. Yu, *Angew. Chem. Int. Ed.* **2009**, 48, 5094-5115; e) R. G. Bergman, *Nature* **2007**, 446, 391-393.
- [15] a) H. Yi, G. Zhang, H. Wang, Z. Huang, J. Wang, A. K. Singh, A. Lei, *Chem. Rev.* **2017**, 117, 9016-9085; b) J.-T. Yu, C. Pan, *Chem. Commun.* **2016**, 52, 2220-2236.
- [16] D. Lapointe, K. Fagnou, *Chem. Lett.* **2010**, 39, 1118-1126.
- [17] a) Y. Boutadla, D. L. Davies, S. A. Macgregor, A. I. Poblador-Bahamonde, *Dalton Trans.* **2009**, 5820-5831; b) Y. Boutadla, D. L. Davies, S. A. Macgregor, A. I. Poblador-Bahamonde, *Dalton Trans.* **2009**, 5887-5893.
- [18] J. Oxgaard, W. J. Tenn, R. J. Nielsen, R. A. Periana, W. A. Goddard, *Organometallics* **2007**, 26, 1565-1567.
- [19] a) D. Zell, M. Bursch, V. Müller, S. Grimme, L. Ackermann, *Angew. Chem. Int. Ed.* **2017**, 56, 10378-10382; b) H. Wang, M. Moselage, M. J. González, L.

- Ackermann, *ACS Catal.* **2016**, 6, 2705-2709; c) D. Santrač, S. Cella, W. Wang, L. Ackermann, *Eur. J. Org. Chem.* **2016**, 2016, 5429-5436; d) R. Mei, J. Loup, L. Ackermann, *ACS Catal.* **2016**, 6, 793-797; e) W. Ma, R. Mei, G. Tenti, L. Ackermann, *Chem. Eur. J.* **2014**, 20, 15248-15251.
- [20] a) S. R. Neufeldt, M. S. Sanford, *Acc. Chem. Res.* **2012**, 45, 936-946; b) L. Ackermann, *Top. Organomet. Chem.* **2007**, 24, 35-60.
- [21] W. Ma, P. Gandeepan, J. Li, L. Ackermann, *Org. Chem. Front.* **2017**, 4, 1435-1467.
- [22] Average price in october 2017 in \$ per Oz: Rh 1027, Ir 968, Pt 947, Pd 885, Ru 65, Co 1.7, <http://www.platinum.matthey.com/prices/price-charts>, <https://www.lme.com/Metals/Minor-metals/Cobalt#tabIndex=0>, 23.08.2017
- [23] a) M. Moselage, J. Li, L. Ackermann, *ACS Catal.* **2016**, 6, 498-525; b) W. Liu, L. Ackermann, *ACS Catal.* **2016**, 6, 3743-3752; c) L. C. M. Castro, N. Chatani, *Chem. Lett.* **2015**, 44, 410-421; d) J. Yamaguchi, K. Muto, K. Itami, *Eur. J. Org. Chem.* **2013**, 19-30; e) G. Cera, L. Ackermann, *Top. Organomet. Chem* **2016**, 374, 191-224.
- [24] a) T. Yoshino, S. Matsunaga, *Adv. Synth. Catal.* **2017**, 359, 1245-1262; b) N. Yoshikai, *ChemCatChem* **2015**, 7, 732-734; c) N. Yoshikai, *Bull. Chem. Soc. Jpn.* **2014**, 87, 843-857; d) N. Yoshikai, *J. Syn. Org. Chem. Jpn.* **2014**, 72, 1198-1206; e) K. Gao, N. Yoshikai, *Acc. Chem. Res.* **2014**, 47, 1208-1219; f) L. Ackermann, *J. Org. Chem.* **2014**, 79, 8948-8954.
- [25] M. S. Kharasch, E. K. Fields, *J. Am. Chem. Soc.* **1941**, 63, 2316-2320.
- [26] a) I. U. Khand, G. R. Knox, P. L. Pauson, W. E. Watts, *J. Chem. Soc., Perkin Trans. 1* **1973**, 975-977; b) I. U. Khand, G. R. Knox, P. L. Pauson, W. E. Watts, *J. Chem. Soc. D* **1971**, 36a.
- [27] a) H. Bönemann, *Angew. Chem.* **1985**, 97, 264-279; b) H. Bönemann, *Angew. Chem.* **1978**, 90, 517-526.
- [28] F. Hebrard, P. Kalck, *Chem. Rev.* **2009**, 109, 4272-4282.
- [29] a) S. Murahashi, S. Horie, *J. Am. Chem. Soc.* **1956**, 78, 4816-4817; b) S. Murahashi, *J. Am. Chem. Soc.* **1955**, 77, 6403-6404.
- [30] a) S. Camadanli, R. Beck, U. Flörke, H.-F. Klein, *Dalton Trans.* **2008**, 5701-5704; b) R. Beck, H. Sun, X. Li, S. Camadanli, H.-F. Klein, *Eur. J. Inorg. Chem.* **2008**, 3253-3257; c) H.-F. Klein, S. Camadanli, R. Beck, D. Leukel, U. Flörke, *Angew. Chem. Int. Ed.* **2005**, 44, 975-977; d) H.-F. Klein, R. Beck, U. Flörke, H.-J. Haupt, *Eur. J. Inorg. Chem.* **2003**, 1380-1387; e) H.-F. Klein, S. Schneider, M. He, U. Flörke, H.-J. Haupt, *Eur. J. Inorg. Chem.* **2000**, 2295-2301; f) H.-F. Klein, M. Helwig, U. Koch, U. Flörke, H.-J. Haupt, *Z. Naturforsch. B* **1993**, 48, 778-784.
- [31] Q. Chen, L. Ilies, E. Nakamura, *J. Am. Chem. Soc.* **2011**, 133, 428-429.
- [32] B. Punji, W. Song, G. A. Shevchenko, L. Ackermann, *Chem. Eur. J.* **2013**, 19, 10605-10610.
- [33] a) K. Gao, T. Yamakawa, N. Yoshikai, *Synthesis* **2014**, 46, 2024-2039; b) K. Gao, N. Yoshikai, *J. Am. Chem. Soc.* **2013**, 135, 9279-9282.
- [34] Selected examples: a) E. Peris, *Chem. Rev.* **2017**, 10.1021/acs.chemrev.6b00695; b) M. N. Hopkinson, C. Richter, M. Schedler, F. Glorius, *Nature* **2014**, 510, 485-496; c) *N-Heterocyclic Carbenes* (Ed.: S. P. Nolan), Wiley-VCH, Weinheim, **2014**; d) H. D. Velazquez, F. Verpoort, *Chem. Soc. Rev.* **2012**, 41, 7032-7060; e) S. Díez-González, N. Marion, S. P. Nolan, *Chem. Rev.* **2009**, 109, 3612-3676.
- [35] a) M. Seki, *Org. Process Res. Dev.* **2016**, 20, 867-877; b) L. Ackermann, *Org. Process Res. Dev.* **2015**, 19, 260-269; c) J. Yamaguchi, A. D. Yamaguchi, K. Itami, *Angew. Chem. Int. Ed.* **2012**, 51, 8960-9009.
- [36] W. Song, L. Ackermann, *Angew. Chem. Int. Ed.* **2012**, 51, 8251-8254.
- [37] K. Gao, P.-S. Lee, C. Long, N. Yoshikai, *Org. Lett.* **2012**, 14, 4234-4237.
- [38] Prices for Grignard reagents: CyMgCl (1.3 M, 100 mL): 45€ (Sigma Aldrich); *t*-BuCH<sub>2</sub>MgCl (1.0 M, 100 mL): 1100€ (Sigma Aldrich). Prices from october 2017.



- [39] J. Li, L. Ackermann, *Chem. Eur. J.* **2015**, *21*, 5718-5722.
- [40] G. Halbritter, F. Knoch, A. Wolski, H. Kisch, *Angew. Chem. Int. Ed. Engl.* **1994**, *33*, 1603-1605.
- [41] a) Z. Ding, N. Yoshikai, *Angew. Chem. Int. Ed.* **2012**, *51*, 4698-4701; b) P.-S. Lee, T. Fujita, N. Yoshikai, *J. Am. Chem. Soc.* **2011**, *133*, 17283-17295; c) K. Gao, P.-S. Lee, T. Fujita, N. Yoshikai, *J. Am. Chem. Soc.* **2010**, *132*, 12249-12251.
- [42] B. J. Fallon, E. Derat, M. Amatore, C. Aubert, F. Chemla, F. Ferreira, A. Perez-Luna, M. Petit, *J. Am. Chem. Soc.* **2015**, *137*, 2448-2451.
- [43] L. Ilies, Q. Chen, X. Zeng, E. Nakamura, *J. Am. Chem. Soc.* **2011**, *133*, 5221-5223.
- [44] K. Gao, N. Yoshikai, *Angew. Chem. Int. Ed.* **2011**, *50*, 6888-6892.
- [45] K. Gao, N. Yoshikai, *J. Am. Chem. Soc.* **2011**, *133*, 400-402.
- [46] V. Galamb, G. Palyi, F. Ungvary, L. Marko, R. Boese, G. Schmid, *J. Am. Chem. Soc.* **1986**, *108*, 3344-3351.
- [47] D. Zell, M. Bursch, V. Müller, S. Grimme, L. Ackermann, *Angew. Chem. Int. Ed.* **2017**, *56*, 10378-10382.
- [48] W. Xu, J. H. Pek, N. Yoshikai, *Adv. Synth. Catal.* **2016**, *358*, 2564-2568.
- [49] P.-S. Lee, N. Yoshikai, *Org. Lett.* **2015**, *17*, 22-25.
- [50] U. Koelle, B. Fuss, M. V. Rajasekharan, B. L. Ramakrishna, J. H. Ammeter, M. C. Boehm, *J. Am. Chem. Soc.* **1984**, *106*, 4152-4160.
- [51] T. Yoshino, H. Ikemoto, S. Matsunaga, M. Kanai, *Angew. Chem. Int. Ed.* **2013**, *52*, 2207-2211.
- [52] T. Yoshino, H. Ikemoto, S. Matsunaga, M. Kanai, *Chem. Eur. J.* **2013**, *19*, 9142-9146.
- [53] H. Ikemoto, T. Yoshino, K. Sakata, S. Matsunaga, M. Kanai, *J. Am. Chem. Soc.* **2014**, *136*, 5424-5431.
- [54] D. J. Schipper, M. Hutchinson, K. Fagnou, *J. Am. Chem. Soc.* **2010**, *132*, 6910-6911.
- [55] *CRC Handbook of Chemicals and Physics* (Ed.: W. M. Haynes), CRC Press, Boca Raton, **2015**.
- [56] H. Ikemoto, R. Tanaka, K. Sakata, M. Kanai, T. Yoshino, S. Matsunaga, *Angew. Chem. Int. Ed.* **2017**, *56*, 7156-7160.
- [57] J. Guilhaumé, S. Halbert, O. Eisenstein, R. N. Perutz, *Organometallics* **2012**, *31*, 1300-1314.
- [58] J. Li, L. Ackermann, *Angew. Chem. Int. Ed.* **2015**, *54*, 3635-3638.
- [59] D.-G. Yu, T. Gensch, F. de Azambuja, S. Vásquez-Céspedes, F. Glorius, *J. Am. Chem. Soc.* **2014**, *136*, 17722-17725.
- [60] A. B. Pawar, S. Chang, *Org. Lett.* **2015**, *17*, 660-663.
- [61] D. Lapointe, K. Fagnou, *Chem. Lett.* **2010**, *39*, 1118-1126.
- [62] A. B. Pawar, D. M. Lade, *Org. Biomol. Chem.* **2016**, *14*, 3275-3283.
- [63] a) X.-Y. Shi, K.-Y. Liu, J. Fan, X.-F. Dong, J.-F. Wei, C.-J. Li, *Chem. Eur. J.* **2015**, *21*, 1900-1903; b) K. Shin, J. Ryu, S. Chang, *Org. Lett.* **2014**, *16*, 2022-2025; c) S. De Sarkar, L. Ackermann, *Chem. Eur. J.* **2014**, *20*, 13932-13936; d) S. Sueki, Y. Guo, M. Kanai, Y. Kuninobu, *Angew. Chem. Int. Ed.* **2013**, *52*, 11879-11883; e) K. Muralirajan, K. Parthasarathy, C.-H. Cheng, *Org. Lett.* **2012**, *14*, 4262-4265; f) K. D. Hesp, R. G. Bergman, J. A. Ellman, *J. Am. Chem. Soc.* **2011**, *133*, 11430-11433; g) P. Hong, H. Yamazaki, K. Sonogashira, N. Hagihara, *Chem. Lett.* **1978**, *7*, 535-538.
- [64] J. Li, L. Ackermann, *Angew. Chem. Int. Ed.* **2015**, *54*, 8551-8554.
- [65] J. R. Hummel, J. A. Ellman, *Org. Lett.* **2015**, *17*, 2400-2403.
- [66] *Modern Heterocyclic Chemistry* (Eds.: J. Alvarez-Builla, J. J. Vaquero, J. Barluenga), Wiley-VCH, Weinheim, **2011**.
- [67] *Transition Metal-Catalyzed Heterocycle Synthesis via C-H Activation* (Ed.: X.-F. Wu), Wiley-VCH, Weinheim, **2016**.

- [68] L. F. Tietze, G. Brasche, K. Gericke, *Domino Reactions on Organic Synthesis*, Wiley-VCH, Weinheim, **2006**.
- [69] J. R. Hummel, J. A. Ellman, *J. Am. Chem. Soc.* **2015**, *137*, 490-498.
- [70] a) Y. Lian, T. Huber, K. D. Hesp, R. G. Bergman, J. A. Ellman, *Angew. Chem. Int. Ed.* **2013**, *52*, 629-633; b) Y. Lian, R. G. Bergman, L. D. Lavis, J. A. Ellman, *J. Am. Chem. Soc.* **2013**, *135*, 7122-7125.
- [71] H. Wang, J. Koeller, W. Liu, L. Ackermann, *Chem. Eur. J.* **2015**, *21*, 15525-15528.
- [72] B. Sun, T. Yoshino, M. Kanai, S. Matsunaga, *Angew. Chem. Int. Ed.* **2015**, *54*, 12968-12972.
- [73] M. Sen, D. Kalsi, B. Sundararaju, *Chem. Eur. J.* **2015**, *21*, 15529-15533.
- [74] Solvent prices (p.A. grade) per Liter: HFIP: 414 € (Sigma Aldrich), TFE: 318 € (Sigma Aldrich), DCE: 115 € (Sigma Aldrich). Prices from September 2017.
- [75] a) X. Zhang, D. Chen, M. Zhao, J. Zhao, A. Jia, X. Li, *Adv. Synth. Catal.* **2011**, *353*, 719-723; b) P. C. Too, Y.-F. Wang, S. Chiba, *Org. Lett.* **2010**, *12*, 5688-5691.
- [76] Selected reviews: a) G. Fumagalli, S. Stanton, J. F. Bower, *Chem. Rev.* **2017**, *117*, 9404-9432; b) M. Murakami, N. Ishida, *J. Am. Chem. Soc.* **2016**, *138*, 13759-13769; c) E. T. C. Vogt, B. M. Weckhuysen, *Chem. Soc. Rev.* **2015**, *44*, 7342-7370; d) L. Souillart, N. Cramer, *Chem. Rev.* **2015**, *115*, 9410-9464; e) T. Xu, A. Dermenci, G. Dong, *Top. Curr. Chem.* **2014**, *346*, 233-257; f) F. Chen, T. Wang, N. Jiao, *Chem. Rev.* **2014**, *114*, 8613-8661; g) K. Ruhland, *Eur. J. Org. Chem.* **2012**, 2683-2706; h) T. Seiser, T. Saget, D. N. Tran, N. Cramer, *Angew. Chem. Int. Ed.* **2011**, *50*, 7740-7752; i) M. Murakami, T. Matsuda, *Chem. Commun.* **2011**, *47*, 1100-1105; j) M. Murakami, M. Makino, S. Ashida, T. Matsuda, *Bull. Chem. Soc. Jpn.* **2006**, *79*, 1315-1321; k) C.-H. Jun, *Chem. Soc. Rev.* **2004**, *33*, 610-618.
- [77] a) P. E. M. Siegbahn, *J. Phys. Chem.* **1995**, *99*, 12723-12729; b) J. A. M. Simoes, J. L. Beauchamp, *Chem. Rev.* **1990**, *90*, 629-688; c) J. A. Labinger, J. E. Bercaw, *Organometallics* **1988**, *7*, 926-928.
- [78] H. Yorimitsu, K. Oshima, *Bull. Chem. Soc. Jpn.* **2009**, *82*, 778-792.
- [79] C. F. H. Tipper, *J. Chem. Soc.* **1955**, 2043.
- [80] D. M. Adams, J. Chatt, R. G. Guy, N. Sheppard, *J. Chem. Soc.* **1961**, 738-742.
- [81] N. A. Bailey, R. D. Gillard, M. Keeton, R. Mason, D. R. Russell, *Chem. Commun.* **1966**, 396-398.
- [82] Tipper's "PtCl<sub>2</sub>" resulted from treating platinum with chlorine gas. As this reaction also leads to over oxidation to Pt(IV), it is assumed that he unknowingly used H<sub>2</sub>PtCl<sub>6</sub> for his pioneer work.
- [83] P. R. Khoury, J. D. Goddard, W. Tam, *Tetrahedron* **2004**, *60*, 8103-8112.
- [84] a) M. Murakami, H. Amii, K. Shigeto, Y. Ito, *J. Am. Chem. Soc.* **1996**, *118*, 8285-8290; b) M. Murakami, H. Amii, Y. Ito, *Nature* **1994**, *370*, 540-541.
- [85] M. Murakami, T. Itahashi, Y. Ito, *J. Am. Chem. Soc.* **2002**, *124*, 13976-13977.
- [86] a) L. Souillart, E. Parker, N. Cramer, *Angew. Chem. Int. Ed.* **2014**, *53*, 3001-3005; b) E. Parker, N. Cramer, *Organometallics* **2014**, *33*, 780-787.
- [87] L. Souillart, N. Cramer, *Angew. Chem. Int. Ed.* **2014**, *53*, 9640-9644.
- [88] C. Aissa, A. Fürstner, *J. Am. Chem. Soc.* **2007**, *129*, 14836-14837.
- [89] T. Seiser, O. A. Roth, N. Cramer, *Angew. Chem. Int. Ed.* **2009**, *48*, 6320-6323.
- [90] J.-Q. Wu, Z.-P. Qiu, S.-S. Zhang, J.-G. Liu, Y.-X. Lao, L.-Q. Gu, Z.-S. Huang, J. Li, H. Wang, *Chem. Commun.* **2015**, *51*, 77-80.
- [91] D. Zell, Q. Bu, M. Feldt, L. Ackermann, *Angew. Chem. Int. Ed.* **2016**, *55*, 7408-7412.
- [92] T. H. Meyer, W. Liu, M. Feldt, A. Wuttke, R. A. Mata, L. Ackermann, *Chem. Eur. J.* **2017**, *23*, 5443-5447.
- [93] A. M. Dreis, C. J. Douglas, *J. Am. Chem. Soc.* **2009**, *131*, 412-413.

- [94] J. Wang, W. Chen, S. Zuo, L. Liu, X. Zhang, J. Wang, *Angew. Chem. Int. Ed.* **2012**, *51*, 12334-12338.
- [95] Y. Terao, H. Wakui, T. Satoh, M. Miura, M. Nomura, *J. Am. Chem. Soc.* **2001**, *123*, 10407-10408.
- [96] Y. Terao, H. Wakui, M. Nomoto, T. Satoh, M. Miura, M. Nomura, *J. Org. Chem.* **2003**, *68*, 5236-5243.
- [97] H. Li, Y. Li, X.-S. Zhang, K. Chen, X. Wang, Z.-J. Shi, *J. Am. Chem. Soc.* **2011**, *133*, 15244-15247.
- [98] K. Chen, H. Li, Y. Li, X.-S. Zhang, Z.-Q. Lei, Z.-J. Shi, *Chem. Sci.* **2012**, *3*, 1645-1649.
- [99] K. Chen, H. Li, Z.-Q. Lei, Y. Li, W.-H. Ye, L.-S. Zhang, J. Sun, Z.-J. Shi, *Angew. Chem. Int. Ed.* **2012**, *51*, 9851-9855.
- [100] X.-S. Zhang, Y. Li, H. Li, K. Chen, Z.-Q. Lei, Z.-J. Shi, *Chem. Eur. J.* **2012**, *18*, 16214-16225.
- [101] E. Ozkal, B. Cachera, B. Morandi, *ACS Catal.* **2015**, *5*, 6458-6462.
- [102] T. Okazawa, T. Satoh, M. Miura, M. Nomura, *J. Am. Chem. Soc.* **2002**, *124*, 5286-5287.
- [103] M. Nilsson, *Acta. Chem. Scand.* **1966**, *20*, 423-426.
- [104] A. G. Myers, D. Tanaka, M. R. Mannion, *J. Am. Chem. Soc.* **2002**, *124*, 11250-11251.
- [105] a) D. Tanaka, S. P. Romeril, A. G. Myers, *J. Am. Chem. Soc.* **2005**, *127*, 10323-10333; b) D. Tanaka, A. G. Myers, *Org. Lett.* **2004**, *6*, 433-436.
- [106] a) L. J. Goossen, P. P. Lange, N. Rodríguez, C. Linder, *Chem. Eur. J.* **2010**, *16*, 3906-3909; b) L. J. Goossen, F. Manjolinho, B. A. Khan, N. Rodríguez, *J. Org. Chem.* **2009**, *74*, 2620-2623; c) L. J. Goossen, N. Rodríguez, C. Linder, *J. Am. Chem. Soc.* **2008**, *130*, 15248-15249; d) L. J. Goossen, N. Rodríguez, B. Melzer, C. Linder, G. Deng, L. M. Levy, *J. Am. Chem. Soc.* **2007**, *129*, 4824-4833; e) L. J. Goossen, G. Deng, L. M. Levy, *Science* **2006**, *313*, 662-664.
- [107] P. Forgione, M.-C. Brochu, M. Stóngé, K. H. Thesen, M. D. Bailey, F. Bilodeau, *J. Am. Chem. Soc.* **2006**, *128*, 11350-11351.
- [108] M. Nakano, H. Tsurugi, T. Satoh, M. Miura, *Org. Lett.* **2008**, *10*, 1851-1854.
- [109] F. Bilodeau, M.-C. Brochu, N. Guimond, K. H. Thesen, P. Forgione, *J. Org. Chem.* **2010**, *75*, 1550-1560.
- [110] C. Li, P. Li, J. Yang, L. Wang, *Chem. Commun.* **2012**, *48*, 4214-4216.
- [111] G. Cahiez, H. Avedissian, *Tetrahedron Lett.* **1998**, *39*, 6159-6162.
- [112] J. Barluenga, C. Valdés, in *Modern Heterocyclic Chemistry, Vol. 1* (Eds.: J. Alvarez-Builla, J. J. Vaquero, J. Barluenga), Wiley-VCH, Weinheim, **2011**, pp. 2875-2911.
- [113] Z. Zhou, G. Liu, Y. Chen, X. Lu, *Adv. Synth. Catal.* **2015**, *357*, 2944-2950.
- [114] a) J. Li, K. Korvorapun, S. De Sarkar, T. Rogge, D. J. Burns, S. Warratz, L. Ackermann, *Nat. Commun.* **2017**, *8*, 15430; b) J. Li, S. Warratz, D. Zell, S. De Sarkar, E. E. Ishikawa, L. Ackermann, *J. Am. Chem. Soc.* **2015**, *137*, 13894-13901; c) N. Hofmann, L. Ackermann, *J. Am. Chem. Soc.* **2013**, *135*, 5877-5884.
- [115] a) Y. Ogiwara, M. Tamura, T. Kochi, Y. Matsuura, N. Chatani, F. Kakiuchi, *Organometallics* **2014**, *33*, 402-420; b) Y. Matsuura, M. Tamura, T. Kochi, M. Sato, N. Chatani, F. Kakiuchi, *J. Am. Chem. Soc.* **2007**, *129*, 9858-9859.
- [116] K. Gao, T. Yamakawa, N. Yoshikai, *Synthesis* **2014**, 2024-2039.
- [117] a) R. A. Amos, J. A. Katzenellenbogen, *J. Org. Chem.* **1977**, *42*, 2537-2545; b) J. Eames, Gregory S. Coumbarides, Michael J. Suggate, N. Weerasooriya, *Eur. J. Org. Chem.* **2003**, 634-641; c) A. Berkessel, M. L. Sebastian-Ibarz, T. N. Müller, *Angew. Chem. Int. Ed.* **2006**, *45*, 6567-6570.
- [118] M. I. Soleilhavoup, G. Bertrand, *Acc. Chem. Res.* **2015**, *48*, 256-266.
- [119] V. Lavallo, Y. Canac, B. Donnadiou, W. W. Schoeller, G. Bertrand, *Science* **2006**, *312*, 722-724.
- [120] L. Ackermann, *Isr. J. Chem.* **2010**, *50*, 652-663.

- [121] a) W. Song, S. Lackner, L. Ackermann, *Angew. Chem. Int. Ed.* **2014**, *53*, 2477-2480; b) J. Yi, L. Yang, C. Xia, F. Li, *J. Org. Chem.* **2015**, *80*, 6213-6221; c) Z. Ruan, S. Lackner, L. Ackermann, *ACS Catal.* **2016**, *6*, 4690-4693; d) Z. Ruan, S. Lackner, L. Ackermann, *Angew. Chem. Int. Ed.* **2016**, *55*, 3153-3157.
- [122] L. Ackermann, A. V. Lygin, *Org. Lett.* **2011**, *13*, 3332-3335.
- [123] After storing for two years, all employed vinyl acetates afforded the same purity as determined by  $^1\text{H}$ -NMR.
- [124] a) Y. Ding, W. Wang, Z. Liu, *Phosphorous Sulfur Silicon Relat. Elem.* **1996**, *118*, 113-116; b) M. G. Silvestri, M. P. Hanson, J. G. Pavlovich, L. F. Studen, M. S. DeClue, M. R. DeGraffenreid, C. D. Amos, *J. Org. Chem.* **1999**, *64*, 6597-6602; c) M. L. Maddess, M. Lautens, *Synthesis* **2004**, 1399-1408; d) M. I. Boultsadakis-Arapinis, M. N. Hopkinson, F. Glorius, *Org. Lett.* **2014**, *16*, 1630-1633.
- [125] a) M. Moselage, N. Sauermann, S. C. Richter, L. Ackermann, *Angew. Chem. Int. Ed.* **2015**, *54*, 6352-6355; b) N. Sauermann, Master-Thesis, Georg-August-Universität Göttingen, **2014**.
- [126] a) J.-B. Xia, S.-L. You, *Organometallics* **2007**, *26*, 4869-4871; b) C. Pi, Y. Li, X. Cui, H. Zhang, Y. Han, Y. Wu, *Chem. Sci.* **2013**, *4*, 2675-2679; c) D.-W. Gao, Q. Yin, Q. Gu, S.-L. You, *J. Am. Chem. Soc.* **2014**, *136*, 4841-4844; d) C. Kornhaas, C. Kuper, L. Ackermann, *Adv. Synth. Catal.* **2014**, *356*, 1619-1624; e) *Ferrocenes: Homogeneous Catalysis, Organic Synthesis, Materials Science* (Eds.: A. Togni, T. Hayashi), Wiley-VCH, Weinheim, **2008**.
- [127] K. Sünkel, S. Weigand, *Inorg. Chim. Acta* **2011**, *370*, 224-229.
- [128] L. A. Lopez, E. Lopez, *Dalton Trans.* **2015**, *44*, 10128-10135.
- [129] S. Takebayashi, T. Shibata, *Organometallics* **2012**, *31*, 4114-4117.
- [130] a) M. Piotrowicz, J. Zakrzewski, *Organometallics* **2013**, *32*, 5709-5712; b) D.-W. Gao, Y. Gu, S.-B. Wang, Q. Gu, S.-L. You, *Organometallics* **2016**, *35*, 3227-3233.
- [131] K. S. Singh, P. H. Dixneuf, *Organometallics* **2012**, *31*, 7320-7323.
- [132] J. F. Hartwig, *Organotransition Metal Chemistry: From Bonding to Catalysis*, University Science Books, **2010**.
- [133] É. Bélanger, J.-F. Paquin, in *Encyclopedia of Reagents for Organic Synthesis*, John Wiley & Sons, Ltd, **2001**.
- [134] G. R. Humphrey, J. T. Kuethe, *Chem. Rev.* **2006**, *106*, 2875-2911.
- [135] W. Li, L.-H. Weng, G.-X. Jin, *Inorg. Chem. Commun.* **2004**, *7*, 1174-1177.
- [136] a) A. S. Tsai, M. I. Brasse, R. G. Bergman, J. A. Ellman, *Org. Lett.* **2011**, *13*, 540-542; b) C. Feng, D. Feng, T.-P. Loh, *Org. Lett.* **2013**, *15*, 3670-3673; c) H. Wang, B. Beiring, D.-G. Yu, K. D. Collins, F. Glorius, *Angew. Chem. Int. Ed.* **2013**, *52*, 12430-12434; d) H. Wang, N. Schröder, F. Glorius, *Angew. Chem. Int. Ed.* **2013**, *52*, 5386-5389; e) C. Feng, D. Feng, T.-P. Loh, *Chem. Commun.* **2015**, *51*, 342-345.
- [137] a) T. Gensch, S. Vásquez-Céspedes, D.-G. Yu, F. Glorius, *Org. Lett.* **2015**, *17*, 3714-3717; b) Y. Suzuki, B. Sun, K. Sakata, T. Yoshino, S. Matsunaga, M. Kanai, *Angew. Chem. Int. Ed.* **2015**, *54*, 9944-9947.
- [138] a) M. Moselage, N. Sauermann, J. Koeller, W. Liu, D. Gelman, L. Ackermann, *Synlett* **2015**, 1596-1600; b) J. Koeller, Master-Thesis, Georg-August-Universität Göttingen, **2015**.
- [139] G. S. Kumar, M. Kapur, *Org. Lett.* **2016**, *18*, 1112-1115.
- [140] a) D.-H. Wang, K. M. Engle, B.-F. Shi, J.-Q. Yu, *Science* **2010**, *327*, 315-319; b) H. M. L. Davies, J. R. Manning, *Nature* **2008**, *451*, 417-424.
- [141] a) R. B. Dateer, S. Chang, *J. Am. Chem. Soc.* **2015**, *137*, 4908-4911; b) H. Yan, H. Wang, X. Li, X. Xin, C. Wang, B. Wan, *Angew. Chem. Int. Ed.* **2015**, *54*, 10613-10617.
- [142] A. Lerchen, S. Vásquez-Céspedes, F. Glorius, *Angew. Chem. Int. Ed.* **2016**, *55*, 3208-3211.

- [143] a) O. Daugulis, J. Roane, L. D. Tran, *Acc. Chem. Res.* **2015**, *48*, 1053-1064; b) G. Rouquet, N. Chatani, *Angew. Chem. Int. Ed.* **2013**, *52*, 11726-11743; c) T. Satoh, M. Miura, *Chem. Eur. J.* **2010**, *16*, 11212-11222; d) R. Giri, B.-F. Shi, K. M. Engle, N. Maugel, J.-Q. Yu, *Chem. Soc. Rev.* **2009**, *38*, 3242-3272; e) L. Ackermann, R. Vicente, A. R. Kapdi, *Angew. Chem. Int. Ed.* **2009**, *48*, 9792-9826.
- [144] a) J. Cornella, I. Larrosa, *Synthesis* **2012**, 653-676; b) N. Rodriguez, L. J. Goossen, *Chem. Soc. Rev.* **2011**, *40*, 5030-5048.
- [145] J. Li, L. Ackermann, *unpublished results*.
- [146] a) D. D. Gaikwad, A. D. Chapolikar, C. G. Devkate, K. D. Warad, A. P. Tayade, R. P. Pawar, A. J. Domb, *Eur. J. Med. Chem.* **2015**, *90*, 707-731; b) A. Thangadurai, M. Minu, S. Wakode, S. Agrawal, B. Narasimhan, *Med. Chem. Res.* **2012**, *21*, 1509-1523.
- [147] a) S. Shu, Z. Fan, Q. Yao, A. Zhang, *J. Org. Chem.* **2016**, *81*, 5263-5269; b) T. Mita, H. Tanaka, K. Michigami, Y. Sato, *Synlett* **2014**, *25*, 1291-1294; c) S. Asako, J. Norinder, L. Ilies, N. Yoshikai, E. Nakamura, *Adv. Synth. Catal.* **2014**, *356*, 1481-1485; d) S. Oi, H. Sasamoto, R. Funayama, Y. Inoue, *Chem. Lett.* **2008**, *37*, 994-995.
- [148] L. Ackermann, R. Vicente, H. K. Potukuchi, V. Pirovano, *Org. Lett.* **2010**, *12*, 5032-5035.
- [149] D. M. Alonso, S. G. Wettstein, J. A. Dumesic, *Green Chem.* **2013**, *15*, 584-595.
- [150] a) B. C. Norris, D. G. Sheppard, G. Henkelman, C. W. Bielawski, *J. Org. Chem.* **2011**, *76*, 301-304; b) Y. Wu, S. Wang, X. Zhu, G. Yang, Y. Wei, L. Zhang, H.-b. Song, *Inorg. Chem.* **2008**, *47*, 5503-5511; c) F. Paul, S. Moulin, O. Piechaczyk, P. Le Floch, J. A. Osborn, *J. Am. Chem. Soc.* **2007**, *129*, 7294-7304; d) H. A. Duong, M. J. Cross, J. Louie, *Org. Lett.* **2004**, *6*, 4679-4681; e) J.-S. Tang, J. G. Verkade, *Angew. Chem. Int. Ed. Engl.* **1993**, *32*, 896-898.
- [151] A. K. Mukerjee, R. Ashare, *Chem. Rev.* **1991**, *91*, 1-24.
- [152] a) K. B. Wiberg, *Acc. Chem. Res.* **1999**, *32*, 922-929; b) W. Walter, E. Schaumann, *Chem. Ber.* **1971**, *104*, 4-10.
- [153] a) J. Zhang, R. Shrestha, J. F. Hartwig, P. Zhao, *Nat Chem* **2016**, *8*, 1144-1151; b) N. Y. P. Kumar, A. Bechtoldt, K. Raghuvanshi, L. Ackermann, *Angew. Chem. Int. Ed.* **2016**, *55*, 6929-6932; c) L. Huang, A. Biafora, G. Zhang, V. Bragoni, L. J. Gooßen, *Angew. Chem. Int. Ed.* **2016**, *55*, 6933-6937; d) A. Biafora, T. Krause, D. Hackenberger, F. Belitz, L. J. Gooßen, *Angew. Chem. Int. Ed.* **2016**, *55*, 14752-14755.
- [154] M. Pichette Drapeau, L. J. Gooßen, *Chem. Eur. J.* **2016**, *22*, 18654-18677.
- [155] *Catalytic Hydroarylation of Carbon-Carbon Multiple Bonds* (Eds.: L. Ackermann, T. B. Gunnoe, L. Habgood), Wiley-VCH, Weinheim, **2017**.
- [156] a) M. Moselage, J. Li, F. Kramm, L. Ackermann, *Angew. Chem. Int. Ed.* **2017**, *56*, 5341-5344; b) F. Kramm, Master-Thesis, Georg-August-Universität Göttingen, **2016**.
- [157] a) C. Kashima, S. Hibi, T. Maruyama, K. Harada, Y. Omote, *J. Heterocyclic Chem.* **1987**, *24*, 637-639; b) J. P. Wibaut, J. W. P. Boon, *Helv. Chim. Acta* **1961**, *44*, 1171-1190.
- [158] N. Gulia, O. Daugulis, *Angew. Chem. Int. Ed.* **2017**, *56*, 3630-3634.
- [159] J. Li, L. Ackermann, *Nat. Chem.* **2015**, *7*, 686-687.
- [160] S. Warratz, L. Ackermann, *unpublished results*.
- [161] M. Moselage, K. Korvorapun L. Ackermann, *unpublished results*.
- [162] N. Sauermann, J. Loup, D. Kootz, V. R. Yatham, A. Berkessel, L. Ackermann, *Synthesis* **2017**, 3476-3484.
- [163] D. Schmiel, H. Butenschön, *Eur. J. Org. Chem.* **2017**, 3041-3048.
- [164] a) W. Liu, S. C. Richter, Y. Zhang, L. Ackermann, *Angew. Chem. Int. Ed.* **2016**, *55*, 7747-7750; b) M. Kim, S. Sharma, N. K. Mishra, S. Han, J. Park, M. Kim, Y. Shin, J. H. Kwak, S. H. Han, I. S. Kim, *Chem. Commun.* **2014**, *50*, 11303-11306.

- [165] P. Anbarasan, K. Ramachandran, *Eur. J. Org. Chem.* **2017**.
- [166] Q. Lu, S. Vásquez-Céspedes, T. Gensch, F. Glorius, *ACS Catal.* **2016**, 6, 2352-2356.
- [167] W. L. F. Armarego, C. Chai, *Purification of Laboratory Chemicals 7th Edition*, Butterworth-Heinemann, Oxford, **2012**.
- [168] X. Qin, H. Liu, D. Qin, Q. Wu, J. You, D. Zhao, Q. Guo, X. Huang, J. Lan, *Chem. Sci.* **2013**, 4, 1964-1969.
- [169] A. C. Rojas, J. K. Crandall, *J. Org. Chem.* **1975**, 40, 2225-2229.
- [170] I. Dubovyk, I. D. G. Watson, A. K. Yudin, *J. Org. Chem.* **2013**, 78, 1559-1575.
- [171] D. Hoppe, R. Hanko, A. Brönneke, F. Lichtenberg, E. van Hülse, *Chem. Ber.* **1985**, 118, 2822-2851.
- [172] D. A. Evans, H.-J. Song, K. R. Fandrick, *Org. Lett.* **2006**, 8, 3351-3354.
- [173] M. J. Mio, L. C. Kopel, J. B. Braun, T. L. Gadzikwa, K. L. Hull, R. G. Brisbois, C. J. Markworth, P. A. Grieco, *Org. Lett.* **2002**, 4, 3199-3202.
- [174] B. Lu, C. Li, L. Zhang, *J. Am. Chem. Soc.* **2010**, 132, 14070-14072.
- [175] a) J. C. Antilla, J. M. Baskin, T. E. Barder, S. L. Buchwald, *J. Org. Chem.* **2004**, 69, 5578-5587; b) A. Correa, C. Bolm, *Adv. Synth. Catal.* **2007**, 349, 2673-2676.
- [176] A. Thurkauf, X.-S. He, H. Zhao, J. Peterson, X. Zhang, R. Brobeck, J. Krause, G. Maynard, A. Hutchison, *Vol. US 6723743 B1*, Neurogen Corporation, USA, **2004**.
- [177] Y. Yamane, X. Liu, A. Hamasaki, T. Ishida, M. Haruta, T. Yokoyama, M. Tokunaga, *Org. Lett.* **2009**, 11, 5162-5165.
- [178] M.-Z. Lu, C.-Q. Wang, S.-J. Song, T.-P. Loh, *Org. Chem. Front.* **2017**, 4, 303-307.
- [179] S. Oi, Y. Tanaka, Y. Inoue, *Organometallics* **2006**, 25, 4773-4778.
- [180] Z. Jia, T. Nagano, X. Li, A. S. C. Chan, *Eur. J. Org. Chem.* **2013**, 858-861.
- [181] S. Doherty, J. G. Knight, C. R. Addyman, C. H. Smyth, N. A. B. Ward, R. W. Harrington, *Organometallics* **2011**, 30, 6010-6016.
- [182] H.-R. Bjørsvik, V. Elumalai, *Eur. J. Org. Chem.* **2016**, 5474-5479.
- [183] J. Jiang, W.-M. Zhang, J.-J. Dai, J. Xu, H.-J. Xu, *J. Org. Chem.* **2017**, 82, 3622-3630.
- [184] L. Ackermann, P. Novák, R. Vicente, N. Hofmann, *Angew. Chem. Int. Ed.* **2009**, 48, 6045-6048.
- [185] Y. Sunada, H. Soejima, H. Nagashima, *Organometallics* **2014**, 33, 5936-5939.
- [186] P. Maslak, P. E. Fanwick, R. D. Guthrie, *J. Org. Chem.* **1984**, 49, 655-659.

## Curriculum Vitae

### Personal Information

---

Name: Marc Philipp Moselage  
Date of Birth: 09.08.1987  
Place of Birth: Verl  
Nationality: German

### Academic Education

---

09/2013-xx/2017      **PhD Thesis** (Supervisor: Prof Dr. L. Ackermann) at the Georg-August-University Göttingen  
  
Title: *C–H and C–C Activation by Cobalt and Ruthenium Catalysis*

10/2010-03/2013      **Master of Science (M. Sc.)** in Chemistry at Bielefeld University, Final Grade: 1.1  
  
**Master Thesis** (Supervisor Prof. Dr. T. Glaser), Title: *Synthesis and Characterization of Thiophloroglucin Ligands for Single Molecule Magnets.*

10/2007-08/2010      **Bachelor of Science (B. Sc.)** in Chemistry at Bielefeld University, Final Grade: 1.2  
  
Bachelor Thesis (Supervisor Prof'in Dr. A. Godt), Title: *Synthesis of Alkylable Linkers for Metal-Organic Frameworks.*

### School Education

---

08/1998-06/2007      Gymnasium Verl, Abitur Grade: 1.4  
  
08/1994-07/1998      Grundschule Kaunitz

### Teaching Experiences

---

07/2017-08/2017      Principal assistant of the practical course "Catalysis"

04/2017-08/2017	Lecture assistant of the course "Modern Aspects in Catalysis"
10/2016-02/2017	Assistant within the FoLL Programm (Forschungsorientiertes Lehren und Lernen)
10/2016-12/2016	Lecture assistant of the course "Introduction to Catalysis"
07/2016-08/2016	Principal assistant of the practical course "Catalysis"
04/2016-08/2016	Lecture assistant of the course "Modern Aspects in Catalysis"
10/2015-12/2015	Lecture assistant of the course "Introduction to Catalysis"
07/2015-08/2015	Principal assistant of the practical course "Catalysis"
04/2015-08/2015	Lecture assistant of the course "Modern Aspects in Catalysis"
10/2014-12/2014	Lecture assistant of the course "Introduction to Catalysis"
07/2014-08/2014	Assistant of the practical course "Catalysis"
01/2014-04/2014	Assistant of the practical course "Chemistry for Medicine Students"

### **Industrial Experiences**

---

10/2011-03/2012	<p>Internship at Merck KGaA in Darmstadt, Division Merck Serono</p> <p>Topic: "Synthesis of organic molecules as potential antitumor agents"</p>
-----------------	--

### **Publications**

---

- 6) **M. Moselage**, J. Li, F. Kramm, L. Ackermann, "*Ruthenium(II)-Catalyzed C–C Arylations and Alkylations: Decarbonylative C–C Functionalizations*" *Angew Chem. Int. Ed.* **2017**, 56, 5341-5344.
- 5) H. Wang, **M. Moselage**, M. J. González, L. Ackermann, "*Selective Synthesis of Indoles by Cobalt(III)-Catalyzed C–H/N–O Functionalization with Nitrones*" *ACS Catal.* **2016**, 6, 2705-2709.



- 4) **M. Moselage**, J. Li, L. Ackermann "Cobalt-Catalyzed C–H Activation" *ACS Catal.* **2016**, 6, 498-525. (Review)
  
- 3) **M. Moselage**, N. Sauermann, J. Koeller, W. Liu, D. Gelman, L. Ackermann "Cobalt(III)-Catalyzed Allylation with Allyl Acetates by C–H/C–O Cleavage" *Synlett* **2015**, 1596-1600.
  
- 2) **M. Moselage**, N. Sauermann, S. C. Richter, L. Ackermann, "C–H Alkenylations with Alkenyl Acetates, Phosphates, Carbonates and Carbamates by Versatile Cobalt Catalysis at 23 °C" *Angew. Chem. Int. Ed.* **2015**, 54, 6352-6355 (selected as hot paper).
  
- 1) B. Feldscher, E. Krickemeyer, **M. Moselage**, H. Theil, V. Hoeke, Y. Kaiser, A. Stammler, H. Bögge, T. Glaser "An Inverted Tripelsalen Ligand by a Convergent Synthesis and its Influence on Trinuclear Fe<sup>III</sup><sub>3</sub> Complexes" *Sci. China: Chem.* **2012**, 55, 951-966.

## Conferences

---

09/2014	<i>Sustainability in Chemistry</i> , Erlangen, Germany (Poster Presentation)
06/2015	<i>18<sup>th</sup> IUPAC International Symposium on Organometallic Chemistry Directed Towards Organic Synthesis</i> (OMCOS 18), Barcelona-Sitges, Spain (Poster Presentation)
04/2016	<i>7<sup>th</sup> Münster Symposium on Cooperative Effects in Chemistry</i> , Münster, Germany (Poster Presentation)
06/2016	<i>3<sup>rd</sup> International Symposium on C–H Activation</i> , Montreal, Canada (Poster Presentation)
09/2017	<i>ICASEC Summer School 2017</i> , Göttingen, Germany (Poster Presentation) ( <b>Poster Prize</b> )

## **Erklärung**

Ich versichere, dass ich die vorliegende Dissertation in dem Zeitraum von August 2013 bis Oktober 2017 am Institut für Organische und Biomolekulare Chemie der Georg-August-Universität Göttingen

auf Anregung und unter Anleitung von

**Herrn Prof. Dr. Lutz Ackermann**

selbstständig durchgeführt und keine anderen als die angegebenen Hilfsmittel und Quellen verwendet habe.

Göttingen, den 20.10.2017

---